

Exploration and Development of Valorisation Routes for Citrus and Potato Waste using Green Methodologies

Joseph A. Houghton

Doctor of Philosophy

University of York

Chemistry

October 2017

“The Earth,” he said, “is a large and very complex lifeboat. We still do not know what can or can’t be done with a proper distribution of resources and it is notorious that to this very day we have not really made an effort to distribute them. In many places on Earth, food is wasted daily, and it is that knowledge that drives hungry men mad.”

– Isaac Asimov

Dedication

I would like to dedicate this body of work to my family. I would not be where I am without your love and support. Thank you.

Abstract

This thesis aimed to establish biorefinery schemes for two large-volume waste feedstocks (citrus juicing waste and potato waste) adhering to the 12 principles of green chemistry and in accordance with the Sustainable Development Goals set out by the United Nations.

A citrus waste biorefinery based around microwave technology was developed, with multiple products. Citrus oil was extracted via microwave-assisted steam distillation (2.4% dry weight) with comparable quality citrus oil extracted via conventional steam distillation. High-methoxyl pectin was extracted under acid-free conditions with microwaves (15.36% dry weight). Pectin showed good gelling capabilities and passed industrial food standard tests. The cellulosic residue remaining after microwave extractions showed good water binding capacity for use as a rheology modifier. Collaboration with Brazilian company Agroterenas generated a map of processing and waste treatment at a modern citrus juicing plant. Industrial citrus juicing waste from Agroterenas was subjected to microwave-assisted pectin extraction (21.19% dry weight). The impact of Huanglongbing disease (HLB) on pectin content was explored with a reduction of 38% in infected oranges.

Proteins were successfully extracted from waste potatoes and identified by SDS-PAGE followed by MALDI-TOF/TOF-MS. The protease inhibitors present in the protein were isolated and purified for potential application as appetite suppressants. The purified protease inhibitors were subjected to crystallisation screening with the aim of gaining a crystal structure of the protein. While crystals were obtained, work is needed to obtain a crystal with good diffraction. Complexation studies were performed on the protease inhibitor and its target enzymes, trypsin and chymotrypsin. A stable complex was isolated via size exclusion chromatography and analysed via SDS-PAGE and LC-MS/MS demonstrating that all three proteins were present.

Finally, pectin from citrus waste was tested in a materials application. Porous, carbonaceous materials created from the pectin dubbed 'Pecbon' were tested in CO₂ capture and compared to activated carbon. Pecbon carbonised to 800 °C (P800) was found to adsorb 2.05 ± 0.24 mmol/g CO₂, showing similar performance to activated carbon (2.12 ± 0.05 mmol/g).

Contents

Abstract	v
List of figures	xiii
List of tables	xix
Acknowledgements	xxv
Declaration	xxvii
1 General Introduction	1
1.1 General Background	3
1.1.1 Global Situation	3
1.1.1.1 Sustainable Development Goals	4
1.1.2 Food Waste – Crisis and Opportunity	6
1.1.2.1 The Food Crisis – from Hunger to Climate Change	8
1.1.3 Green Chemistry and the 12 Principles	10
1.1.3.1 Drivers for Green Chemistry	12
1.1.4 The Biorefinery Concept	13
1.1.5 Future Outlook	15
1.2 Aims and Objectives – an Overview	16
2 Experimental	19
2.1 Acid-Free Microwave Based Biorefinery Scheme for Orange Waste	21
2.1.1 Biomass Preparation	21
2.1.2 D-Limonene Extraction	21
2.1.2.1 Conventional Hydro/Steam-Distillation	21
2.1.2.2 Microwave Assisted Steam Distillation	22
2.1.2.3 Optimisation of Citrus Oil Extraction	23
2.1.2.4 Characterisation of Citrus Oil	23
2.1.3 Pectin Extraction and Characterisation	24
2.1.3.1 Conventional Acid-Assisted Extraction	24
2.1.3.2 Acid-Free Microwave-Assisted Extraction	24

2.1.3.3	Characterisation of Pectin	25
i.	ATR-IR	25
ii.	Degree of Esterification	25
iii.	Galacturonic Acid Content	26
iv.	Test for Residual Solvents in Pectin	26
v.	Test for Total Insolubles in Pectin	28
vi.	Test for Metal Content in Pectin	28
vii.	Gelling Tests	29
2.1.4	Agroterenas Case Study	30
2.1.4.1	Biomass Preparation	30
2.1.4.2	Pectin Extraction	30
2.1.5	Pilot-Scale Study for Pectin Extraction	31
2.2	Proteins from Potatoes	32
2.2.1	Potato Fruit Juice Production	32
2.2.2	Protein Purification and Drying	32
2.2.3	Protein Analysis	32
2.2.3.1	SDS-PAGE	32
2.2.3.2	Protein Identification via Proteomics	33
i.	MALDI-TOF/TOF-MS	33
ii.	LC-MS/MS	35
2.2.4	Protein Purification	37
2.2.5	Crystallisation	37
2.2.5.1	Sitting Drop Method	37
2.2.5.2	Hanging Drop Method	37
2.2.6	Preliminary Trypsin Inhibition Assay for Protease Inhibitors	38
2.3	Pecbons - a Carbonaceous Material for CO ₂ Capture	39
2.3.1	Pecbon Synthesis	39
2.3.1.1	Carbonisation	39
2.3.1.2	N ₂ adsorption/desorption porosimetry	40
2.3.1.3	CO ₂ /N ₂ Porosimetry	40
2.3.1.4	CO ₂ Pressure Swing	41
2.3.1.5	CO ₂ Enthalpy Measurements	41

3	Acid-Free Microwave Biorefinery Scheme for Citrus Waste	43
3.1	Introduction	45
3.1.1	Oranges	45
3.1.2	Citrus Production and Waste	45
3.1.3	D-Limonene and Essential Oil	47
3.1.3.1	Extraction Methodologies for Essential Oils	48
	i. Soxhlet	48
	ii. Hydrodistillation and Steam-Distillation	48
	iii. Supercritical CO ₂ Extraction	49
	iv. Microwave-Assisted Extraction	49
3.1.4	Pectin: Structure, Market Analysis and Extraction	50
3.1.4.1	Pectin Structure	51
3.1.4.2	Pectin Market Analysis	52
3.1.4.3	Extraction Methodologies	56
	i. Traditional: Acid-Catalysed	56
	ii. Enzyme-Assisted Extraction	57
	iii. Ultrasound-Assisted Extraction	58
	iv. Subcritical Water or Super-Hot Water Extraction	58
	v. Microwave Assisted Extraction	60
	vi. Combined Techniques	61
3.2	Specific Aims and Objectives	62
3.3	Results and Discussion	63
3.3.1	Citrus Oil	63
3.3.1.1	Varietal Yields	63
3.3.1.2	Method Optimisation	64
3.3.1.3	Characterisation of Citrus Oil	67
3.3.2	Pectin	71
3.3.2.1	Varietal Yields	71
3.3.2.2	Characterisation of Pectin	72
	i. Visual Appearance	72
	ii. ATR-IR	74
	iii. Degree of Esterification	74
	iv. Gelling Tests	75

v. Total and Acid-Insoluble Content	78
vi. Nitrogen Content	79
vii. Metal Content	79
3.3.3 Cellulosic Residue Valorisation	81
3.3.3.1 Water Binding	81
3.3.4 Flavonoids	82
3.3.5 Agroterenas Case Study and Potential Improvements	83
3.3.5.1 Company Information	84
3.3.5.2 Process	84
3.3.5.3 HLB and Effect on Industrial Orange Juice Production	86
3.3.5.4 Potential Improvements to the Agroterenas Process	87
3.3.5.5 Pectin Isolation Studies	88
i. Characterisation of Pectin Produced from Bagasse	89
ii. Characterisation of Pectin Produced from Healthy and HLB Oranges	90
iii. Characterisation of Pectin Obtained from Yellow Water	91
3.3.6 Pilot-Scale Extraction	93
3.3.6.1 Pilot-Scale Pectin Characterisation	94
i. ATR-IR Characterisation	94
ii. Quality Tests	95
3.4 Conclusions	96
4 Protein from Potatoes	99
4.1 Introduction	101
4.1.1 Production and Waste	101
4.1.2 Potato Valorisation	102
4.1.3 Obesity	103
4.1.3.1 Economic Burden	105
4.1.4 Potato Starch	105
4.1.5 Vegetable Protein Market Analysis	106
4.1.5.1 Potato Proteins Market Analysis and Applications	108
4.1.6 Potato Protein Quality and Extraction	110
4.1.7 Protein Purification Methods	113
4.1.7.1 Ultrafiltration	113

4.1.7.2	Chromatography	114
i.	Anion Exchange	114
ii.	Size Exclusion	114
4.1.8	Specific Proteins of Interest – Protease Inhibitors	115
4.1.9	Potential Potato Biorefinery	116
4.1.10	Research Opportunities	118
4.2	Specific Aims and Objectives	119
4.3	Results and Discussion	120
4.3.1	Protein Yield	120
4.3.1.1	Protein Characterisation	120
i.	SDS-PAGE Analysis	120
ii.	Protein Identification via Proteomics	121
4.3.1.2	Purification of Protease Inhibitors	126
4.3.1.3	Crystallisation Studies	132
iii.	Initial X-ray Diffraction Studies	140
4.3.1.4	Protease Inhibitor Complexation Studies	140
4.3.1.5	Preliminary Trypsin Inhibition Assays	143
4.4	Conclusions	146
5	Pecbons – a Carbonaceous Material for CO₂ Capture	147
5.1	Introduction	149
5.1.1	Carbon Dioxide Capture	150
5.1.1.1	Key Challenges	151
5.1.1.2	Traditional CO ₂ methodology	152
5.1.1.3	Emerging CO ₂ Capture Methodologies	152
i.	Physical Absorbents	153
ii.	Adsorption	153
5.1.2	Carbonaceous, Mesoporous Materials	156
5.1.2.1	Carbonaceous Materials – Background and Production	156
5.1.2.2	Starbons [®]	159
5.1.2.3	Pecbons	160
5.2	Specific Aims and Objectives	164
5.3	Results and Discussion	165
5.3.1	N ₂ adsorption/desorption porosimetry	165

5.3.2	CO ₂ Pressure Swing Adsorption studies	168
5.3.3	Enthalpy of Adsorption	169
5.3.3.1	CO ₂ /N ₂ Swing	169
5.3.3.2	Water Saturated CO ₂ /N ₂ Swing	171
5.3.4	CO ₂ /N ₂ Porosimetry	174
5.3.5	SEM Analysis	176
5.3.6	Relationship Between Physical Properties and CO ₂ Adsorption	178
5.3.7	Effect of Material Preparation Methodology on CO ₂ Adsorbance Capacities	180
5.4	Conclusions	182
6	Future Work and Concluding Remarks	183
6.1	Future Work	185
6.1.1	Acid-Free Microwave Biorefinery Scheme for Citrus Waste	185
6.1.1.1	Full Analysis of Pectin Extraction from Agroterenas Case Study	185
6.1.1.2	Scale-Up to Pilot-Scale	185
6.1.1.3	Mixed Feedstocks	185
6.1.1.4	Combined Extraction Techniques	186
6.1.1.5	Other Valorisation Options – Proteins	186
	i. Protein Content	187
	ii. SDS-PAGE	188
	iii. Identification of Proteins via Proteomics	188
6.1.1.6	Full Life Cycle Assessment of Described Citrus Waste Biorefinery	191
6.1.2	Proteins from Potatoes	191
6.1.2.1	Testing in Food Applications	191
	i. Testing of Extracted Protease Inhibitors as Appetite Suppressants	191
6.1.2.2	Full Protease Inhibition Analysis	192
6.1.2.3	Crystallisation of Protease Inhibitor-Enzyme Complex	192
6.1.2.4	Full Life Cycle Assessment of Protein Extraction from Potatoes	192
6.1.3	Pecbons – a Carbonaceous Material for CO ₂ Capture	192

6.1.3.1	Different Material Production Methodologies	192
6.1.3.2	Full Characterisation	193
	i. Surface Chemistry Analysis	193
	ii. Isotherms with Water and Mixed Gas Analysis	193
	iii. Further Analysis into Physical Properties and CO ₂ Adsorption Capacity	194
6.2	Concluding Remarks	195
Appendix		197
A.1	Chapter 2	199
	A.1.1 List of Equipment	199
A.2	Chapter 3	203
A.3	Chapter 4	205
A.4	Chapter 5	232
Abbreviations		239
Bibliography		243

List of Figures

1.1	Proportions of Waste from Different Sectors Generated in the EU. ¹⁹	7
1.2	Circular Bio-economy	13
1.3	Scheme for a General Biorefinery	14
2.1	Microwave assisted steam distillation apparatus set-up: (1) vacuum pump; (2) condensers; (3) 45 rotative Milestone RotoSYNTH MW system; (4) MW vessel. ⁵¹	23
2.2	Sample loadings for SDS-PAGE	33
3.1	General structure of orange	45
3.2	Global Sweet Orange Production from 1961-2013 ⁶³	46
3.3	Example setup for combined microwave-assisted extraction and hydrodistillation	50
3.4	General Structure of Pectin ⁹⁴	51
3.5	General Structure for the Smooth Region of Pectin	51
3.6	Global Pectin Sales in MT from 2011-2016(Estimated)	52
3.7	Global Pectin Sales by Region (2015)	53
3.8	Simplistic Representation of Different Pectin Types. Top: HM Pectin, Middle: LM Pecin, Bottom: LMA Pectin	54
3.9	Proportion of Different Classes of Pectin Produced	55
3.10	Price of Different Classes of Pectin from 2011-2016(Estimated)	56
3.11	Phase diagram showing subcritical (red dashed area) and supercritical (above the critical point) areas	59
3.12	Citrus Oil Yields Obtained from citrus from Different Countries	63
3.13	Essential Oil Yields Obtained from Different Citrus Fruits	67
3.14	Pectin Yields Obtained from Citrus Sources from Different Countries	71
3.15	Visual Appearance of Pectins Extracted from Different Sources	73
	(a) Commercial Pectin	73
	(b) South Africa – Orange	73
	(c) Spain – Orange (Waxed)	73
	(d) Mexico – Lime	73
	(e) Italy – Lemon	73

(f) Spain – Orange (Unwaxed)	73
3.16 ATR-IR of Pectin Extraction from South Africa Oranges Compared to Commercial Pectin	74
3.17 Degree of Esterification for Extracted Pectins	75
3.18 Gels Formed from Different Pectins	76
3.19 Hardness of Pectin Gels from Different Sources	77
3.20 ¹ H NMR spectrum of Hesperidin Standard (red), Washed (blue), and Unwashed (green) Samples	82
3.21 ¹ H NMR spectrum for hesperidin standard, with peak assignments indicated, performed in D ₂ O and DMSO to suppress signals due to alcohol protons	83
3.22 Simplified Agroterenas Process	85
3.23 Orange Showing Symptoms of HLB	87
3.24 ATR-IR of Pectin Extracted from Agroterenas Bagasse	89
3.25 Pectin Yields from Healthy and HLB Infected Oranges	90
3.26 ATR-IR of Pectin Extracted from Healthy and HLB Infected Oranges	91
3.27 ATR-IR of Pectin Precipitated from the Yellow Water	92
3.28 Pectin Extracted from Different Brazilian Samples	93
(a) Pectin Extracted from Bagass Supplies by Agroterenas	93
(b) Pectin Extracted from Healthy Oranges	93
(c) Pectin Extracted from Oranges Infected with HLB	93
(d) Pectin Extracted from Yellow Water	93
3.29 ATR-IR of Pectin Extracted at Pilot Scale	94
4.1 Global Potato Production ¹³⁵	101
4.2 Prevalence of overweight and obesity in over 20 year olds from 1975-2014 ¹⁴⁸	104
4.3 Global Potato Protein Production ¹⁶¹	109
4.4 Potential Potato Biorefinery ¹⁵³	117
4.5 SDS-PAGE of the Protein Extracted from the Different Varieties	120
4.6 Four Bands Analysed Through Proteomics Assigned Band 1-4 from Bottom to Top	121
4.7 Full PI2 Amino Acid Sequence	124
4.8 Amino Acid Sequence for Chain A	125
4.9 Amino Acid Sequence for Chain B	125

4.10	Initial 1 mL Q Column of Crude Potato Protein	127
4.11	SDS-PAGE Gel Image Looking at the Maximums of Each Peak in the Anion Exchange Chromatogram	127
4.12	SDS-PAGE Gel Image of Fractions A9-b4	128
4.13	Mono Q Polishing Step	129
4.14	SDS-PAGE Gel Image of Fractions Around the Main Peak in the Mono-Q Chromatogram	129
4.15	SEC Chromatogram	130
4.16	SDS-PAGE Gel Image of Fractions of the Main Peaks in the SEC Chromatogram	131
4.17	Initial Crystal Formed in Sitting Drop Screens	132
4.18	Initial Crystal Formed in Sitting Drop Screens	133
4.19	Potential Protein Crystals Formed in Initial Hanging Drop Screen	135
	(a) Crystal Formed in Condition 2A	135
	(b) Crystal Formed in Condition 1C	135
4.20	Potential Protein Crystals Formed in Second Hanging Drop Screen	136
	(a) Potential Crystals Formed in Condition 2A by Industrial Protein	136
	(b) Potential Crystals Formed in Condition 2A by Industrial Protein	136
4.21	Crystals Showing Small, Rapidly Grown Structures	137
4.22	Potential Protein Crystals Showing Promising Morphology	139
	(a) Small Crystal Shards, Showing Hard Straight Edges	139
	(b) Rectangular Crystals, Showing Limited Polarisability	139
	(c) More Crystals with Rectangular Morphology	139
	(d) Large 'Snowflake' Crystals, Strong Polarisability	139
	(e) Single Large Crystal with Semi-Straight Edges	139
	(f) More Examples of Larger 'Snowflake' Crystals	139
4.23	NATIVE gel of Complexation Test	141
4.24	SDS-PAGE of the Potential Complex	142
4.25	Trypsin Assay Showing Fluorescence where un-inhibited Trypsin is Present	144
5.1	Structure of primary alkanolamine MEA	152
5.2	Robeson Plot Showing the Upper Bound Limit	155
5.3	Phase Diagram for Water and TBA	162

5.4	Physisorption Isotherms for Different Materials. From Top to Bottom: Activated Carbon, P800, S800 and A800.	167
5.5	mmol CO ₂ Adsorbed per g Material	169
5.6	Heat Flow and Weight Change During CO ₂ Adsorption and Desorption using P800 at 308 K	170
5.7	Enthalpy of Adsorption/Desorption Determined via CO ₂ /N ₂ Swing Experiments	171
5.8	Heat Flow and Weight Change During Water Saturated CO ₂ Adsorption and Desorption using P800 at 308 K	172
5.9	Enthalpy of Adsorption and Desorption of CO ₂ under Dry and Wet Conditions for Activated Carbon (AC), Pecbon 800 (P800), Starbon [®] 800 (S800) and Algibon 800 (A800)	173
5.10	Chemisorption Isotherms for Different Samples at 308K for both CO ₂ and N ₂	175
5.11	SEM Images of different samples	177
	(a) SEM images of Activated Carbon 10,000x	177
	(b) SEM images of Activated Carbon 20,000x	177
	(c) SEM images of P800 10,000x	177
	(d) SEM images of P800 20,000x	177
	(e) SEM images of A800 10,000x	177
	(f) SEM images of A800 20,000x	177
	(g) SEM images of S800 10,000x	177
	(h) SEM images of S800 20,000x	177
5.12	Analysis of BET Surface Area against CO ₂ Adsorption Capacity	178
5.13	Analysis of Micropore Volume against CO ₂ Adsorption Capacity	179
5.14	Analysis of Micropore Volume against BET Surface Area	180
6.1	SDS-PAGE gel for orange protien	188
A.1	ATR-IR of Pectin Extracted from Oranges (Spain – Waxed)	203
A.2	ATR-IR of Pectin Extracted from Oranges (Spain – Non-Waxed)	203
A.3	ATR-IR of Pectin Extracted from Lemons (Italy)	204
A.4	ATR-IR of Pectin Extracted from Limes (Mexico)	204
A.5	Guide to Amino Acids for Reference	205
A.6	Isotherms for Different Samples	234

(a) Isotherm for P300	234
(b) Isotherm for P450	234
(c) Isotherm for P600	234
A.7 DSC Traces for A800, S800 and AC on Addition of CO ₂ and N ₂	235
(a) Heat Flow and Weight Change on Addition of CO ₂ and N ₂ to A800	235
(b) Heat Flow and Weight Change on Addition of CO ₂ and N ₂ to P450	235
(c) Heat Flow and Weight Change on Addition of CO ₂ and N ₂ to P600	235
A.8 DSC Traces for P300, P450 and P600 on Addition of CO ₂ and N ₂	236
(a) Heat Flow and Weight Change on Addition of CO ₂ and N ₂ to P300	236
(b) Heat Flow and Weight Change on Addition of CO ₂ and N ₂ to P450	236
(c) Heat Flow and Weight Change on Addition of CO ₂ and N ₂ to P600	236
A.9 DSC Traces for A800, S800 and AC on Addition of Moisture Loaded CO ₂ and N ₂	237
(a) Heat Flow and Weight Change on Addition of Moisture Loaded CO ₂ and N ₂ to P300	237
(b) Heat Flow and Weight Change on Addition of Moisture Loaded CO ₂ and N ₂ to P450	237
(c) Heat Flow and Weight Change on Addition of Moisture Loaded CO ₂ and N ₂ to P600	237
A.10 DSC Traces for P300, P450 and P600 on Addition of Moisture Loaded CO ₂ and N ₂	238
(a) Heat Flow and Weight Change on Addition of Moisture Loaded CO ₂ and N ₂ to P300	238
(b) Heat Flow and Weight Change on Addition of Moisture Loaded CO ₂ and N ₂ to P450	238
(c) Heat Flow and Weight Change on Addition of Moisture Loaded CO ₂ and N ₂ to P600	238

List of Tables

1.1	Sustainable Development Goals	4
1.2	12 Principles of Green Chemistry	11
2.1	Solid State CPMAS NMR Conditions	25
2.2	GC-FID Conditions for Residual Solvent Analysis	27
2.3	Reagents for Fraunhofer Gelling Test	29
2.4	Reagents for University of York Gelling Test	30
2.5	Experimental Conditions for Pectin Extraction in Brazil	30
2.6	Reagents used for Pectin Production	39
2.7	Pectin Carbonisation Parameters	40
3.1	Experimental Conditions and Yields for One-Step Citrus Oil Extraction	65
3.2	Experimental Conditions and Yields for Two-Step Citrus Oil Extraction at WOP:H ₂ O ratio of 1:1.5	66
3.3	Optimal Reaction Conditions for Citrus Extraction from WOP	67
3.4	Citrus Oil Analysis from Optimised Microwave Assisted Distillation and Steam Distillation	68
3.5	Citrus Oil Analysis from Different Sources via Optimised Microwave Assisted Steam Distillation	70
3.6	Visco-elastic Properties of Pectins Extracted from Different Sources	78
3.7	CHN Analysis of Microwave Extracted Pectin	79
3.8	ICP Data for Acid-Free Microwave Extracted Pectin	80
3.9	Water binding capacity of residual cellulose created from conventional pectin extraction and acid-free microwave extraction pectin, compared with industrially used cellulosic water binders	81
3.10	Pectin Scale up Conditions	94
3.11	Quality Tests for Pilot-Scale Pectin	95
4.1	Typical losses from potato production ¹³⁶	102
4.2	Basic Nutritional Value for Potato ¹⁴²	103
4.3	Protein Quality from Different Plant and Animal Sources ¹⁶¹	106
4.4	Potato Protein Production (MT) by Region (2012-2017) ¹⁶¹	109

4.5	Amino Acid Profile for Potato Protein with Bold Showing Essential Amino Acids ¹⁶⁶	111
4.6	Different Protein Yields and Properties with Regard to Precipitation Method ¹⁴³	112
4.7	Proteomics Analysis of Potato Protein	122
4.8	Proteomics Data For Potato Band at 15 kDa	123
4.9	Proteomics Analysis of Potato Protein at roughly 90 kDa	126
4.10	Conditions for NATIVE gel Complex Test	141
4.11	Layout of Plate for Trypsin Inhibition Assay	144
4.12	Trypsin Inhibition Assay Conditions	144
5.1	Composition of gases by weight in both postcombustion and precombustion processes ¹⁸⁶	151
5.2	Porosity Analysis of Pecbons	165
5.3	Maximum Adsorption of CO ₂ and N ₂ onto Materials as Determined by Chemisorption Experiments	176
6.1	CHN Analysis of Dry Orange Peel Before and After Microwave Extraction	187
6.2	Proteomics Analysis of Orange Protein	189
6.3	Proteomics Data For Orange Protein	190
A.1	GC-TOF Specification	199
A.2	Ultra-Filtration cartridge properties	201
A.3	Proteomics Data For Potato Band 1	206
A.4	Proteomics Data For Potato Band 2	206
A.5	Proteomics Data For Potato Band 3	207
A.6	Proteomics Data For Potato Band 4	207
A.7	Proteomics Data For Potato Band 1 at 90 kDa	208
A.8	Proteomics Data For Potato Band 2 at 90 kDa	208
A.9	Proteomics Data For Orange Band 1	209
A.10	Proteomics Data For Orange Band 2	209
A.11	Proteomics Data For Orange Band 3	209
A.12	Index Formulation Hampton Research - Copyright 2016 Part 1	210
A.13	Index Formulation Hampton Research - Copyright 2016 Part 2	211
A.14	Index Formulation Hampton Research - Copyright 2016 Part 3	212

A.15 Index Formulation Hampton Research - Copyright 2016 Part 4	213
A.16 PEG ION Formulation Hampton Research - Copyright 2016 Part 1	214
A.17 PEG ION Formulation Hampton Research - Copyright 2016 Part 2	215
A.18 PEG ION Formulation Hampton Research - Copyright 2016 Part 3	216
A.19 PEG ION Formulation Hampton Research - Copyright 2016 Part 4	217
A.20 Molecular Interactions PACT <i>premier</i> TM Crystallisation Screen Part 1	218
A.21 Molecular Interactions PACT <i>premier</i> TM Crystallisation Screen Part 2	219
A.22 Molecular Interactions PACT <i>premier</i> TM Crystallisation Screen Part 3	220
A.23 PDB Minimal Crystallisation Screen Part 1	221
A.24 PDB Minimal Crystallisation Screen Part 2	222
A.25 PDB Minimal Crystallisation Screen Part 3	223
A.26 PDB Minimal Crystallisation Screen Part 4	224
A.27 Qiagen [®] MPD Screen Conditions Part 1	225
A.28 Qiagen [®] MPD Screen Conditions Part 2	226
A.29 Qiagen [®] MPD Screen Conditions Part 3	227
A.30 HT Formulation Hampton Research - Copyright 2016 Part 1	228
A.31 HT Formulation Hampton Research - Copyright 2016 Part 2	229
A.32 HT Formulation Hampton Research - Copyright 2016 Part 3	230
A.33 HT Formulation Hampton Research - Copyright 2016 Part 4	231
A.34 Activated Carbon CO ₂ Pressure Swing 10 bar pressure for 30mins	232
A.35 Pecbon 300 CO ₂ Pressure Swing 10 bar pressure for 30mins	232
A.36 Pecbon 450 CO ₂ Pressure Swing 10 bar pressure for 30mins	232
A.37 Pecbon 600 CO ₂ Pressure Swing 10 bar pressure for 30mins	233
A.38 Pecbon 800 CO ₂ Pressure Swing 10 bar pressure for 30mins	233
A.39 Starbon 800 CO ₂ Pressure Swing 10 bar pressure for 30mins	233
A.40 Algibon 800 CO ₂ Pressure Swing 10 bar pressure for 30mins	233

Acknowledgements

First and foremost, I would like to thank my supervisor Dr. Avtar Matharu and the Green Chemistry Centre of Excellence at the University of York for giving me the opportunity to study for a PhD in an area I am truly passionate about.

To my many collaborators over the last three years, thank you. Working as part of a team towards a more sustainable future has been one of the most rewarding parts of the last three years. Below are some of the people who have been instrumental in this work.

Acid-Free Microwave Biorefinery Scheme for Orange Waste

Dr. Lucie Pfaltzgraff deserves special mention for pioneering the work comprised within this chapter and for inspiring me during my MChem year to continue studying green chemistry.

Dr. Julen Bustamante, Edu de Melo, Hao Xia, Dr. Hannah Briers, Dr. Thomas Dugmore, Dr. Rob Mcelroy, Iris Houthoff and Sytze van Stempvoort, thank you all for aiding in the work detailed in this chapter.

Proteins from Biomass

Special thanks have to go to Rachel Bates, Dr. Tim Ganderton and Dr. Christian Roth for all the help you have given me on the biological side of this product, it has been a pleasure learning so much about a new area. Thank you as well for being patient with a chemist thrown into a biology-heavy project.

Mesoporous Materials

Special thanks to Jennifer Attard for helping in the pecbon creation, Roxana Milescu for the Algibon and Starbon production and Dr. Xiao Wu for helping design experiments.

Finally, I would like to thank those of you who have made the last three years such a pleasure, Stefan Lawrenson, Xiao Wu, Tabitha Petchey, Ian Ingram, Katie Lamb, Anna Zhenova, Rob McElroy and Thomas Attard, Jonny Ruffell among many others. You have made the last three years a joy.

Declaration

The research described in this thesis is original work, which I undertook at the University of York during 2014–2017. This work has not previously been presented for an award at this, or any other, University. All sources are acknowledged as References. Except where stated, all of the work contained within this thesis represents the original contribution of the author. Certain parts of the work described herein were undertaken in collaboration with other researchers, they are fully acknowledged below:

Chapter	Section	Collaborator	Institution
3	Citrus Oil Extraction, Optimisation and Characterisation	Dr. Julen Bustamante Sytze van Stempvoort	University of York University of York
3	Pectin Extraction and Characterisation	Dr. Julen Bustamante Eduardo M. de Melo Dr. Lucie A. Pfaltzgraff	University of York University of York University of York
3	Agroterenas Process Mapping	Jose Vega Barbero	Stockholm Environment Institute at York
3	Scale up	Eduardo M. de Melo Dr. Hannah Briers Dr. Thomas Dugmore Dr. Rob McElroy	University of York University of York Univeristy of York University of York
4	Starch and Protein Extraction	Asila Al Rushaidi Xinyi Zhou	University of York University of York
4	Proteomics Analysis	Rachel Bates	University of York
4	Purification and Crystallisation	Dr. Tim Ganderton	University of York
4	Scale up	Alison Wright	Branston Ltd
5	Pecbon Creation	Jennifer Attard	University of York

Some parts of this thesis have been published in journals; where items were published jointly with collaborators, the author of this thesis is responsible for the material presented here. For each published item the primary author is the first listed author. Publications are listed at the beginning chapter to which they relate, as well as below.

Publications

Chapter 1

1. Matharu, A.S.; de Melo, E.M.; Houghton, J.A. 'Food Supply Chain Waste: A Functional Periodic Table of Biobased Resources', in *Waste Biorefinery: Perspectives and Challenges*, Elsevier. **2017**. Accepted and uploaded as Chapter 7 on Elsevier EMSS system
2. Matharu, A.S.; de Melo, E.M.; Houghton, J.A. 'Green Chemistry: Opportunities from food supply chain waste' in *Resource Nexus*, Routledge. **2017**. Accepted as Chapter 30
3. Dugmore, T. I.; Clark, J. H.; Bustamante, J.; Houghton, J. A.; Matharu, A. S. *Top. Curr. Chem.* **2017**, *375*, 46.
4. Xia, H.; Houghton, J. A.; Clark, J. H.; Matharu, A. S. *ACS Sus. Chem. Eng.* **2016**, *4*, 6002–6009.
5. Matharu, A. S.; de Melo, E. M.; Houghton, J. A. *Bioresource Technol.* **2016**, *215*, 123–130.
6. Attard, T. M.; Hunt, A. J.; Matharu, A. S.; Houghton, J. A.; Polikarpov, I. '2. Biomass as a Feedstock,' In *Introduction to Chemicals from Biomass*; John Wiley & Sons, Ltd: **2015**, pp 31–52.

Chapter 3

7. Matharu, A. S.; Houghton, J. A.; Lucas-Torres, C.; Moreno, A. *Green Chem.* **2016**, *18*, 5280–5287.
8. Bustamante, J.; van Stempvoort, S.; Garcia-Gallarreta, M.; Houghton, J. A.; Briers, H. K.; Budarin, V. L.; Matharu, A. S.; Clark, J. H. *J. Clean. Prod.* **2016**, *137*, 598–605.

How to Use this Thesis

This thesis is designed for use by undergraduate, postgraduate and experienced researchers in the area of green and sustainable science. It is divided into the following chapters.

1. General Introduction

This section gives an overview of global situation with regards to sustainability, waste production and green chemistry. It puts the project into a global social and economic perspective and covers drivers for research and development into the area of chemistry explored within this thesis.

2. Experimental

Methods used within this thesis are covered in this chapter. It is split into three sections corresponding to each of the following three chapters.

3. Acid-Free Microwave Biorefinery Scheme for Orange Waste

Within this chapter an introduction to citrus juicing waste volumes and relating issues along with current and future valorisation routes is given followed by the results obtained within this project along with discussion of the findings. A conclusion of the findings is given at the end of the chapter.

4. Proteins from Biomass

The need for an increase in global vegetable protein is very topical. An introduction to vegetable protein with specific focus on potato protein is given at the beginning of this chapter followed by the results obtained within this project along with discussion of the findings. A conclusion highlighting the main results is also included. For when amino acid sequences are used, a guide to the 20 most common amino acids is included in the appendix (figure A.5 – figure created by Compound Interest – <http://www.compoundchem.com/>)

5. Mesoporous Materials from Biomass

A literature review based around current production of mesoporous materials from biomass along with their potential utilisation within the application of CO₂ capture is given followed by the results obtained within this project and discussion of the findings. A conclusion highlighting the main findings is also included.

6. Future Work and Concluding Remarks

Concluding remarks regarding the work included in this thesis along with future work needing to be performed are provided in this chapter.

Chapter 1

General Introduction

1. Matharu, A.S.; de Melo, E.M.; Houghton, J.A. 'Food Supply Chain Waste: A Functional Periodic Table of Biobased Resources', in *Waste Biorefinery: Perspectives and Challenges*, Elsevier. **2017**. Accepted and uploaded as Chapter 7 on Elsevier EMSS system
2. Matharu, A.S.; de Melo, E.M.; Houghton, J.A. 'Green Chemistry: Opportunities from food supply chain waste' in *Resource Nexus*, Routledge. **2017**. Accepted as Chapter 30
3. Dugmore, T. I.; Clark, J. H.; Bustamante, J.; Houghton, J. A.; Matharu, A. S. *Top. Curr. Chem.* **2017**, *375*, 46.
4. Xia, H.; Houghton, J. A.; Clark, J. H.; Matharu, A. S. *ACS Sus. Chem. Eng.* **2016**, *4*, 6002–6009.
5. Matharu, A. S.; de Melo, E. M.; Houghton, J. A. *Bioresource Technol.* **2016**, *215*, 123–130.
6. Attard, T. M.; Hunt, A. J.; Matharu, A. S.; Houghton, J. A.; Polikarpov, I. *In Introduction to Chemicals from Biomass*; John Wiley & Sons, Ltd: **2015**, pp 31–52.

1.1 General Background

1.1.1 Global Situation

This century is providing unprecedented challenges to our planet, with humanity's anthropogenic impact causing myriad problems that we can no longer afford to ignore. Natural resource depletion, food and water scarcity, environmental degradation, exceptionally high waste production and negative climate change are just some of the problems being compounded by an ever increasing population. But while these challenges are clearly numerous and hard to solve immediately, this does afford an immense opportunity to design and safe-guard an efficient, sustainable future which allows for the continued technological and economic growth of humanity while also protecting against climate change and finite resource depletion.^{1,2}

Global population has increased by 24% from 1900 to 2010 with an average yearly increase of 1.2% over the last 10 years.³ This rapid increase is adding strain to the already stressed finite resources available globally, with crude oil being the basis of most of the chemical and materials industry⁴ and a large proportion of global energy coming from non-renewable sources.⁵ This increase in population, along with the increased industrialisation and development of developing countries^{6,7} means that the challenge of resource distribution and sustainability is becoming increasingly prominent.

Steps are already being taken to alleviate many of these problems however, with better communication and sharing of technological innovations globally it is possible to create a more educated and responsible global society capable of predicting the long term effect of its actions on the planet and societal infrastructure. Initiatives to mitigate climate change, abolish world hunger, reduce waste production and increase industrial efficiency and robustness are becoming global phenomena with multiple countries beginning to work together to bring about global change.

'Sustainability' is becoming a very important concept in modern society and has to encompass both economic, social and environmental values to be effective. Sustainability is the concept of allowing the lifestyle of the present, without compromising the ability of future generations to live an equivalent lifestyle, or to improve upon it.^{8,9}

1.1.1.1 Sustainable Development Goals

In 2015, the United Nations (UN) recognised the importance of sustainability on the future of society and so, organised a Sustainable Development Summit to discuss the report: ‘Transforming our World: the 2030 Agenda for Sustainable Development.’ Within this report are detailed 17 Sustainable Development Goals (SDGs, table 1.1) that build on the Millennium development goals (MDGs).¹⁰

Table 1.1 – Sustainable Development Goals

Goal 1	End poverty in all its forms everywhere.
Goal 2	End hunger, achieve food security and improved nutrition and promote sustainable agriculture.
Goal 3	Ensure healthy lives and promote well being for all at all ages.
Goal 4	Ensure inclusive and equitable quality education and promote lifelong learning opportunities for all.
Goal 5	Achieve gender equality and empower all women and girls.
Goal 6	Ensure availability and sustainable management of water and sanitation for all.
Goal 7	Ensure access to affordable, reliable, sustainable and modern energy for all.
Goal 8	Promote sustained, inclusive and sustainable economic growth, full and productive employment and decent work for all.
Goal 9	Build resilient infrastructure, promote inclusive and sustainable industrialisation and foster innovation.
Goal 10	Reduce inequality within and among countries.
Goal 11	Make cities and human settlements inclusive, safe, resilient and sustainable.
Goal 12	Ensure sustainable consumption and production patterns.
Goal 13	Take urgent action to combat climate change and its impacts.
Goal 14	Conserve and sustainably use the oceans, seas and marine resources for sustainable development.
Goal 15	Protect, restore and promote sustainable use of terrestrial ecosystems, sustainably manage forests, combat desertification, and halt and reverse land degradation and halt biodiversity loss.
Goal 16	Promote peaceful and inclusive societies for sustainable development, provide access to justice for all and build effective, accountable and inclusive institutions at all levels.
Goal 17	Strengthen the means of implementation and revitalise the Global Partnership for Sustainable Development.

The SDGs encompass a broad range of issues ranging from poverty and world peace to sustainable industry and agriculture and certain goals are particularly relevant to this body of work, namely goals 2, 12 and 13. Each goal is further subdivided into several more specific ‘targets’ which shed light on how the suggested goal could be achieved. Each of the relevant goals is explored in more detail below with respect to the specific targets that are relevant to this body of work.

Goal 2. End hunger, achieve food security and improve nutrition and promote sustainable agriculture.

While the majority of this goal lies outside the scope of this project, the focus on sustainable agriculture is of relevance as detailed in target 4.

Target 4: By 2030, ensure sustainable food production systems and implement resilient agricultural practices that increase productivity and production.

Goal 12. Ensure sustainable consumption and production patterns.

This is by far the most relevant goal to this project with targets 3 and 5 being of particular interest.

Target 3: By 2030, halve per capita global food waste at the retail and consumer levels and reduce food losses along production and supply chain, including post-harvest losses.

Target 5: By 2030, substantially reduce waste generation through prevention, reduction, recycling and reuse.

Waste is a serious problem in modern society. This is highlighted by the emphasis put on it within the sustainable development goals. A greater exploration into the issues surrounding waste is given in the next section.

Goal 13. Take urgent action to combat climate change and its impacts.

Climate change, and in particular green-house gas emission, is certainly not a new concept, but its importance on a sustainable future is beyond question, hence the urgency emphasised within this SDG. The issues arising from climate change and how they relate to this project are explored later in this chapter.

1.1.2 Food Waste – Crisis and Opportunity

Biomass accounts for roughly 32% of yearly processed material, with subsequently high amount of waste being produced. One large area of biomass processing worldwide is the food industry, and waste from the food industry poses both a colossal challenge and a very tantalising opportunity to the global economy.¹¹

Food waste is defined as ‘wholesome edible material intended for human consumption, arising at any point in the Food Supply Chain (FSC) that is instead discarded, lost, degraded or consumed by pests.’¹² Approximately one-third of all food produced for human consumption ends up as waste, amounting to over 1.3 billion tons annually.¹³ Per capita food waste in developed regions of the world such as Europe and North America range from 280-300 kg/year.¹⁴ This is a huge volume of waste being produced annually, and with landfill gate taxes increasing in value within recent years,^{15,16} industries are being forced to acknowledge the massive economic and environmental burden that food waste represents.

The UK is currently the highest generator of food waste in Europe, with 14 million tons being produced in 2013,¹⁷ 7.2 million tons of which is generated in UK households and 4.3 million tons from the FSC.¹⁸ In the EU roughly 90 million tonnes of food waste is generated annually, with around 39% of that from the manufacturing sector, 42% from households, 14% from the food service and 5% from retail/ wholesale (figure 1.1).¹⁹

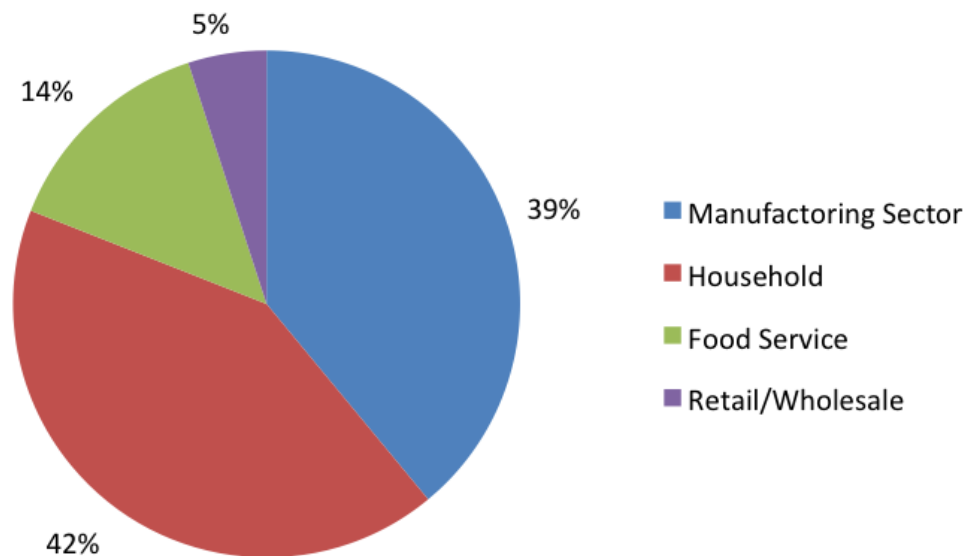


Figure 1.1 – Proportions of Waste from Different Sectors Generated in the EU.¹⁹

Food waste is being recognised as a serious issue by some of the world’s leading governing bodies. For example, the French parliament unanimously passed a bill in 2016 in an effort to reduce food waste from large supermarkets. This bill adds an article (L. 541-15-3) into the French environmental code, outlining a hierarchical approach to reducing food waste starting with prevention; followed by use of unsold food fit for human consumption via donation or reprocessing; then followed by recovery for animal feed; and finally for use as a compost or for energy recovery. This bill prevents supermarkets from deliberately spoiling food (usually by pouring bleach over it) which was and is a common practice in many places around the world.

It is infamous that so much food is wasted globally on a daily basis, while such a high percentage of the global population still live in abject poverty, where malnutrition and undernourishment are serious concerns. This global imbalance along with the growing population and hence requirements for more and more food needing to be produced is leading to a crisis of food production and even distribution.

1.1.2.1 The Food Crisis – from Hunger to Climate Change

While in recent years global hunger has been gradually declining, an estimated 795 million people worldwide are still undernourished, equating to roughly 1 in 9 people suffering from hunger. While this is a dramatic reduction from the previous decade (roughly 18.6% of the population undernourished), it is still a long way from being a comfortable worldwide situation.²⁰

The Global Hunger Index (GHI) is often used as a simple metric for analysing the current standings of world hunger.²¹ The International Food Policy Research Institute (IFPRI) calculate the GHI yearly based on the following four indicators:

1. **Undernourishment:** the percentage of undernourished people in a population.
2. **Child Wasting:** Proportion of children under the age of five who have low weight for their height.
3. **Child Stunting:** Proportion of children under the age of five who have low height for their age.
4. **Child Mortality:** Mortality rate for children under the age of five.

The GHI ranges from 0 (being no global hunger) to 100 which would be a catastrophic prevalence of world hunger. The year 2016 marked a reduction of 29% from 2000 with the GHI score dropping from 30.0 (classed as ‘serious’ but approaching ‘alarming’) to 21.3 (still classed as ‘serious’, but approaching ‘moderate’).

While world hunger appears to be on the decline, challenges still remain as to how enough food is going to be produced to sustain the growing population. It has been predicted that within the next 40 years, food production will have to be doubled to accommodate the increase in population and adhere to the SDG’s aim to reduce world hunger.^{22,23}

Protein is being heralded as one of the most important macronutrients to take into consideration when looking to future expansions of global food production, not only because it is a vital macronutrient within the human diet, but also because the anthropogenic contributions to the nitrogen cycle are 100-200% compared to the contribution to the carbon cycle by mineral fuel combustion (1-2%).²⁴

For every 1 kg of animal protein produced, roughly 6 kg of plant protein is needed to feed the animal. This equates to only 15% of the protein and energy inputted by the plant feedstock ending up as human nutrition, with the other 85% being wasted. This also means that 85% of the nitrogen inputted into the system in the form of fertiliser ends up as waste. This is incredibly resource inefficient, and while currently economically viable, given the need to double the global food production by 2050, the future might have to see a reduction in the amount of animal protein consumed by humans, and a proportional increase in the amount of plant protein consumed.

Within the UK it has been estimated that roughly 50% of greenhouse gas emissions could be attributed to meat consumption and that the economic cost on the National Health Service due to illness and early death relating to excessive meat consumption was roughly £1.28 billion.²⁵ It has also been estimated that the amount of GHG emitted per person with a high (>100 g/day) meat diet is roughly double that of a person with a vegan diet.²⁶

It is evident that with future global food production having to undertake such a vast increase, and to abide by the SDGs relating to reduction in climate change and biodiversity loss, that there is most likely have to be a trend towards more plant based proteins and a move away from the heavily animal protein dominated diet most of the western world is currently used to. This will bring about a host of new challenges, with more focus having to put upon the essential amino acid content and quality of plant based proteins if there is hope for them to replace or partly replace their animal based counterparts.

When greenhouse gas emission is spoken about, the majority of the time it is in reference to the burning of fossil fuels, and while this is a major contributor to global GHG emissions, it is not the only source. Food waste is now recognised as a large contributor to the yearly global GHG emissions.²⁶⁻²⁸ If food waste was a country, it

would be the third largest GHG emitter behind the USA and China.²⁹

Production phase GHG emissions from food waste have more than tripled in the past 40 years, rising from 680 Mt in 1961 to 2.2 Gt CO₂ equivalent (CO₂e) in 2011. Not only is this in and of itself a very obvious problem, the scope of the issue increases again when the GHG produced from food waste per capita is taken into account, this showed a 44% increase over the past 40 years with values increasing from 225 kg CO₂e per capita in 1961 to 323 kg CO₂e per capita in 2011. Therefore, not only is the GHG from food waste increasing with the population (and hence the global food production) but it is also increasing in amount per capita. This is most likely due to the increased prevalence of developing countries adopting a ‘western’ diet, high in animal protein, refined oils and sugars, with accompanying high GHG emissions.³⁰ With food production having to increase in tandem with the growing population, food waste is going to become an ever increasing problem with relation to GHG emissions and climate change if the practices surrounding industrial food production are not changed.

While food waste is a large contributor to global GHG emissions, fossil fuel burning for energy is still one of the major contributors to global CO₂ emissions. Renewable energy sources, while undoubtedly attractive, are still decades from full implementation in most parts of the world, especially in developing countries. Ways of reducing the CO₂ emissions from conventional fossil fuel burning is therefore a very topical and interesting area of research, with work being done into different CO₂ scrubbing methodologies. This is covered in further detail in Chapter 5 of this thesis.

1.1.3 Green Chemistry and the 12 Principles

Green chemistry is one of the fastest growing areas of chemistry and is set to continue to expand and become increasingly important over the next century, with government and national policies becoming stricter on chemical practices. The general definition of green chemistry came about in the early 1990s: ‘the design of chemical products and process to reduce or eliminate the use and generation of hazardous substances’³¹ It was realised that this definition required some expanding upon, so Paul Anastas and John Warner set out the twelve principles of green chemistry (table 1.2) in 1998.^{32–35} These were intended to cover all considerations when a new chemical methodology was designed.

Table 1.2 – 12 Principles of Green Chemistry

Principle	Explanation
1. Prevention.	It is better to prevent waste than to treat waste after it has been created.
2. Atom Economy.	Methods should be designed to maximise the incorporation of all materials used in the process into the final product.
3. Less Hazardous Chemical Syntheses.	Synthetic methods should be designed to use and generate substances that possess little or no toxicity to human health/the environment.
4. Designing Safer Chemicals.	Chemical products should be designed to affect their desired function while minimising toxicity.
5. Safer Solvents and Auxiliaries.	The use of auxiliary substances (e.g. solvents) should be made unnecessary wherever possible and innocuous when used.
6. Design for Energy Efficiency.	Energy requirements of chemical processes should be minimised. Ambient temperature/pressure ideal.
7. Use of Renewable Feedstocks.	A raw material or feedstock should be renewable whenever possible.
8. Reductive Derivatives.	Unnecessary derivatisation (use of blocking groups, protection/ deprotection etc.) should be minimised or avoided if possible.
9. Catalysis.	Catalytic reagents are superior to stoichiometric reagents.
10. Design for Degradation.	Chemical products should be designed so that at the end of their function they break down into innocuous degradation products and do not persist in the environment.
11. Real-time Analysis for Pollution Prevention.	Analytical methodologies need to be developed to allow for real-time monitoring and control prior to the formation of hazardous substances.
12. Inherently Safer Chemistry for Accident Prevention.	Substances and the form of a substance used should be chosen to minimise the potential for chemical accidents (explosions, fires etc.)

The concept of design is central to the green chemistry ideology, with everything being taken into account during the design phase of the process, meaning excessive or hazardous waste, dangerous chemicals, excessive solvent or high temperatures or pressures during the method have to be justified and removed if at all possible.³⁶

From an industrial point of view, new legislation arising from green chemical philosophy is often a benefit to the industry. Not only does it improve public perception of the chemical industry (which is often quite negative) but also usually ends up profiting the industry via the reduction of waste produced, limiting unnecessary solvent usage and expensive reaction conditions and increasing efficiency within the process.³⁷

1.1.3.1 Drivers for Green Chemistry

There are many global drivers for the adoption of green chemistry into the chemical and material industry; the principles of green chemistry fit very well with the sustainable development goals, with beneficial effects on climate change, industrial efficiency, waste management and safety within industry. From a purely economic standpoint however, green chemistry still makes a lot of sense due to the fact that the price for non-renewable feedstocks such as crude oil is incredibly volatile and will inevitably begin to increase as global stocks dwindle.^{38,39} The increasing price for commodities by 147% since the turn of the century provides evidence of this.⁴⁰

The use of biomass as a feedstock for the chemical, fuel and materials industries is an attractive alternative to the use of finite resources such as crude oil, as they are usually readily available in large volumes and renewable. The use of biomass waste is theoretically an even more attractive concept as this takes care of two problems with one solution; the need to reduce waste production globally, and the need for a high volume, renewable feedstock.

The chemical industry cracks crude oil into simple platform molecules, and then builds these up into high value application molecules. In the case of biomass, the reversal is often true. Biomass already contains complex molecules that can be extracted in their present state without any need for adding functionalisation. This is particularly true for molecules containing hetero atoms, as these are commonly found in biomass but have to be engineered from the hydrocarbons commonly produced from crude oil cracking.

Biomass also allows for a circular bio-economy (figure 1.2),^{41,42} with the CO₂ emissions from the production of chemicals and fuels being recycled back into the biomass feedstock.

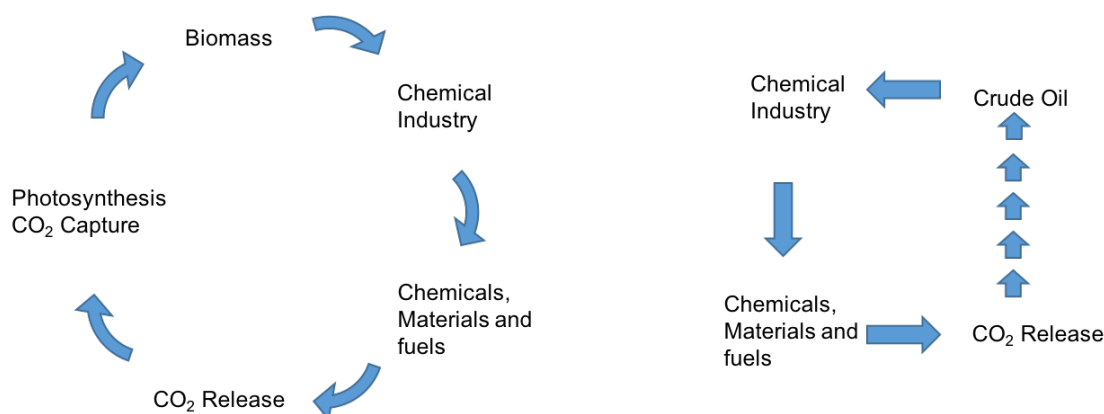


Figure 1.2 – Circular Bio-economy

Utilisation of biomass waste as a feedstock for the chemical, fuel and materials industry also allows for direct re-use back into industry. This fits nicely into the circular economy ideology and shows a ‘cradle to cradle’ approach as opposed to a ‘cradle to grave’ route which represents materials ending up as waste at the end of their life span.^{43,44} A common way of looking at use of biomass in this way is the ‘biorefinery’ concept: replacing conventional oil refinery with a biomass equivalent. This ideology is expanded upon in the next section.

1.1.4 The Biorefinery Concept

Utilisation of waste generally involves increasing its value. This process is known as valorisation which allows for either full or partial re-use, energy recovery or conversion of the waste into more useful products. Valorisation routes for bio-waste are often conducted using the ‘biorefinery’ concept which is comparable to that of a conventional refinery; it is designed to maximise outputs, not only in the procurement of product, but also in energy recovery.^{45–47} Originally designed purely for the procurement of biofuels, biorefineries have expanded to cover a host of different products, ranging from platform chemicals and plastics, to minerals and precious metals (figure 1.3).

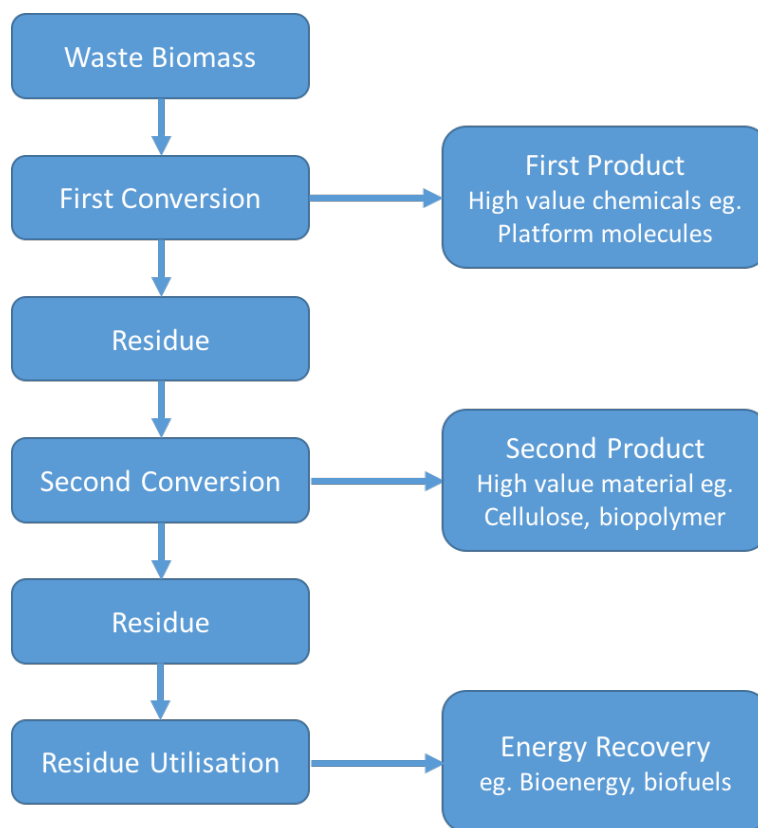


Figure 1.3 – Scheme for a General Biorefinery

While the concept of a biomass based biorefinery appears on the surface a perfect solution to the global reliance on non-renewable feedstocks for chemicals, fuel and energy, it is not without challenges. Issues can arise from using biomass that could potentially be used for food as a feedstock for a biorefinery. The ‘food vs fuel’ debate⁴⁸ is a serious political issue but can be circumvented by using waste biomass only within the biorefinery scheme. Issues also arise from the complexity and heterogeneous nature of a lot of potential biomass feedstocks, maintaining uniformity within a biorefinery and coping with seasonal and production variations within the feedstock is a serious challenge.⁴⁹

The challenges associated with biorefinery implementation has triggered a vast increase in research within this field, with the number of scientific publications relating to biorefineries increasing nearly 800 fold within the last 15 years.⁴⁷ The majority of the research being done into biorefineries focusses on technological innovations to make processing more efficient, cost effective, and robust.

1.1.5 Future Outlook

This coming century will no doubt provide many challenges to overcome, with global population putting stress on the finite global resources, food production and the environment. There is a great opportunity for progressive thinking and research into how to achieve the sustainable development goals set out by the United Nations to ensure a future with enough resources, energy and food for humanity to continue its economic, technological and social growth.

Research into areas surrounding food waste and anthropogenic CO₂ emissions is clearly needed for the realisation of the Sustainable Development Goals, and the development of a truly sustainable future. The work included in this thesis aims to add to the research being done into the field of food waste valorisation and biorefinery development as well as into sequestration of CO₂ from mixed gas streams.

1.2 Aims and Objectives – an Overview

The aim within this body of work was to target two large volume food waste feedstocks and, through a biorefinery approach, valorise to value added products such as essential oils, pectin, cellulose with high water binding capacities, proteins, enzyme inhibitors for diet control and potential CO₂ adsorbers. It was important when designing and implementing the biorefinery schemes that the 12 principles of green chemistry, as well as the Sustainable Development Goals, were taken into account.

1.2.1 Citrus Juicing Waste: from Citrus Oil to Pectin

Citrus waste is a high volume feedstock that causes myriad issues with regards to waste disposal. The aim was to create a microwave-based biorefinery system that adhered to the 12 principles of green chemistry as well as the Sustainable Development Goals, while also maximising products obtained. When designing the biorefinery the following attributes were deemed important.

- i. Use of a renewable resource.
- ii. Allow the extraction of added-value chemical components.
- iii. Reduce energy consumption through avoidance of a drying and/or a pre-treatment stage.
- iv. Avoid the use of acid and/or additives in the process especially for pectin extraction, which currently requires mineral acid and generates significant volumes of acidic waste.
- v. Utilise optimised microwave technology.
- vi. Avoid or limit the use of solvent to food grade solvents only.

The aim was to produce three products through this biorfinery system. First, citrus oil extracted via open vessel microwave-assisted steam distillation, with competitive yield and quality when compared to current industrial extraction methodologies. Second, pectin extracted via acid-free closed-vessel microwave-assisted hydrothermal treatment, with competitive yield and quality along with the improvement to waste treatment

practices through the lack of acid. Third, the residual cellulosic matter remaining after the first two extractions, utilisation of this solid matter would result in zero solid waste resulting from this biorefinery.

Initial scale up of this biorefinery was also an aim within this project, to demonstrate its effectiveness at pilot scale prior to scaling up to industrial scale.

1.2.2 Potato Waste: the Importance of Vegetable Proteins

Potato waste valorisation, especially regarding the protein content, is an area of great potential considering the rapidly increasing demand for vegetable proteins globally. The aim in this body of work was to extract, characterise and purify proteins present within potato waste using green methodologies such as membrane separation.

Special interest was given to the protease inhibitors present within potato protein, due to their documented appetite suppressing effect on mammals.⁵⁰ Purification of these protease inhibitors from crude potato protein extract using chromatographic methods was an aim. Characterisation of the resulting purified protease inhibitor via both crystallisation testing and complexation studies to determine activity regarding its target enzymes was an important aspect of this work.

1.2.3 Carbonaceous Pectin for CO₂ Capture

The pectin extracted from the acid-free microwave-assisted citrus waste biorefinery has potential to be used to create a carbonaceous mesoporous material. The aim was to utilise this material as a potential adsorbent for CO₂ which could be envisaged in a future industrial application such as remediation of CO₂ from flue gas.

Green methodologies should be used for the creation of the material, utilising templating with Tertiary Butyl Alcohol (TBA) and water and drying via lyophilisation to create the adsorbent. The aim was to test the CO₂ adsorption capacity and behaviour of the pectin-based carbonaceous material in comparison to activated carbon and carbonaceous materials that have proven attractive for this application, as well as compare the physical properties of both materials.

Chapter 2

Experimental

All chemicals, reagents and buffers were purchased from Sigma Aldrich unless specified otherwise. A full list of equipment used can be found in the appendix, section A.1.1, where analysis was outsourced to other companies, full details of the company are given.

2.1 Acid-Free Microwave Based Biorefinery Scheme for Orange Waste

2.1.1 Biomass Preparation

Initial extractions were carried out on oranges and other citrus provided by Chingford Fruits (Dartford, UK). They included oranges from both South Africa and Spain (both un-waxed and waxed in the case of Spanish oranges), limes from Mexico and lemons from Italy.

Later extractions were performed using a range of citrus: sweet oranges (*Valencia Late* and *Navel Powell* varieties, grown in Spain), lemons (*Primofiore* variety, grown in Spain), limes (*Tahiti* variety, grown in Brazil), satsumas (*Nihowase* variety, grown in South Africa) and grapefruits (*Star Ruby* variety, grown in South Africa) all of which were purchased from Morrisons (York, UK).

All these citrus samples were juiced using a conventional juicer within 24 h of receiving, the resulting peel/pulp was macerated in a Retsch, GM 300 food processor at 2500 rpm for approximately 5 minutes until rough uniformity was obtained. This macerated sample was frozen at -5 °C until needed.

2.1.2 D-Limonene Extraction

2.1.2.1 Conventional Hydro/Steam-Distillation

For conventional hydro-distillation a Clevenger apparatus was used, extractions were carried out at 100 °C for 240 minutes. The oil was then separated from the aqueous phase by simple liquid separation using a separating funnel. Oil obtained was stored at 5 °C until analysis could be run.

2.1.2.2 Microwave Assisted Steam Distillation

For microwave-assisted steam distillation a Milestone RotoSYNTH microwave was used with a 4 L Pyrex[®] reactor vessel. This vessel was connected to a condenser located outside the microwave to cool the vapour phase created through the microwave process. The condensed liquid was collected in a round bottomed flask with a dual neck, the other neck was connected to another condenser and finally a vacuum pump so the entire system could be run under reduced pressure (figure 2.1).

Different conditions were tested (see section 3.3.1.2), but the general procedure involved placing a total volume of 1.5 L of WOP/water into the reactor vessel and then irradiating the vessel while rotating it to reduce the chance of hot spots. Different irradiation powers, WOP:water ratios, time under irradiation and pressures were tested and the condensate collected and the oil separated as for the conventional hydro-distillation. The oil was once again stored at 5 °C until analysis could be performed.

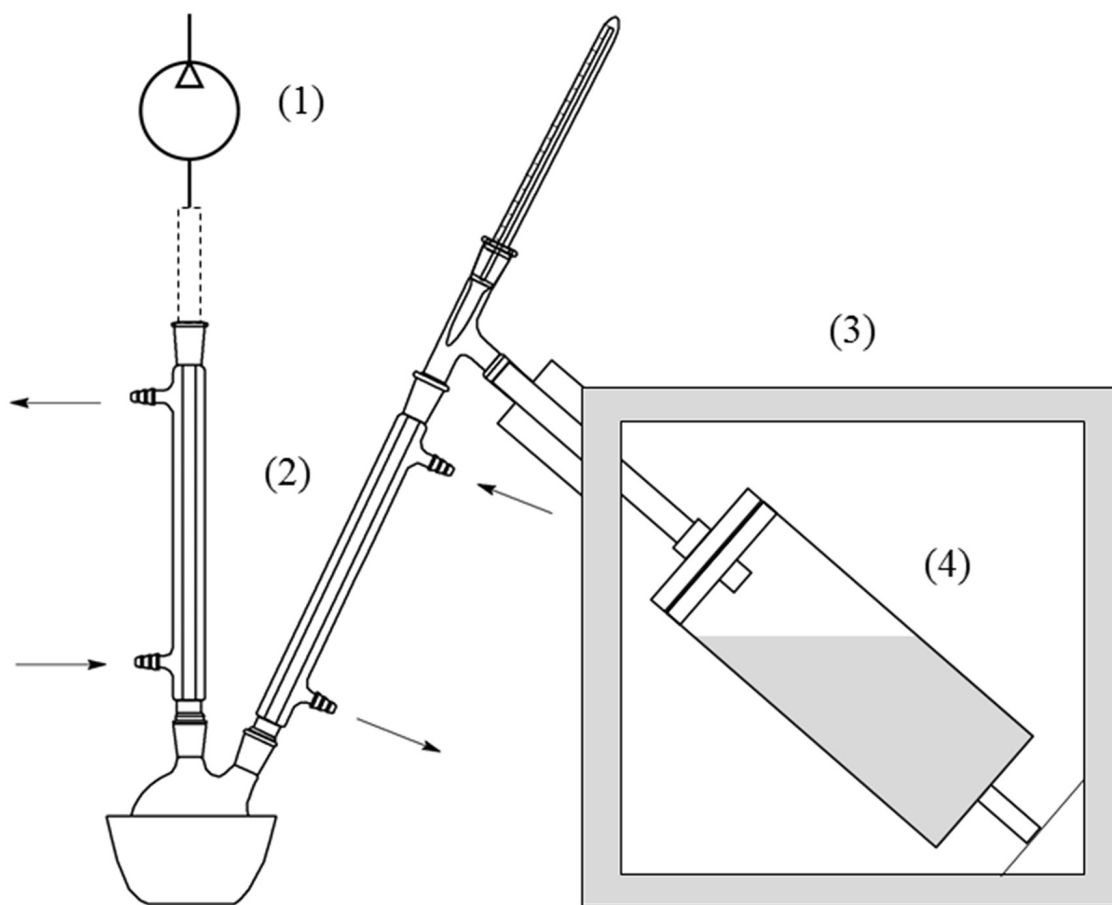


Figure 2.1 – Microwave assisted steam distillation apparatus set-up: (1) vacuum pump; (2) condensers; (3) 45 rotative Milestone RotoSYNTH MW system; (4) MW vessel.⁵¹

2.1.2.3 Optimisation of Citrus Oil Extraction

Design Of Experiment (DOE) experiments for multiple variable testing was performed for the method optimisation focussing on power, pressure, time, ratio of waste citrus peel to water and multiple step extraction. Full details of experiments run can be found in section 3.3.1.2.

2.1.2.4 Characterisation of Citrus Oil

Citrus oil was analysed via GC-TOF using an Agilent 6890 GC coupled with a Pegasus IV TOF mass spectrometer (Leco) full specs can be found in the list of equipment. A 1 μL sample was injected with a 100:1 split ratio, the oven program was isothermal at

40 °C for 2 minutes, then ramped at 5 °C min⁻¹ to 300 °C and held for 2 minutes. Mass spectra were generated at 230 °C and 70 eV. The mass range of data collected was 20-450 m/z and was collected at 20 scans/s. The resulting spectra were analysed using ChromaTof 4.5 software with reference to either standards run through the same system or via spectral matches to the NIST 05 and Wiley 7 libraries.

2.1.3 Pectin Extraction and Characterisation

2.1.3.1 Conventional Acid-Assisted Extraction

Biomass was prepared as described previously and conventional acid hydrolysis was performed based on the methodology given by Kratchanova *et al.*⁵² Orange peel (25 g) was added to de-ionised water (250 mL) and the pH adjusted to 1.5 using 0.5 M aqueous HCl. This mixture was then heated to 80 °C for 1 h. The solid residue was separated using vacuum filtration and stored at 5 °C for further analysis. The aqueous phase containing the dissolved pectin was worked up as described later in this chapter.

2.1.3.2 Acid-Free Microwave-Assisted Extraction

Pectin extractions were performed using the optimised conditions on the CEM Mars 6 closed vessel Microwave, 1800 W, 2.45 GHz using EasyPrep Plus Easy Prep Teflon 100 mL closed vessels on different varieties of oranges from different countries. Waste Orange Peel (WOP) (4 g) was combined with distilled water (70 mL) and a microwave safe stirrer bar in a 100 mL microwave vessels. Six of these vessels were prepared and placed inside the Mars microwave in a symmetric fashion to ensure even energy distribution. These vessels were then heated to 120 °C over 7.5 minutes, then held at that temperature for a further 17.5 minutes, then cooled to room temperature. The solid residue was filtered using a Buchner vacuum filtration system and the pectin worked up as follows.

Ethanol (roughly two volumes) was added to the pectin containing aqueous solution in order to precipitate the pectin. This mixture was stirred for 15 minutes and left to stand overnight to complete the precipitation process. The ensuing pectin was separated using a Thermo Scientific Heraeus Magafuge 40R centrifuge at a speed of 3000 rpm with an acceleration of 9 and deceleration of 3 RCF (Relative Centrifuge Force). The pectin

pellet was suspended in ethanol, re-centrifuged and isolated again. This was performed twice, and the last ethanol re-suspension was performed using hot ethanol and sample was filtered using a sintered glass funnel under vacuum while still hot.

Finally, pectin was dissolved in a minimum amount of water in a appropriately sized round bottomed flask and then freeze dried using a VirTis SP Scientific sentry 2.0 freeze drier held between -105 °C and -110 °C at a vacuum of 27 mT.

2.1.3.3 Characterisation of Pectin

i. ATR-IR

The pectin extracted was analysed via ATR-IR using a Bruker Vertex 70 spectrometer equipped with a Specac Golden gate. Spectra was taken from 4000 cm^{-1} to 600 cm^{-1} at 32 scans, with a spectral resolution of 2 cm^{-1} with a blank window for background.

ii. Degree of Esterification

Degree of Esterification was determined via solid state ^{13}C CPMAS NMR. Spectra were obtained using a 400 MHz Bruker Avance III HD spectrometer equipped with a Bruker 4mm H(F)/X/Y triple-resonance probe and 9.4T Ascend[®] superconducting magnet. Experiments were performed using the conditions given in table 2.1.

Table 2.1 – Solid State CPMAS NMR Conditions

Contact pulse	1 ms linearly ramped
Spinning rate	12000 \pm 2Hz
Recycle Delay	5 s (optimised)
Scans	200-300

Chemical shifts were reported with respect to TMS and were referenced using adamantane 29.5 ppm as an external reference.

The CPMAS ^{13}C NMR spectra allowed the degree of esterification (DE) of the extracted pectin to be determined using the integral ratio $\text{Int}_{\text{OCH}_3}/\text{Int}_{\text{C(O)OR}}$ as

outlined by Synytsya *et al.*⁵³

iii. Galacturonic Acid Content

Pectin (1 g) was accurately weighed and transferred to a beaker containing 100 mL 60% ethanol and 5 mL 37 wt% HCl and stirred for 10 minutes. The mixture was then transferred to a sintered glass funnel and filtered under vacuum. The pectin was washed with HCl-ethanol (6 x 15 mL) followed by 60% ethanol (15 mL volumes) multiple times. A final wash with ethanol (20 mL) was performed and the pectin was dried under high vacuum and stored in a desiccator. Exactly 25% of the resulting mass of pectin (equating to 0.25 g of the unwashed pectin) was transferred into a 250 mL conical flask, moistened with ethanol (2 mL) and then dissolved in distilled water (50 mL). Phenolphthalein (5 drops) were added and this solution was titrated with 0.1 M NaOH. The amount of titre needed was recorded.

To the titrated mixture, exactly 10 mL of 0.5 M aqueous NaOH was added and the solution was shaken vigorously, 10 mL of 0.5 M HCl was then added and the solution shaken until the pink colour disappeared. This solution was again titrated with 0.1 M NaOH until a faint pink colour persisted after vigorous shaking. The amount of titre required was recorded, tests were run in triplicate and the average value reported.

The percentage galacturonic acid was calculated via equation 2.1.⁵⁴

$$\% \text{ Galacturonic Acid} = \frac{(19.41 \times [V_1 + V_2]) \times 1000}{S} \quad (2.1)$$

Where:

V_1 = The first titre volume.

V_2 = The second titre volume.

S = the weight of the washed and dried sample in mg.

iv. Test for Residual Solvents in Pectin

Standard stock solution: 5 g of methanol, ethanol and 2-propanol were accurately weighed out and added to 500 mL of de-ionised water in a 1000 mL volumetric flask

which was then made up to the mark with de-ionised water. This was the standard stock solution used herein.

Internal standard solution: 5 g of 2-butanol was accurately weighed and added to 500 mL of de-ionised water in a 1000 mL volumetric flask and made up to the mark with de-ionised water. This solution was used as the internal standard herein.

Calibration Solution: 2.0 mL of the standard stock solution and 2.0 mL of the internal standard solution were pipetted into a 200 mL volumetric flask and made up to the mark with de-ionised water, 1 g of this solution was then accurately weighed into a head space vial ready for GC analysis.

Test Sample: Pectin (1 g) and sucrose (5 g) were weighed out and added slowly to a 100 mL conical flask containing 95 mL water and 1.0 mL internal standard solution equipped with a magnetic stirrer bar under fast stirring. This flask was stoppered and left under stirring for 2 h until all the pectin and sucrose had been fully dissolved. An aliquot (1 g) of this solution was accurately weighed out into a headspace vial for GC analysis.

Both the sample, the blank and calibration samples were analysed via GC-FID using the conditions shown in table 2.2.

Table 2.2 – GC-FID Conditions for Residual Solvent Analysis

Carrier Gas	Helium
Flow Rate	208 kPa, 5 mL/min

After analysis the percentage residual solvent was calculated using equation 2.2.

$$Residual\ Solvent\ (\%) = \frac{(R_{Sample} \times W_{Standard} \times M_{Standard})}{(R_{Standard} \times W_{Sample} \times M_{Sample} \times 1000)} \times 100 \quad (2.2)$$

Where:

R_{sample} = the relative peak area of the sample

$R_{standard}$ = the relative peak area of the standard

W_{sample} = the weight of sample (g)

W_{standard} = the weight of solvent used for the standard stock solution

M_{sample} = the weight of sample solution used for the GC analysis

M_{standard} = the weight of calibration solution used for the GC analysis

v. Test for Total Insolubles in Pectin

A 70 mm glass fiber filter paper was dried in an oven set at 105 °C for 1 h. This filter paper was then transferred to a desiccator containing silica gel to cool, the filter paper was then weighed accurately and the weight recorded. Pectin (0.5 g) was loaded into a 250 mL beaker and 2-propanol (2.5 mL) was added to disperse the sample. Under magnetic stirring, 0.03 M sodium hydroxide (50 mL) solution containing 0.1% (w/w) ethylene diamine tetra-acetic acid (Na salt) was added after being filtered through filter paper. This solution was stirred for 30 minutes at room temperature before being heated to boiling. The hot solution was then filtered through the pre-weighed filter paper under vacuum, the beaker was rinsed with water (5 x 100 mL) at 50 °C and filtered through the same filter paper. The filter paper was then once again dried at 105 °C for 1h, transferred to a desiccator to cool and accurately weighed. The percentage of total insolubles was calculated using equation 2.3.

$$\text{Total Insolubles (\%)} = \left[\frac{M_2 - M_1}{S} \right] \times 100 \quad (2.3)$$

Where:

M_1 = the weight of the filter paper prior to filtration

M_2 = the weight of the filter paper post filtration

S = the weight of pectin used

vi. Test for Metal Content in Pectin

Elemental analysis of samples was outsourced to Yara UK where analysis was performed on samples via documented In-house method 1.17 using microwave digestion with nitric

acid analysis by Inductively Coupled Plasma Atomic Emission Spectroscopy (ICP-OES) to determine their elemental composition with particular focus on the metal content.

vii. Gelling Tests

Initial gelling tests were outsourced to the Fraunhofer Institute, Germany, the methodology shown below was employed. Subsequent samples were analysed in-house using the methodology titled the ‘University of York Method’.

Fraunhofer Method: The pectin and 50% of the sugar were mixed homogeneously in dry state. This mixture was added to water and stirred at room temperature. Afterwards, the homogeneous solution was heated up to 100 °C. At this point, the remaining (50%) sugar was added while continuous stirring and heating of the solution. The pH of the solution was adjusted to 3-3.5 using a buffer solution. Excess of water was evaporated until the original volume was obtained. Finally, the pectin solution was allowed to cool down to room temperature and stored at 5 °C overnight. The amounts of the reagents used for this test are shown in table 2.3.

Table 2.3 – Reagents for Fraunhofer Gelling Test

Reagent	Amount (%)	Amount (g)
Pectin	1.0	0.5
Sucrose	59	29.5
Water	40	20

University of York Method: The pectin and 50% of the sugar were added to the buffer solution (pH 3-3.5) while continuous stirring and left to dissolve overnight to ensure the homogeneity of the solution. Afterwards, the solution was heated up to its boiling point and, after cooling, the remaining 50% of sugar was added. At this point, the solution was heated again (100 °C) with continuous stirring. After reaching its boiling point, the solution was allowed to cool down to room temperature and stored in the fridge overnight. The amounts of the reagents used for this test are shown in table 2.4.

Table 2.4 – Reagents for University of York Gelling Test

Reagent	Amount (%)	Amount (g)
Pectin	1.0	0.5
Sucrose	60	30
Water	39	19.5

2.1.4 Agroterenas Case Study

2.1.4.1 Biomass Preparation

Both healthy and HLB diseased oranges were juiced by hand using a commercially available juicer, the resulting peel/pulp was macerated using a food processor until rough uniformity was obtained. The bagasse sample was obtained from Agroterenas was already macerated. The samples were re-refrigerated at 5 °C until needed.

2.1.4.2 Pectin Extraction

For pectin extraction orange peel (1 g) was weighed and placed inside a 30 mL Anton Paar microwave vessel along with a microwave safe stirrer bar, and deionised water (17.5 mL). The vessel was placed inside an Anton Paar Monowave 300 Microwave Synthesis Reactor. The conditions used for the extraction are given in table 2.5.

Table 2.5 – Experimental Conditions for Pectin Extraction in Brazil

Ramp Rate	10 °C/min
Holding Temperature	120 °C
Time at Temperature	17.5 minutes

Once the time under irradiation was finished the sample was cooled to room temperature by flowing nitrogen and removed from the microwave. The sample was then filtered to remove the solid residue and the aqueous solution added to an excess of ethanol under

stirring to precipitate the pectin. This sample was stored at 5 °C overnight to complete the precipitation process. The pectin was separated via centrifugation using a Centrifuge eppendorf 5810 R at 7000 rpm with an acceleration of 9 and deceleration of 1 RCF and washed 3 times with ethanol (with further centrifugation between washes) the final step was performed using hot ethanol. The final washed pectin was dissolved in a minimum of water and freeze-dried using a Liofilizador E-C Modulyo freeze drier.

Also, biomass was received from Agrotomas to the UK and pectin extraction was performed as described earlier utilising the MARS microwave in the Green Chemistry Centre of Excellence (GCCE).

2.1.5 Pilot-Scale Study for Pectin Extraction

Scale up of the pectin extraction was carried out using a bespoke large-scale microwave rig, the exact information relating to this rig is confidential and will therefore not be included in this body of work. Once acid-free microwave assisted extraction of pectin had been performed, the slurry of aqueous pectin and residual orange peel was filtered through a muslin cloth to remove most of the solid residue. The liquid fraction was then centrifuged using a Lemitec MD 60 decanter centrifuge with a throughput of 1-30 L/h in-line centrifuge to remove all of the solid matter from the aqueous pectin. The volume of water was then reduced using a Buchi Kilo Suite (ATEX Rated 65 L vessel) pilot scale glass reactor suite to concentrate the sample to allow for less ethanol to be used in the precipitation step. Pectin precipitation and work up was performed as described previously, but scaled up appropriately. A VirTis Genesis 35 EL freeze drier equipped with 5 Shelves (each 273 x 521 mm) was used to dry the pectin.

2.2 Proteins from Potatoes

2.2.1 Potato Fruit Juice Production

Potatoes were chopped into small (roughly 1 inch) pieces and macerated in a Retsch, GM 300 food processor at 2500 rpm for approximately 3 minutes. Sodium metabisulfite was added to the potato fruit juice at this point to prevent browning. The potato fruit juice was centrifuged in a Thermo Scientific Heraeus Megafuge 40R centrifuge at 3000 rpm for 20 minutes to remove the residual starch and fibre from the aqueous fraction. The supernatant was then filtered utilising a Büchner filter under vacuum to obtain a clarified sample.

2.2.2 Protein Purification and Drying

To purify the protein fraction present in the potato fruit juice (PFJ), 250 mL of the PFJ was run through a KrosFlo Research III Tangential Flow Filtration System using a mPES MidiKros filter module. This removed the low molecular weight (<10 kDa) components present in the PFJ. Both the retentate (protein fraction) and the permeate (low molecular weight fraction) were retained for analysis. 200 mL of the retentate was freeze-dried using a VirTis SP Scientific sentry 2.0 freeze drier and the mass of protein recovered was recorded and the yield calculated using equation 2.4:

$$Yield \% = \frac{[(Protein\ mass\ g/200\ ml) \times Total\ PFJ\ ml]}{g\ starting\ raw\ potato} \times 100 \quad (2.4)$$

2.2.3 Protein Analysis

2.2.3.1 SDS-PAGE

Sodium Dodecyl Sulfate-Polyacrylamide Gel Electrophoresis (SDS-PAGE) was performed on a XCell SureLoc Mini-Cell Electrophoresis System using NuPAGE Bis-Tris Mini Gels (Graduated). The samples were prepared by accurately weighing out 10 mg of the dried, purified protein, adding 2.5 μ L of the loading buffer, 100 μ L of the reducing agent and

220 μL deionised water, this was vortexed to ensure mixing and heated at 70 $^{\circ}\text{C}$ for 10 minutes.

Initial runs were performed using varying amounts of the sample created above in the SDS-PAGE gel to determine the optimum protein concentration for analysis, 10 μL , 20 μL , 30 μL , and 40 μL loadings were tested and the order of loadings on the SDS-PAGE gel is shown in figure 2.2, with red representing the protein standards, white a blank lane and the darkness of the colour in the remaining representing the differing loading amounts (darker represents higher loading.)

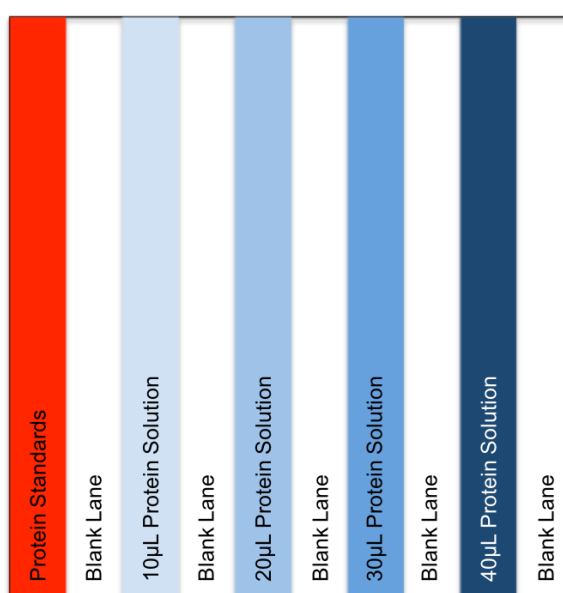


Figure 2.2 – Sample loadings for SDS-PAGE

2.2.3.2 Protein Identification via Proteomics

i. MALDI-TOF/TOF-MS

In-gel tryptic digestion was performed after reduction with DTE and *S*-carbamidomethylation with iodoacetamide. Gel pieces were washed two times with 50% (v:v) aqueous acetonitrile containing 25 mM ammonium bicarbonate, then once with acetonitrile and dried in a vacuum concentrator for 20 min. Sequencing-grade, modified porcine trypsin (Promega) was dissolved in the 50 mM acetic acid supplied by the manufacturer, then diluted 5-fold by adding 25 mM ammonium bicarbonate to give a final trypsin concentration of 0.02 g/L. Gel pieces were rehydrated by adding 10 L of

trypsin solution, and after 5 min enough 25 mM ammonium bicarbonate solution was added to cover the gel pieces. Digests were incubated overnight at 37 °C.

A 1 L aliquot of each peptide mixture was applied directly to the ground steel MALDI target plate, followed immediately by an equal volume of a freshly-prepared 5 mg/mL solution of 4-hydrox- α -cyano-cinnamic acid (Sigma) in 50% aqueous (v:v) acetonitrile containing 0.1% trifluoroacetic acid (v:v).

Positive-ion MALDI mass spectra were obtained using a Bruker ultraflex III in reflectron mode, equipped with a Nd:YAG smart beam laser. MS spectra were acquired over a mass range of m/z 800-5000. Final mass spectra were externally calibrated against an adjacent spot containing 6 peptides (des-Arg1-Bradykinin, 904.681; Angiotensin I, 1296.685; Glu1-Fibrinopeptide B, 1750.677; ACTH (1-17 clip), 2093.086; ACTH (18-39 clip), 2465.198; ACTH (7-38 clip), 3657.929.). Monoisotopic masses were obtained using a SNAP averagine algorithm (C 4.9384, N 1.3577, O 1.4773, S 0.0417, H 7.7583) and a S/N threshold of 2.

For each spot the ten strongest peaks of interest, with a S/N greater than 30, were selected for MS/MS fragmentation. Fragmentation was performed in LIFT mode without the introduction of a collision gas. The default calibration was used for MS/MS spectra, which were baseline-subtracted and smoothed (Savitsky-Golay, width 0.15 m/z , cycles 4); monoisotopic peak detection used a SNAP averagine algorithm (C 4.9384, N 1.3577, O 1.4773, S 0.0417, H 7.7583) with a minimum S/N of 6. Bruker flexAnalysis software (version 3.3) was used to perform the spectral processing and peak list generation for both the MS and MS/MS spectra.

Tandem-mass spectral data were submitted to database searching using a locally-running copy of the Mascot program (Matrix Science Ltd., version 2.1), through the Bruker BioTools interface (version 3.2). Search criteria included: Enzyme, Trypsin; Fixed modifications, Carbamidomethyl (C); Variable modifications, Oxidation (M); Peptide tolerance, 100 ppm; MS/MS tolerance, 0.5 Da; Instrument, MALDI-TOF-TOF (The version and size of the database can be obtained from the Mascot result page.).

ii. LC-MS/MS

In-gel Digestion: Two size exclusion derived samples and a 1:1:1 equivalent mixture of protease inhibitor, trypsin and chymotrypsin were diluted into NuPAGE LDS sample buffer (Life Technologies) before heating at 70 °C for 10 mins. Denatured samples were run into a 7 cm NuPAGE Novex 10% Bis-Tris gel (Life Technologies) at 200 V for 6 mins. Gels were stained with SafeBLUE protein stain (NBS Biologicals) for a minimum of 1 h before destaining with ultrapure water for a minimum of 1 h. Coomassie stained gel segments were split for parallel in-gel digestion with trypsin and Asp-N endoproteases, which was performed after reduction with DTE and *S*-carbamidomethylation with iodoacetamide. Gel pieces were washed two times with 50% (v:v) aqueous acetonitrile containing aqueous 25 mM ammonium bicarbonate, then once with acetonitrile before drying in a vacuum concentrator for 20 min. A 0.2 μ g aliquot of sequencing grade modified porcine trypsin (Promega) or metallo-endoprotease Asp-N (Sigma) was added before incubation at 37 °C for a further 24 h.

Analysis: Peptide mixture was loaded onto a nanoAcquity UPLC system (Waters) equipped with a nanoAcquity Symmetry C18, 5 μ m trap (180 μ m x 20 mm Waters) and a nanoAcquity HSS T3 1.8 μ m C18 capillary column (75 m x 250 mm, Waters). The trap wash solvent was 0.1% (v/v) aqueous formic acid and the trapping flow rate was 10 μ L/min. The trap was washed for 5 min before switching flow to the capillary column. Separation used a gradient elution of two solvents (solvent A: aqueous 0.1% (v/v) formic acid; solvent B: acetonitrile containing 0.1% (v/v) formic acid). The capillary column flow rate was 350 nL/min and the column temperature was 60 °C. The gradient profile was linear 2-35% B over 20 mins. All runs then proceeded to wash with 95% solvent B for 2.5 min. The column was returned to initial conditions and re-equilibrated for 25 min before subsequent injections.

The nanoLC system was interfaced with a maXis HD LC-MS/MS system (Bruker Daltonics) with CaptiveSpray ionisation source (Bruker Daltonics). Positive ESI-MS and MS/MS spectra were acquired using AutoMSMS mode. Instrument control, data acquisition and processing were performed using Compass 1.7 software (microTOF

control, Hystar and DataAnalysis, Bruker Daltonics). Instrument settings were: ion spray voltage: 1,450 V, dry gas: 3 L/min, dry gas temperature 150 °C, ion acquisition range: m/z 150-2,000, MS spectra rate: 5 Hz, MS/MS spectra rate: 5 Hz at 2,500 cts to 25 Hz at 250,000 cts, cycle time: 1 s, quadrupole low mass: 300 m/z, collision RF: 1,400 Vpp, transfer time 120 ms. The collision energy and isolation width settings were automatically calculated using the AutoMSMS fragmentation table, absolute threshold 200 counts, preferred charge states: 2 – 4, singly charged ions excluded. A single MS/MS spectrum was acquired for each precursor and former target ions were excluded for 0.8 min unless the precursor intensity increased fourfold.

Data Processing: Tandem-mass spectra derived from trypsin digested samples were searched against an in-house database (1,022 sequences; 397,544 residues) containing trypsin, chymotrypsin, Asp-N and serine protease inhibitor sequences. Searches were submitted to a locally-running copy of the Mascot program (Matrix Science Ltd., version 2.5.1), through the Bruker ProteinScape interface (version 2.1). Search criteria specified: Enzyme, Trypsin; Fixed modifications, Carbamidomethyl (C); Variable modifications, Oxidation (M); Peptide tolerance, 10 ppm; MS/MS tolerance, 0.1 Da; Instrument, ESI-QUAD-TOF. Results were filtered to accept only peptides with an expect score of 0.05 or lower. LC-MS/MS chromatograms from Asp-N digested samples in Bruker .d format were imported into Progenesis QI and LC-MS runs aligned. Precursor ion intensities were normalised against total intensity for each acquisition. A combined peak list was exported in .mgf format for database searching against the unrestricted UniProt database (554,860 sequences; 198,649,153 residues) concatenated with serine protease inhibitor sequences. Mascot Daemon (version 2.5.1, Matrix Science) was used to submit the search to a locally-running copy of the Mascot program (Matrix Science Ltd., version 2.5.1). Search criteria specified: Enzyme, none; Fixed modifications, Carbamidomethyl (C); Variable modifications, Oxidation (M); Peptide tolerance, 30 ppm; MS/MS tolerance, 0.1 Da; Instrument, ESI-QUAD-TOF. Search results were filtered to require a minimum expect score of 0.05. The Mascot .XML result file was imported into Progenesis QI and peptide identifications associated with precursor peak areas. Relative quantification was performed using the Top3 approach, taking the normalised intensity for the three most responsive peptides from each identified protein and comparing these intensities between the size exclusion fractions and the pooled standard.

2.2.4 Protein Purification

Protein purification was performed on a GE Healthcare Life Sciences ÄKTA Pure M25 Equipped with a multiple wavelength UV detector, conductivity monitoring and pH monitoring. Protein was loaded onto either a GE Healthcare Life Sciences HiTrap Q HP sepharose FastFlow anion exchange column, a Mono-Q 5/50 GL anion exchange column or a Sephadex S-75 size exclusion column. For anion exchange columns the starting buffer was 30 mMol Tris base at pH 7.8 and through a linear salt gradient the ending buffer was 30 mMol Tris base at pH 7.8 with 1 M NaCl. The concentration of NaCl was taken from 0% to 70% over 15 column volumes and then held at 100% for 10 column volumes to make sure all protein was eluted from the column. Fractions were collected using a 96-well plate. Size exclusion columns were run with a 30 mMol Tris base buffer at pH 7.8 and the fractions, once again, collected using a 96-well plate. All buffers were made using analytical grade chemicals purchased from Sigma Aldrich.

2.2.5 Crystallisation

2.2.5.1 Sitting Drop Method

Sitting drop crystallisation screens were conducted using a TTP Labtech Mosquito Crystal liquid handling robot in conjunction with a Hydra II 96-well dispensing robot. All screen conditions were obtained from either Hampton Research or Molecular Dimensions, full detail on the screens used can be found in the appendix tables A.12-A.33. Once set up, a protective film was applied to ensure a sealed environment was achieved for crystallisation studies. Crystal growth was observed manually using an optical microscope equipped with a polarising lens filter.

2.2.5.2 Hanging Drop Method

Hanging drop optimisation screens were performed manually using 24-well plates. The appropriate reservoir conditions were made using analytical grade chemicals purchased from Sigma Aldrich and 0.5 mL of each was transferred into the appropriate reservoir in the crystal tray. Glass slides were first cleaned thoroughly and then the protein

was spotted onto the slide using a Gilson pipette (the volume depended on the crystal conditions being tested), then an amount of reservoir solution was also spotted onto the protein on the slide with a Gilson pipette. The slide was then flipped and placed onto the corresponding well in the crystal tray. The wells were greased prior to affixing the slide to ensure a good seal was obtained. Once all the slides had been affixed to the crystal tray, manual observation of the seal was conducted using an optical microscope to ensure that each hanging drop well was entirely sealed. Crystal growth was once again observed manually using an optical microscope with a polarising lens filter.

2.2.6 Preliminary Trypsin Inhibition Assay for Protease Inhibitors

Trypsin inhibition was measured fluorometrically using Boc-Gln-Ala-Arg-7-amido-4-methylcoumarin hydrochloride based on the work done by Kawabata et al.⁵⁵ Different samples were prepared containing either just 0.2 mM Boc-Gln-Ala-Arg-7-amido-4-methylcoumarin hydrochloride, this substrate plus 10 nM bovine trypsin, or the substrate, trypsin and protease inhibitor ranging from 200 nM to 5 nM. These samples were left to incubate for 1 h and there were analysed visually using an excitation of 380 nm.

2.3 Pecbons - a Carbonaceous Material for CO₂ Capture

2.3.1 Pecbon Synthesis

Pecbon was produced from the acid-free microwave-assisted extracted pectin using the conditions and methodology reported by Dr. Aleksandra Borisova,⁵⁶ as shown in table 2.6.

Table 2.6 – Reagents used for Pecbon Production

Solvent Ratio (H ₂ O:TBA)	Pectin: Solvent Ratio	Pectin (g)
75:25 by wt	1:10 by wt	0.5

Ten separate samples were made up according to the conditions given above and after dissolving the pectin in the solvent mixture (with the aid of sonication) the samples were placed in 100 mL round bottomed flasks and freeze dried under the same conditions as for standard pectin drying.

2.3.1.1 Carbonisation

Carbonisation of the dried Pecbon was performed based on the work of Dr. Aleksandra Borisova using a Barnstead Thermolyne 6000 furnace, under an inert atmosphere using the conditions given in table 2.7, for Pecbons carbonised at different temperatures, the same procedure is followed but only up to the target temperature.

Table 2.7 – Pecbon Carbonisation Parameters

Temperature (°C)	Ramp Rate (°C/min)	Hold Time (h)
Room Temperature	–	–
100	5.0	1
210	0.3	1
400	0.3	–
600	1.0	–
800	3.0	–

2.3.1.2 N₂ adsorption/desorption porosimetry

Nitrogen-physisorption adsorption measurements were carried out at 77 K using a Micromeritics ASAP 2020 volumetric adsorption analyser. Prior to measurements the powdered samples (0.1g) were degassed under vacuum at 110 °C for 6 h. Analysis of pore distribution has been done by standard procedures.^{57–59} The Brunauer, Emmet and Teller (BET) adsorption isotherm equation was used to determine surface area, the Barret-Joyner-Halenda (BJH) equation was used to determine the volume of mesopores and pore-size distribution, and the t-plot was used for evaluation of micropore volumes of the carbonaceous materials.

2.3.1.3 CO₂/N₂ Porosimetry

The adsorption isotherms of N₂ and CO₂ at a temperature of 308 K and gas pressure up to 100 kPa were measured volumetrically by using a Micromeritics ASAP 2020 volumetric adsorption analyser. Temperatures were achieved by the supplied tube oven. Before analysis, powdered samples (roughly 0.1 g) were degassed under vacuum at 120 °C for 4h. Helium gas was used to determine the free space of the system. The degassing procedure under vacuum was repeated on the same sample between measurements. Ultrahigh purity grade N₂, CO₂ and He was purchased from BOC and used as received.

2.3.1.4 CO₂ Pressure Swing

To explore the CO₂ capacity of the materials, a pressure/vacuum swing adsorption/desorption cycle was set up. This also allowed the reversibility of adsorption to be explored. Powdered samples (roughly 0.1g) were degassed using a Micromeritics ASAP 2020 volumetric adsorption analyser at 110 °C for 16 h to ensure the complete removal of residual solvent and water. The samples were cooled to room temperature while still under vacuum. The samples were then weighed and transferred to sample vials fitted with caps, the vial, cap and sample were weighed accurately under air. A needle was inserted through the cap and the vial was placed in a pressure reactor and pressurised to 10 bar with CO₂ for 30 minutes to ensure sample saturation. The pressure vessel was opened and the needle removed before the vial was once again accurately weighed. The sample was then held under vacuum until the original weight was again obtained. The mass of the CO₂-saturated and CO₂-free materials were obtained for each of 5 cycles and used to calculate the mmols of CO₂ adsorbed per gram of sample. Prior to analysis the empty vials, caps and needle were run under the same conditions without sample to take into account the difference in weight attributed by CO₂ adsorption onto the cap/needle and the difference in weight associated with filling the vial with CO₂ as opposed to air. The weight increase observed for the empty vials were subtracted from the results obtained using the samples.

2.3.1.5 CO₂ Enthalpy Measurements

The CO₂ adsorption behaviour of samples was explored using a Stanton Redcroft STA 780 thermal analyser, using alumina crucibles. 5.0 mg of sample was loaded into the alumina crucible and placed inside the analyser. The heat was ramped to 373 K at 10 K min⁻¹ and held for 1 h under flowing N₂ gas (60 mL min⁻¹) to ensure removal of residual water in the sample. Once cool, the heat was ramped to 308 K at a rate of 1 °C min⁻¹ under flowing N₂ gas (60 mL min⁻¹). A three-way valve was employed to allow the flowing gas to be swapped from N₂ to CO₂ and the mass of CO₂ adsorbed and the associated heats of adsorption were determined by differential scanning calorimetry (DSC) under these conditions. For moisture-loaded experiments the same procedure was followed but gaseous water was introduced into the CO₂ stream via heated gas syringe.

Chapter 3

Acid-Free Microwave Biorefinery Scheme for Citrus Waste

1. Matharu, A. S.; Houghton, J. A.; Lucas-Torres, C.; Moreno, A. *Green. Chem.* **2016**, *18*, 5280–5287.
2. Bustamante, J.; van Stempvoort, S.; Garcia-Gallarreta, M.; Houghton, J. A.; Briers, H. K.; Budarin, V. L.; Matharu, A. S.; Clark, J. H. *J. Clean. Prod.* **2016**, *137*, 598–605.

3.1 Introduction

3.1.1 Oranges

Oranges (sweet orange – *Citrus sinensis*) are believed to have originated in Southeast Asia. Orange trees reach fruit bearing age after 3 years and full production at 10-12 years.⁶⁰ Citrus fruit (including sweet orange) is generally separated into two sections: peel and flesh (figure 3.1). The peel further comprises of flavedo and albedo. The flavedo (otherwise known as the exocarp - 10% (w/w) of the whole fruit) describes the outermost layer of the fruit which contains cellulose, oil glands and pigments, and the albedo (25%) which is the innermost layer of the peel and is generally rich in pectin.^{61,62}

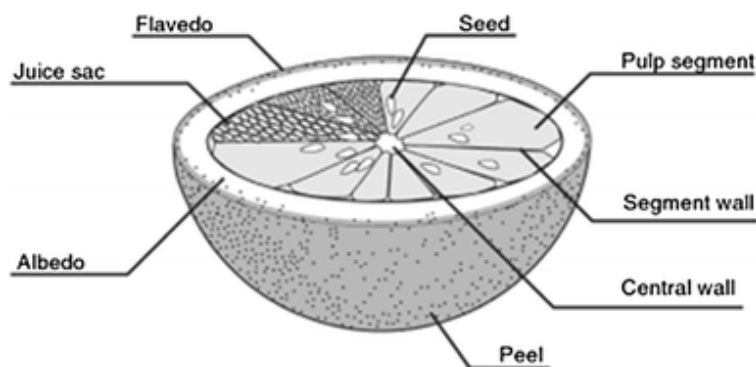


Figure 3.1 – General structure of orange

3.1.2 Citrus Production and Waste

Global citrus production reached roughly 140 million tonnes in 2014 (the top ranked among global fruit crops) with sweet oranges representing 61.1% of this value (86 million tonnes).⁶¹ As shown in figure 3.2, global orange production has increased by 22% in the last 20 years and is continuing to rise.⁶³

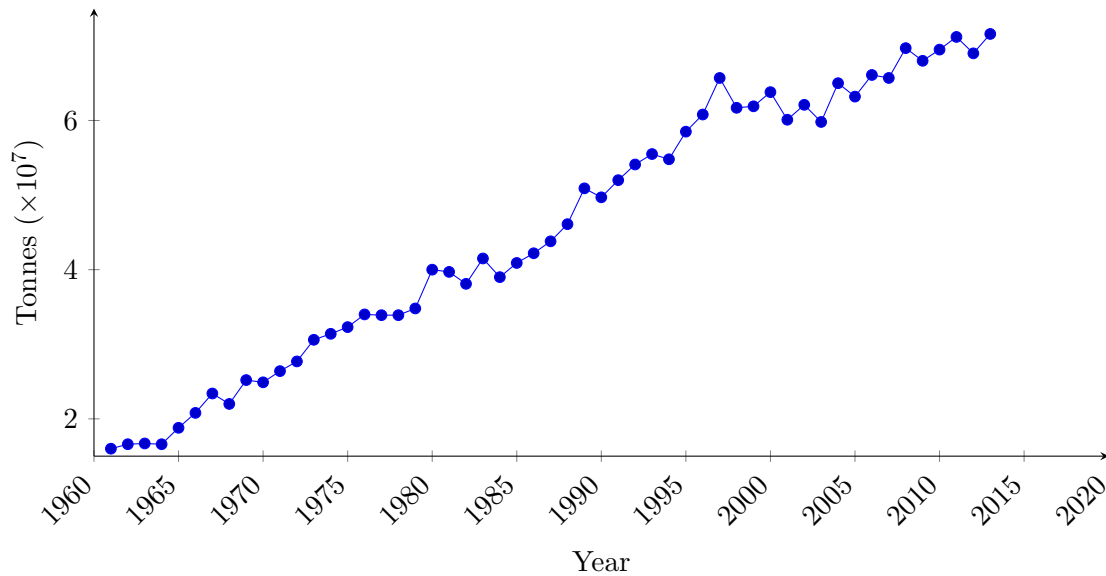


Figure 3.2 – Global Sweet Orange Production from 1961-2013⁶³

Oranges are commonly either eaten fresh or used to produce orange juice, with approximately 40-60% of oranges being used for the latter. Although orange juice production has decreased in recent years, from just over 2.1 million tonnes in 2013-2014 to just under 1.8 million tonnes in 2014-2015,⁶⁴ this still represents a huge amount of waste being generated because roughly 50-60% of the orange, by weight, is wasted during the juicing process.⁶⁵ This amounts to roughly 0.9 million tonnes of orange waste being produced within 2014-2015 from fresh juice production alone (not counting production of juice concentrate which represents another large contributor of orange waste). The waste produced from the production of orange juice consists of roughly 60-65% w/w peel and 30-35% w/w of internal tissue or pulp and 0-10% seeds.⁶⁶

Orange waste poses a real problem, not only due to its volume but also due a highly fermentable carbohydrate content; this can cause issues with accelerated degradation as well as uncontrolled methane production if the citrus waste is simply left to decompose back into the soil.⁶⁷ The only other common use for citrus waste is cattle feed, which poses its own challenges: feedstock must be dried to <10% water content, which is a costly process, and the resulting feed has only 6% protein. This low nutrition content along with its bitter taste, limits the amount of citrus waste that can be incorporated into cattle feed.⁶⁸ Incineration is another option, but this produces greenhouse gases and is therefore not ideal.⁶¹ Modern methods such as biogas production have been suggested for utilising citrus waste, but again, the properties of the waste provides problems, this

time the D-limonene content.⁶⁹ D-limonene is a potent anti-microbial agent⁷⁰ and so the use of microbes for production of biogas is hindered by the large concentration of limonene (90% of orange essential oil as 2-3% of dry matter of the orange),⁶⁵ to allow for biogas production, the limonene content has to be reduced to 0.05% at which point it is no longer toxic to the microbes, this involves a pre-treatment step which can be very costly.^{71,72}

It is clear that the vast global production of oranges and the associated waste disposal problems make this feedstock extremely attractive for valorisation in a biorefinery, not only eliminating the waste but recovering valuable chemicals and materials.

3.1.3 D-Limonene and Essential Oil

Citrus essential oils are usually found within the flavedo, or exocarp, of the fruit. They are primarily volatile compounds, (85-99%) with the majority of these being monoterpenes and sesquiterpenes. By far the most abundant of these is D-limonene. The D-limonene content of sweet oranges varies depending on season, variety and source location, but is usually in the range of 68-98% w/w of the essential oils present in the fruit. In orange peel waste, the essential oil content is roughly 0.5% by wet weight, the majority of this is D-limonene.⁷³

Limonene is a cyclic monoterpene that is produced by citrus as an anti-microbial to protect the outermost layer of the fruit. Limonene exists as D- and L-stereoisomers with D- being the prevalent isomer in oranges. It has been shown that D-limonene is toxic to *Saccharomyces cerevisiae* in any concentration above 0.025%.⁷⁴ Limonene is highly lipophilic with very low solubility in water (0.101 mM at 25 °C).

Extraction of D-limonene is a common valorisation route for citrus waste that is already commercially implemented, as shown later in the Agrotrenas case study (section 3.3.5). Limonene is most commonly used in the cosmetics and food industries, which value its fragrance and antioxidant properties respectively.⁷⁵ More recent research on limonene focuses on its apolar solvent properties,⁷⁶ exploring its use as a bio-derived green solvent for research and manufacture.⁷⁷ Limonene also shows promise as an insecticide, which could help reduce reliance on synthetic pesticides that are often damaging to human health.⁷⁸

3.1.3.1 Extraction Methodologies for Essential Oils

There are a host of different methodologies for extracting lipophilic components from biomass. A selection is now reviewed.

i. Soxhlet

Soxhlet extraction is one of the most well-known and commonly used solid-liquid extraction techniques. Soxhlet extraction comprises a vessel containing solvent which is heated to boiling allowing the gaseous solvent to rise up a condenser where it is condensed and collected in a thimble containing the biomass to be extracted. Once filled a siphon mechanism empties the thimble back into the solvent reservoir, this process can be repeated as many times as is necessary. This technique works well for extraction of citrus essential oil, using lipophilic solvents such as hexane⁶⁵ to selectively extract the apolar terpenes from citrus peel waste. Hexane is a good extraction solvent – its low boiling point of 69 °C reduces energy use, and it has a high affinity for apolar compounds. However, residual hexane can create issues when the limonene is to be used in the food industry. Hexane is on the SIN list⁷⁹ as a Substance of Very High Concern (SVHC) under the criteria set up by REACH⁸⁰ (Regulation, Evaluation and Authorisation of CHEMicals). The maximum allowed value for hexane in components destined for the food industry is 5-30 mg/kg.⁶⁶ So limonene destined for food applications would require a stringent method of removing residual hexane from limonene.

ii. Hydrodistillation and Steam-Distillation

Hydrodistillation relies on the principle that the boiling point of a mixture of immiscible liquids is lower than the boiling point of each liquid on its own. This phenomenon is due to the vapor pressure of the mixture affecting the temperature of evaporation. Boiling occurs when the vapor pressure of the liquid is equal to the pressure above the liquid. For a mixture of immiscible liquids being agitated – exposing both liquids to the gas phase of the vessel – the total vapor pressure is equal to the sum of the individual vapor pressures of the components.

The change in individual vapor pressure upon heating can be found using the Clausius-Clapeyron Equation (equation 3.1).

$$\ln \frac{P_2}{P_1} = \frac{\Delta H_{vap}}{R} \left(\frac{1}{T_1} - \frac{1}{T_2} \right) \quad (3.1)$$

Steam distillation exposes cell membranes in biomass to hot water vapor, pressurising and then bursting them. Essential oil within is released and carried by the water vapor. The vapor penetrates better into the cellulosic matrix than its liquid counterpart due to the intrinsically lower viscosity of vapors, allowing more efficient extraction of the essential oil. However, this method requires long extraction times at high temperatures, which is expensive and can destroy thermally labile components within the extracted oil.⁸¹

iii. Supercritical CO₂ Extraction

One of the most common modern methods for extracting non-polar, thermally labile compounds from biomass is via supercritical fluids. When holding a solvent above its critical point in both temperature and pressure, the solvent exhibits the diffusivity of a gas while retaining the high solvent loading of a liquid, allowing for increased mass transfer and rate of extraction.⁸² CO₂ is the most commonly used solvent as it has a relatively low critical temperature (31.2 °C) and pressure (72.9 bar),⁸³ it is both chemically and physically inert, is low cost and is easy to remove from both residual biomass and products by simply reducing the pressure to revert it to its gaseous state.⁸⁴

This technique is not without drawbacks, however. The solvent itself might be cheap, but the equipment needed to perform supercritical fluid extraction is costly, as is the energy to maintain the pressures necessary to perform the extraction.⁸¹ The efficacy of extraction is also affected by the water content of the sample, with a water content above 23% reducing extraction efficiency.⁸⁵ The high water content of biomass necessitates a costly drying step to facilitate efficient supercritical extraction.

iv. Microwave-Assisted Extraction

Microwaves offer many advantages over conventional methods for biomass extraction

including: more uniform heating, drastically lower extraction temperatures and times, and more controllable heat transfer.^{86,87} Because microwaves heat the water within the sample, there is no need for a drying step in the extraction process; in fact, the native water aids in the extraction. Similar to steam distillation, the microwaves increase internal pressure and burst the cell membranes of the citrus peel waste, allowing for more efficient mass transfer of the limonene, and hence, higher yields. Combining microwave power with steam-distillation retains all the benefits of microwave extraction – lower extraction times and temperatures, reduced energy usage, and higher extraction yield⁵¹ – while allowing easy separation of the essential oil from the collected solvent after hydrodistillation.⁸⁸ An example apparatus showing the combination of these techniques is shown in figure 3.3.

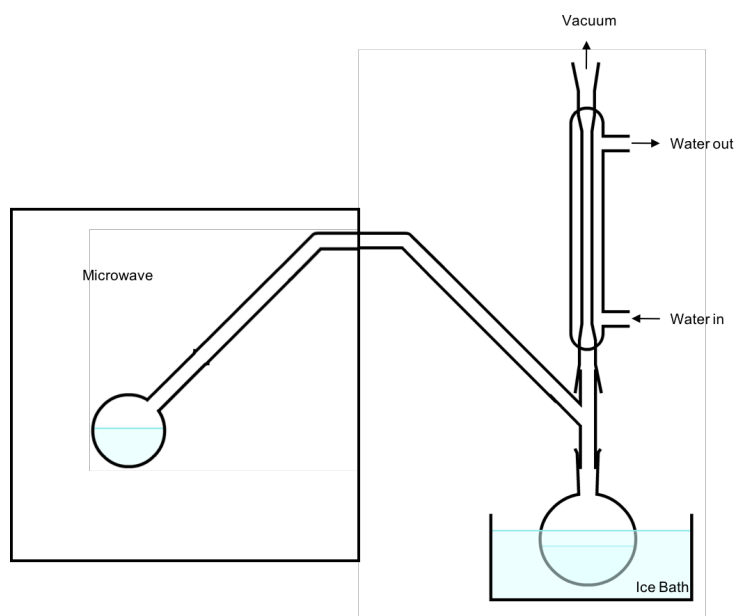


Figure 3.3 – Example setup for combined microwave-assisted extraction and hydrodistillation

3.1.4 Pectin: Structure, Market Analysis and Extraction

Pectin extraction is a common valorisation method for fruit waste,^{89–91} because pectin is usually present in high concentrations. Pectin has many applications in food, cosmetics and pharma industries.⁹²

3.1.4.1 Pectin Structure

Pectins are complex polysaccharides present in non-woody biomass, mainly in the primary cell wall and intercellular regions.⁹³ They are composed of a α -(1-4)-D-galacturonic acid polymer chain which, when unbranched, is known as homogalacturonan (HG), or the ‘smooth region’, and a ‘hairy’ region which is comprised of branched neutral sugar chains (figure 3.4 and 3.5).

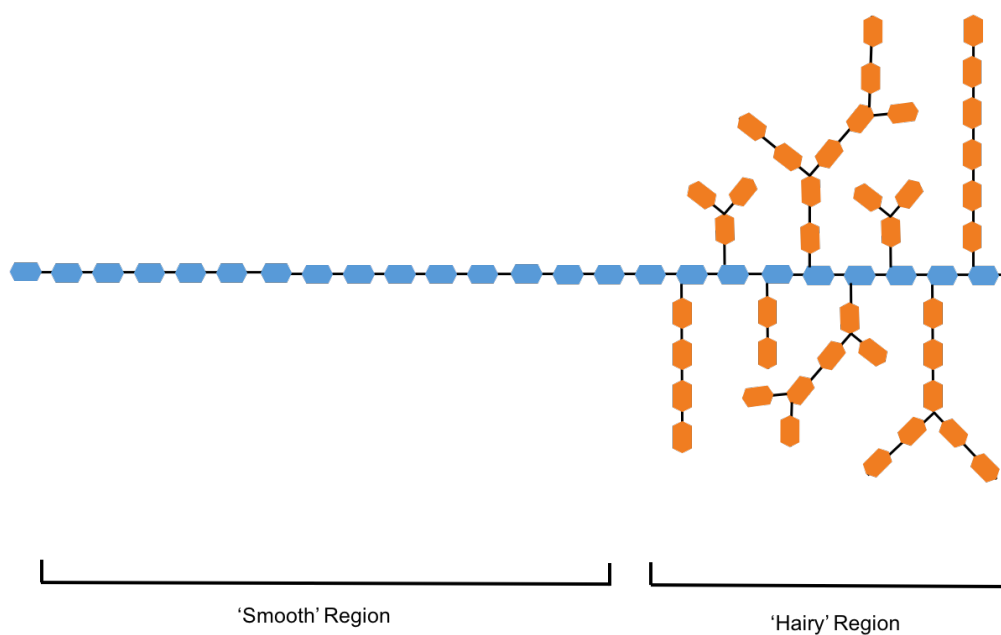


Figure 3.4 – General Structure of Pectin⁹⁴

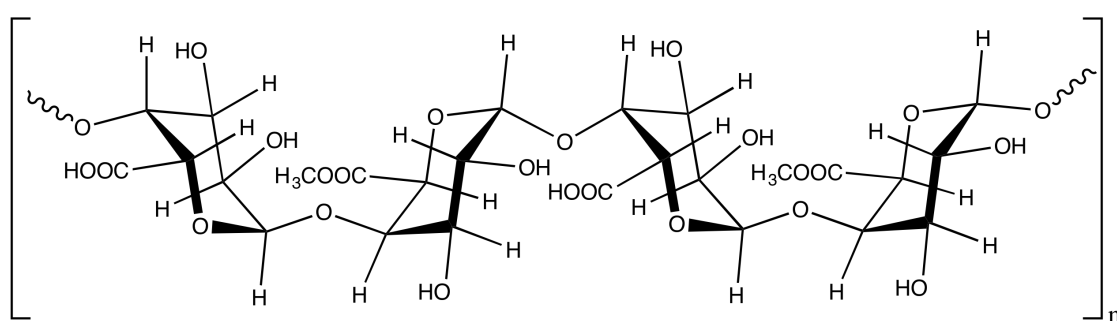


Figure 3.5 – General Structure for the Smooth Region of Pectin

3.1.4.2 Pectin Market Analysis

The pectin industry has been showing steady growth over the last 5 years, with 52000 MT sold in 2011 increasing to 61000 MT in 2016 (figure 3.6), an increase of nearly 17% over 5 years. Revenue from pectin sales rose from \$700 M in 2011 to \$1100 M in 2016, representing a 54% increase.⁹⁵

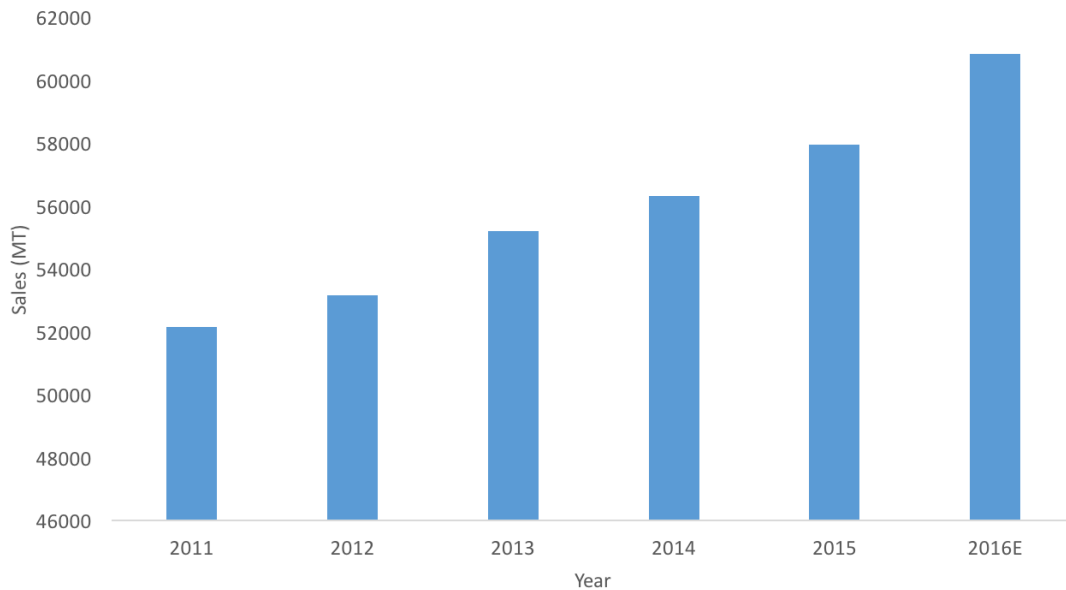


Figure 3.6 – Global Pectin Sales in MT from 2011-2016(Estimated)

Europe is the largest seller of pectin, with roughly 40% of pectin sales occurring within this region. North America and Asia are both large sellers with 23% and 22% of the market, respectively (figure 3.7). Interestingly, South America, which is one of the global leaders in production of citrus, the main feedstock for pectin, has a relatively low global pectin sale proportion — with only 11% of global pectin sales occur within this region. This could either mean that there is a lot of under-utilised citrus feedstock within this region, or that the pectin is either produced or sold overseas.

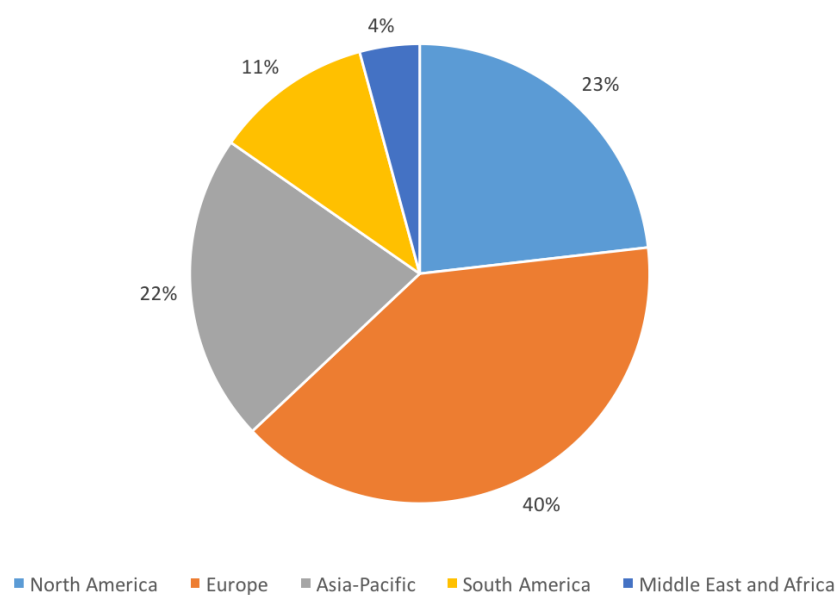


Figure 3.7 – Global Pectin Sales by Region (2015)

The growth of the pectin market shows no sign of slowing down; in fact, it seems to be increasing. This is going to put strain on current industrial producers of pectin, requiring additional feedstocks and more efficient extraction methodologies. Waste disposal issues will become even more of an issue.

Pectin can be segregated into three classes depending on its degree of esterification and amidation (figure 3.8).

High Methoxyl Pectin (Degree of Esterification (DE) >50%): Pectin with a high degree of esterification is termed ‘High Methoxyl’ (HM) with more than 50% of the carboxyl groups in the methyl ester state rather than the free carboxylic acid.

Low Methoxyl Pectin (DE <50%): Pectin with a low degree of esterification is termed ‘low methoxyl’ (LM) with less than 50% of the carboxyl groups in the methyl ester state rather than the free carboxylic acid.

Low Methoxyl-Amidated Pectin (LMA): Pectin that has been treated with ammonia to produce a product with less than 50% methoxyl groups and between 5 and 25% amidated groups.

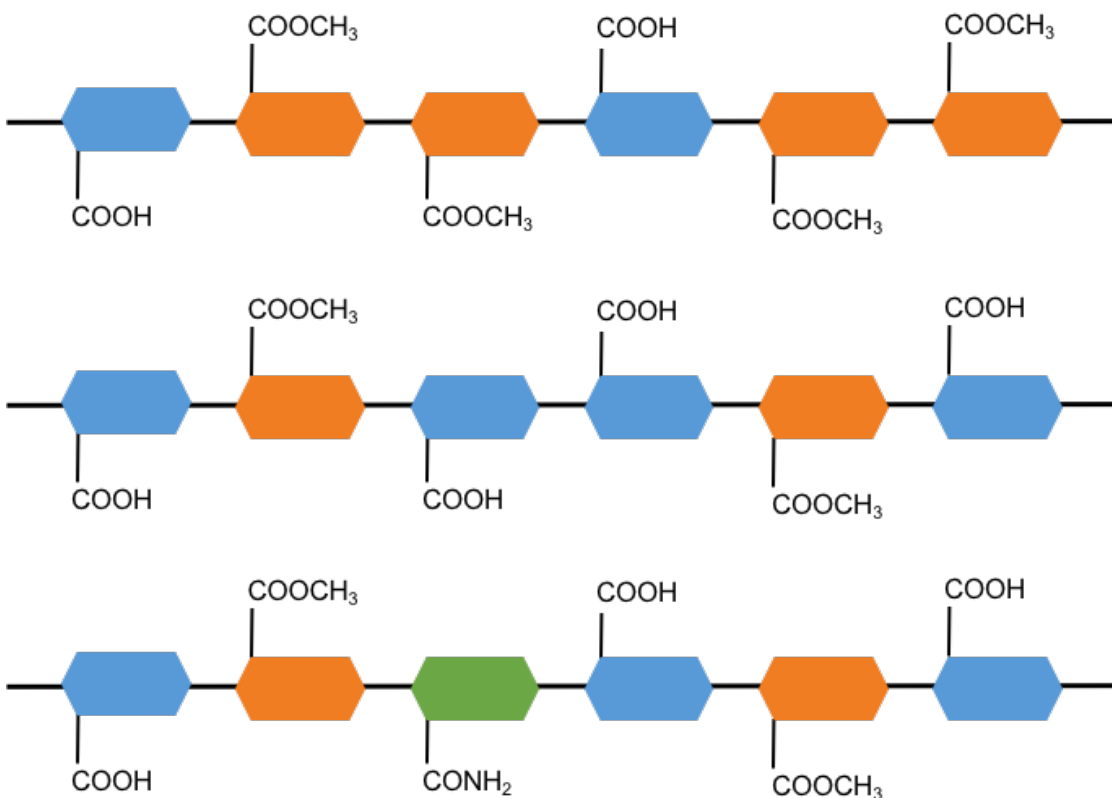


Figure 3.8 – Simplistic Representation of Different Pectin Types. Top: HM Pectin, Middle: LM Pectin, Bottom: LMA Pectin

HM pectin is by far the most common, with 77.14% of the market in this kind of pectin (figure 3.9). This is mainly due to its extensive use within the food industry. The high degree of esterification lends itself to use as a gelling agent due to rapid gelation. LM pectin and LMA pectin have much lower market shares (16.17% and 6.69%, respectively). They are used for low-volume applications within the cosmetic, food and pharmaceutical industries, lowering demand for bulk material.

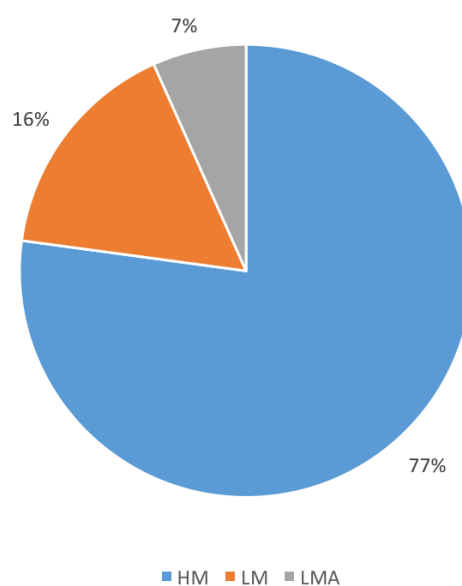


Figure 3.9 – Proportion of Different Classes of Pectin Produced

Sales of the different classes of pectin have all seen an increase in the last 5 years, with high methoxyl pectin showing a 13% increase in sales volume from 41263 MT in 2011 to 46741 MT in 2016, low methoxyl pectin had a 30% increase in sales volume going from 7657 MT in 2011 to 9940 MT in 2016 and low methoxyl-amidated pectin had a 20% increase in sales volume, from 3239 MT in 2011 to 4149 MT in 2016. A similar trend is seen when the revenue from each of the pectin types is explored with a 51% increase in revenue from high methoxyl pectin observed from 2011 to 2016, a 68% increase in revenue from low methoxyl pectin and a 60% increase in revenue from low methoxyl-amidated pectin across the same time period.

The disparity between the percentage increase in sales volume and sales revenue across the last 5 years can be explained by the increasing cost of pectin per ton (figure 3.10). The price of HM pectin per ton increased by 33% from 2011 to 2016, LM pectin increased 30% and LMA pectin increased by 25% across this time period.

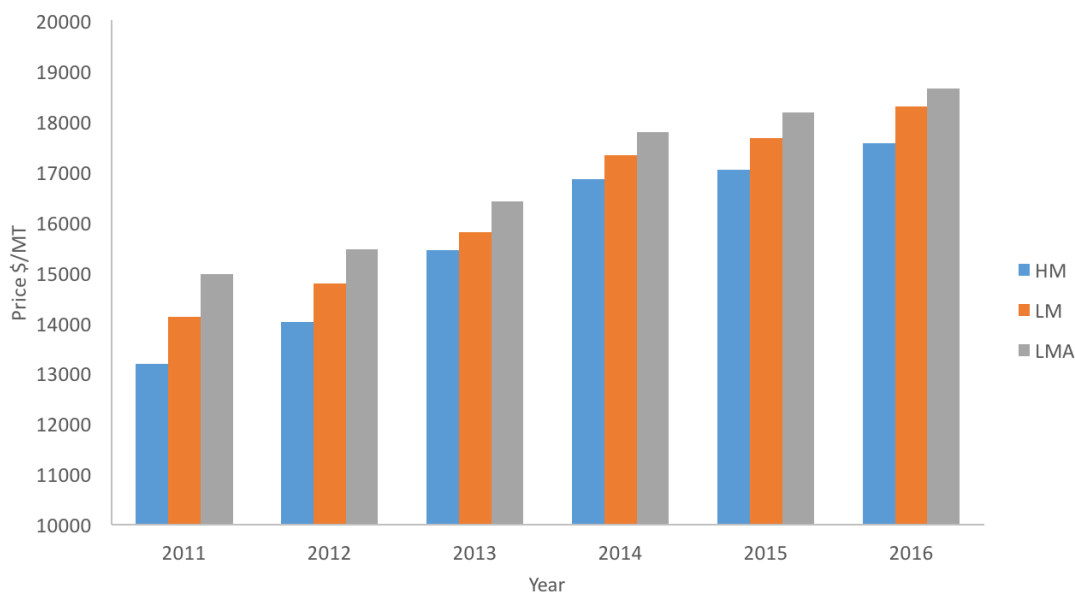


Figure 3.10 – Price of Different Classes of Pectin from 2011-2016(Estimated)

3.1.4.3 Extraction Methodologies

i. Traditional: Acid-Catalysed

Conventional extraction methodologies for pectin involve heating the biomass in acidic water (pH 1.5-3.0) to a temperature of 60-100 °C for several hours.⁹⁶ This practice is not only time-and energy-consuming, but also causes problems with the extracted pectin and waste streams. Large volumes of acid waste are produced by this extraction methodology, which is problematic at the industrial scale, requiring costly and time consuming waste treatment steps.

While acid extraction can give a high yield, it is not selective, yielding pectin with a high neutral sugar content.⁹⁷ Long extraction time⁹⁸ at elevated temperatures can also cause thermal degradation of the pectin,^{99,100} lowering the average molecular mass,^{101,102} which leads to an irreversible decrease in the viscosity and gel strength achieved by the pectin.^{103,104} It can therefore be clearly seen the need for new green extraction methodologies to be pioneered for the extraction and isolation of food grade pectin from biomass.

ii. Enzyme-Assisted Extraction

Enzymes are already commonly used within the juicing industry to reduce cloudiness caused by suspended pectin.¹⁰⁵ While these enzymes degrade pectin to enable easy removal from the juice, other enzymes can aid in the extraction of pectin while retaining its structural and functional properties.

Citrus peel waste biomass comprises of an entangled network of polysaccharides, including cellulose, hemicellulose, pectin and proteins. These interact to create a matrix that makes up the cell wall of the plant. Disentangling this matrix to remove a specific component is difficult, even given the specific solubility of pectin in water, but enzymes can selectively destroy polysaccharides; this is one of their purposes in nature. Enzymes such as cellulases, hemicellulases, proteases and pectinases all degrade individual components of the cell wall, with differing degrees of selectivity depending on the enzyme.¹⁰⁶ Therefore, enzymes with limited pectinolytic activity but extensive activity towards the other polysaccharides could be used for pectin extraction, selectively destroying the cell wall while preserving the pectin within, this would allow the solvent easier access of the pectin molecules. This, however, requires in depth knowledge of the enzymatic activity of the enzymes used, as well as the optimal conditions needed for each, if multiple enzymes are employed.¹⁰⁷ Depending on the enzymes used, this approach could eliminate both acid waste and heat.¹⁰⁸ The gentle nature of this extraction ensures that the pectin recovered is of a high degree of esterification and molecular weight.^{109,110}

The drawbacks of this technique are mainly in the scale-up needed to bring it into an industrial context. Enzymes can be expensive, so obtaining them in quantities large enough to cope with the industrial scale of orange peel waste production is challenging. Due to the highly specific conditions each enzyme requires to work effectively, controlling large-scale production would also be difficult.¹⁰⁸

iii. Ultrasound-Assisted Extraction

Ultrasound is a promising technique for biomass extraction. Sound waves with frequencies above 20 kHz cause expansion and compression cycles through a medium, which can be solid, liquid or gas. In a liquid, these ultrasonic waves create cavities that grow during the expansion cycle and collapse during the compression cycle, resulting in localised temperatures of around 5000 °C and pressures of 1000 atm.¹¹¹ This can rupture cell walls, allowing the solvent easier access to pectin.

The two most common methods for ultrasound extraction are bath and probe; these both have advantages and disadvantages. The bath allows larger volumes of biomass to be processed, but lacks uniformity in ultrasound energy distribution.¹¹² The probe system has a more uniform energy distribution, but the ultrasound intensity declines with distance from the probe-emitter, limiting the volume of biomass that can be processed.¹¹³

The conditions of the extraction are also important to consider. Ultrasound extraction systems usually allow for the control of temperature, pressure, frequency and time, but another important consideration is the ratio of sample to solvent. Higher ratios, attenuate the ultrasound energy, leading to non-optimal extraction conditions.¹¹⁰

iv. Subcritical Water or Super-Hot Water Extraction

Subcritical water extraction, refers to heating water over its boiling point (100 °C) and under its critical point (374 °C),^{114,115} while retaining an elevated pressure high enough to keep the water in its liquid state (figure 3.11). This allows for potentially fast, cheap, green extraction at relatively low temperatures.^{116,117}

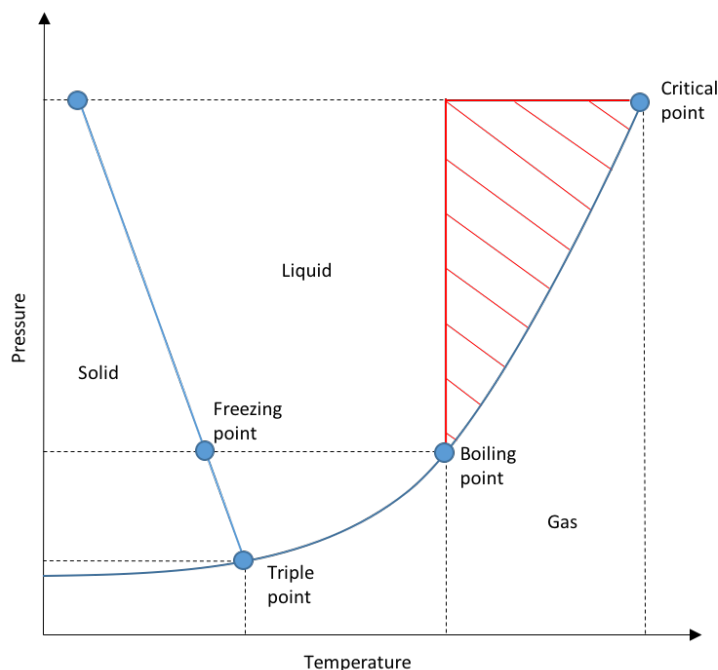


Figure 3.11 – Phase diagram showing subcritical (red dashed area) and supercritical (above the critical point) areas

Subcritical water extraction differs from steam distillation and hydro-distillation because, while the temperature is higher than in those two methodologies, the extraction time is usually much shorter, allowing retention of thermally labile/volatile components.

Because heating water changes its solvent properties¹¹⁸ including its dielectric constant and Hansen solubility parameters, the extraction conditions will affect the applicability of the method for extraction of certain compounds.¹¹⁹ Hence, optimisation studies taking into account the temperature, pressure, run time and particle size would have to be performed to enable efficient pectin extraction. Care would have to be taken to avoid thermal hydrolysis and degradation of the extracted pectin.

Another attractive characteristic of subcritical water extraction is its suitability for flow processing, so more efficient continuous flow extraction rather than batch process is achievable with this methodology.¹¹⁰

v. Microwave Assisted Extraction

Microwave assisted extraction of pectin has been explored as a greener alternative to the classical acid assisted extraction technique.^{98-100,120} Microwaves have a lower operating cost than conventional heating, and can have advantageous effects on biomass that facilitate pectin extraction.

Microwaves can achieve homogeneous heating of a sample, with none of the inconvenient temperature gradient seen with conventional heating. This results in a more efficient heating for large quantities of sample, as well as allowing more control throughout the heating process. The fact that microwaves affect polar molecules turns the high water content of waste citrus biomass into an advantage, allowing for the microwaves to directly affect the water within the biomass.¹²¹ Increased inter-cellular pressure causes the cells to rupture and increases the capillary porous nature of the biomass. The pectin, normally contained within cell walls, can then be more easily extracted. Microwave treatment of orange peel can increase surface area more than four-fold in comparison to a control sample.¹²²

With all thermal treatment of biomass for pectin extraction, there is a danger of thermally decomposing the pectin.¹²³ Microwave treatment holds an advantage here as well – processing temperature can be achieved faster, so heating times are vastly reduced. Time under irradiation is an important factor to consider when designing microwave-assisted extraction methodologies, as it is not only the most energy-intensive step energy-wise, but also the step that most heavily affects pectin yield and quality.¹²⁴

Another parameter to consider when designing the methodology is the ratio of sample to solvent. An advantage of microwave treatment is a reduction of solvent needed for the desired effect. However, with too little solvent, the pectin forms a colloid with the water, increasing viscosity and reducing extraction efficiency. This saturation limit is important to take into account when using reduced solvent for microwave treatment.¹²⁵ If a closed-vessel microwave system is used, then temperatures of above 100 °C can be achieved and the advantages of subcritical water can be exploited. However, elevated temperatures will promote thermal degradation of the pectin, so care has to be taken.

Microwave power is another factor to take into consideration when using microwave-assisted extraction techniques. The power determines the speed at which the desired

temperature can be achieved, and as stated before, this is one of the most important factors in maximising yield without thermally degrading the pectin.¹²⁴

Acids can be used within microwaves, as their oppositely charged ions (eg. H^+ and Cl^-) can be affected by microwave radiation.¹²³ The issues of acid waste management remain, and acid extraction in a microwave gives similar pectin yields to aqueous microwave extraction. Furthermore, water-extracted pectin has better properties than acid extracted.¹²⁶

Another beneficial effect of microwaves is inactivation of pectolitic enzymes within the orange peel. These enzymes interact with the pectin present in the peel and reduce its solubility, degree of esterification, molecular mass and gel strength. Thus, microwave treatment to inactivate such enzymes increases yield and quality of pectin obtained.¹²²

vi. Combined Techniques

With so many promising methodologies being explored for more efficient, greener techniques for extraction of pectin from waste biomass, the logical approach is to combine two or more complementary techniques. This could increase pectin yield and quality while reducing time, energy and solvent usage during the extraction.

Some techniques are intrinsically incompatible, such as enzymatic extraction and microwave heating. Because enzymes are vulnerable to heat, the microwave treatment would most probably destroy the enzymes before they had a chance to aid in the extraction of pectin. Other techniques, however, could work together within the same system, for example, ultrasound extraction and microwave heating.^{127,128} These two approaches use different forms of radiation: electromagnetic in the case of microwaves, and sound waves in the case of sonication. Both forms of energy could be used in combination on the same sample, with potentially advantageous results.¹²⁹

3.2 Specific Aims and Objectives

The aims within this chapter focus on the development of comprehensive citrus waste biorefinery based around acid-free microwave treatment with three specific objectives:

- i. To extract, with competitive yield and minimal energy and solvent expenditure, citrus oil from waste citrus biomass using microwave technology.
- ii. To extract, with competitive yield and industrially acceptable quality, pectin from waste citrus biomass utilising microwave technology.
- iii. To utilise the residual cellulosic residue after microwave extraction of both citrus oil and pectin.

Through collaborative work with a citrus juicing company, the resulting biorefinery method should be applied to industrial citrus waste samples to prove its efficacy with a ‘real-world’ feedstock, as well as explore the effects of diseased oranges on the biorefinery yields.

Preliminary studies should be performed on scaling the process up to pilot-scale to prove suitability for industrialisation.

3.3 Results and Discussion

3.3.1 Citrus Oil

3.3.1.1 Varietal Yields

As detailed in the introduction to this chapter, citrus oil extraction via steam distillation is a well-established valorisation route for oranges. This method has many disadvantages, including high energy use and difficulties in heating large volumes of biomass evenly. Microwave technology is a relatively new technology within the field of citrus oil extraction that could potentially solve many of these issues.

Citrus peel from different sources was exposed to microwave radiation as outlined within the experimental section (2.1.2), giving the yields shown in figure 3.12.

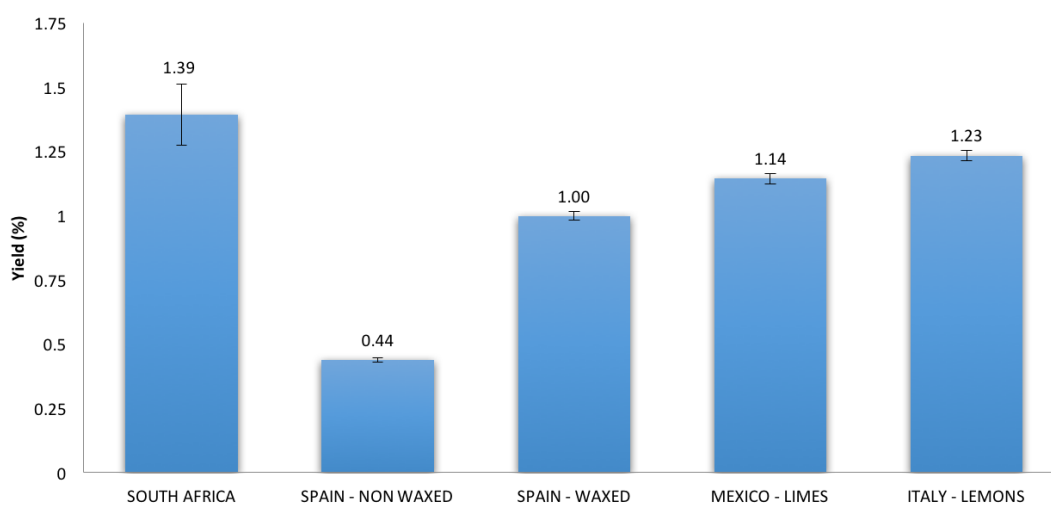


Figure 3.12 – Citrus Oil Yields Obtained from citrus from Different Countries

The citrus oil yield on a dry basis ranged from 0.44% to 1.39%. The oil yield from non-waxed Spanish oranges gives an interesting insight into the importance of wax when transporting oranges. As citrus oil is volatile, it appears that a great deal is lost in the transport of non-waxed oranges from Spain to the UK. While this does not necessarily

impact industrial citrus oil manufacturers, as they will probably extract the oil close to the orange plantation to reduce transportation costs, it is worth knowing that oranges stored for extended periods of time un-waxed will have a lower citrus oil yield.

These extractions were done via a one-step heating methodology described in the experimental section (2.1.2). In order to select the most efficient, affordable conditions for extraction, various parameters were tested, as described below.

3.3.1.2 Method Optimisation

The extraction process for citrus oil was optimised by altering the conditions of the microwave extraction. The parameters explored were: power (in both one-step and two-step extractions), pressure, time and ratio of Waste Orange Peel (WOP) to water. Initially, a one-step extraction procedure was explored. Each of the reaction parameters was altered, resulting yields recorded, and it was found that time and ratio of WOP to water have the largest effect on citrus oil yield. Table 3.1 shows full experimental conditions and yields.

Table 3.1 – Experimental Conditions and Yields for One-Step Citrus Oil Extraction

Run	Power (W)	Pressure (mbar)	Time (min)	Ratio (WOP:H ₂ O)	Yield (% - dry basis)
1	600	1013	30	1:1.5	1.402
2	800	400	45	1:1.5	1.822
3	600	700	18	1:2.5	1.121
4	400	100	19	1:2.5	0.140
5	1000	1013	14	1:5	0.514
6	600	500	15	1:5	0.467
7	700	600	18	1:2.5	1.042
8	900	800	15	1:3.5	1.636
9	500	500	30	1:3.5	1.168
10	675	475	43	1:1.5	1.509
11	400	400	44	1:2.5	1.542
12	300	300	43	1:5	1.168
13	600	400	35	1:2.5	1.523
14	600	1013	24	1:5	1.449
15	700	900	19	1:3.5	0.607
16	400	250	35	1:3.5	0.748
17	600	800	25	1:2.5	1.626

Working under the assumption that the citrus oil extraction begins after the water in the reaction vessel starts boiling, a second set of experiments was designed. In these, boiling temperature was achieved as fast as possible using maximum power; then, once boiling, the power was lowered to maintain evaporation at a lower energy cost. This two-step approach allows for maximum time boiling while minimising energy input. Table 3.2 details all the experimental parameters used, as well as the yields of this two-step process.

Table 3.2 – Experimental Conditions and Yields for Two-Step Citrus Oil Extraction at WOP:H₂O ratio of 1:1.5

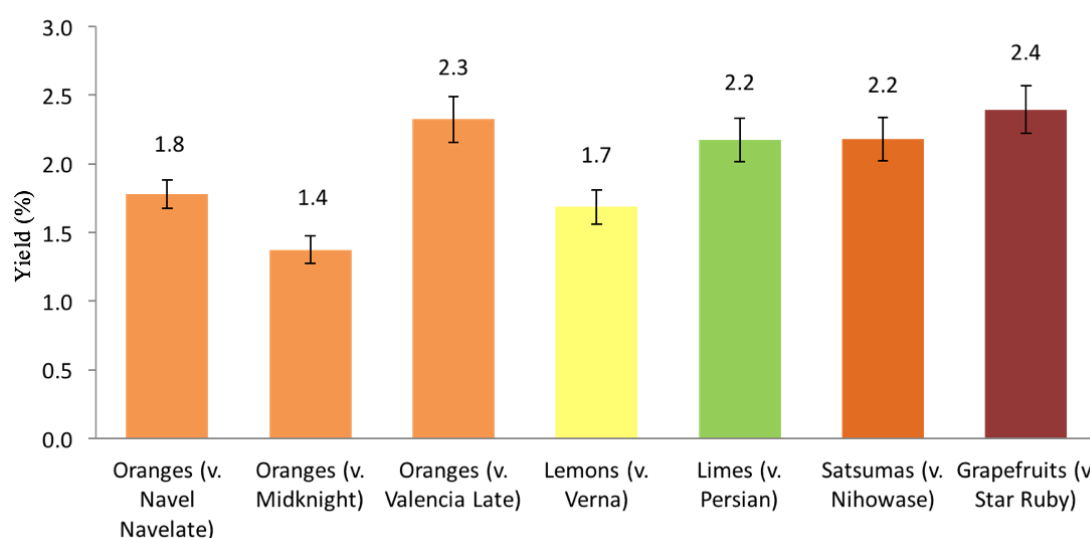
Run	Method	Power (W)	Pressure (mbar)	Time (min)	Yield (% - dry basis)
	First step	1200	800	5	
1	Second step	400	800	5	0.888
2	Second step	400	800	15	1.402
3	Second step	400	800	30	1.729
	First step	982	500	5	
4	Second step	250	500	5	1.360
5	Second step	250	500	15	1.790
6	Second step	250	500	30	1.869
	First step	785	300	5	
7	Second step	250	300	5	1.215
8	Second step	250	300	15	1.776
9	Second step	250	300	30	1.822

From these results it was determined that the optimal conditions for citrus oil extraction from WOP were as reported in table 3.3. Although run number 6 gave a slightly higher yield it was decided that slightly increased yield was not worth the increased energy usage to achieve a power of 982 W as opposed to 785 W in the chosen run (9).

Table 3.3 – Optimal Reaction Conditions for Citrus Extraction from WOP

	Power (W)	Pressure (mbar)	Time (min)	Ratio
First Step	785	300	5	1:1.5
Second Step	250	300	20	1:1.5

With this new, optimised methodology, experimental runs were done on citrus from a variety of sources, with the results shown in figure 3.13.

**Figure 3.13** – Essential Oil Yields Obtained from Different Citrus Fruits

As can be seen from figure 3.13, citrus oil yields were improved in all the citrus biomass samples tested, with a maximum yield of 2.4% (grapefruit) being achieved.

3.3.1.3 Characterisation of Citrus Oil

Citrus oil obtained from both traditional steam distillation (Oranges (v. Navel Navelate) 1.7% yield) and the optimised microwave-assisted steam distillation method (Oranges (v. Navel Navelate) 1.8% yield) were analysed via GC-MS – with standards run using GC-FID for confirmation of assignments – primarily to determine D-limonene content, but also to test the effect of different extraction methods on other constituents of the oils

extracted. The results of this analysis are given in table 3.4.

Table 3.4 – Citrus Oil Analysis from Optimised Microwave Assisted Distillation and Steam Distillation

Compound	Steam Distillation (SD) (%)	Microwave Distillation (MD) (%)	Difference (MD-SD)
Monoterpenes	98.56	99.34	0.78
D-Limonene	96.75	97.38	0.63
γ-Terpinene	–	0.04	0.04
β-Pinene	0.05	0.06	0.01
α-Pinene	0.32	0.39	0.07
R-β-Myrcene	0.74	0.79	0.05
Sabinene	0.49	0.50	0.01
α-Terpinolene	0.20	0.18	-0.02
Oxygenated Monoterpenes	0.14	0.14	–
Linalool	0.05	0.05	–
Terpinene-4-ol	0.01	0.01	–
Terpineol	0.01	0.01	–
Eucalyptol	0.07	0.06	-0.01
Sesquiterpenes	–	0.01	0.01
<i>Trans</i>-α-Bergamotene	–	0.01	0.01
Unidentified	1.3	0.51	–

The results show that the oils extracted by both methods are broadly similar, with the optimised microwave-assisted extraction yielding slightly higher D-limonene content (0.63% higher) with a correspondingly higher total monoterpene content (0.78% higher). The citrus oil extracted via the optimised microwave-assisted extraction is of very similar quality to that of the conventional steam distillation.

Citrus oils extracted from different sources using the same optimised microwave-assisted steam distillation are broadly similar across orange varieties, but other citrus fruits (lemon, lime, satsuma and grapefruit) show marked differences, with much lower D-limonene content and correspondingly higher amounts of other terpenes. Table 3.5 shows the full analysis of citrus oil from different sources.

Table 3.5 – Citrus Oil Analysis from Different Sources via Optimised Microwave Assisted Steam Distillation

Compound	Orange Nn	Orange M	Orange V1	Lemon	Lime	Satsuma	Grapfruit
	%						
Monoterpenes	99.34	98.54	98.51	96.84	96.10	97.36	98.39
D-Limonene	97.38	96.36	96.54	68.42	61.93	92.98	89.20
γ -Terpinene	0.04	0.04	0.04	11.35	16.93	0.08	4.82
β -Pinene	0.06	0.07	0.07	12.31	11.36	0.28	1.59
α -Pinene	0.39	0.41	0.35	1.89	2.35	0.79	0.96
R-β-Myrcene	0.79	0.90	0.84	0.83	0.90	2.01	0.93
M-3Carene	–	0.90	–	0.12	0.17	0.16	–
Sabinene	0.50	0.46	0.53	1.00	0.77	0.57	0.23
α -Thujene	–	–	–	0.33	0.46	0.22	0.17
p-Cymene	–	–	–	0.19	0.21	–	0.10
Terpinene	–	–	–	0.13	0.29	0.02	0.05
α -Terpinolene	0.18	0.22	0.13	0.27	0.74	0.25	0.33
Oxygenated monoterpenes	0.14	0.16	0.16	1.36	1.19	0.46	0.19
Linalool	0.05	0.08	0.07	0.10	0.14	0.20	0.02
Terpinene-4-ol	0.01	0.01	0.01	0.42	0.39	0.02	0.04
Geraniol acetate	–	–	–	0.41	0.10	0.09	0.02
Terpineol	0.01	0.01	0.01	0.32	0.39	0.10	0.04
Eucalyptol	0.06	0.07	0.06	0.12	0.16	0.05	0.06
Sesquiterpenes	0.01	0.51	0.52	0.10	1.04	0.06	0.09
Valencene	–	–	0.08	0.02	0.01	0.05	0.04
β -Elemene	–	–	–	–	–	–	0.01
Trans-α-Bergamotene	0.01	–	0.01	– 0.08	0.16	0.01	0.04
β -Bisabelene	–	0.51	0.43	–	0.87	–	–
Oxygenated Sesquiterpenes	–	–	–	0.24	0.66	0.13	0.01
Z-Citral	–	–	–	0.16	0.29	–	0.01
E-Citral	–	–	–	0.07	0.38	0.13	–
Other Oxygenated Compounds	–	0.01	–	0.13	0.23	0.02	0.04
Neryl acetate	–	0.01	–	0.13	0.23	0.02	0.04
Unidentified	0.51	0.78	0.81	1.46	1.00	1.99	1.33

3.3.2 Pectin

3.3.2.1 Varietal Yields

The pectin yields via acid-free closed vessel microwave extraction, as outlined in the experimental (2.1.3), with respect to citrus from different sources are shown in figure 3.14.

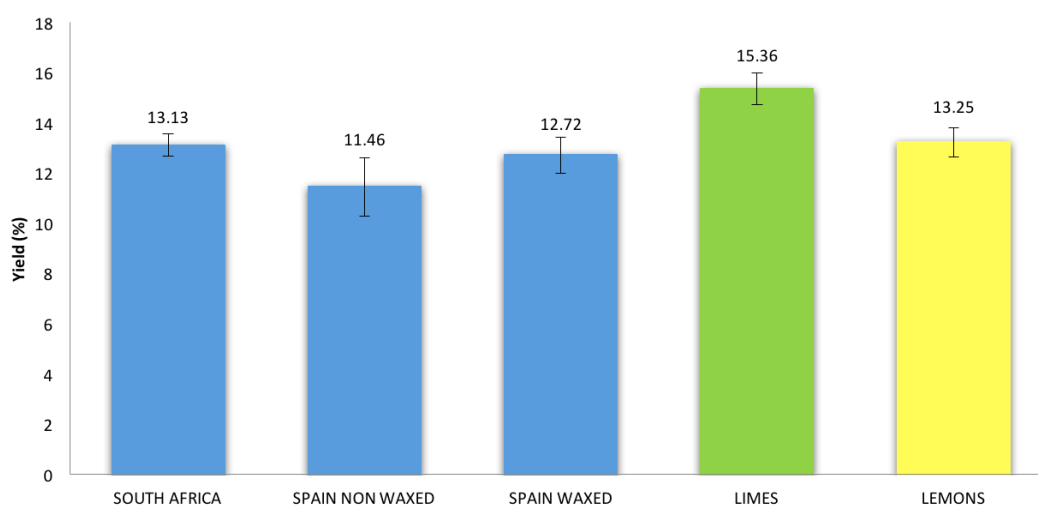


Figure 3.14 – Pectin Yields Obtained from Citrus Sources from Different Countries

Pectin yields were found to vary slightly depending on the citrus sources, with less than 1% difference between the yields from oranges sourced in Spain (12.72% on a dry weight basis) and South Africa (13.13% on a dry weight basis). Interestingly a reduction in yield is observed in the non-waxed oranges again – a 1.26% drop compared to waxed oranges from the same source. This reduction is not as significant as that of the citrus oil, but as pectin is a non-volatile component of the biomass cell walls, it is intriguing that there is a reduction at all. It is probably due to the preservative effect of wax – non-waxed varieties are more likely to be susceptible to pectin-degrading enzymes than their waxed counterparts. The acid-free closed vessel microwave methodology was tested on other citrus fruit (namely limes and lemons) to test its validity across different biomass types; pectin yields were 15.36% and 13.25%, respectively.

3.3.2.2 Characterisation of Pectin

In commercialising pectin, certain standards have to be met to ensure the pectin is safe for human consumption and of a quality appropriate for industrial food use. Tests were designed based on an industrial specification document prepared at the 71st JECFA (2009) and published in FAO JECFA Monographs 7 (2009). The results of these tests, as well as comments on their importance, are given below.

i. Visual Appearance

Pectin obtained from citrus is described as white, yellowish, light greyish or light brownish powder. The extracted pectin conforms to this appearance (figure 3.15), although grinding was required to obtain a powder. The freeze-drying route formed white polymeric pectin in large sheets which had to be broken apart to extract them from the drying vessel. Loss on drying was also negligible, as freeze-drying is a thorough drying method. Samples showed less than 8% loss after drying in an oven at 110 °C for 2 h.



Figure 3.15 – Visual Appearance of Pectins Extracted from Different Sources

ii. ATR-IR

ATR-IR analysis shows a good correlation between extracted pectin and commercial pectin. The characteristic adsorption bands at $1700\text{-}1740\text{ cm}^{-1}$, corresponding to the methyl ester/acid group, can clearly be seen in both spectra (figure 3.16). In addition, the -CH_3 bending absorption band associated with the esterified CH_3 can be seen at $1350\text{-}1450\text{ cm}^{-1}$. The IR spectra for the other experimentally derived pectin samples are given in the appendix, figures A.1-A.4.

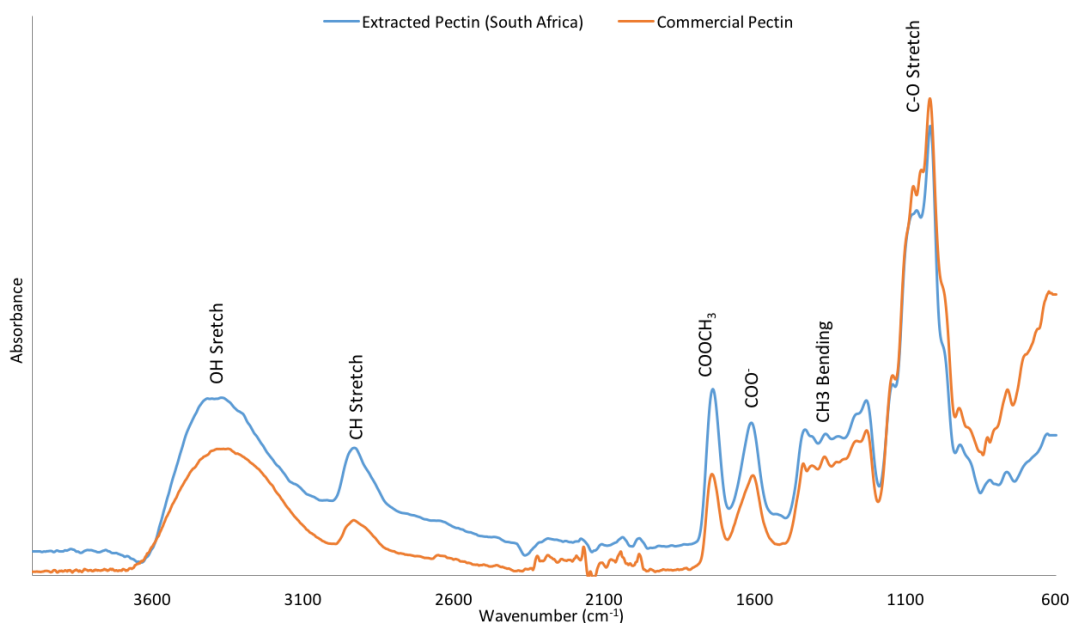


Figure 3.16 – ATR-IR of Pectin Extraction from South Africa Oranges Compared to Commercial Pectin

iii. Degree of Esterification

The Degree of esterification (DE) is an important factor in pectin quality. It is directly proportional to the speed at which the pectin can gel, with high-DE pectins gelling faster than low-DE pectins. For food applications that rely on gelation ability, high-DE pectins are preferred. The DE was determined for all extracted pectins produced via the solid state NMR method and compared to commercial pectin (figure 3.17).

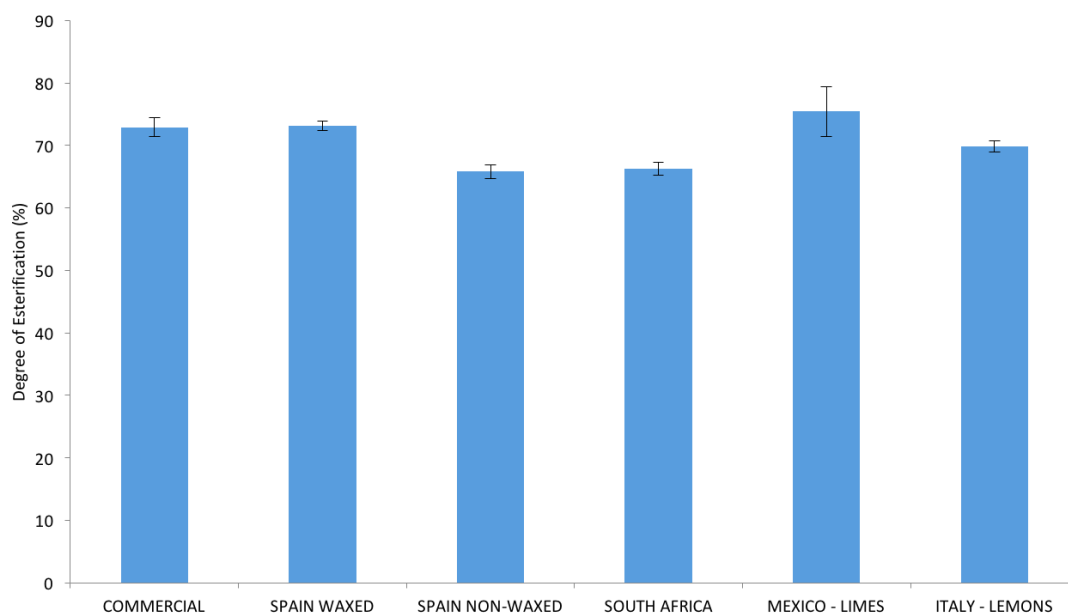


Figure 3.17 – Degree of Esterification for Extracted Pectins

Figure 3.17 shows that all pectins extracted can be classed as high-DE (>50%) and are all comparable with the commercial pectin. There is little difference in DE between pectin obtained from different sources, indicating that extraction method is the most important factor for DE.

iv. Gelling Tests

Gelation is a key parameter for pectin. Initial gelation tests were run in-house via the method outlined in the experimental section (2.1.3.3). As a qualitative analysis, the vessels were turned upside down to see if the gel had formed (figure 3.18).

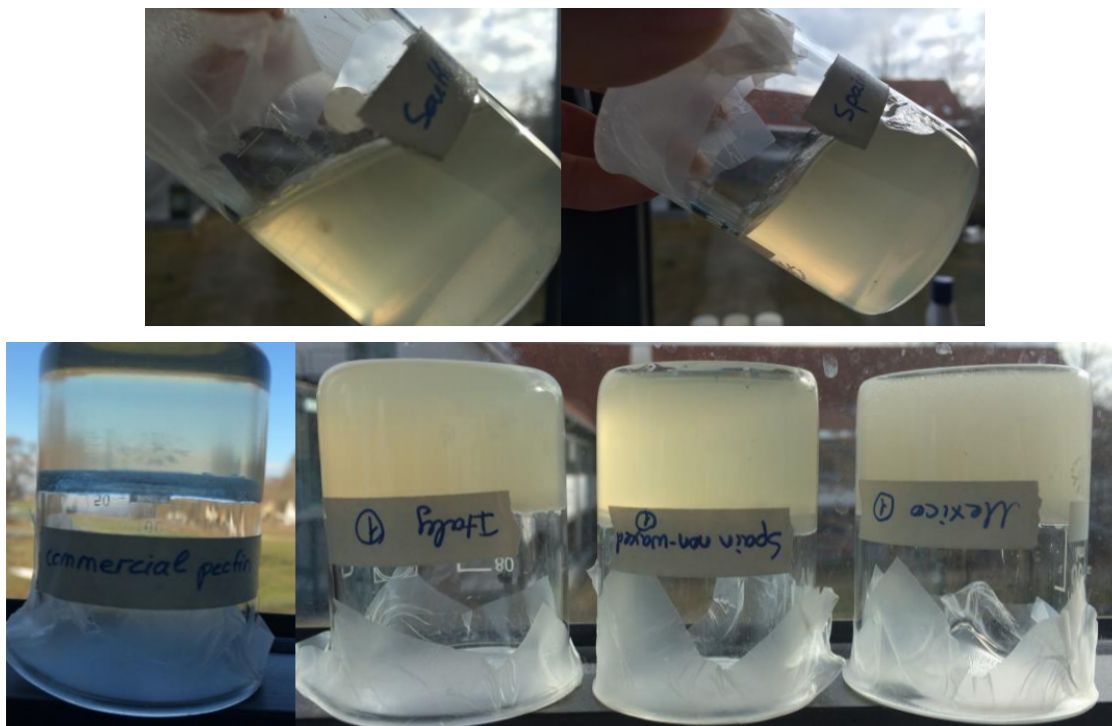


Figure 3.18 – Gels Formed from Different Pectins

More in-depth gel analysis was outsourced to the Fraunhofer Institute for Process Engineering and Packaging IVV, Germany, This analysis was to quantify hardness (figure 3.19) and visco-elastic properties (table 3.6) of the gels formed.

Interestingly, the results from the Fraunhofer report indicate that degree of esterification or methylation is not the sole contributing factor to gel properties – physical characteristics of the pectin also play a large part. During freeze-drying the pectin is dissolved in a minimal amount of water and then hung on the freeze-drier, as described in the experimental section (2.1.3.2). The ratio of water to pectin heavily influences the appearance of the pectin obtained, but almost all freeze-dried pectin ends up as large, polymeric ‘chunks’, whereas industrial spray-dried pectin ends up as a fine powder. This difference was shown to have a significant effect on gel hardness, with pectins that formed large and hard ‘chunks’ tending to form weaker gels. The pectins sent to Fraunhofer could be divided into two groups, with the first group consisting of pectins obtained from oranges from South Africa and waxed oranges from Spain and displaying relatively large, hard ‘chunks’ of pectin indicating a low water:pectin ratio when freeze drying. The second group consisted of the pectin obtained from the non-waxed Spanish oranges, and the limes and lemons from Mexico and Italy

respectively; these pectins were composed of smaller flakes of lower density, indicating a higher water:pectin ratio when freeze-dried, (see earlier figure 3.15). Figure 3.19 shows the gel hardness of the extracted pectins in comparison to commercial citrus pectin for reference. The measured gel hardness correlated to the appearance of the pectin with the denser, larger, hard ‘chunks’ of pectin showing lower hardness.

In solids gelation is more efficient with high surface areas, so it is reasonable that the powdered and less dense pectins form stronger gels. To improve gelation a grinding step was added to the pectin extraction process.

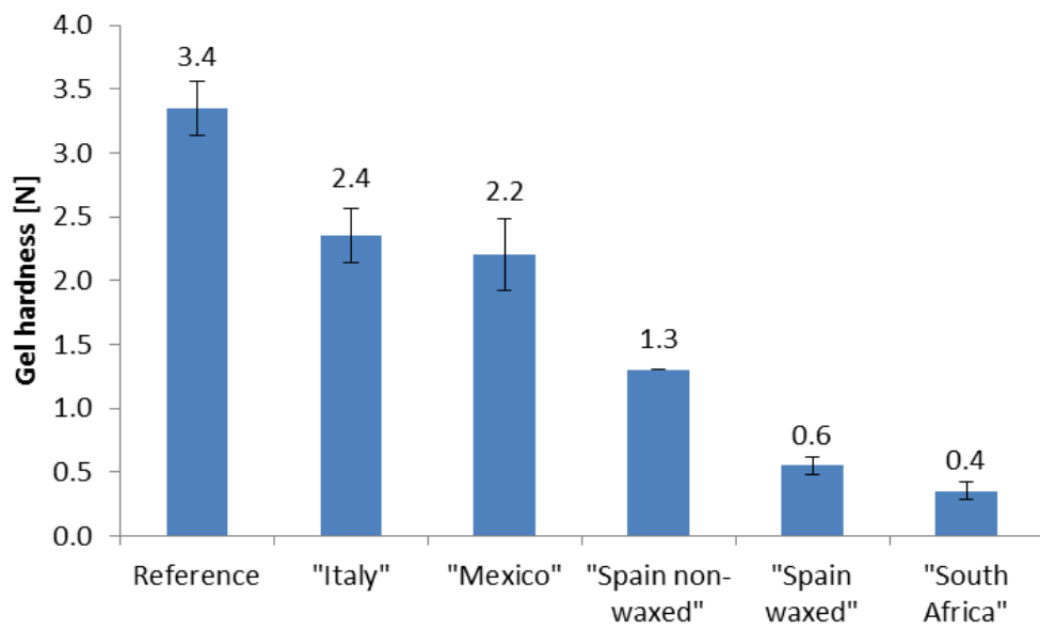


Figure 3.19 – Hardness of Pectin Gels from Different Sources

To further analyse the properties of the gels created from the extracted pectin, the visco-elastic behavior of the gels was explored. The properties measured were the storage modulus (G') which indicates the elastic behavior of the gel, the loss modulus (G'') which describes the viscous nature of the gel, the complex shear modulus (G^*), which is a sum of G' and G'' that gives an indication of the overall visco-elastic behaviours of the gel and the dynamic Weissenberg number (W'), which is the ratio of storage to loss moduli. The results are shown in table 3.6.

Table 3.6 – Visco-elastic Properties of Pectins Extracted from Different Sources

Sample	Loss Modulus, G'' (Pa)	Storage Modulus, G' (Pa)	Complex Shear Modulus, G^* (Pa)	Weissenberg Number, W'
Commercial Pectin	121.8 ± 6.7	1002.9 ± 35.3	1081.9 ± 35.3	8.2 ± 1.0
South Africa – Orange	90.6 ± 4.0	234.7 ± 5.8	252.1 ± 4.4	2.7 ± 0.2
Spain – Orange (non-waxed)	73.4 ± 42.5	455.0 ± 124.6	461.4 ± 130.1	7.0 ± 2.1
Spain – Orange (waxed)	65.6 ± 40.1	239.2 ± 113.5	248.2 ± 120.2	3.9 ± 0.6
Mexico – Lime	267.0 ± 82.2	1578.1 ± 386.9	1600.7 ± 395.1	6.0 ± 0.4
Italy – Lemon	156.3 ± 18.2	1352.2 ± 70.8	1361.4 ± 70.6	8.8 ± 1.1

The visco-elastic analysis indicates, again, that the texture of the pectin obtained can greatly impact its gel properties. Pectin samples with small, low-density flakes exhibit highly elastic behavior with high complex shear modulus and Weissenberg numbers comparable to those of commercial pectin, whereas samples with hard, high-density textures show similar viscous and elastic moduli and low Weissenberg numbers.

v. Total and Acid-Insoluble Content

The industrial standard for total insoluble content is up to 3% by weight, and for acid-insoluble ash, up to 1% by weight. Results indicated that the total insoluble content was 0.6%, far below the allowed 3%, and total insolubles were also below the limit for acid insoluble ash content. Tests were run on pectin obtained from South Africa oranges in duplicate and the average result taken as indicative measures for all pectin produced.

vi. Nitrogen Content

To conform to industrial standards, pectin cannot have a nitrogen content of over 2.5% after acid and ethanol washes. To test this, unwashed pectin was assessed for C, H and N content. The results of this test are given in table 3.7.

Table 3.7 – CHN Analysis of Microwave Extracted Pectin

Element	% C	% H	% N	% Rest
First test	35.94	4.89	0.02	59.15
Second test	35.93	4.79	0.04	59.24
Mean	35.935	4.839	0.031	–

The mean value for nitrogen present within the pectin, even prior to the acid/ethanol wash, was 0.031%, showing that the pectin extracted via the acid-free microwave-assisted method passes this industrial purity test.

vii. Metal Content

Analysis of the metal content was performed to make sure that the pectin extracted was in accordance with the industrial standards for food-grade pectin. The areas of importance are the toxic metals, namely lead (Pb), mercury (Hg) and arsenic (As) all of which are below 5 ppm and therefore within the ranges allowed for food grade pectin. For full elemental analysis results see table 3.8.

Table 3.8 – ICP Data for Acid-Free Microwave Extracted Pectin

Element	Amount Present (ppm)	Element	Amount Present (ppm)
Ag	0.01	Na	60.06
Al	159.82	Ni	<0.01
As	4.22	P	2354.71
Au	<0.01	Pb	<0.01
B	<0.01	Pd	<0.01
Ba	39.16	Pt	<0.01
Be	<0.01	Rb	23.46
Bi	<0.01	S	5266
Ca	12012.90	Sb	<0.01
Cd	0.23	Sc	0.20
Co	<0.01	Se	<0.01
Cr	2.65	Si	278.25
Cu	57.11	Sn	<0.01
Fe	96.76	Sr	74.41
Hg	<0.01	Te	<0.01
K	4032.87	Ti	13.80
La	13.18	Tl	5.70
Li	0.56	V	0.24
Mg	1725.15	W	7.53
Mn	12.43	Zn	27.55
Mo	<0.01	Zr	1.62

3.3.3 Cellulosic Residue Valorisation

After extraction of citrus oil and pectin, a cellulosic residue remains. If the biorefinery ideology is to be fully adopted for citrus feedstock, this residue must be viewed as another feedstock for value-added products. The main component of this residue is insoluble ligno-cellulose. Cellulose is used commercially for a variety of applications such as water binding agents.

3.3.3.1 Water Binding

Tests of water binding capacity for the residual citrus fibers left after pectin extractions were outsourced to CyberColloids Ltd, who performed the analysis. The results of their analysis are given in table 3.9.

Table 3.9 – Water binding capacity of residual cellulose created from conventional pectin extraction and acid-free microwave extraction pectin, compared with industrially used cellulosic water binders

Sample	Gram bound water/gram of fibre		
	Cold Mixed	Cold Sheared	Hot Sheared
Conventionally Extracted Pectin	6.32	7.33	9.95
Acid-free Microwave Extracted Pectin	5.43	13.79	14.77
Herbacel AQ plus Citrus	9.99	12.38	12.54
Citri-fi 100 FG (Fiberstar)	5.36	7.04	7.68

The results show that for both the acid-free microwave-assisted extraction and the conventional acid-catalysed extraction, under cold mixing without shear the water binding are quite similar similar to those of the commercially available Citri-fi 100 FG produced by Fiberstar. When shear is added, however, the acid-free microwave-assisted extracted pectin outperforms fiber produced by conventional acid extraction by a noticeable margin, and when compared to the commercially available Herbacel AQ plus Citrus produced by Herbacel – one of the best performing water-binding citrus fibers

available – it performs similarly, and even slightly better.

These results indicate that the residual citrus fiber left after extraction of citrus oil and pectin is well suited for applications as a water-binder within the food industry, and the microwave extraction process improves the properties of the resulting citrus fibers.

3.3.4 Flavonoids

After microwave pectin extraction, refrigeration of the aqueous pectin overnight resulted in formation of a white precipitate which was isolated and washed multiple times with deionised water to give an average yield of 35 g/kg WOP extracted. The solid was believed to be hesperidin as evidenced by ^1H NMR spectroscopy with respect to commercial hesperidin (figures 3.20 and 3.21).

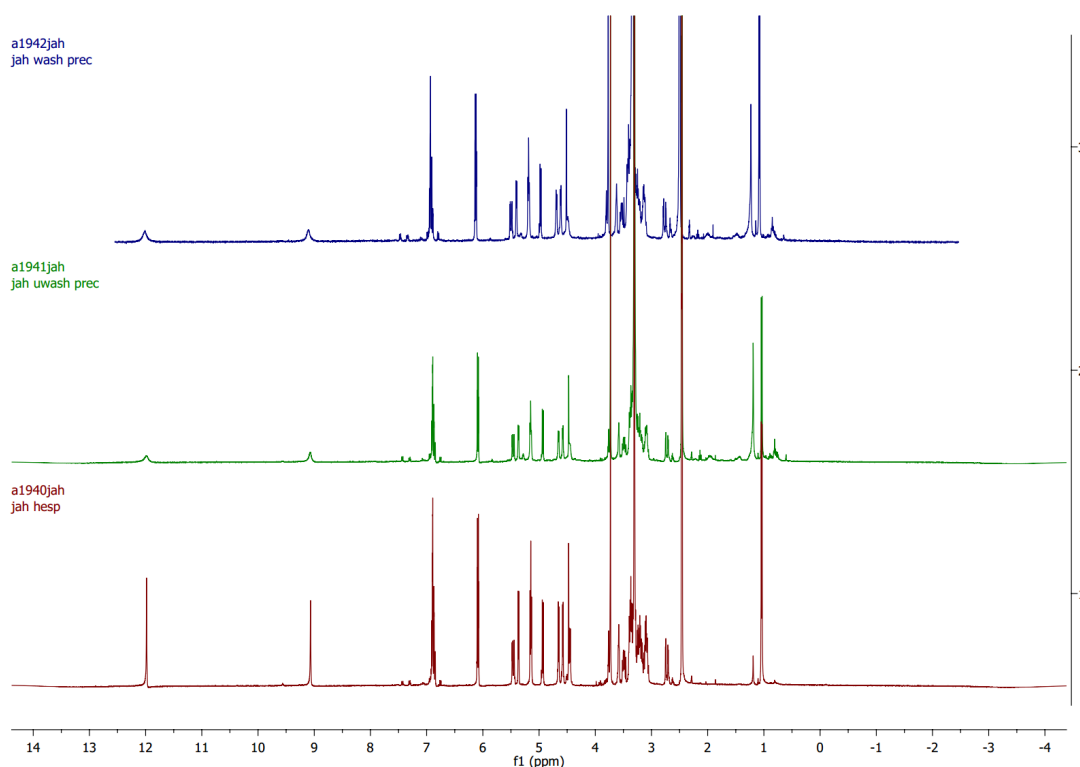


Figure 3.20 – ^1H NMR spectrum of Hesperidin Standard (red), Washed (blue), and Unwashed (green) Samples

The NMR spectra of the washed, unwashed and standard samples are all similar, with the main difference being the peak at roughly 1.25 ppm. This indicates that the precipitate formed is indeed hesperidin, but potentially with a small amount of impurity. This

result suggests that simple cooling of the aqueous pectin might be sufficient to remove a relatively pure hesperidin fraction from the extraction – from the NMR there is little difference between the washed and unwashed samples.

To allow analysis of extracted hesperidin via NMR, attempts were made to assign the proton NMR of hesperidin standard. To aid in assignment, a proton NMR spectrum was obtained of hesperidin standard in DMSO with a small amount of D₂O added to suppress labile alcohol proton signals. This allowed the signals associated with the alcohol groups to be more easily assigned. See figure 3.21 for assignments of the alcohol suppressed proton NMR spectrum of hesperidin standard.

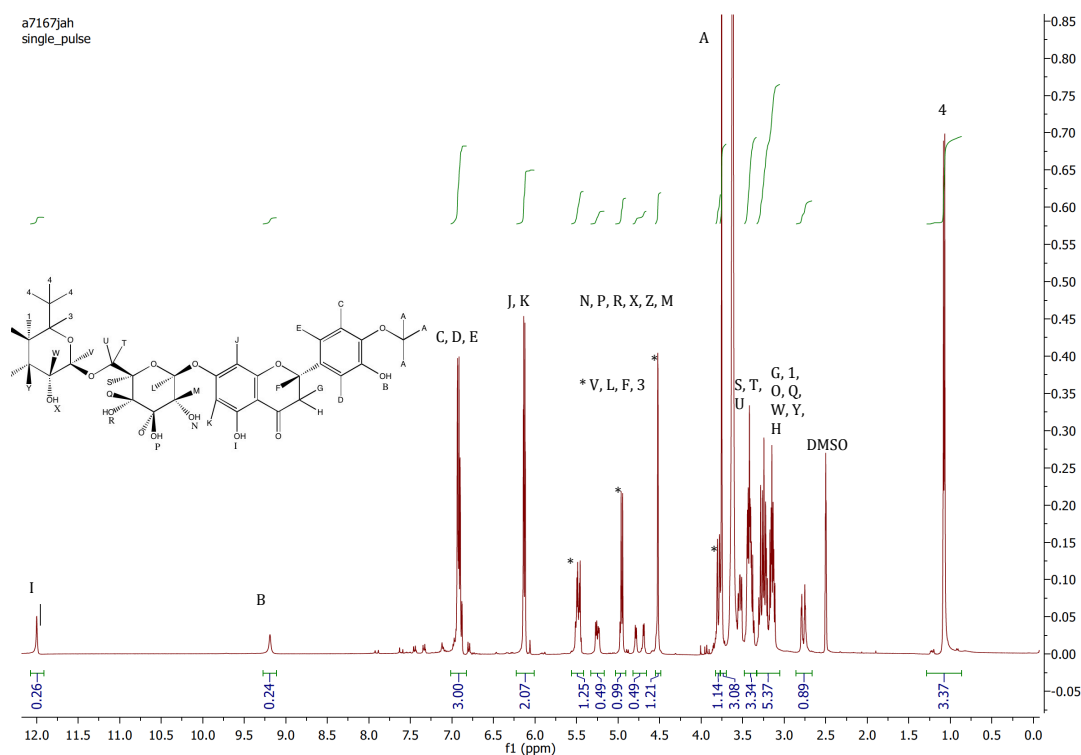


Figure 3.21 – ¹H NMR spectrum for hesperidin standard, with peak assignments indicated, performed in D₂O and DMSO to suppress signals due to alcohol protons

3.3.5 Agroterenas Case Study and Potential Improvements

Herein results from a three-month work placement in Brazil working in collaboration with Agroterenas Citrus are reported.

3.3.5.1 Company Information

Agroterenas Citrus, is a subsidiary of Agroterenas S.A. and was founded in 2006. Based in Santa Cruz do Rio Pardo, São Paulo State, Brazil, it primarily produces orange juice and related byproducts. A total of 8000 hectares of orange trees are spread across three farms, giving a total of roughly 2.5 million orange trees of fruit-bearing age, mostly of Pera variety. In the central juicing plant, 115 oranges are juiced per minute, equating to roughly 490-610 tonnes of oranges processed daily during juicing season. In addition to orange juice, the company also produces 1800 kg of essential oil, 1000 kg of D-limonene and 250 tonnes of semi-dried citrus biomass daily. Very little in the Agroterenas process goes to waste. Water is either recycled into the system or used to irrigate the fields, and the bagasse formed from the peel and pulp is sent to animal feed.

3.3.5.2 Process

Over the course of several site visits, interviews, and meetings, a map of the full Agroterenas juicing process was created, including steps from field to packaging. Figure 3.22 shows an excerpt of the map created representing the processes, inputs, outputs and waste from the juicing and essential oil extraction of oranges.

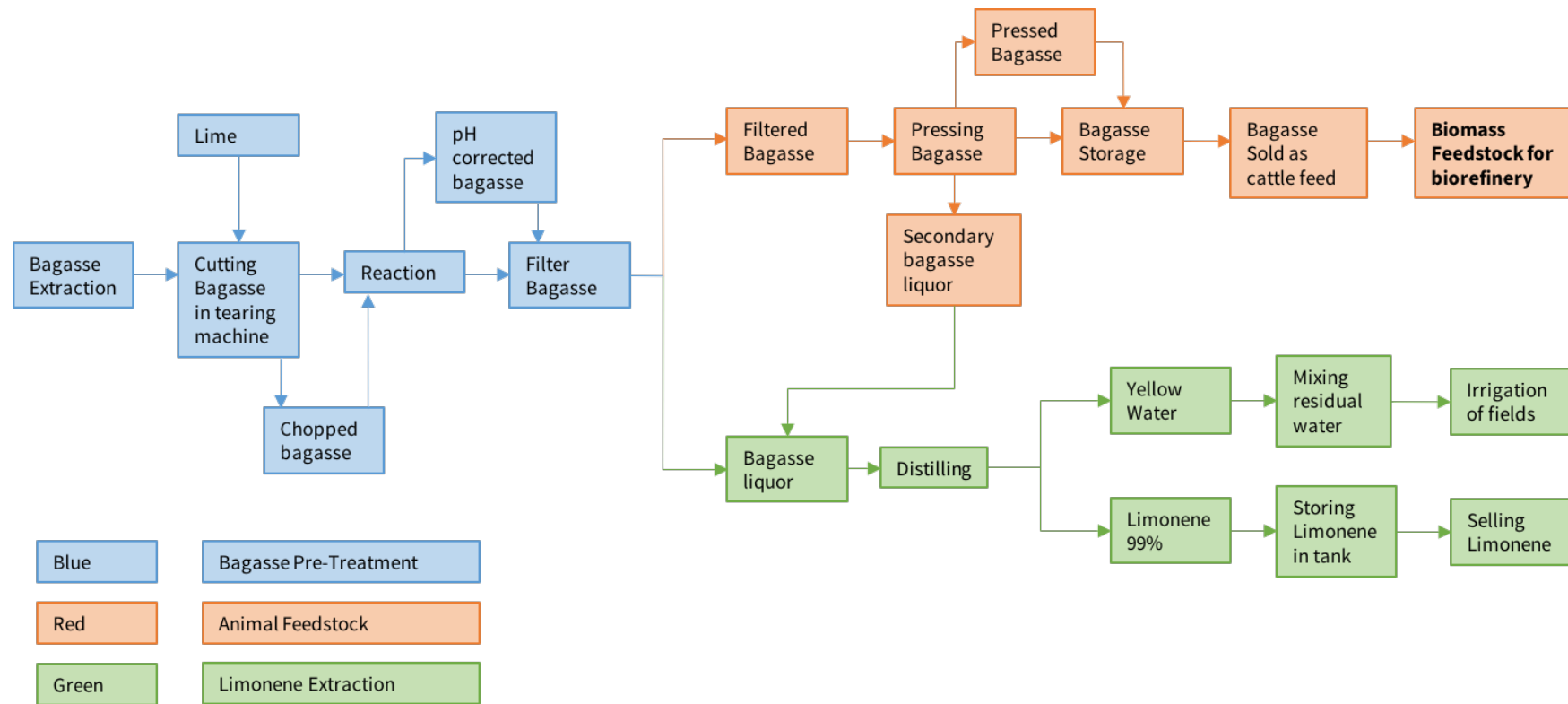


Figure 3.22 – Simplified Agrotrenas Process

Quality Control: The quality control step of the industrial process makes sure that no rotten or highly damaged fruit are sent for juicing. Fruits with diseases such as Huanglongbing (HLB) are also removed at this point, as they increase the bitterness of the juice extracted.

Juicing and Essential Oil extraction: The juicing stage simultaneously extracts juice and essential oil from the oranges. Agroterenas produces 6000 kg of orange juice and 1800 kg of essential oil per day using this simultaneous extraction technology. After the initial extraction, the pulp is washed to create a secondary juice, which is then blended into the first juice. The essential oil is purified and removed from the residual pulp via washing with water and centrifugation to create 98% pure oil, the wax still present is then removed to create a 100% pure oil ready to be sold.

Bagasse Creation and Limonene Extraction: The residual solid from the juice and essential oil extraction is macerated with lime to correct the pH. The bagasse ‘liquor’ is then separated from the solid by rotary filtration. The remaining solid is pressed to remove residual water and stored for use as animal feed, producing 250 tonnes per day. The bagasse ‘liquor’ is distilled to yield limonene with a 99% purity, which is stored for sale.

Other Products: During juice extraction, juice must be concentrated and separated from an aqueous phase, an oil phase and a Valencia oil phase. This is achieved via distillation. Each of these products are stored separately for sale. The yield of Valencia oil per day is 0.005 kg.

3.3.5.3 HLB and Effect on Industrial Orange Juice Production

HLB or Huanglongbing is a disease that affects citrus fruit and is caused by a phloem-limiting bacteria. In Brazil, the American form of HLB (*Candidatus Liberibacter americanus*) is of greatest concern and it was first identified in 2004.¹³⁰ The main symptoms that appear in the fruit are:¹³⁰ small, asymmetrical fruit, vascular columella stained orange/brown, aborted seeds, an abnormally thick rind or ‘pith’, an acidic/bitter taste to the juice obtained, reduction in fruit size, premature fruit drop, and the stem end can remain yellow as the fruit ripens (should go green).

Soon after infection, the tree becomes economically unviable, and serves as a source of infection for other trees. Therefore, infected trees are removed and burnt as soon as they are identified. This makes HLB a very damaging disease that not only lessens an individual tree's production of oranges, but actually removes the tree from the farm.



Figure 3.23 – Orange Showing Symptoms of HLB

The fruit from an infected tree will not necessarily show any of these symptoms, depending on disease stage, but these symptoms reduce juice quality significantly.

The potential economic impact of HLB is immense. Galvão de Miranda *et al.* predicted that by 2028, annual production of oranges in the São Paulo region will have fallen by 12 million tonnes if the spread of HLB is left unchecked.¹³¹ In Florida, almost 100% of orange orchards are infected with HLB, with approximately 70-80% of trees infected and losing production. Since 2006, HLB has cost Florida's economy roughly \$2.63 billion, with a further \$20 million a year being spent on research into control methodologies for HLB.¹³²

3.3.5.4 Potential Improvements to the Agroterenas Process

Within the Agroterenas process there are two main areas that could be improved upon. First, the utilisation of the *agua amarella* – yellow water – while the yellow water is currently recycled back into the system, is it most likely full of flavonoids and sugars

from the orange processing. If an extraction/water cleaning step was added, valuable compounds could potentially be obtained from the yellow water while still allowing the purified water to be re-used within the system.

The second area that could be improved upon is the utilisation of the bagasse produced after the extraction of both juice and essential oils. Currently it is used to extract non-food-grade limonene (due to the use of lime) and then sold for animal feed for R\$20 per tonne. First, the limonene extraction step could be performed without the use of lime, allowing for higher-value, food-grade limonene to be produced. Second, if the residual feedstock were used for pectin extraction instead of for animal feed, the value of the biomass per tonne could be greatly increased. Pectin yields from orange peel can approach 18% on a dry matter basis. With the water content of the bagasse produced in Agroterenas being roughly 20%, this equates to a potential pectin yield of about 14%.

Industrial juicing practices are aimed at maximising juice yield while also extracting value-added products, such as essential oils and limonene, from the orange bagasse. The process has been optimised for the re-use of water within the system, with very little loss of waste water. There is, however, the issue of the waste bagasse after limonene extraction. There is potential here for valorisation, as well as improving the current limonene extraction methodology with greener alternatives.

3.3.5.5 Pectin Isolation Studies

First, pectin extraction was performed on the waste biomass currently used as a low-value cattle feed. Two samples of the bagasse taken straight from the Agroterenas product line were removed, one dried as-is and the other processed to remove seeds and juice sacs before drying. This processing was done by Agroterenas and reportedly could be scaled up without too much difficulty. Both were then shipped to the UK for extraction using the microwave facilities at the Green Chemistry Center of Excellence. The pectin yield from the dried bagasse was 7.67% by weight and the pectin yield from the processed bagasse without seeds or juice sacs was 21.19%. This dramatic difference suggests that pectin yield from waste biomass is greatly increased if an extra step to remove seeds and juice sacs is employed.

i. Characterisation of Pectin Produced from Bagasse

Visually, the pectin obtained is very similar to that obtained from other lab experiments, being white and, due to the freeze-drying process; frozen into a matrix. Figure 3.28 shows a sample of the pectin obtained from bagasse from *Agroterenas*, along with other pectin samples obtained from the work performed in Brazil. Through ATR-IR analysis it can be proven that pectin was extracted by assignment of the characteristic absorption bands as shown in figure 3.24

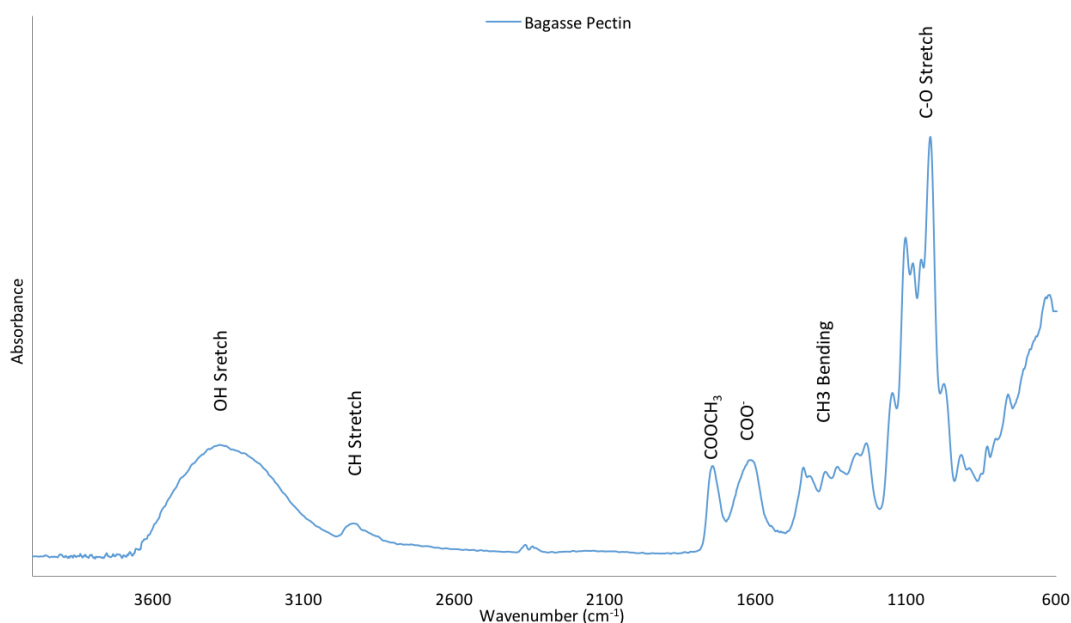


Figure 3.24 – ATR-IR of Pectin Extracted from *Agroterenas* Bagasse

Second, pectin content of oranges infected with HuangLongBing disease (HLB) was analysed, it is known that HLB has detrimental effects on juice quality, but it was unclear how HLB would affect the yield and quality of pectin extracted from infected oranges.

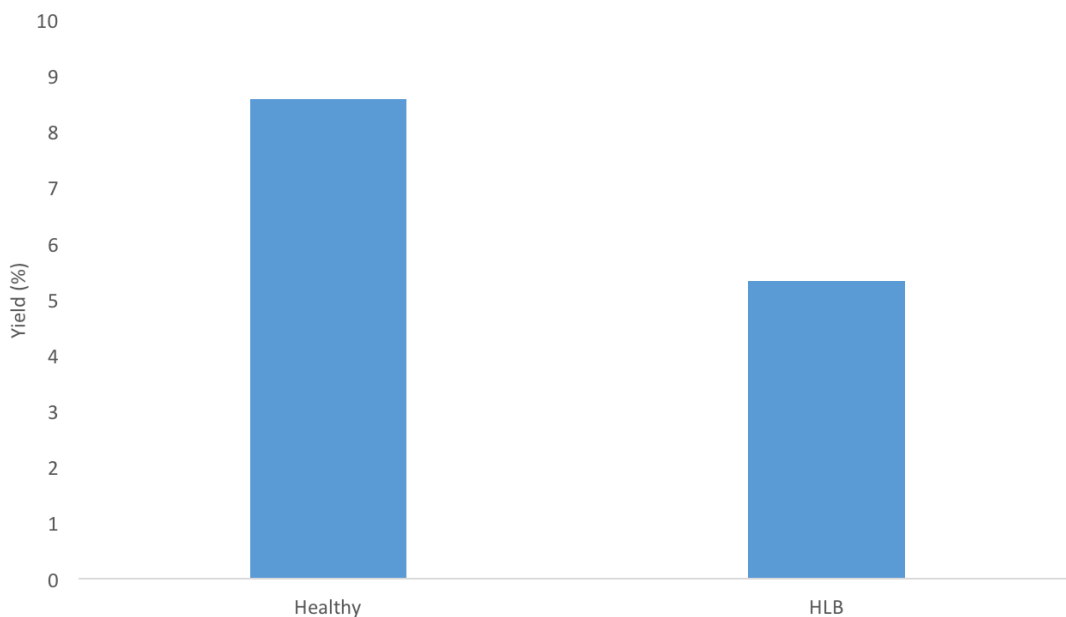


Figure 3.25 – Pectin Yields from Healthy and HLB Infected Oranges

The results shown in figure 3.25 suggest that HLB reduces the amount of pectin that can be extracted from the citrus peel. This is unexpected, as one of the observable symptoms of HLB is a thickening of the pith in affected oranges, which should result in more pectin per fruit. The analysis performed was based on waste orange peel only, so the yield of pectin per fruit is not known and could be greater. The amount of waste peel would be higher from each infected fruit, but less pectin can be extracted from the same amount of peel compared to a healthy orange.

These results show that, not only does the addition of HLB-infected fruit into the juicing plant negatively affect the quality of the resulting juice, but if a pectin extraction step was added into the industrial operation, HLB-infected fruit would also negatively affect the yield of pectin.

ii. Characterisation of Pectin Produced from Healthy and HLB Oranges

Visually, the pectin obtained from both the healthy oranges and HLB infected oranges were very similar (and comparable to all other extracted pectins) being white and polymeric (figure 3.28). ATR-IR analysis of the two pectins shows broad similarities (figure 3.26) with a slightly higher relative intensity for the COOCH_3 absorption band for healthy oranges. This could indicate a slightly higher degree of esterification for this

pectin.

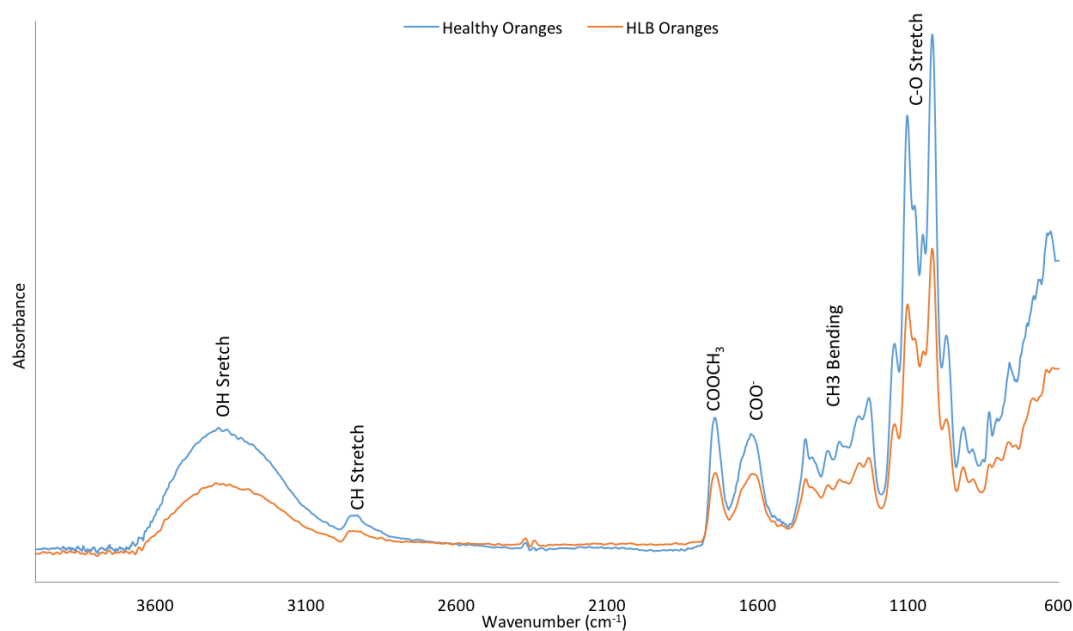


Figure 3.26 – ATR-IR of Pectin Extracted from Healthy and HLB Infected Oranges

Third, work was started into potential utilisation of the ‘agua amarela,’ or yellow water – the processing water used within several stages of the Agroterenas process. The yellow water was observed to be highly viscous, and had a high quantity of insoluble precipitate. The high viscosity might suggest the presence of pectin. This was investigated by adding ethanol to a sample of the yellow water, as outlined earlier in the lab-based pectin extraction. A precipitate formed upon addition of ethanol, and this precipitate was washed and dried like earlier pectin extracts. ATR-IR confirmed the precipitate to be pectin.

iii. Characterisation of Pectin Obtained from Yellow Water

Visually, the pectin obtained from the yellow processing water from Agroterenas was a white powder, differing from other extracted pectins by the fact it did not form polymeric sheets on freeze-drying, potentially indicating a lower average molecular mass (figure 3.28). Analysis via ATR-IR (figure 3.27) shows a much lower absorption band for COOCH_3 , perhaps indicating a very low degree of esterification, or that impurities were present. More work would have to be done characterising this pectin to confirm.

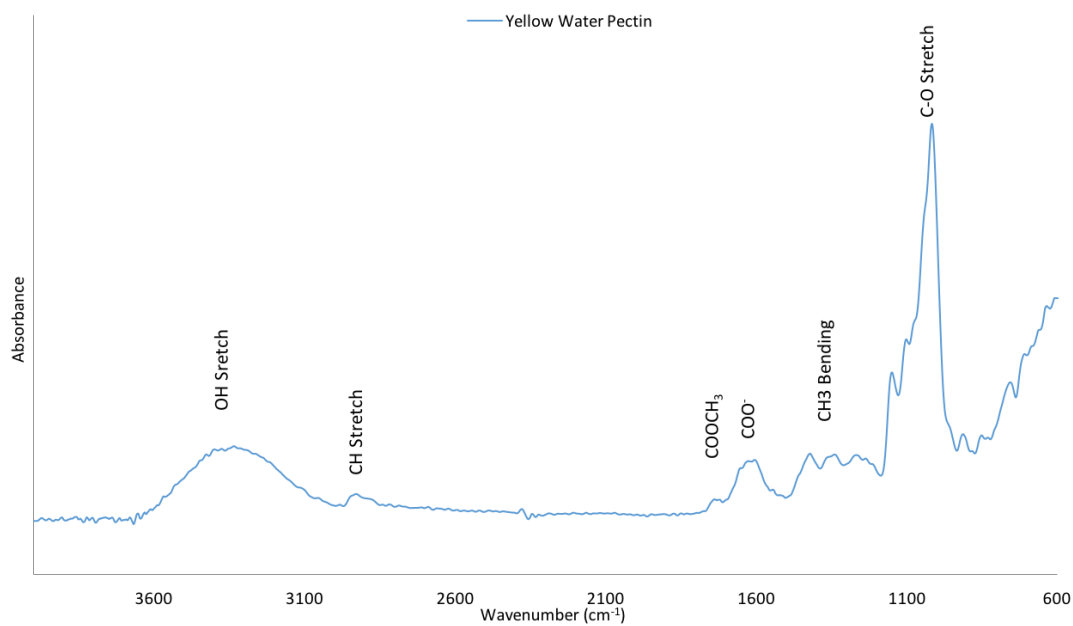
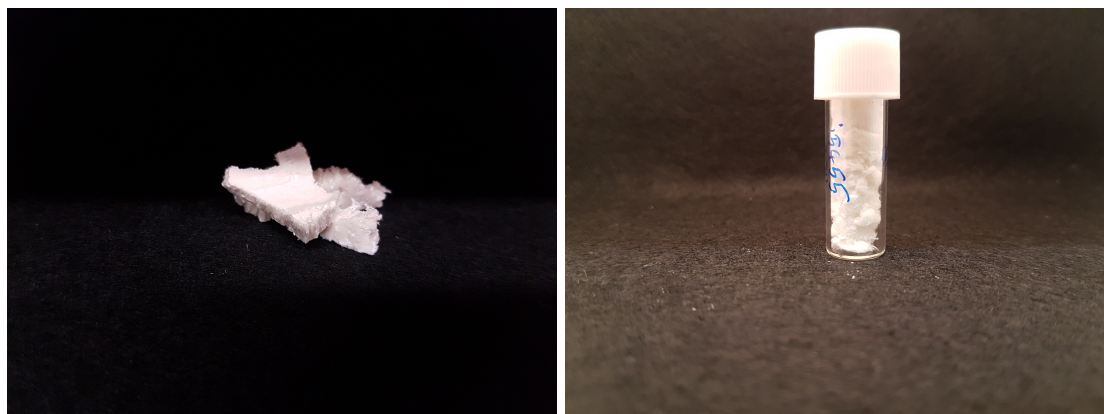


Figure 3.27 – ATR-IR of Pectin Precipitated from the Yellow Water

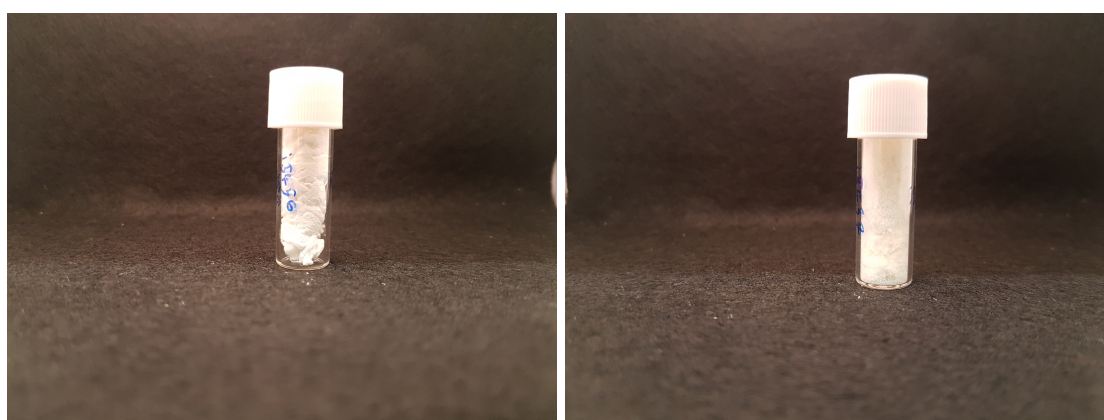
The solid precipitate present in the yellow water prior to addition of ethanol was found to be hesperidin via NMR. Unfortunately, there was insufficient time to determine the percentage of hesperidin present in the yellow water before returning to York.

Tests for presence of other flavanoids and sugars were also designed and begun but due to time constraints this work was not completed.



(a) Pectin Extracted from Bagass Supplies by Agroterenas

(b) Pectin Extracted from Healthy Oranges



(c) Pectin Extracted from Oranges Infected with HLB

(d) Pectin Extracted from Yellow Water

Figure 3.28 – Pectin Extracted from Different Brazilian Samples

3.3.6 Pilot-Scale Extraction

Commercialisation of pectin extraction requires scaling up the methodologies from the lab scale to pilot scale, and eventually to industrial scale. The exact design and nature of the microwave apparatus used are confidential and shall not be discussed in this thesis. Equipment limitations prevented removal of all the aqueous medium from the large scale microwave, resulting in yields that were lower than expected. Taking the pectin yield from an aliquot of the aqueous phase and multiplying by the known amount of aqueous phase (including the percentage that could not be recovered) a theoretical yield of pectin can be obtained for a more optimised microwave rig.

Taking several aliquots from several different runs gave an average theoretical pectin

yield of 12.3% on a dry weight basis, and while this is lower than the yields observed at the lab scale, full optimisation on the large scale microwave has not been performed. This yield was obtained using the conditions given in table 3.10.

Table 3.10 – Pectin Scale up Conditions

WOP:Water Ratio	5:16
Temperature	95 °C
Power	6 kW
Flow Rate	260 L min ⁻¹

3.3.6.1 Pilot-Scale Pectin Characterisation

i. ATR-IR Characterisation

ATR-IR spectroscopy was performed on the pectin obtained from the scale-up experiments. Figure 3.29 shows the spectra. The spectra aligns well with other extracted and commercial pectin with the distinctive absorptions at 1700-1740 cm⁻¹ and 1350-1450 cm⁻¹ both being present.

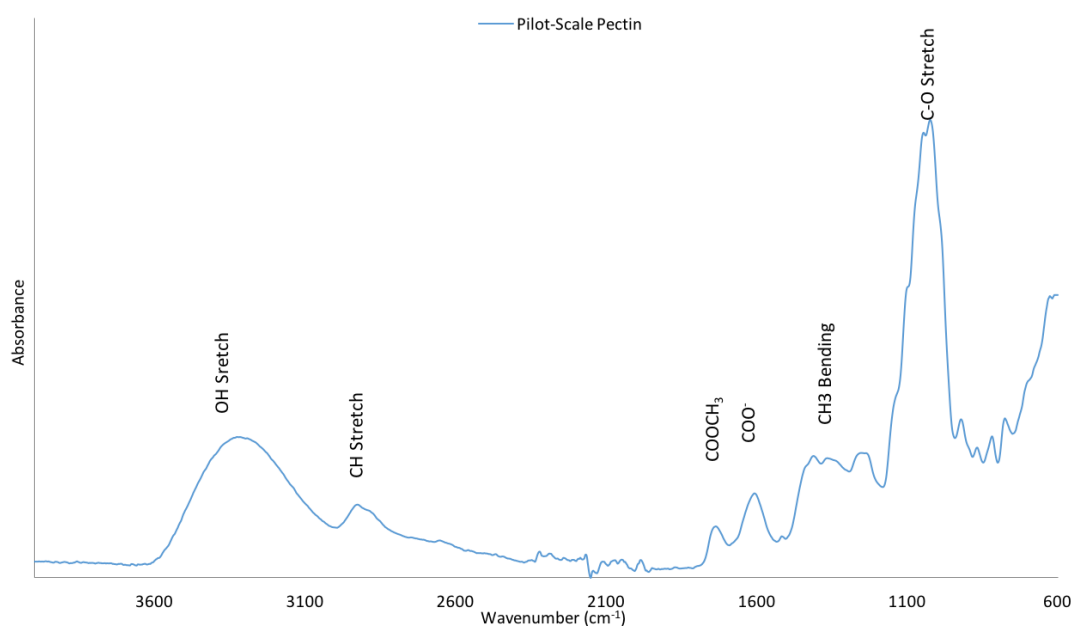


Figure 3.29 – ATR-IR of Pectin Extracted at Pilot Scale

ii. Quality Tests

Quality tests were performed on the pectin obtained from the scale-up experiments. The pectin obtained passed in all criteria tested, as shown in table 3.11. Degree of esterification was also calculated via solid state NMR and confirmed via titration, as described in the experimental section (2.1.3.3). The measured value of 72.8% means the extracted pectin can be classified as high methoxyl (HM) pectin.

Table 3.11 – Quality Tests for Pilot-Scale Pectin

Test	Pass Criteria	Experimental Result
Loss on Drying	<12%	8.98%
Residual Solvents	<1%	Trace
Degree of Esterification	Class Dependent	72.8%
Galacturonic Acid Content	>65%	72.3%
Total Insolubles	<3%	0.29%
Nitrogen Content	<2.5%	0.29%

While microwave extraction at pilot scale has been proven possible, optimisation of the extraction conditions and further exploration of the effect of scale-up on pectin quality must be carried out before this system can be utilised at an industrial scale. However, this work demonstrates that high-methoxyl pectin of high purity can be extracted on a large scale via acid-free microwave-assisted extraction. The future of this line of work is detailed in the general conclusions and future work section.

3.4 Conclusions

The work conducted in this chapter has proven the potential for a complete citrus waste biorefinery using acid-free microwave extraction technology. Through the use of green chemistry approaches, a biorefinery with four distinct products has been designed and tested.

Citrus oil extraction via microwave-assisted steam distillation has been proven effective, with yields of up to 2.4% on a dry weight basis. Citrus oil quality was comparable, and in some cases better than citrus oil obtained via conventional steam distillation. The experimental parameters were optimised to identify a method that maximises yield while minimising power input and processing time.

Pectin extraction is conventionally performed using mineral acid. This work has proven the feasibility of an acid-free microwave-assisted extraction method. Maximum pectin yield obtained from citrus waste was 15.36% on a dry weight basis and characterisation of the product showed that it was a high-methoxyl pectin with industrially desirable gelation properties. The extracted pectin passed all standard food industry tests. It was also found that hesperidin could be isolated from the sample, adding another product into this biorefinery scheme.

The cellulosic residue remaining after both microwave treatments was tested for water binding capacity, with the potential for application as a rheology modifier in food. The water-binding capacity was comparable to industrially leading citrus fibre products in both cold- and hot-sheared applications, and was comparable to other commercial citrus fibre products in cold mixed applications, confirming its usefulness.

A three-month placement in Brazil was also undertaken during this project in order to engage with citrus juicing company Agroterenas, mapping their current industrial process and testing real-world citrus waste in the proposed biorefinery system. Bagasse obtained from Agroterenas underwent pectin extraction via the acid-free microwave-assisted method, giving a yield of 21.19%. Repeat experiments would have to be performed before this value was certain, but this result suggests that the proposed biorefinery system could work well on industrial samples. Another aim of the Brazilian partnership was exploration of the impact of disease on pectin yield. With this in mind

oranges infected with HLB were tested alongside healthy oranges. It was found that the pectin yield of oranges infected with HLB was reduced by 38% indicating that infected oranges are undesirable for pectin extraction as well as juicing. Exploratory work was also performed on the yellow processing water used by Agroterenas in the juicing process; this process water was found to contain small amounts of pectin and also had a large quantity of hesperidin, confirming findings by Agroterenas.

Finally, initial scale up tests were performed on bespoke microwave equipment with promising results. Pectin was successfully extracted, precipitated and dried, and the quality of the extracted pectin was similar to that of pectin extracted at lab-scale. Further optimisation of the equipment and method must be performed to maximise yield, allow for continuous flow processing and minimise energy usage.

Citrus waste is a challenging global problem, not only due to the large scale of the industry, but because the waste is difficult to handle safely. The work performed during this project has shown that a microwave-based biorefinery for orange waste is an attractive prospect for future citrus waste processing.

Chapter 4

Protein from Potatoes

1. Dugmore, T. I.; Clark, J. H.; Bustamante, J.; Houghton, J. A.; Matharu, A. S. *Top. Curr. Chem.* **2017**, *375*, 46.
2. Matharu, A. S.; de Melo, E. M.; Houghton, J. A. *Bioresource Technol.* **2016**, *215*, 123–130.

4.1 Introduction

The potato is a tuberous crop from the Solanaceae family. It originated in the Andes and was introduced to areas outside the Andes some 400 years ago. There are roughly 5000 different varieties worldwide, the main grown species is *Solanum tuberosum* which is a tetraploid with 48 chromosomes.¹³³ It is the world's fourth-largest food crop, following maize, wheat, and rice, it is therefore the largest non-grain food crop grown globally.¹³⁴ Within developed countries potatoes make up roughly 130 kcal of the average person's daily calorie intake and globally accounts for roughly 2% of the world's energy supply.¹³³

4.1.1 Production and Waste

Global production of potatoes reached 370 million tonnes in 2013 (figure 4.1), with the UK alone producing 5.5 million tonnes.¹³⁵ Potato production has seen a gradual increase over the past 15 years from roughly 270 million tonnes in 1990 to 370 million tonnes in 2013.

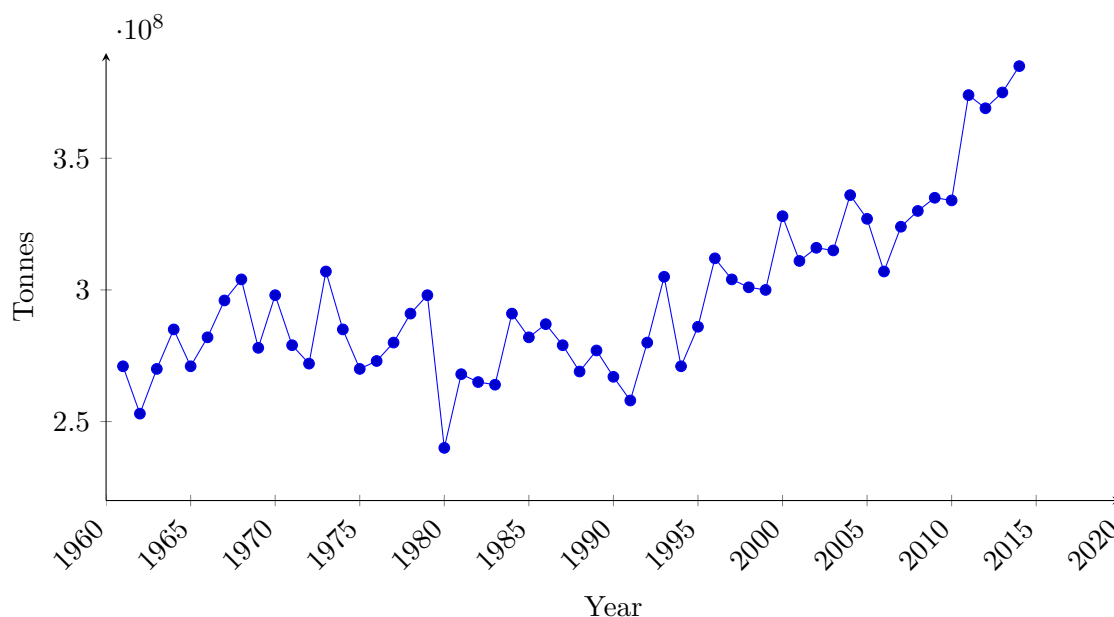


Figure 4.1 – Global Potato Production¹³⁵

As with all agricultural products potatoes suffer losses at many stages of the process from farm to fork, the main causes of loss from the food supply chain are summarised in table 4.1.

Table 4.1 – Typical losses from potato production¹³⁶

Loss Stage	Percentage Loss
Field Loss	1-2
Grading Loss	3-13
Storage Loss	3-5
Packing Loss	20-25
Retail Waste	1.5-3

Potatoes are the UK's fourth most produced crop¹³⁵ and when considering the amount of waste created in the food supply chain it can be seen that valorisation of potato waste is an important consideration for the UK's waste streams as well as potentially being a lucrative source of raw materials such as starch and protein.

4.1.2 Potato Valorisation

Potato valorisation has been the subject of extensive scientific research over the last decade or so,^{137,138} with companies such as Cyvex and Solanic now commercialising this research, by producing a range of potato-based products. A common valorisation route for lower grade potatoes is drying and grinding into 'potato flakes,'^{139,140} which is a common practice to produce a stable, long-life potato based product for use in applications such as instant mashed potato. This methodology of drying and grinding potatoes into a flour/flake substance is widely used globally.¹⁴¹ This is, however, a relatively low value valorisation route.

As shown in table 4.2, potatoes are a nutritional source of starch, carbohydrates, fibre and proteins. Starch comprises roughly 19% of the potato by weight; and proteins, roughly 2% by weight.¹⁴²

Table 4.2 – Basic Nutritional Value for Potato¹⁴²

Nutrient	Raw Potatoes (g/kg)
Water	781.0
Total Nitrogen	3.1
Protein	19.0
Fat	1.0
Starch	187.0
Carbohydrates	196.0
Fibre (Total)	28.0
Sugar (Total)	9.0
Energy	820

The proteins within potato include protease inhibitors which have been shown to have an appetite suppressing effect on mammals.^{143,144} Protease inhibitors, are a new development within the scope of potato valorisation with companies like Cyvex and Kemin Health beginning to market products such as Solthin and Slendesta, which are comprised of PI2 (protease inhibitor 2 from potatoes) as appetite suppressing supplements, to help target the global obesity epidemic.¹⁴⁵ A short review on the current state of global obesity and comments on the economic effects is included.

4.1.3 Obesity

Obesity is a serious problem in the modern world, therefore the appetite suppressing potential of protease inhibitors is of significance to the health/diet sector. In 2010, it was estimated that 3.4 million deaths could be attributed to obesity, with 3.9% life-years lost and 3.8% of disability-adjusted life-years. The proportion of adults classed as overweight (BMI of 25 kg/m² or above) and obese (BMI of 30 kg/m² or above) combined increased by 27.5% in adults and 47.1% in children from 1980-2013 with 857 million individuals being classed as overweight or obese in 1980 increasing to 2.1 billion in 2013. While the rate of increase has slowed down in the last decade, there is no evidence of it decreasing.^{146,147}

The increase in overweight and obese persons globally is represented in figure 4.2.

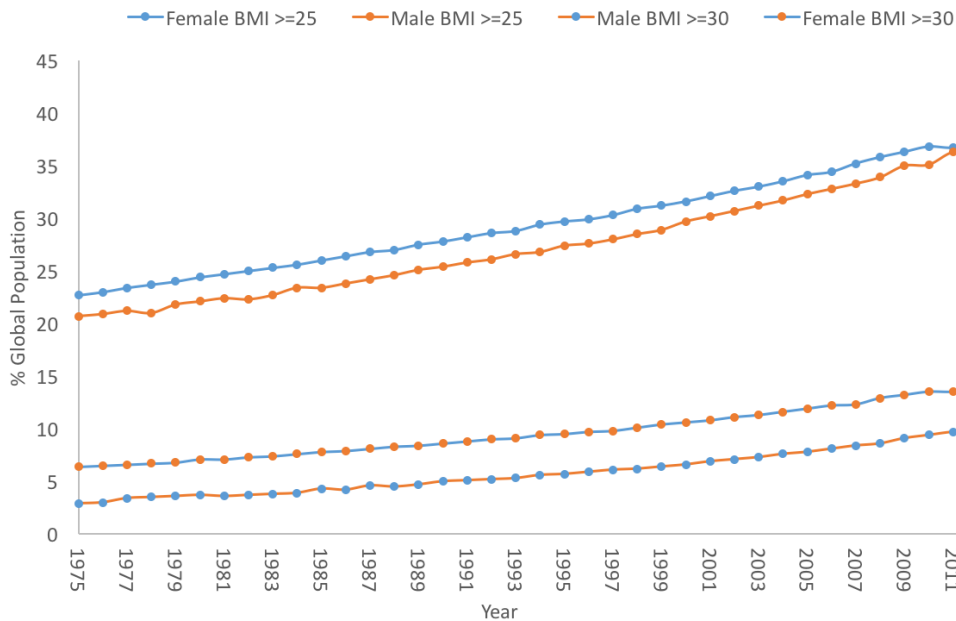


Figure 4.2 – Prevalence of overweight and obesity in over 20 year olds from 1975-2014¹⁴⁸

When obesity is compared to other health damaging risk factors, such as smoking and excessive alcohol consumption, it reveals an interesting variability between how these three risk factors negatively affect the quality of life in an individual when approaching the end of life. Of the three, smoking has the largest effect on life expectancy with an average reduction of 4.0 years at age 55, excessive alcohol consumption reduced life expectancy by 2.8 years, and, interestingly, obesity only showed a reduction of 1.4 years. This only tells half the story however, because if years lived with disability are analysed for these three risk factors a different trend is observed, with smoking having 3.8 years of disability affected life after age 55, excessive alcohol consumption 3.1 years, and obesity having the highest at 5.9 years lived with disability.¹⁴⁹ So while obesity is maybe not the highest risk factor for mortality, it does heavily influence quality of life and cause myriad other co-morbid conditions.

The most effective method for weight loss remains restriction of energy intake, and so obesity is most commonly treated with diet and exercise, but while theoretically the best approach, this often fails due to patient non-compliance. The two FDA approved drug therapeutics for obesity (sibutramine and orlistat) have a 2-year persistent rate of

less than 2%, this shows that the development of new methodologies for weight loss and food intake control without side effects are needed. Protease inhibitors are an attractive alternative as they are already present in food and therefore can be marketed as a ‘food supplement’ as opposed to a drug, which simplifies the legislative procedures required when producing this material, as it does not require as stringent FDA approval.¹⁵⁰

4.1.3.1 Economic Burden

Not only does the rapid increase in obesity over the past century cause issues for average life expectancy and health, it also has a detrimental economic effect on the countries health-care system. Obesity has recently been officially recognised as a disease in many countries, this puts greater emphasis on the health-care system confronting obesity to negate or minimise its adverse health effects. While there is undoubtedly a large financial cost associated with obesity in and of itself, co-morbid conditions directly related to obesity have to also be taken into account, chronic conditions such as myocardial infarction, stroke, asthma, hypertension, cancer and type 2 diabetes have all been shown to be promoted by obesity.^{147,151,152} Due to the wide spread effect of obesity on not only the subjects health, but also their susceptibility to other diseases, predicting the financial burden that this disease has on society is problematic, with different studies using different methodologies with resulting differences in the predicted cost per capita and nationwide costs.

Kim *et al.* analysed the results and methodologies from 12 studies predicting the economic cost of obesity in the USA. The average annual medical spending attributed to an obese individual was found to be on average \$1901 (with values ranging from \$1239-\$2582 depending on the study) in 2014, and with the prevalence of obesity within the USA this results in a national spending of \$149.4 billion annually.¹⁵¹

4.1.4 Potato Starch

Potato starch production is an established industry.¹⁵³⁻¹⁵⁵ Companies in Denmark have been producing potato starch since the 1900s, currently Denmark is the largest producer per capita of potato starch in the world with production reaching around 175,000 tonnes in 2012, 75% of potatoes grown in Denmark are grown for industrial

processing,¹⁵⁶ rather than human consumption. Starch is commonly used in food applications, industrial processes, in pet and animal feed, in paper production and as a base for natural polymers.^{155,157,158}

The current starch production process produces large volumes of aqueous waste which contain a high concentration of protein,¹⁵³ and due to increasing global demand for vegetable proteins, protein extraction from potatoes is now becoming increasingly important.^{143,159,160}

4.1.5 Vegetable Protein Market Analysis

The vegetable protein market has seen a marked increase in recent years and is predicted to continue to rise, with the meat substitute market alone being expected to reach \$5.81 billion by 2022. There is also concern growing over the amount of vegetable protein needing to be incorporated into animal feed to allow for the increased food demand. The last ten years has seen a rise of over 50% of the amount of protein needed for animal feed, amounting to over 250 million tonnes annually, with a corresponding rise in price for these vegetable based proteins.

Within the vegetable protein market, protein quality is often the most important feature because, if attempting to replace protein obtained from meat or dairy, there are certain standards that must be adhered to. Table 4.3 shows comparisons of different proteins, including potato protein, using different quality indexes.

Table 4.3 – Protein Quality from Different Plant and Animal Sources¹⁶¹

Quality Index	Potato Protein	Soy Protein	Wheat Protein	Rice Protein	Casein	Beef	Poultry
CS	57-69	42-48	30-49	47	54	69	59-63
EAAI	48-83	71	64	79	80	80	72-78
BV	65-94	64-80	66	80	80	70-75	77
PER	0.95-2.3	1.3-2.3	0.77	1.76	2.5-2.9	2.1-2.5	2.1-2.5
NPU	60-73	61-64	45-51	–	67-72	68-79	68-77

As can be seen from table 4.3, potato protein, although having a large variation in quality, generally scores highly in the quality index. It is generally better than other vegetable protein sources such as soy, wheat and rice, and in some cases can be comparable to animal protein sources such as beef and poultry. This high quality makes potato protein an attractive market opportunity as a high-end vegetable protein.

The definitions for the different protein quality indexes and how they are found are detailed below.¹⁶²

CS – Chemical Score

Finding the chemical score for a given protein requires the content of each essential amino acid to be expressed as a percentage of the content of the same amino acid in a standard protein (most commonly egg protein). The amino acid with the lowest percentile is identified as the limiting amino acid and this percentage is given as the proteins chemical score.

EAAI – Essential Amino Acid Index

The essential amino acid index is calculated as the geometric mean of the ratios of the essential amino acids found in the sample protein to those in a standard protein (most commonly egg protein). More on the EAAI score of potato protein is given later in this chapter.

PER – Protein Efficiency Ratio

Protein efficiency ratio defines the weight gain per weight of sample protein eaten, usually measured in rats.

BV – Biological value

The biological value of a protein is defined as the proportion of absorbed nitrogen that is retained for maintenance and/or growth. It is usually calculated via equation 4.1:

$$BV = \frac{[I - (F - F_k) - (U - U_k) - (S - S_k)]}{[I - (F - F_k)]} \quad (4.1)$$

Where:

I – Intake Nitrogen

F – Faecal Nitrogen

F_k – metabolic nitrogen (endogenous faecal)

U – urinary nitrogen

U_k – endogenous urinary nitrogen

S – Integumental and miscellaneous nitrogen

S_k – Obligatory integumental and miscellaneous nitrogen

NPU – Net Protein Utilisation

Net protein utilisation is defined as the proportion of nitrogen that is retained after consumption. It is therefore a product of the biological value and digestibility of the sample protein. It can be found using the equation 4.2:

$$NPU = BV \times D \quad (4.2)$$

Where digestibility D is defined using the equation 4.3.

$$D = \frac{[I - (F - F_k)]}{I} \quad (4.3)$$

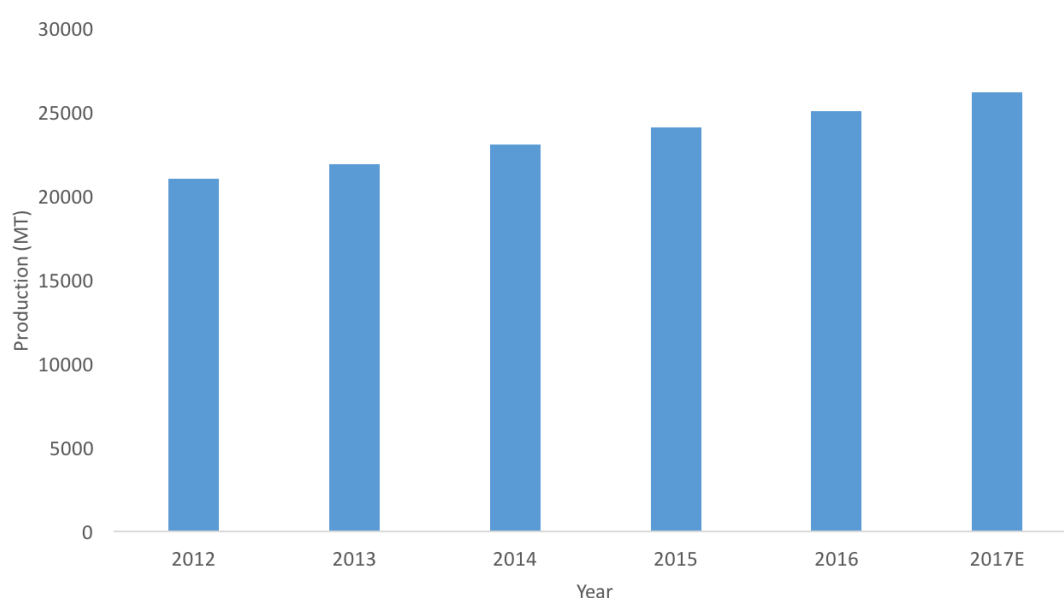
4.1.5.1 Potato Proteins Market Analysis and Applications

The global potato protein market value reached \$73M in 2016 and is predicted to increase to \$93M by 2022 with a compound annual growth rate (CAGR) of 4.21% over this time period, based on an average growth rate of 3% CAGR between 2012-2016.¹⁶¹

Global potato protein production (table 4.4 and figure 4.3) reached 25,064 MT in 2016, roughly 75% of which comes from Europe with China and North America producing 14% and 7% respectively. From 2012 to 2017 (estimated) the global potato protein production has increased by roughly 19%.¹⁶¹ This number is likely to continue to increase over the next decade due to the increased demand for vegetable based proteins.

Table 4.4 – Potato Protein Production (MT) by Region (2012-2017)¹⁶¹

Region	2012	2013	2014	2015	2016	2017 estimated
North America	1,384	1,456	1,528	1,591	1,667	1,746
Europe	15,858	16,453	17,343	18,076	18,771	19,541
China	2,779	2,937	3,066	3,239	3,408	3,590
India	265	276	288	301	317	331
Other	749	780	820	861	901	950
Global	21,035	21,902	23,045	24,068	25,064	26,158

**Figure 4.3** – Global Potato Protein Production¹⁶¹

Potato protein can be broadly separated into three classes; low-purity potato protein (less than 70% protein content), medium-purity potato protein (between 70 and 80% protein content), and high-purity potato protein (above 80% protein content). Currently, the most produced class is the medium-purity, with roughly 61% of the total potato protein produced globally falling within this classification. The high-purity potato protein accounts for roughly 24% of the total global production and low-purity roughly 15%.¹⁶¹ If revenue market share is compared for each of the three potato protein classes, the

percentage of the market share relating to high-purity protein rises to 33%, low-purity falls to 6% while medium purity potato protein remains largely the same, accounting for 61% of the revenue market share.¹⁶¹

While by far the highest use for potato protein currently is in the feed industry with almost 85% of the global potato protein market share being devoted to feed applications, there is also myriad higher value applications that potato protein lends itself to within the human food industry. The properties of the protein extracted from potatoes, namely its foaming, gelation and emulsion abilities, allow this protein to be incorporated into products such as ice creams, mousses, whipped cream, crème fraiche, bavarois and cappuccinos. Its nutritional profile also makes in an attractive addition into more products including yoghurt, sour cream, custard, low-fat spreads, quiche fillings, mayonnaise and salad dressings. Potato protein usage within the food industry reached 3779 MT in 2016 and is predicted to reach 4826 MT in 2022 according to current growth trends.¹⁶¹

4.1.6 Potato Protein Quality and Extraction

Potato protein is considered higher quality than most other plant or vegetable proteins due to the relatively high concentration of lysine.^{143,161,163} Lysine is an essential amino acid that the human body cannot produce and therefore must be obtained through diet. Lysine is not commonly present in abundance within proteins available from plant crops including cereals.^{143,164} It has been stated that potato protein quality is roughly 70% that of whole egg protein, with respect to the amino acid composition using Essential Amino Acid Index (EAAI) estimation.^{164,165} See table 4.5 summarising the amino acid profile for potato protein.

Table 4.5 – Amino Acid Profile for Potato Protein with Bold Showing Essential Amino Acids¹⁶⁶

Amino Acid	Unit	Average
Alanine	% of Protein	3.6
Arginine	% of Protein	3.5
Aspartic Acid	% of Protein	16.7
Cystine	% of Protein	0.9
Glutamic Acid	% of Protein	16.4
Glycine	% of Protein	3.1
Histidine	% of Protein	1.6
Isoleucine	% of Protein	3.5
Leucine	% of Protein	5.1
Lysine	% of Protein	4.9
Methionine	% of Protein	1.0
Phenylalanine	% of Protein	3.8
Proline	% of Protein	2.8
Serine	% of Protein	3.5
Threonine	% of Protein	3.8
Tryptophan	% of Protein	1.5
Tyrosine	% of Protein	4.2
Valine	% of Protein	5.1

Protein Recovery from potato fruit juice (PFJ) has had extensive research performed, and while the extraction methodology, as stated earlier, is already part of the established starch process, the precipitation conditions have been shown to have an effect on the properties of the protein recovered. Some of the precipitation methods explored within the literature are shown in table 4.6, with comments on the properties of the extracted protein. Table 4.6 gives the maximum extraction yield, purification factor and the proportions of the different proteins for each precipitation method. As can be seen the highest yield is obtained from the ammonium sulphate precipitation with a value of 98.8%, the protein recovered has a good purification factor (2.99) although the best purity is obtained using FeCl_3 as the precipitation agent (6.24).

Table 4.6 – Different Protein Yields and Properties with Regard to Precipitation Method¹⁴³

Precipitation agent	Max Protein Yield (%)	Purification factor	Patatin (%)	PI 25-21 kDa (%)	PI 20-15 kDa (%)	PI <15 kDa (%)	HMW Proteins (%)
Thermal/Acid	90.2	0.74	37.9	0.0	20.2	31.3	10.7
Acid	64.7	1.26	11.1	9.9	15.3	17.4	46.4
FeCl_3	75.2	6.24	21.7	18.7	23.2	34.3	2.0
MnCl_2	16.8	1.52	20.4	0.0	30.9	44.2	4.6
Ethanol	55.2	3.79	37.7	8.0	22.4	26.5	5.4
$(\text{NH}_4)_2\text{SO}_4$	98.9	2.99	31.1	7.6	23.7	26.3	11.3

As can be seen from table 4.6, potato protein has three main components: patatin (the most abundant protein found in potatoes), protease inhibitors (PI) and high molecular weight (HMW) proteins.

There are other methods for gaining a powdered protein from an aqueous medium, one such technique is freeze drying or lyophilization. Drying the protein via freeze drying has the advantage of not having elevated temperatures associated with it, this means that protein denaturation is kept to a minimum.^{167,168} One of the disadvantages of freeze drying, or any drying technique, is that it is not selective, meaning that the product recovered from drying includes every soluble constituent within the aqueous sample, be it protein, sugar, polyphenolic etc. In consideration of this, a suitable purification step to compliment the drying step should be employed to ensure protein purity.

4.1.7 Protein Purification Methods

General methods for protein purification are reviewed, these are applicable to vegetable protein (eg. potato protein) purification.

4.1.7.1 Ultrafiltration

Ultrafiltration is a method of separating macromolecules based on their size,¹⁶⁹ it is most commonly performed using a porous membrane and uses pressure within the system to force the liquid sample through the membrane allowing small macromolecules through and retaining the larger macromolecules.¹⁷⁰ Ultrafiltration membranes have a 'molecular weight cut-off point', but due to there always being a range of pore sizes present within membranes, this cut off point is an averaged value so it is important to choose a molecular weight cut-off point sufficiently different to the desired molecule for purity to be achieved.¹⁷¹ The method can be seen as analogous with the principles of gel filtration, but with only two resulting fractions, one above the molecular cut-off point (retentate) and one below the molecular weight cut-off point (filtrate). It is, therefore, less discriminating than gel filtration but works very well when removing two components with very different molecular weights (such as proteins from low molecular weight salts/flavonoids etc.) or when working with large volumes as it is easily scaled up.

Ultrafiltration is most commonly used as a method for concentrating a dilute protein solution, this is done by choosing a molecular weight cut-off point that allows all non-protein molecules through, allowing for the removal of water while retaining the protein in a reduced-volume solution. This method does not, however, completely remove impurities from the solution as it is limited by the volume of the solution, so even low molecular weight impurities are not entirely removed. Diafiltration is a method that overcomes this problem, it involves replacing any volume of solution lost with either pure water, or buffer, meaning that the concentration of the protein remains the same, allowing for complete removal of impurities present.¹⁶⁰

There are techno-economic disadvantages to ultrafiltration however, if solid particulate matter is present within the solution then membrane fouling can easily occur,¹⁵⁹ lowering

the life time of the membrane and reducing the efficiency of the process. There can also be issues when separating proteins. Protein aggregation at a certain concentration may lead to membrane fouling and loss of protein within the solution.

4.1.7.2 Chromatography

If a protein is required to be purified from the protein pool in a solution, then ultrafiltration is no longer the best technique to use and often chromatography is employed.¹⁷² Chromatographic purification of proteins is most commonly based on two properties of the protein in question; its molecular size and isoelectric point, or the proteins net charge.

i. Anion Exchange

Anion exchange chromatography separates substances based on their charge utilising an ion exchange resin that commonly contains positively charged groups and hence binds to negatively charged substrates.¹⁷³ This works well for proteins due to the fact they usually have a charge associated with them. Proteins are usually dissolved in a high pH buffer to allow for the maximum of negatively charged species to be present and then run through the anion exchange column. Once bound to the column, there are two methods for eluting the protein off. Firstly, by gradually increasing the salt concentration within the elution buffer, meaning the negatively charged ion of the salt competes with the protein for the positively charged binding sites eventually leading to elution of the protein. Secondly, by gradually decreasing the pH of the elution buffer resulting in more positively charged proteins which eventually get released from the resin.^{171,173} The elution time for both methods rely entirely on the negative charge on the protein, and this is then related to the protein isoelectric point, or the pH at which the net charge of a protein is zero.¹⁷⁴

ii. Size Exclusion

Size Exclusion Chromatography (SEC) is a technique for separating proteins based on their size, this technique is analogous with ultrafiltration. Ultrafiltration allows small molecules through and not larger molecules, essentially meaning that you get two fractions: one below the molecular cut off and one above. Whereas, size exclusion

chromatography allows for full separation of proteins based on size. This is achieved by passing the protein solution through a highly porous stationary phase with a large range of pore sizes, smaller proteins can enter into more pores and so have a slower elution time to that of larger proteins which cannot enter into as many of the pores. This allows for fractions of the elute to be collected and only the protein of interest to be concentrated down for further analysis/processing. One important requirement for SEC is that the protein not interact with the stationary phase, otherwise protein would be held in the resin rather than eluting off. SEC is often run in a simple buffer with no change in eluting buffer throughout the run.

4.1.8 Specific Proteins of Interest – Protease Inhibitors

As mentioned previously, potato proteins have a specific group of inhibitors which are of significance to the health and diet industry¹⁷⁵ for their appetite suppressing effects on mammals,¹⁴⁷ they are serine protease inhibitors which show specific inhibition of trypsin and chymotrypsin.

Protease inhibitors are a class of proteins that inhibit specific proteases: endopeptidases and exopeptidases. The inhibition is caused by the protein forming a complex with the protease, therefore inhibiting their proteolytic activity. Protease inhibitors are usually specific to one of the four mechanistic classes of proteolytic enzymes (serine, cysteine, aspartic and metallo-proteases), with the majority being active for serine proteases; they are usually of low molecular weight (5-25 kDa).

It has been hypothesised that protease inhibitors are present in plants as a defence mechanism against insects; this is due to the effect that protease inhibitors have on the digestive physiology of insects (and other animals).^{176–180} Animals usually require proteolysis to degrade proteins into the constituent amino acids for use within the body, therefore, protease inhibitors can affect the growth and development of animals eating food with high levels of protease inhibitors. This is less of a problem regarding human consumption as most of the food with high levels of protease inhibitors are cooked, which denatures and, therefore, deactivates the inhibitors. Trypsin inhibitors (a common family of protease inhibitors) also have adverse effects on animals due to the fact that they interfere with the degradation of monitor peptides which regulate the

release of a polypeptide hormone called cholecystokinin (CCK) which in turn controls several processes, including gall-bladder contraction, gut mobility, pancreatic secretions and appetite.¹⁸¹ This can be a serious problem if protease inhibitors constitute a large part of an animals diet causing several problems involving the pancreas and gut and loss of appetite potentially leading to starvation and hence death.¹⁷⁸ The antinutritional nature of protease inhibitors is an effective defence mechanism against insects, particularly when the plant has a high level of protease (trypsin) inhibitors, when inhibitors are present at over 10% of the insects diet they become toxic.

Potato protease inhibitors are a major family of inhibitors present in nature and they have two main groups, protease inhibitor I (PI1) and protease inhibitor II (PI2). PI1 has only chymotrypsin inhibition activity while PI2 has both chymotrypsin and trypsin inhibition activity, it has been proven by Johnson *et al.* that trypsin inhibition is responsible for the inhibition of growth within insects.

Within humans, protease inhibitor II acts in broadly the same way as with insects; inhibiting trypsin and chymotrypsin which are responsible for the digesting CCK. This results in an elevated level of CCK in postprandial plasma which in turn reduces appetite. This phenomenon has been proven to occur in numerous animal and clinical studies,^{150,175,182–184} and has been quoted to have no short-term adverse effects.¹⁷⁵ Studies have not been carried out on the long-term health benefits/issues associated with regular consumption of PI2 at concentrations capable of inducing this appetite suppressing effect in humans and so requires further investigation.

4.1.9 Potential Potato Biorefinery

Starch and protein extraction from potato are complimentary processes. This is due to the fact that the aqueous waste from potato starch extraction already contains the majority of the protein present within potato tubers. This makes protein extraction not so much a separate extraction step, but more a waste treatment method, removing protein from the aqueous medium, which not only makes the waste water easier to deal with (showing reduced foaming and microbial issues) but also adds potato protein as a product into the process line.

This integrated biorefinery approach to treatment of either feedstock potatoes or potato waste can be designed as a process line as shown in figure 4.4, with the classical starch extraction running down the left side of the figure and the protein extraction step and waste treatment steps on the right.

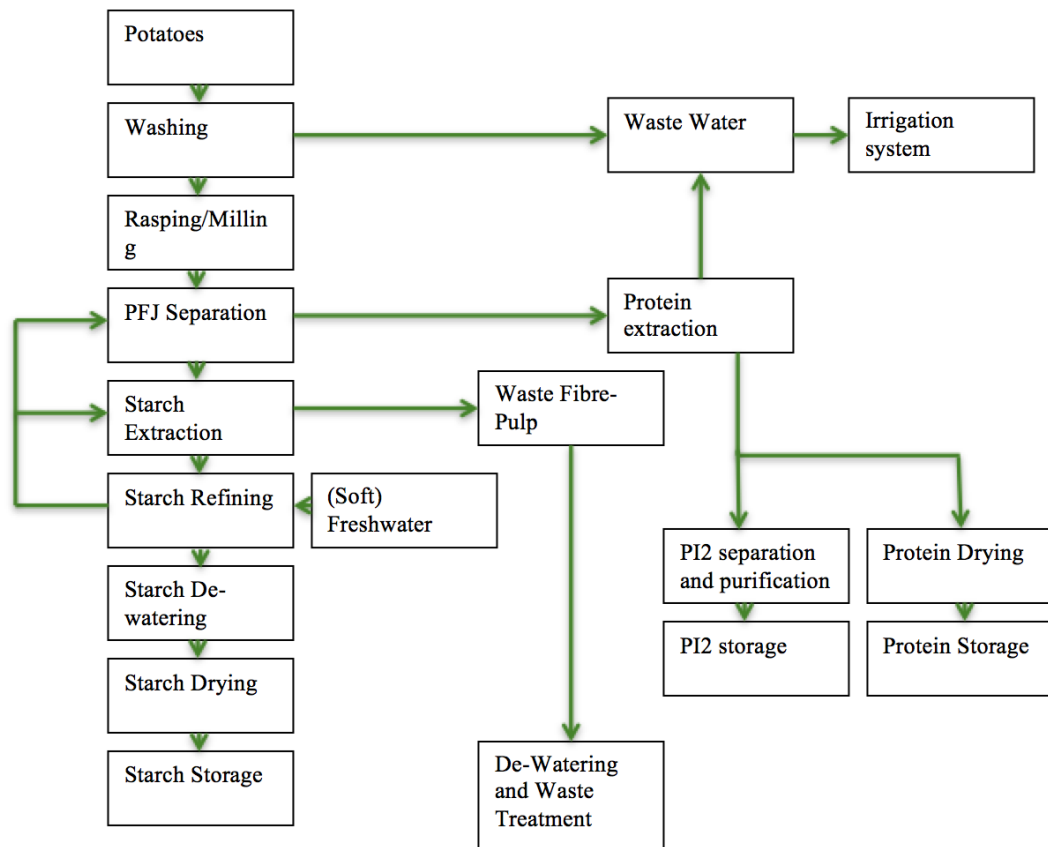


Figure 4.4 – Potential Potato Biorefinery¹⁵³

4.1.10 Research Opportunities

Population increases are putting strain on the current food supply chain, and the need to convert from the current heavily animal-protein reliant dietary tendencies to a more vegetable-protein based diet is going to become increasingly obvious within the next few decades. Potato protein extraction is an attractive addition to established starch production industries as well as a way to valorise potato waste produced throughout the food supply chain, this is due to potato proteins high quality and relatively high abundance.

Advanced uses for constituents within the potato protein is also of interest as use of their anti-nutrition, or appetite suppressing properties could have high-end applications within the health and fitness industry and add more economic drive for a biorefinery scheme to be applied to potato waste/starch industry water waste.

4.2 Specific Aims and Objectives

The aims within this chapter focus on sequential extraction of starch and protein from potato tubers utilising ultrafiltration as a crude purification methodology for the extracted protein. Followed by full identification of the proteins present via SDS-PAGE and MALDI-TOF/TOF-MS analysis. Further purification of specific protease inhibitors present in the crude potato protein due to their documented appetite suppressing effect should be attempted. Identification of protease inhibitors, complexation studies between extraction protease inhibitor and target enzymes, as well as initial crystallisation studies should also be attempted.

4.3 Results and Discussion

4.3.1 Protein Yield

Protein extraction was carried out from the aqueous phase left over from starch extraction as described in the experimental section (2.2.2) with rough yields of 1.1% being obtained. It was found that care had to be taken to thoroughly remove all solid particulate matter prior to ultrafiltration to avoid fouling of the membrane. Optimisation of the protein extraction was not the aim of this thesis as characterisation, identification and purification of the different fractions were the main aims, so no more analysis will be performed on protein yields from waste potatoes.

4.3.1.1 Protein Characterisation

i. SDS-PAGE Analysis

SDS-PAGE analysis was performed on six potato varieties to determine the different protein distribution of each (figure 4.5).

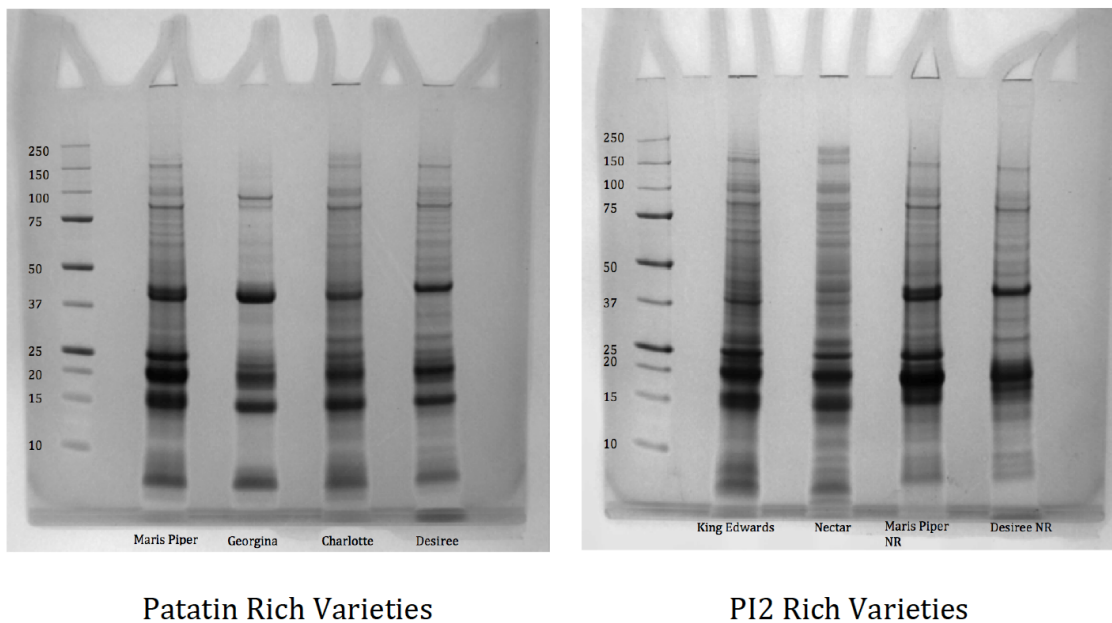


Figure 4.5 – SDS-PAGE of the Protein Extracted from the Different Varieties

The two areas of most interest within the SDS-PAGE are the band at roughly 40 kDa and the bands centred around 20 kDa, these represent patatin and protease inhibitors respectively. Patatin is reported to be the most abundant protein found within potato tubers and as can be seen from the SDS-PAGE images there are a large amount of patatin present within the varieties Maris Piper, Georgina, Charlotte and Desiree. Interestingly the other two varieties, King Edwards and Nectar, have a much lower concentration of patatin and therefore a proportionally higher protease inhibitor content.

ii. Protein Identification via Proteomics

Proteomic analysis was performed on the four bands centred around 20 kDa (the area of interest) as shown in figure 4.6, the results of the proteomic analysis are shown in table: 4.7.

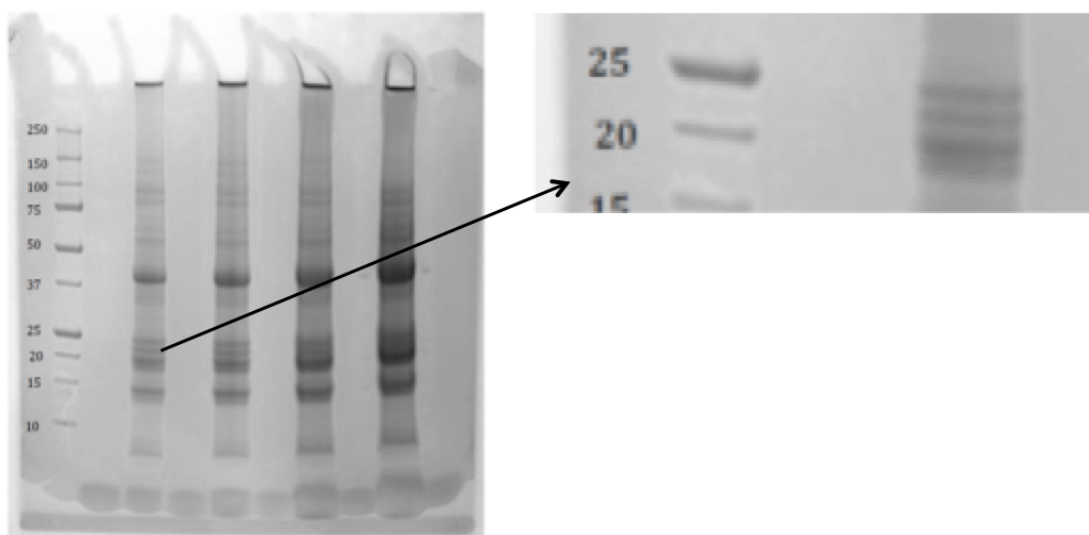


Figure 4.6 – Four Bands Analysed Through Proteomics Assigned Band 1-4 from Bottom to Top

Table 4.7 – Proteomics Analysis of Potato Protein

Band	Protein Match	Molecular Weight of Protein (kDa)
1	PCPI 8.3=cysteine proteinase inhibitor	20.305
1	Cysteine protease inhibitor 9	25.008
1	Aspartic protease inhibitor 8	24.688
2	PCPI 8.3=cysteine proteinase inhibitor	20.305
2	Cysteine protease inhibitor 9	25.008
3	Aspartic protease inhibitor 8	24.688
4	cysteine protease inhibitor 8	21.583
4	cysteine protease inhibitor 9	25.845
4	Aspartic protease inhibitor 8	24.688

Each band was analysed separately according to the methodology outlined in the experimental (2.2.3.2), then the individual peptides found in each band were searched against the NCBI database and the results were compared by their Expect score, which gives a value indicating the likelihood of a false positive. Only values of over 0.05 (1 in 20) are given as an output. Full data regarding the peptide matches and proteins can be found in the appendix, see tables A.3, A.4, A.5 and A.6. These results prove that all the bands are most likely protease inhibitors, either cysteine or aspartic, but not serine protease inhibitors, which are the proteins of interest.

Analysis was also performed into the two bands present at roughly 15 kDa in the SDS-PAGE, the results of which are shown in table 4.8.

Table 4.8 – Proteomics Data For Potato Band at 15 kDa

Observed Mass	Mr (expt)	Mr (calc)	Expect Score	Peptide Match
Protein Serine protease inhibitor 1				
1491.6957	1490.6884	1490.6572	1.1E-06	K.SPNSDAPCANGIFR.Y
1492.7321	1491.7248	1491.6412	7E-06	K.SPNSDAPCANGIFR.Y + Deamidated (NQ)
1348.7361	1347.7288	1347.6419	2E-06	R.YNSDVGPSGTPVR.F
Protein Serine protease inhibitor 2				
1412.8358	1411.8285	1411.7559	6E-05	-.LPSDATPVLDVTGK.E
1506.7489	1505.7416	1505.6569	0.002	K.SPNSDAPCANGIFR.Y + Deamidated (NQ)
1348.7361	1347.7288	1347.6419	2E-06	R.YNSDVGPSGTPVR.F

Three peptide matches to serine protease inhibitor 2 from *Solanum tuberosum* (Potato) giving a protein sequence coverage of 22% and with good expect scores – showing a low probability of a false positive – indicates that, with relative confidence, the band at roughly 15 kDa in the SDS-PAGE gel can be said to be this protein. Although the molecular mass for this protein is roughly 20-21 kDa, the reason it is expressed at 15 kDa within the SDS-PAGE gel is due to the fact that this protein is a hetero-dimeric protein consisting of 2 chains linked by a disulfide bond. This disulfide bond is broken during the preparation of the protein for gel electrophoresis meaning that when analysed the protein is actually present as two non-identical chains, chain ‘A’ having a molecular mass of roughly 16 kDa, and chain ‘B’ having a molecular mass of roughly 4 kDa. Details of the protein and the two chains can be found in figures 4.7, 4.8 and 4.9.

Protease Inhibitor II

Protein nominal mass (Mr)	20331
Molecular formular	C ₈₉₉ H ₁₃₉₁ N ₂₃₅ O ₂₇₉ S ₅
Average molecular weight	20115.4
Monisotopic molecular weight	20103.1

10	20	30	40	50
LPSDATPVLD	VTGKELDSRL	SYRIISTFWG	ALGGDVYLGK	SPNSDAPCAN
60	70	80	90	100
GIFRYNSDVG	PSGTPVRFIF	SSSHFGQGIF	ENELLNIQFA	ISTSKLCVSY
110	120	130	140	150
TIWKVGDYDA	SLGTMLLETG	GTIGQADSSW	FKIVKSSQLG	YNLLYCPVTS
160	170	180		
SSDDQFCSKV	GVVHQNGKRR	LALVNENPLD	VLQFEV	

Figure 4.7 – Full PI2 Amino Acid Sequence

Chain A				
10	20	30	40	50
LPSDATPVLD	VTGKELDSRL	SYRIISTFWG	ALGGDVYL GK	SPNSDAPCAN
60	70	80	90	100
GIFRYNSDVG	PSGTPVRFIG	SSSHFGQGIF	ENELLNIQFA	ISTSKLCVSY
110	120	130	140	150
TIWKVGDYDA	SLGTMLLETG	GTIGQADSSW	FKIVKSSQLG	YNLLYCPVTS

Figure 4.8 – Amino Acid Sequence for Chain A

Chain B			
160	170	180	
SSDDQFC SKV	GVVHQNGKRR	LALV NENPLD	VLFQEV

Figure 4.9 – Amino Acid Sequence for Chain B

There are two disulfide bonds present within this protein, one intrachain bond between amino acids 48 and 97 (shown in red in figure 4.8) and one interchain bond between amino acids 146 and 157 (shown in blue in figures 4.8 and 4.9) linking the two chains together. As mentioned previously, the function of this protein mainly revolves around it being a potent inhibitor of serine proteases, namely trypsin and chymotrypsin but also human leukocyte elastase (HLE). This protein is quoted to not inhibit cysteine and aspartic proteases such as papain, pepsin and cathepsin D. Computational studies predict that the reactive sites for binding to trypsin and chymotrypsin are amino acids 67-68 and 115-116, respectively.

For complete identification of the proteins present in the crude extract, the two low-intensity bands at roughly 80-100 kDa were also analysed via proteomics analysis (shown in the table 4.9 – Band 1 is the lower of the two bands.) Full proteomics data is given in the appendix tables A.7 and A.8. While identification of all proteins present in the crude extract was one of the aims of this project, further work into the high molecular weight proteins was not, so no more analysis was performed on these proteins.

Table 4.9 – Proteomics Analysis of Potato Protein at roughly 90 kDa

Band	Position on Gel (kDa)	Protein Match	Number of Peptide Matches	Exact weight (kDa)	molecular of protein
1	90	Lipoxygenase	5	95.341	
2	95	Linoleate lipoxygenase 1	92 - 6	97.078	

4.3.1.2 Purification of Protease Inhibitors

Purification of the crude protein to yield pure protease inhibitors was performed by applying the protein to an anion exchange HiTrap Q HP sepharose FastFlow (GE Healthcare) connected to an ÄKTA HPLC (GE Healthcare). A linear salt gradient was used to elute the protein with a starting buffer of 30 mMol Tris base at pH 7.8 and ending with a 30 mMol Tris base at pH 7.8 with a 1 M NaCl concentration. The concentration of NaCl was taken from 0% to 70% over 15 column volumes and then held at 100% for 10 column volumes to ensure all protein was eluted from the column. Fractions were collected using a 96-well plate. Fractions with an absorbance response at 280 nm were analysed SDS-PAGE gels with the chromatogram of the run and the related SDS-PAGE testing the main peaks being shown in figure 4.10 and 4.11, respectively.

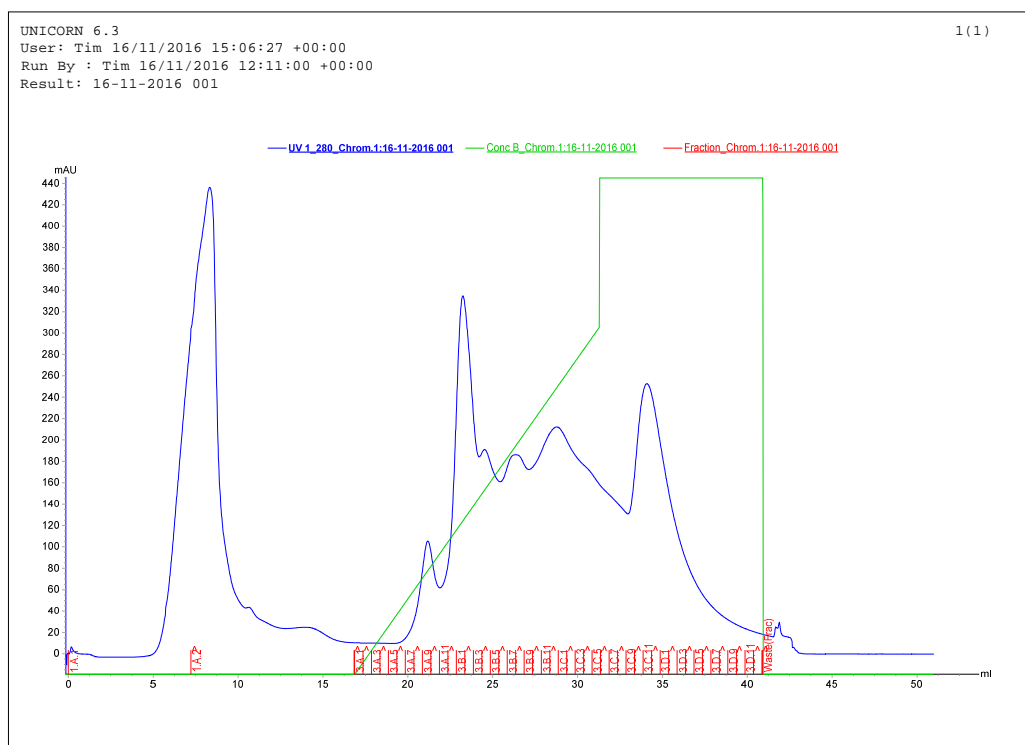


Figure 4.10 – Initial 1 mL Q Column of Crude Potato Protein

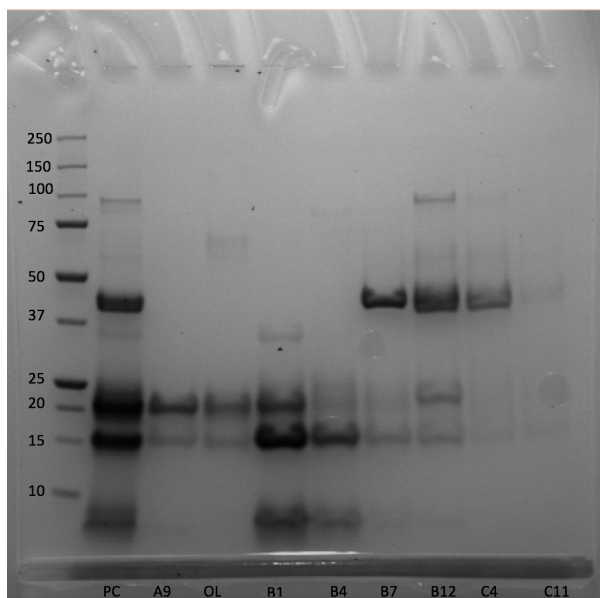


Figure 4.11 – SDS-PAGE Gel Image Looking at the Maximums of Each Peak in the Anion Exchange Chromatogram

Once the peaks representing the desired protein was identified (in this case A9 and B4) a second SDS-PAGE gel was run testing the fractions between those two peaks. The gel image is shown in figure 4.12.

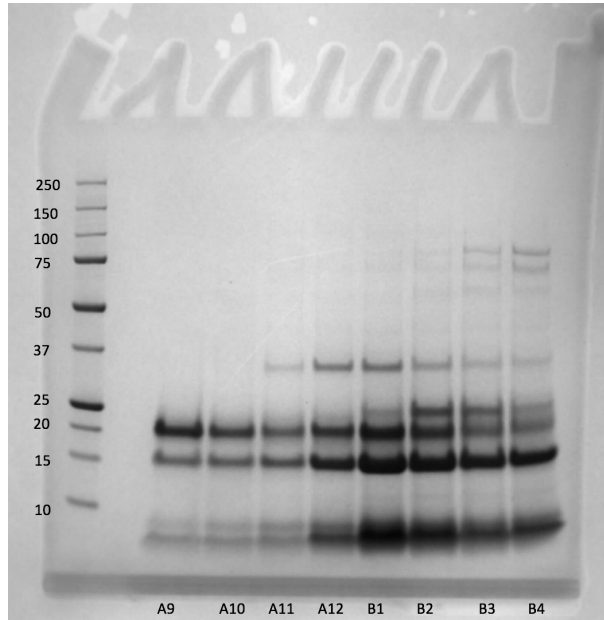


Figure 4.12 – [SDS-PAGE Gel Image of Fractions A9-b4

The bands in the SDS-PAGE image show the desired protein (bands at roughly 20 kDa representing the intact protein and roughly 17 kDa representing one of the degradation products). As the fractions get closer to B4 however, it can be seen that more, high molecular weight, impurities start to be introduced. It was decided, then, to pool the fractions from A6 to A12 to try and maximise protein yield while minimising impurities. These pooled fractions were subjected to a mono-Q anion exchange column to try and ‘polish’ the protein and gain a higher purity (figure 4.13).

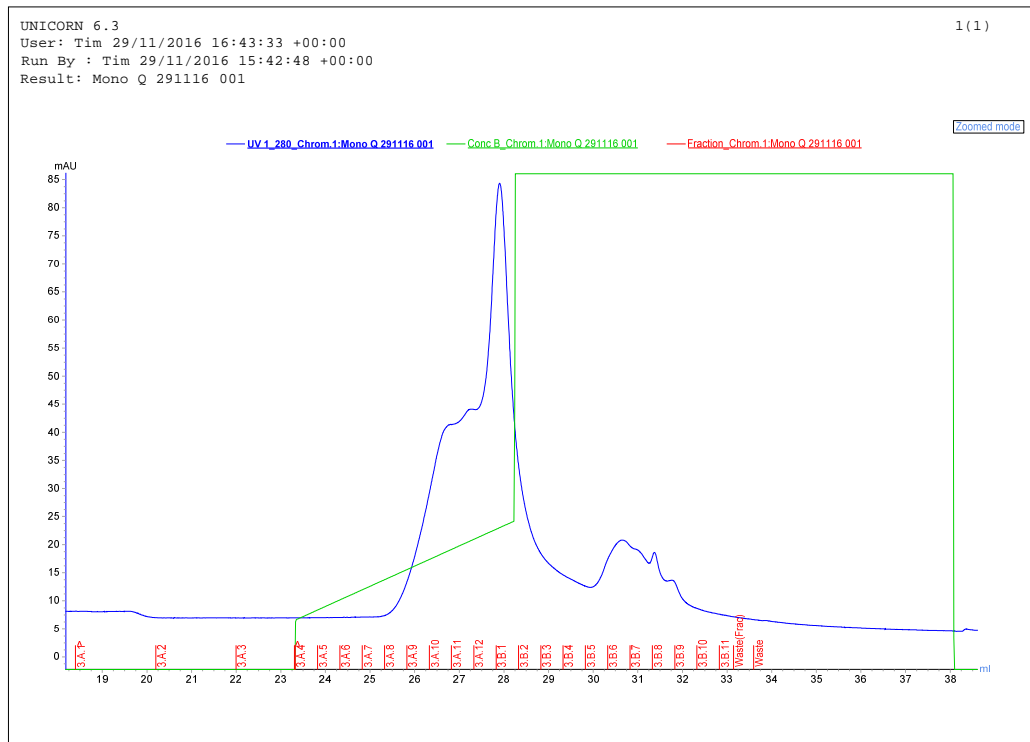


Figure 4.13 – Mono Q Polishing Step

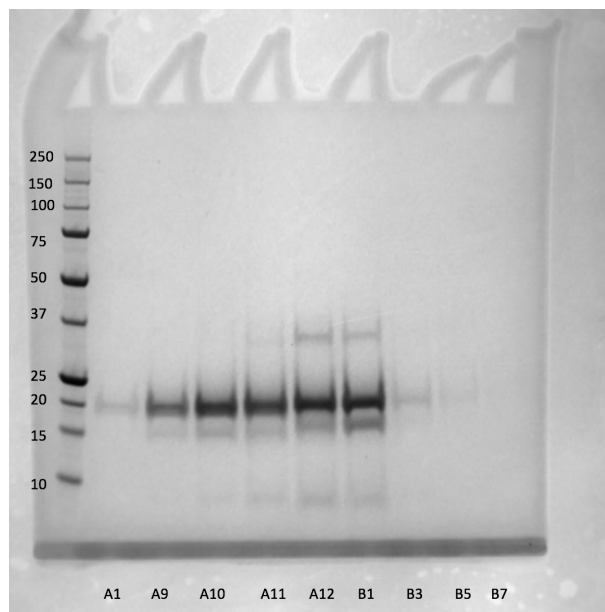


Figure 4.14 – SDS-PAGE Gel Image of Fractions Around the Main Peak in the Mono-Q Chromatogram

From the SDS-PAGE gel image (figure 4.14) it can be seen that the number of impurities has now been reduced to a single impurity at roughly 40 kDa, it was decided to perform size exclusion chromatography to remove this unwanted protein as it is sufficiently different in molecular weight to the desired protein. Fractions A9-B1 were pooled and concentrated until a total volume of roughly 0.5 mL was achieved. This was then subjected to size exclusion chromatography (experimental section 2.2.4) using the same buffer as in previous runs but without the salt gradient. The chromatogram and corresponding SDS-PAGE gel image are given in figure 4.15 and 4.16, respectively.

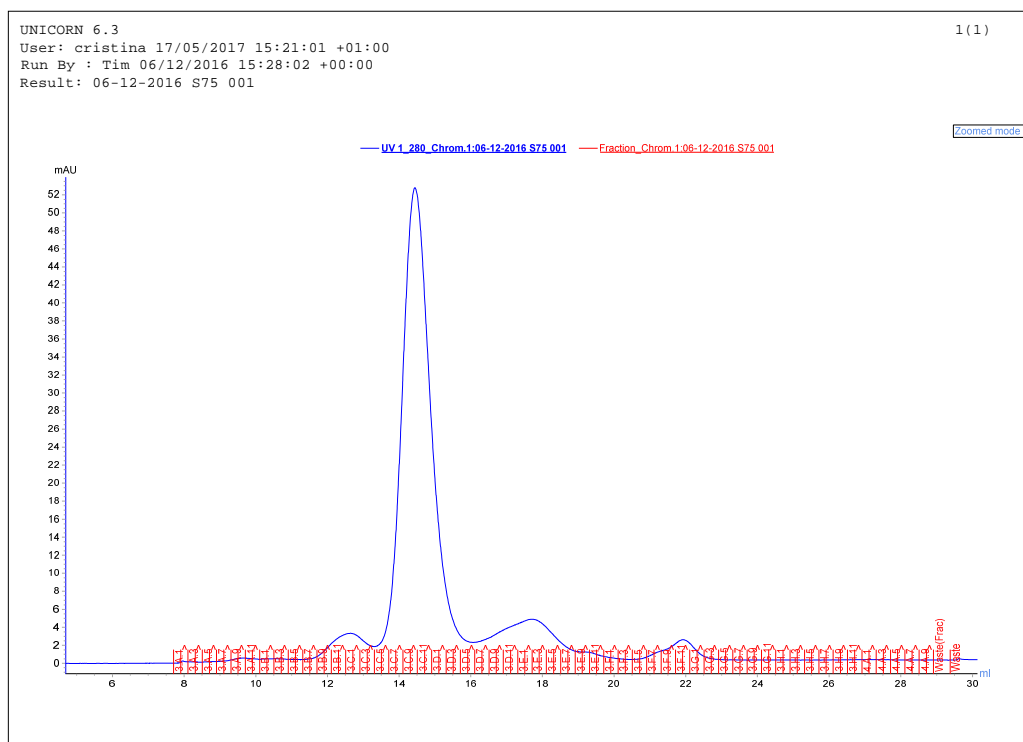


Figure 4.15 – SEC Chromatogram

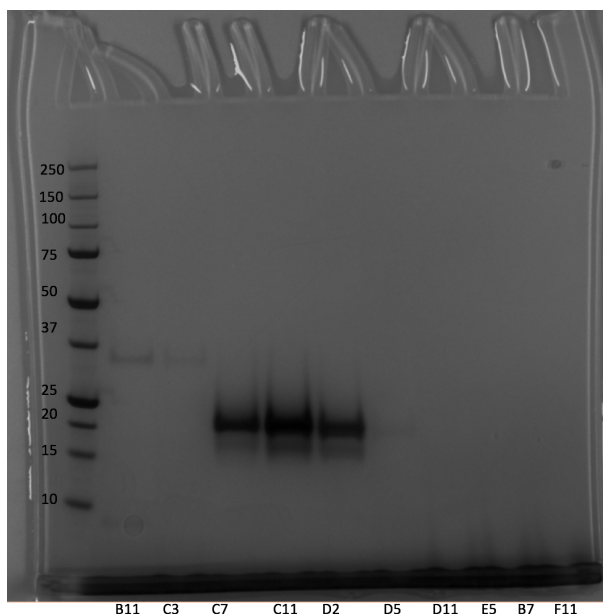


Figure 4.16 – SDS-PAGE Gel Image of Fractions of the Main Peaks in the SEC Chromatogram

The SDS-PAGE image shows a good separation of the proteins with the impurity at roughly 40 kDa being present in the first peak in the chromatogram (represented by the first two lanes in the SDS-PAGE) while the protein of interest along with the lower molecular weight degradation product are found within the second and much larger peak in the chromatogram. The third peak in the chromatogram was proved to be the lower molecular weight (6 kDa) degradation product from the desired protein.

Identification of the protein present in the final purified fractions proved that it was a mixture of the several serine protease inhibitors found within *Solanum tuberosum* (the different serine protease inhibitors would be extortionately difficult to separate as they have differences of only a few amino acids, but do all have the same functionality – inhibiting trypsin and chymotrypsin – which is the desired property of the protein extracted). Subsequent scaled up purification runs were performed missing out the Mono-Q ‘polishing’ step, going straight from the initial anion exchange column to the size exclusion column with good results.

4.3.1.3 Crystallisation Studies

Crystal screening was performed on the purified protein; this was done in an attempt to gain a crystal structure. If a structure was determined, this could then be compared to an industrial standard to see if the extraction and purification process had retained the structural properties of the protein. Two methods were trialled: sitting drop for broad screening, and hanging drop for optimisation.

i. Sitting Drop Method

Initial sitting drop crystallisation screens were carried out on both the purified extracted protein obtained from the anion exchange and SEC chromatography, and commercially available PI2 (Slendesta[®]) for reference. First, the protein was concentrated to roughly 20 mg/mL using centrifugal ultrafiltration with a molecular cut-off of 10 kDa, this concentrated protein sample was loaded into crystal trays using a nanolitre-drop dispensing Mosquito robot, full screen information is available in the appendix (tables A.12-A.33).

After several weeks a small needle (figure 4.17) was observed in one of the trays as shown in figure 4.17 with the following conditions: 0.1 M Tris pH 8, 40% v/v MPD.



Figure 4.17 – Initial Crystal Formed in Sitting Drop Screens

Another screen was then designed focused around the inclusion of MPD, again the full screen information is available in the appendix (tables A.27-A.29).

After several weeks multiple needle-like crystals were observed to be forming in one of the crystal wells, they were much larger than the original crystal and weakly polarised light as shown in figure 4.18 (conditions: 0.2 M di-ammonium phosphate, 40% v/v MPD).

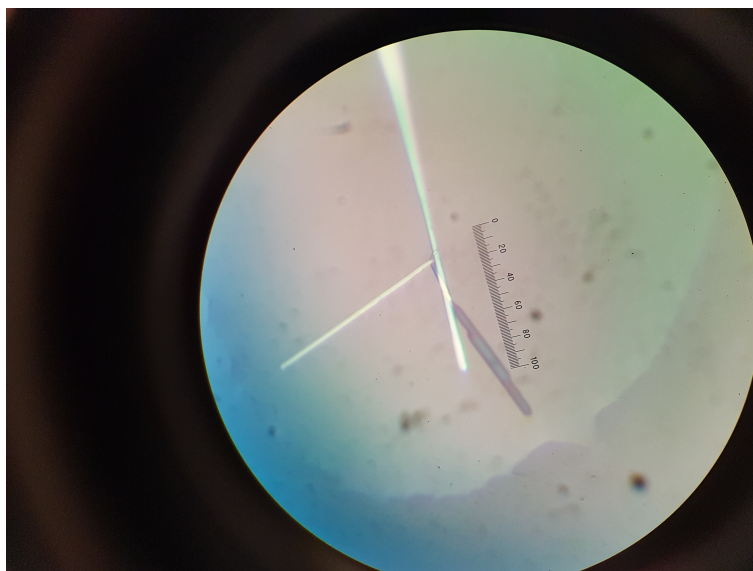


Figure 4.18 – Initial Crystal Formed in Sitting Drop Screens

ii. Hanging Drop Method

Once crystals had been observed forming in the sitting drop screens, optimisation was carried out using manual hanging drop crystal screens. The conditions that had successfully formed a crystal were taken and varied to try and obtain optimal crystallisation parameters. Diammonium phosphate and MPD were the additives that showed crystal formation, so the concentrations of both of these were varied as shown in the following diagrams.

Initial Hanging Drop Tray Layout

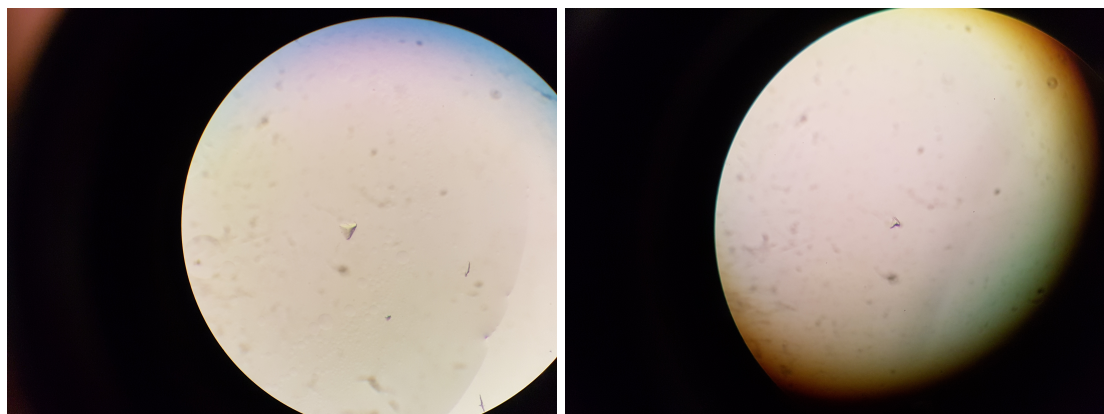
	1	2	3	4	5	6
A	1A	1B	1C	1A	1B	1C
B	2A	2B	2C	2A	2B	2C
C	3A	3B	3C	3A	3B	3C
D	4A	4B	4C	4A	4B	4C

Conditions shown in red text represent protein extracted from native source and black text is protein obtained from industry (Slendesta diet pills).

Hanging Drop Tray Conditions

1A	0.1M Diammonium phosphate 20% v/v MPD	1B	0.2M Diammonium phosphate 20% v/v MPD	1C	0.3M Diammonium phosphate 20% v/v MPD
2A	0.1M Diammonium phosphate 30% v/v MPD	2B	0.2M Diammonium phosphate 30% v/v MPD	2C	0.3M Diammonium phosphate 30% v/v MPD
3A	0.1M Diammonium phosphate 40% v/v MPD	3B	0.2M Diammonium phosphate 40% v/v MPD	3C	0.3M Diammonium phosphate 40% v/v MPD
4A	0.1M Diammonium phosphate 50% v/v MPD	4B	0.2M Diammonium phosphate 50% v/v MPD	4C	0.3M Diammonium phosphate 50% v/v MPD

After approximately 14 days small crystals were observed forming under conditions 2A and 1C (figure 4.19).



(a) Crystal Formed in Condition 2A

(b) Crystal Formed in Condition 1C

Figure 4.19 – Potential Protein Crystals Formed in Initial Hanging Drop Screen

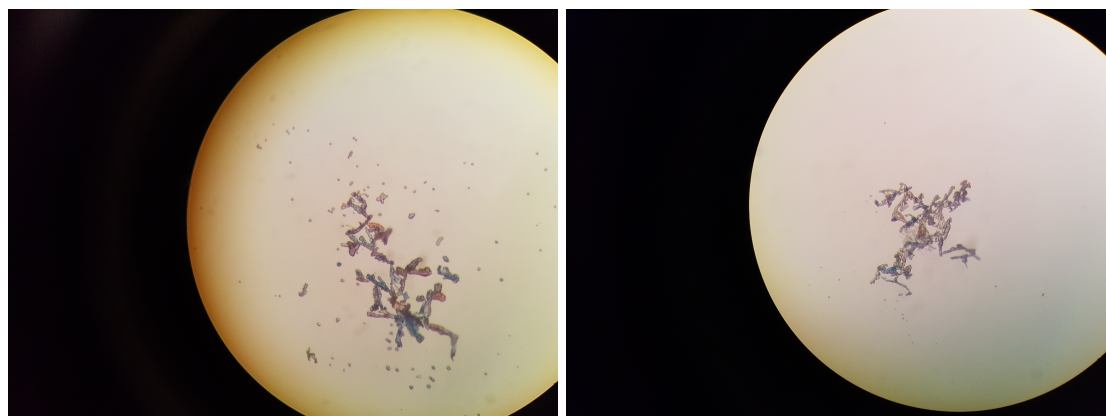
With this in mind a new hanging drop optimisation tray was set up screening conditions around 2A for both extracted protein and industrial protein. The condition was replicated 4 times to allow for micro changes in concentration and environment. For the industrial protein (for which no crystals were observed in the previous hanging drop tray) the concentration of the protein was increased until it was roughly equal to that of the extracted protein (22 mg/mL) in an attempt to more accurately replicate the conditions that formed crystals.

Second Hanging Drop Tray Layout

	1	2	3	4	5	6
A	2A	2A	X	X	X	X
B	2A	2A	X	X	X	X
C	2A	2A	X	X	X	X
D	2A	2A	X	X	X	X

Once again red text indicates extracted protein and black text represents industrial protein. ‘X’ represents a well that is currently not in use. This time, crystals were seen to form rapidly in the wells with the industrial protein, so rapidly, in fact, that the morphology of the crystals suffered, with many small crystals growing interlinked. This poses issues if x-ray diffraction is attempted as individual crystals are not obtained but rather a mass of interlinked small crystals. See figure 4.20 for images of the interlinked

crystals formed.



(a) Potential Crystals Formed in Condition 2A by Industrial Protein (b) Potential Crystals Formed in Condition 2A by Industrial Protein

Figure 4.20 – Potential Protein Crystals Formed in Second Hanging Drop Screen

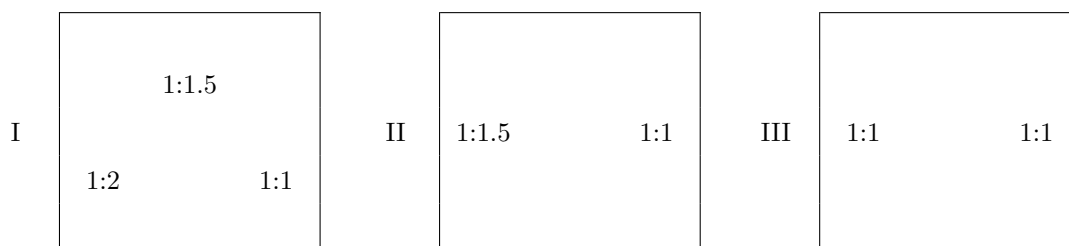
In an attempt to allow the crystals to grow more slowly, more wells were set up in the hanging drop tray using similar conditions to those that developed crystals in the previous trial, but this time, multiple hanging drops were prepared on each slide, and with each drop the ratio between protein and reservoir solution was varied to see how that would affect the crystal growth.

Third Hanging Drop Tray Layout

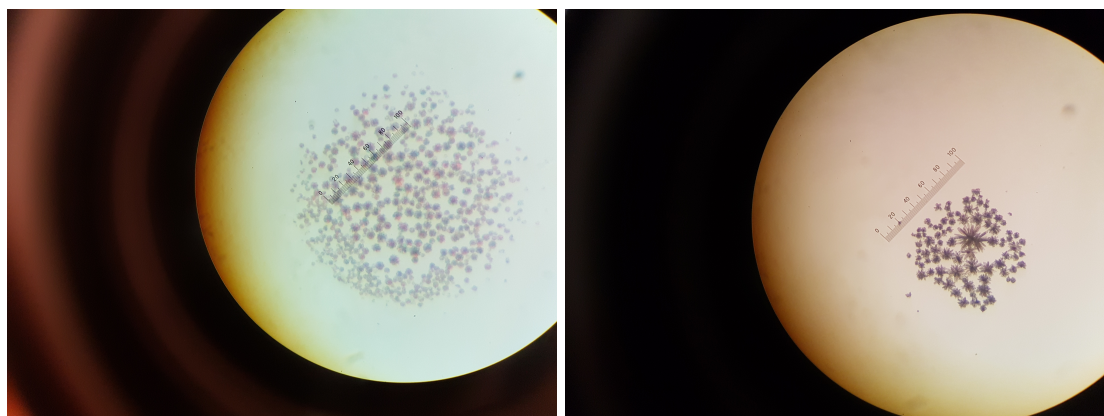
	1	2	3	4	5	6
A	2A	2A	2A ^I	1C ^{II}	X	X
B	2A	2A	2A ^I	2A ^{III}	X	X
C	2A	2A	1A ^{II}	X	X	X
D	2A	2A	2D ^{II}	X	X	X

As before, red represents extracted protein and black represents industrial protein, the superscript numerals indicate what the ratios of each drop were on the slide, these ratios are given below. The first number in the ratio represents the μL of protein used in the drop, and the second number the μL of reservoir solution used in the drop.

Hanging Drop Orientation and Properties

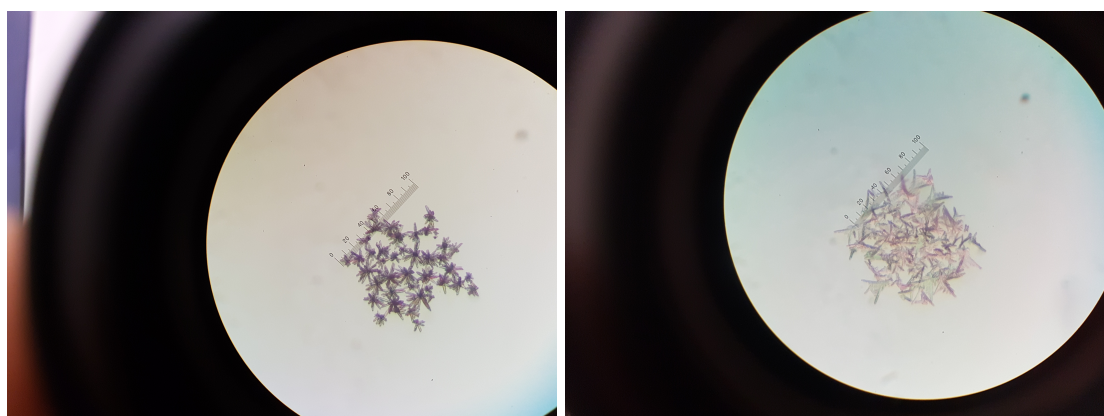


Unfortunately, contrary to the desired effect the crystals grown in this iteration of the optimisation were also formed very rapidly, and therefore were either very small, or formed ‘snowflakes’ which would be hard to break up to get a single crystal from (figure 4.21)



(a) Small, Star Shaped Crystals

(b) Small, Star Shaped Crystals



(c) Medium, Star Shaped Crystals

(d) Snowflake Crystals

Figure 4.21 – Crystals Showing Small, Rapidly Grown Structures

In light of this, a final set of crystallisation parameters were designed, once again with multiple drops on each slide and using broadly the same conditions as before. This time the ratio of protein to reservoir solution was altered again, but also glycerol was included into the reservoir solutions at different concentrations, as this is known to slow down crystal forming.

The experimental crystallisation conditions are given below, with the numerals, once again, indicating the drop pattern on the slide and the superscript letters indicated if, and how much, glycerol was included into the reservoir solution.

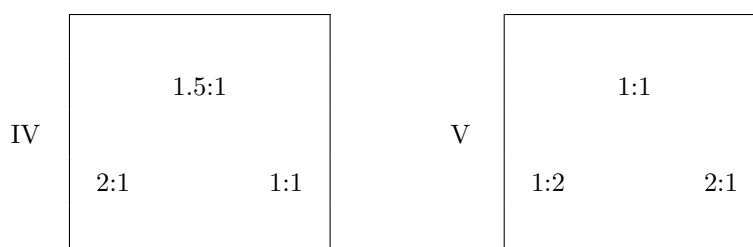
Fourth Hanging Drop Tray Layout

	1	2	3	4	5	6
A	2A	2A	2A ^I	1C ^{II}	1C ^{IV(b)}	1C ^{I(a)}
B	2A	2A	2A ^I	2A ^{III}	2A ^V	1C ^{I(b)}
C	2A	2A	1A ^{II}	1C ^{IV}	2A ^{IV(a)}	2A ^{I(a)}
D	2A	2A	2D ^{II}	1C ^{IV(a)}	2A ^{IV(b)}	2A ^{I(b)}

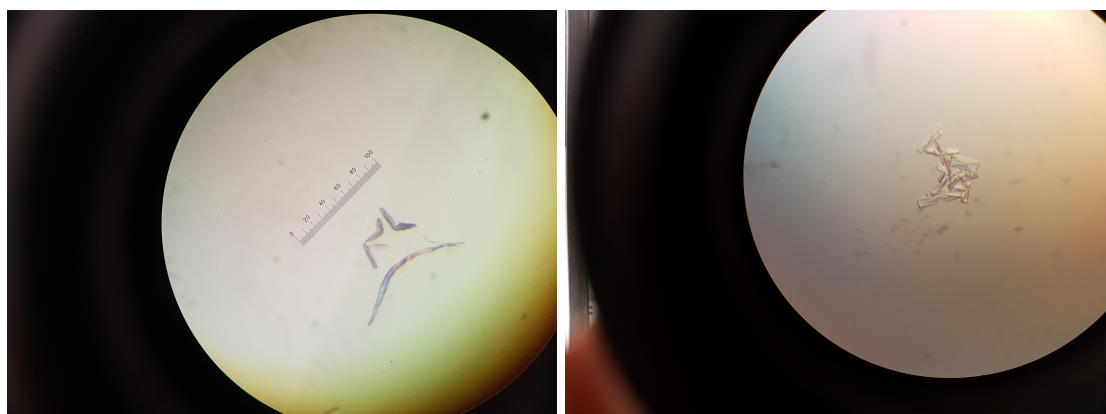
(a) 5% glycerol

(b) 10% glycerol

Hanging Drop Orientation and Properties



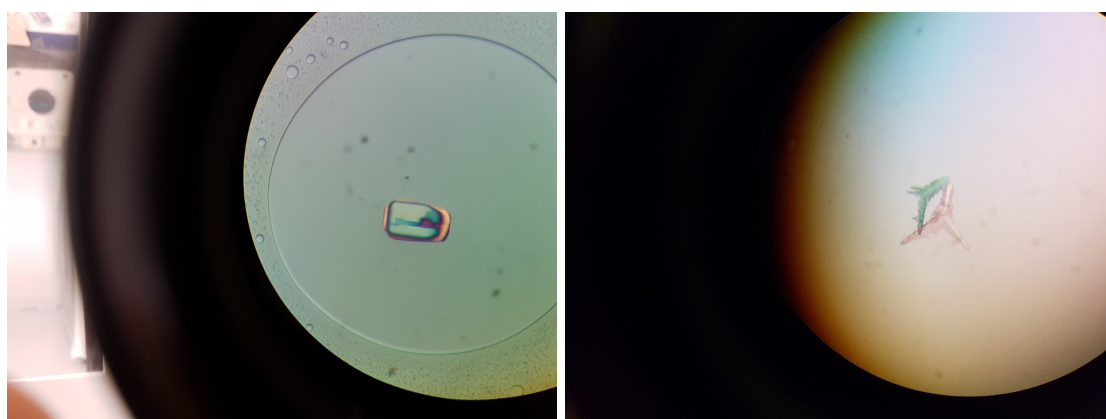
These conditions gave much better crystal morphologies, with sharp, straight edges and large, single crystal structures (figure 4.22)



(a) Small Crystal Shards, Showing Hard Straight Edges (b) Rectangular Crystals, Showing Limited Polarisability



(c) More Crystals with Rectangular morphology (d) Large 'Snowflake' Crystals, Strong Polarisability



(e) Single Large Crystal with Semi-Straight Edges (f) More Examples of Larger 'Snowflake' Crystals

Figure 4.22 – Potential Protein Crystals Showing Promising Morphology

iii. Initial X-ray Diffraction Studies

Initial tests were carried out on crystals obtained from the hanging drop optimisation screens via X-ray facilities within the university, these facilities are used to determine diffraction quality before outsourcing samples for full analysis. Unfortunately the crystals tested either did not diffract well enough to be worth sending for external analysis or showed preliminary data sets indicating small molecular size, this could mean that the crystals formed were due to crystallisation of the salt present within the reservoir solutions. Due to time restraints further tests could not be performed on the crystals to confirm this and more work would therefore have to be done on the optimisation conditions in attempts to yield a protein crystal with favourable diffraction.

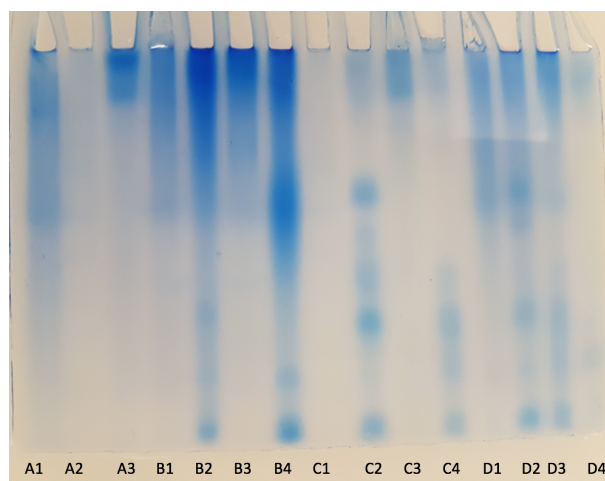
4.3.1.4 Protease Inhibitor Complexation Studies

To begin exploration into how the protease inhibitors inhibit trypsin and chymotrypsin initial work into complexation of the serine protease inhibitor II with trypsin and chymotrypsin, was started. The first test involved simply mixing the proteins in a 1:1:1 w/w ratio. NATIVE gels were run in an attempt to determine if complexation had taken place, pure samples of the PI2, trypsin and chymotrypsin were also run as standards. Unfortunately the initial complexation was a failure as there was little to no change to the bands in the NATIVE gel. It was hypothesised that a metal ion might be required to catalyse the complexation (as there are many metal ions present in the body). Once again PI2, trypsin and chymotrypsin were ran as standards in a NATIVE gel along with test samples mixing the proteins with metal ions. This time it could be seen that the inclusion of certain metal ions makes a marked difference, the three metal ions which showed the largest difference were Fe(III), Ca(II) and Mg(II).

The test was run again using a 5-fold increase in the protein to make the NATIVE gels easier to interpret. The resultant NATIVE gel image is shown in figure 4.23 and shows lanes with the conditions given. Addition of Fe(III) caused a drastic change in the bands present in the NATIVE gel and so indicates it could catalyse complexation.

Table 4.10 – Conditions for NATIVE gel Complex Test

NATIVE gel lane	Test Solution
A1	PI2
A2	Trypsin
A3	Chymotrypsin
B1	PI2 + Trypsin + Mg(II)
B2	PI2 + Chymotrypsin + Fe(III)
B3	PI2 + Chymotrypsin + Ca(II)
B4	PI2 + Trypsin + Chymotrypsin + Fe(III)
C1	Trypsin + Mg(II)
C2	Chymotrypsin + Fe(III)
C4	Chymotrypsin + Trypsin + Fe(III)
D1	PI2 + Trypsin + Fe(III) + Ca(II) + Mg(II)
D2	PI2 + Chymotrypsin + Trypsin + Fe(III) + Ca(II) + Mg(II)
D3	Trypsin + Chymotrypsin + Fe(III) + Ca(II) + Mg(II)

**Figure 4.23** – NATIVE Gel of Complexation Test

The test was once again scaled up, still using a 1:1:1 ratio of the proteins and a 10 mM concentration of Fe(III). A 1.29 mL solution was prepared and subjected to size exclusion chromatography. If the proteins were stably complexed, a fraction with a high molecular weight (faster elution time) when compared to the constituent proteins would

be expected. Pure samples of PI2, trypsin and chymotrypsin were also run through the size exclusion column for reference. The chromatograms of the complexed protein and the standards indicated that a complex was indeed being formed by the appearance of a peak not present in the single protein runs and situated at the start of the chromatogram, this would indicate that a new, higher molecular weight, species was being produced.

In an effort to prove this, the fractions corresponding to the new peak were collected and concentrated for SDS-PAGE followed by MALDI-TOF/TOF-MS analysis. Once again, standards of PI2, trypsin and chymotrypsin were run in the same SDS-PAGE gel for comparison (figure 4.24), the theory being, if all three bands from the standards were present in the 'complexed' protein lane, then the likelihood is that all three proteins were present in a complexed form.

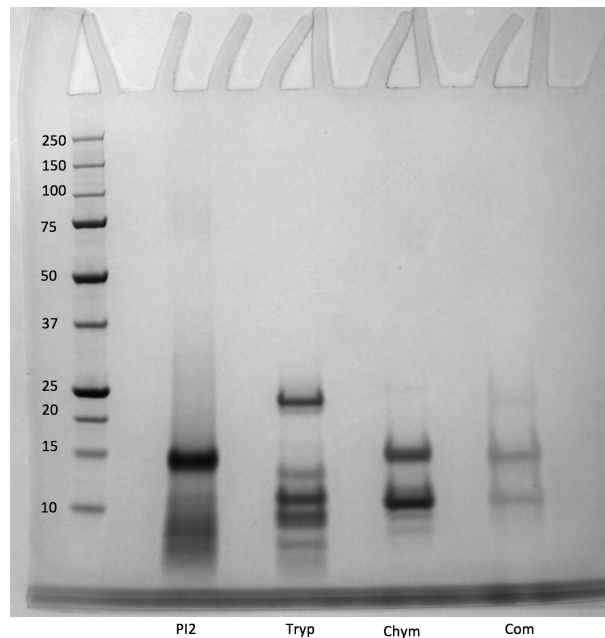


Figure 4.24 – SDS-PAGE of the Potential Complex

While the SDS-PAGE gel indicated that all three were present, the bands for chymotrypsin and PI2 came at very similar places so it could not be confirmed from the SDS-PAGE gel alone whether all three were present. LC-TOF-TOF was performed, the potentially complexed protein was loaded onto a 1D-gel, run into the gel 1 cm, stained with Coomassie, excised and digested with Asp-N protease prior to analysis. The Asp-N was to replace trypsin which had been used for all proteomic analysis prior to this. For obvious reasons, trypsin could not be used to digest this sample as trypsin was one of the proteins potentially present. Initial results from the LC-MS-MS indicated

both trypsin and chymotrypsin being present in abundance, but only a single peptide match to serine protease inhibitors was found and at a much lower intensity, indicating that, if it was present, it would be at a much lower concentration than trypsin and chymotrypsin.

It was hypothesised that while serine protease inhibitors had been successfully analysed by MALDI-TOF/TOF-MS previously, the alternative protease used for digesting the samples (Asp-N) may not be as effective as trypsin was in the initial tests. An experiment was designed with the aim to prove this.

To normalise the relative abundances of the proteins observed from the LC-MS/MS analysis a sample was prepared mixing exact 1:1:1 ratios of the proteins, it was therefore assured that each protein was present in the solution with the same concentration. This solution was then subjected to the same LC-MS/MS analysis as the sampled obtained from size exclusion separation of the potential complex. The results obtained showed a much reduced signal for protease inhibitor II when digested with Asp-N, as predicted. The initial complexed sample along with another complex sample prepared under the same conditions were subjected to analysis via LC-MS/MS again, and the relative abundance values normalised using the run from the known 1:1:1 mixture of proteins. The data showed a similar response for protease inhibitor 2 between the 1:1:1 standard and the complexation tests, suggesting that the protein distribution was approximately 1:1:1 with trypsin and chymotrypsin in the complexed sample. This proves that a stable 1:1 complex had been formed between extracted protease inhibitors and their target enzymes (trypsin and chymotrypsin.)

4.3.1.5 Preliminary Trypsin Inhibition Assays

Preliminary studies into using a fluorescence assay for trypsin inhibition was performed using the methodology outlined by Kawabata *et al.*⁵⁵ using Boc-Gln-Ala-Arg-7-amido-4-methylcoumarin hydrochloride. Different excesses of protease inhibitor were used in relation to trypsin concentration as given in tables 4.11 and 4.12, test samples containing assay only, trypsin only, assay with just trypsin and assay with just PI2 were run for comparison.

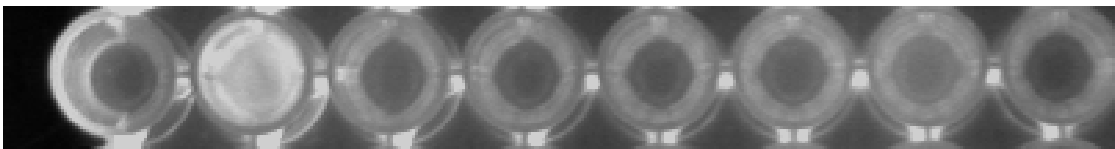
Table 4.11 – Layout of Plate for Trypsin Inhibition Assay

Well Number	1	2	3	4	5	6	7	8
Condition	A	B	C	D	E	F	G	H

Table 4.12 – Trypsin Inhibition Assay Conditions

Condition	Well content
A	Assay only
B	Assay and trypsin
C	Assay, Trypsin and 200 fold excess of protease inhibitor
D	Assay, Trypsin and 100 fold excess of protease inhibitor
E	Assay, Trypsin and 10 fold excess of protease inhibitor
F	Assay, Trypsin and 1:1 excess of protease inhibitor
G	Assay, Trypsin and 0.5:1 excess of protease inhibitor
H	Assay and protease inhibitor

Figure 4.25 shows the wells being excited at a wavelength of 440 nm, this qualitatively shows that trypsin with no protease inhibitor allows the assay to fluoresce strongly while all excesses of protease inhibitor with the exception of 0.5:1 with relation to trypsin show full inhibition of the trypsin and therefore no fluorescence is observed. For 0.5:1 excess of protease inhibitor to trypsin, fluorescence is observed but at a lower intensity than trypsin alone, indicating that there is partial inhibition of trypsin.

**Figure 4.25** – Trypsin Assay Showing Fluorescence where un-inhibited Trypsin is Present

This is a preliminary proof of concept experiment that proves that the use of Boc-Gln-Ala-Arg-7-amido-4-methylcoumarin hydrochloride as an assay for testing trypsin inhibition is applicable to this protein. More work has to be done to quantify this data and to fully explore stoichiometry and rate of inhibition. Initial work was also done into developing a chymotrypsin inhibition assay using *N*-Succinyl-Ala-Ala-Pro-Phe p-nitroanilide based on the work of DelMar *et al.*¹⁸⁵ with limited success and more work needing to be done before credible results can be obtained.

4.4 Conclusions

Demand for vegetable-derived protein is increasing, and will continue to do so as the expanding population puts strain on the food production industry. Waste potatoes are a large volume feedstock that is currently under-utilised, especially in the UK, and there is potential for its valorisation into a high quality protein for food industry purposes, or for fractions to be purified and marketed as high value dietary aids.

The work in this chapter illustrates the potential for use of potato waste as a feedstock for protein extraction. Potato protein has been extracted in yields of roughly 1.1% and purified using ultrafiltration membrane technology. The extracted protein has been fully characterised by SDS-PAGE followed by MALDI-TOF/TOF-MS. Three main protein fractions were identified: patatin (roughly 40 kDa), protease inhibitors (<25 kDa) and high molecular weight proteins (>75 kDa).

The protease inhibitors were purified by a combination of anion exchange and size exclusion chromatography. 1056 different sitting drop crystallisation tests were performed on the purified protein as well as an industrial standard along with 76 manual hanging drop tests. While crystals were produced, more work has to be performed to gain a well-diffracting crystal and to ensure that the crystals formed are not salt.

Complexation tests between the extracted and purified protease inhibitors were performed using their target enzymes, trypsin and chymotrypsin. It was found through screening of different metal ions, that Fe(III) ions play an important role in the stable complexation of protease inhibitors to their target enzymes. Successful complexation of protease inhibitor II to both trypsin and chymotrypsin in the presence of Fe(III) ions was confirmed by LC-MS/MS analysis after size exclusion chromatography.

Chapter 5

Pecbons – a Carbonaceous Material for CO₂ Capture

5.1 Introduction

The need for an efficient, cost effective and easy to implement way of removing CO₂ from mixed gas streams, whether it is precombustion, postcombustion or sweetening of natural gas, is obvious, but there are several difficulties that must be overcome. Advancements in new materials hold the greatest promise for improvements within this field, and any advancement made in this area would not only aid in separation of CO₂ from mixed gas streams but also help in the development of other gas separations, such as solar-to-fuel applications and H₂ production as well as sequestration of atmospheric CO₂ which is going to become increasingly important as greenhouse gas levels continue to rise.

The annual global CO₂ emissions have increased by 80% between 1970 and 2004, this is mainly due to humanities increased reliance on fossil fuels as a combustion medium along with deforestation and chemical processing.¹⁸⁶ CO₂ emissions are the main contributor to anthropogenic climate change (roughly 63% of the gaseous radiative force), with atmospheric CO₂ concentrations increasing from 280 ppm to 380 ppm from the 1700s to 2005.¹⁸⁷

Power generation is currently heavily reliant on coal as its main feedstock. In 2008, 41% of global electricity was generated by coal combustion.¹⁸⁸ In 2005, burning of fossil fuels created 7.9 Gigatonnes of CO₂ with an average increase in atmospheric CO₂ of >2 ppm/year, this amounts to roughly 60% of anthropogenic CO₂ emissions coming from the burning of fossil fuels for energy.^{187,189} Currently only about half of the CO₂ emitted remains in the atmosphere, the rest being removed by land and ocean sinks.¹⁹⁰ However, the amount of CO₂ being removed is becoming lower year by year, indicating an overloading of the natural land and ocean CO₂ sinks.

It is paramount, therefore, for humanity to reduce the amount of anthropogenic CO₂ emissions if the Sustainable Development Goals (SDGs) relating to climate change are to be accomplished. Swapping to a carbon neutral fuel for energy production, or to low emission energy sources such as solar, wind and tidal are attractive and are being adopted by many countries in the developed world. Coal is still predicted to be the main power source for much of the world, however, especially in developing countries for the next few decades. Hence, a way of sequestering CO₂ from coal fire plant emissions is an attractive

area of research.

5.1.1 Carbon Dioxide Capture

Conventional CO₂ capture most commonly utilises amine absorbers and cryogenic coolers, this technology was initially used for separation of CO₂ from natural gas and hydrogen and has been in use since 1930.¹⁹¹ This technology was explored as a potential CO₂ capture agent in 1991 and while the efficacy of this system is beyond dispute, the increase of the energy requirements to the coal plant are large (25-40% assuming a flue gas containing 12-15% CO₂ at 40 °C). This increase in energy requirements is predicted to increase electricity price \$0.06 kWh or an ‘avoided cost of capture’ of \$57-60/tonne CO₂, proving that this method is not currently a cost effective process for the sequestration of CO₂ from coal fire plants. This clearly shows the drive for alternative techniques and materials for CCS (Carbon Capture and Storage).^{186,192,193} For the latter parts of the process, namely the storing, compression and transportation of CO₂, the technologies involved are already well documented and researched and the most economic options are already in use. The majority of the cost of the CCS process is the capture phase, which represents roughly two thirds of the total cost.

There are two main routes used for removal of CO₂ from combustion streams. Firstly postcombustion, removing CO₂ from the flue gas after combustion, this process is characterised by low pressures (ca. 1 bar) and relatively low CO₂ concentrations (ca. 10-15%) with the largest other gas component being N₂.¹⁹⁴ Secondly precombustion, removing CO₂ impurities from gas before being utilised as a fuel. This process is characterised by high pressures (ca. 30 bar) and relatively high concentrations of CO₂ (ca. 35%) and the main other gas component being H₂. Table 5.1 shows the conditions and gas composition for typical postcombustion and precombustion processes.

Table 5.1 – Composition of gases by weight in both postcombustion and precombustion processes¹⁸⁶

Gas	Postcombustion	Precombustion
CO ₂	15-16%	35.5%
H ₂ O	5-7%	0.2%
H ₂	–	61.5%
O ₂	3-4%	–
CO	20 ppm	1.1%
N ₂	70-75%	0.25%
SO _x	<800 ppm	–
NO ₂	500 ppm	–
H ₂ S	–	1.1%
Condition		
Temperature	50-75 °C	40 °C
Pressure	1 bar	30 bar

5.1.1.1 Key Challenges

CO₂ capture has a lot of challenges associated with it, the main issue is that the carbon capture material must be regenerable and in large supply. This is due to the fact that the volume of CO₂ emissions is so large that any material used that is non-regenerable would quickly become exhausted on the global scale.¹⁸⁶ CO₂ capture agents also have to be selective for CO₂ as well as be resistant to fouling from water and particulate matter due to the fact that flue gas is a mixture of gasses and tends to have a lot of fine particulate matter within it.

With regards to CO₂ capture from flue gas, the low pressure, low CO₂ concentration and temperature of the gas stream are all challenges. A material would have to be able to selectively adsorb a large amount of CO₂ from this low pressure, low CO₂ system in order to be effective. These challenges, combined with the importance of developing novel CO₂

capture technologies to limit climate change, make this area of research rapidly growing and dynamic, with novel systems and improvements to traditional methodologies being developed at a rapid rate.

5.1.1.2 Traditional CO₂ methodology

Conventional amine scrubbing of CO₂ relies predominantly on a primary alkanolamine MonoEthanolAmine (MEA - figure 5.1).^{195,196}

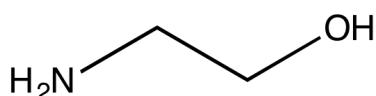


Figure 5.1 – Structure of primary alkanolamine MEA

The process involves a flow of aqueous amine solution (25-30 wt%) running down a tower with the gas introduced at the bottom. The temperature of the gas being 40 °C, the amine reacts with the gaseous CO₂ via a zwitterion mechanism to form a carbamate. This CO₂ enriched amine mixture is then passed into a ‘regeneration’ column where the solvent is heated to 100-140 °C with steam in order to regenerate the solvent. The elevated temperatures required are due to the high heat of formation associated with carbamate production and represents a high energy cost for the regeneration of the solvent. There are also issues related to amine degradation via the presence of oxygen in the flue gas.¹⁹⁷

5.1.1.3 Emerging CO₂ Capture Methodologies

Considerable effort is being put into overcoming the problematic regeneration and chemical degradation present within the current methodology of carbon dioxide capture. The main area of research is into new materials for use within this application.¹⁹² The materials being investigated range from physical absorbents, solid adsorption agents, membranes and metal oxides and are effective through a range of capture mechanisms including pressure/temperature swing, cryogenic distillation, gas hydrate formulation and chemical looping combustion.¹⁹²

i. Physical Absorbents

While technically not being a new technology, swapping the traditional MEA method for a solvent system that selectively dissolves CO₂ under the required conditions and has more favourable regeneration conditions, is an attractive area for research. Solvents such as Selexol (a mixture of dimethylethers of polyethylene glycol)¹⁹⁸ and Rectisol (methanol at -40 °C)¹⁹⁹ are both already used industrially in natural gas sweetening, and have the advantage of having a lower heat requirement for the regeneration step.

ii. Adsorption

Adsorption offers both advantages and disadvantages when compared to absorption. It has a higher energy efficiency when compared to absorption, there are, however, physical limitations. Whereas the CO₂ dissolves into the bulk solvent during the traditional methodology, adsorption requires interaction between the gaseous CO₂ and the surface of the material, this limits efficiency.¹⁹⁸

When considering physical adsorbents as a carbon capture medium, several properties have to be considered. Firstly the adsorption capacity of the material (how much CO₂ can the material adsorb) secondly the balance between the affinity of the material to remove CO₂ from a gas mixture and the amount of energy required to regenerate the material afterwards; and thirdly the selectivity of the material to adsorb CO₂ as opposed to other gasses.^{200,201}

Separation based on adsorption relies on a number of factors which need to be taken into consideration when designing a material for CO₂ capture. Some of them are summarised below:

Molecular sieving – This effect is based on the size or shape exclusion promoted by the material in question.

Thermodynamic equilibrium – Controls the adsorbent-adsorbate surface interactions and can control the preferential adsorption of more thermodynamically favourable adsorbate.

Kinetic effect – Controls the diffusion rate of different components within a gas mixture.

iii. Metal-Organic Frameworks

Metal-Organic Frameworks or MOFs consist of metal ‘nodes’ bridged by organic linking groups to form structured crystalline networks with very large surface areas and extensive porosity. They also have highly tune-able properties depending on the organic and inorganic substituents used in their production. This makes them an interesting material with large scope to be used as a CO₂ capture agent.^{202–205}

Honeycomb structured MOFs have been researched with regards to applications within anthropogenic CO₂ capture. The one-dimensional channels formed by the honeycomb structure allows a high density of the charged metal ions to be exposed. The metal ion choice then is very important as different metal ions could potentially selectively bind to certain gasses.¹⁸⁹ Because of this, MOFs have a large potential for selective CO₂ adsorption from mixed gas streams with high loading capacity due to their large surface area and pore volume.

While the advantages to MOFs are many and varied, they do not come without their own drawbacks. Generally they have lower CO₂ capture potential than other solid materials at low CO₂ partial pressure. They have also been reported to be sensitive to moisture fouling as well as being very expensive to produce with the inorganic ligands and organic linkers being costly to make.²⁰¹ Another issue with use of MOFs is that they are generally synthesised at relatively low temperatures (50-300 °C), this limits their operational and regeneration temperature to below this temperature, this can cause issues especially with regeneration as if there is a high heat of adsorption, high temperatures are usually required to desorb the CO₂.

iv. Membranes

Membranes are an extremely attractive area for research into their utilisation within CO₂ separation from mixed gas streams. They have been shown to have high selectivity, low energy requirements and are highly modular and flexible when it comes to plant design.

When it comes to gas separation, membranes have two characteristics to consider: selectivity and permeability. Unfortunately, these two characteristics are negatively correlated, with highly permeable membranes tending to have poor selectivity, and highly selective membranes tending to have poor permeability. This relationship is shown clearly in a Robeson plot which shows CO₂ selectivity when compared to N₂ against CO₂ permeability (see fig 5.2).^{206,207} The upper bound limit (represented by the solid line with the plot) represents the optimal theoretical limit of membrane performance with respect to permeability and selectivity.

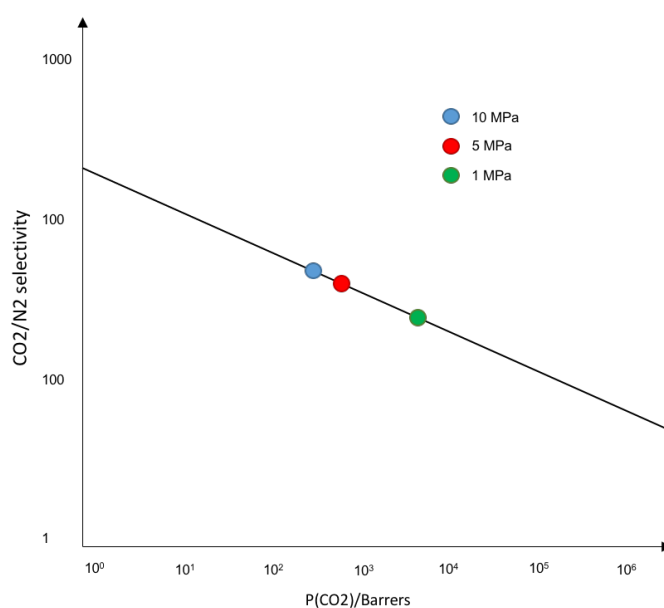


Figure 5.2 – Robeson Plot Showing the Upper Bound Limit

There are other membrane properties that should be considered including robustness and resistance to chemical and/or physical damage within the conditions during gas separation, along with material lifetime and efficacy over time.

While membranes show promise within the application of CO₂ separation, they do tend to have difficulty when trying to separate gas from low pressure streams, such as in flues. The partial pressure of the CO₂ is too low to drive the gas separation, hence compression of the feed gas is often needed to make them economically viable. They also have issues with fouling of the membrane due to the high particulate present in flue gas, this decreases permeability over time which results in short lifetimes for membranes.²⁰⁸

v. Zeolites

Mesoporous materials, namely zeolites, are already used industrially in the production of H₂ in which pure hydrogen needs to be separated from a H₂/CO₂ mixture.²⁰⁹ Zeolites are most often used via a pressure swing adsorption route under elevated pressure (>2 bar), and while the adsorption capacity for these materials is high, they are very sensitive to water present in the gas stream and get easily ‘fouled’ with moisture, resulting in very high temperatures being needed for regeneration (often >300 °C). These materials are also expensive to produce and have issues with CO₂ selectivity unless chemically modified.

5.1.2 Carbonaceous, Mesoporous Materials

Carbonaceous mesoporous materials are an attractive alternative to zeolites due to their relatively inexpensive production and the fact that they are insensitive to moisture.

The material used to create the mesoporous carbonaceous material changes the surface chemistry of the resulting material. This means that different materials could be made which selectively adsorb CO₂ as opposed to N₂ as an example. These materials tend to have a lower heat of adsorption than zeolites, and while this means that they have a lower adsorption capacity, it also means that the regeneration conditions can be milder and therefore more economic, this adsorption capacity can be increased by increasing the pressure of the gas.

The resistance to fouling by water in these materials is mainly due to the hydrophobic nature of their surface, meaning that these materials can still perform their function in humid conditions. Add this to the relatively inexpensive production of carbonaceous materials from large volume and potential waste feedstocks and this material becomes a very viable reagent in the separation of CO₂ from mixed gas streams.

5.1.2.1 Carbonaceous Materials – Background and Production

Carbonaceous materials have been made and utilised for millennia, with carbon black being used in inks and pigments for over 3000 years.²¹⁰ More recently carbonaceous,

porous materials such as Activated Carbons (AC) have become the basis for a rapidly expanding area of research with applications in carbon capture and storage, catalyst supports,²¹¹ adsorbents,^{212,213} water remediation,^{214–216} electrodes²¹⁷ and carbon fuel cells.^{218,219} One of the properties of carbonaceous materials that make them suitable for these applications is their inherent porosity.²¹⁸

Biomass is an attractive feedstock for the production of meso-/micro-porous carbonaceous materials due to its relatively high abundance²²⁰ and renewable nature.²²¹ It is especially attractive if biomass that would otherwise be considered a waste product from other industrial applications is used, because this feedstock is considered ‘low value’ and avoids the controversy of the ‘food vs fuel’ debate.^{48,210,222}

Roughly 80% of the world's production of Activated Carbon (AC) is used in liquid-phase applications such as primary water treatment,²²² preceding other purification techniques. When utilised as an adsorbent, AC performs its function via interactions between the adsorbate and the carbon surface through either electrostatic or non-electrostatic interactions²²² depending on:

- Electrostatic Interactions:
 - The charge density of the carbon surface.
 - The chemical characteristic of the adsorbate.
 - The ionic strength of the solution.
- Non-Electrostatic Interactions:
 - Van der Waals forces.
 - Hydrophobic interactions.
 - Hydrogen bonding.

With regards to the adsorbate, the main properties that influence its adsorption onto AC are:

- *Molecular size* - Determines how accessible the inner porous network present in the AC is to the adsorbate.
- *Solubility* - Determines the degree of hydrophobic interactions between the adsorbate and the carbon surface.
- *pKa* - Determines dissociation of the adsorbate.
- *Nature of substituents* - Depending on whether substituents are electron donating or withdrawing affects non-electrostatic interactions.

When making AC from waste biomass, the physical and chemical characteristics of the biomass heavily effect the nature and performance of the AC formed.^{212,223} AC can come in different forms²²⁴ including Granular Activated Carbon (GAC), Powdered Activated Carbon (PAC), Activated Carbon Fibers (ACF) and Activated Carbon Cloths (ACC). The feedstock used to produce AC dictates the physical form of the resulting material. Hard biomass such as coconut shells and fruit stones tend to yield granular AC²²⁵ with particle sizes above 0.177 mm. Biomass in a powdered or macerated form, such as sawdust, yields powdered AC with particles below 0.177 mm. PAC tends to be more efficient at adsorption due to its smaller particle size,²²⁶ but this does have an adverse effect on the removal of the PAC from the aqueous medium, with separation times being longer than with GAC. While ACF and ACC exhibit interesting properties with regards to pore size distribution and enhanced adsorption properties, their synthesis is more complex and therefore GAC and PAC are by far the mostly widely used.

When considering feedstocks for AC to be created from, it would ideally conform to several prerequisites. Firstly, the feedstock should be abundant and cheap to allow for profitable production to meet potentially growing demand. Secondly, it needs to have a high carbon content and a relatively low inorganic content, the feedstock should also allow easy and cheap activation and show little degradation when aged. Currently, the most commonly used precursor is coal as it is cheap and has relatively large supply.²²⁴ It is, however, a non-renewable resource within a realistic time scale and therefore, fully renewable alternatives will likely be required in the future.

Agricultural waste streams are an attractive alternative feedstock due to myriad reasons. They are very abundant, relatively low cost,²²⁷ they usually have a high carbon content and a comparably low inorganic content, with the added benefit that waste from agriculture is currently a large burden on the environment. Therefore, this waste becomes a very attractive feedstock for AC production.

The standard templating methodology²²⁸ for synthesis of mesoporous carbonaceous materials with tuneable surface and pore size distribution involves using a mesoporous template, most often silica, with a carbon precursor. This carbon precursor is then carbonised and template removed using either hydrofluoric acid or caustic soda. While this method does produce highly ordered mesoporous materials with a large specific volume, the aggressive chemicals used in its production are non-ideal from a green chemistry stand point and also allow for only the production of ACs with inert hydrophobic surfaces. If different surface chemistry is desired then subsequent chemical modifications are needed, this is usually a time consuming and costly process and reduces the porosity of the AC.

5.1.2.2 Starbons[®]

One relatively novel method of producing ordered mesoporous carbonaceous materials is the procedure developed for the production of Starbon[®] and Starbon-like materials.^{229,230} This methodology relies on the feedstock being able to self-assemble into organised nanoscale lamellar structures, in the case of Starbon[®] this is due to the feedstock being starch which is comprised of amylose and amylopectin polymer. As such, this process does not involve the use of a templating agent. Therefore it negates the need for the template removal step, avoiding a lot of the problematic chemicals from the methodology.²²⁹

The original process for Starbon[®] is as follows:²²⁹

Starch Expansion - Firstly the starch is made into a gel in water, this ‘opens’ the dense biopolymer network.

Retrogradation - Starch gels are cooled to partially recrystallise the gel.

Solvent Exchange - The water in the gel is then exchanged for a lower surface tension solvent to limit collapse of the porous network during the drying process.

Drying - Mesoporous materials are then oven dried.

Acid Doping - Material is doped with catalytic amounts of *para*-toluenesulfonic acid allowing for fast carbonisation starting at the pore sites (where the acid is absorbed) and then gradually moves through to the bulk material.

Carbonisation - Dried and doped samples are then carbonised under vacuum at different temperatures to fix the mesoporous pore structure.

While starbon[®] allows for the synthesis of mesoporous carbonaceous materials with high mesoporosity and large pore volumes, there are limitations with this material, mainly due to the fact that catalytic amounts of organic acid have to be added during the synthesis. This can cause limited use of the low temperature carbonaceous materials due to the strong acid adsorption and uneven acid distribution onto the polysaccharide surface. As such, it would be advantageous then to find a new polysaccharide feedstock that has inherent acid properties. This would negate the need to add acid and not only simplify the synthesis of the material, but also allow for a more uniform acidic group distribution throughout the material.²³¹ With all this in mind, pectin is an attractive feedstock as it is a naturally acidic polysaccharide.

5.1.2.3 Pecbons

Pectin is an attractive feedstock for the synthesis of mesoporous carbonaceous material via the ‘soft’ templating method adopted for Starbon[®] because it readily creates gels in water so the gelation step of the synthesis would happen with ease. Pectin is also inherently acidic due to its galacturonic acid backbone; this would negate the need for

catalytic amounts of acid in the synthesis as well as create a porous material with evenly distributed acidic groups.

One of the major pitfalls of the traditional Starbon[®] methodology is the complex and expensive drying process required to form the aerogel from the hydrogel without destruction of the pore structure. This is achieved by solvent exchange of the water for a more volatile solvent such as ethanol followed by utilisation of supercritical CO₂ to drive off the more volatile solvent. The solvent exchange to ethanol allows for the retention of the pore structure due to its lower surface tension, meaning that as it evaporates it does not collapse the pore structure. While this method is undoubtedly effective, it does pose serious challenges to scaling up, and would be economically challenging on an industrial scale.

One drying method with great promise is lyophilisation or freeze-drying. This is due to the fact that lyophilisation avoids issues with liquid-vapour interfaces and surface tension problems by subliming the solvent directly from a solid to gas.²³² A common issue with using lyophilisation for the synthesis of porous materials is the fact that this process usually yields macroporous aerogels with limited mesoporosity.⁵⁶ This issue has been partially resolved by creating hydrogels from aqueous TBA (tertiary butyl alcohol) solutions at their eutectic point (figure 5.3) the eutectic solvent at point B creates microstructured hydrogels which allow production of mesoporous aerogels when using lyophilisation.^{56,233}

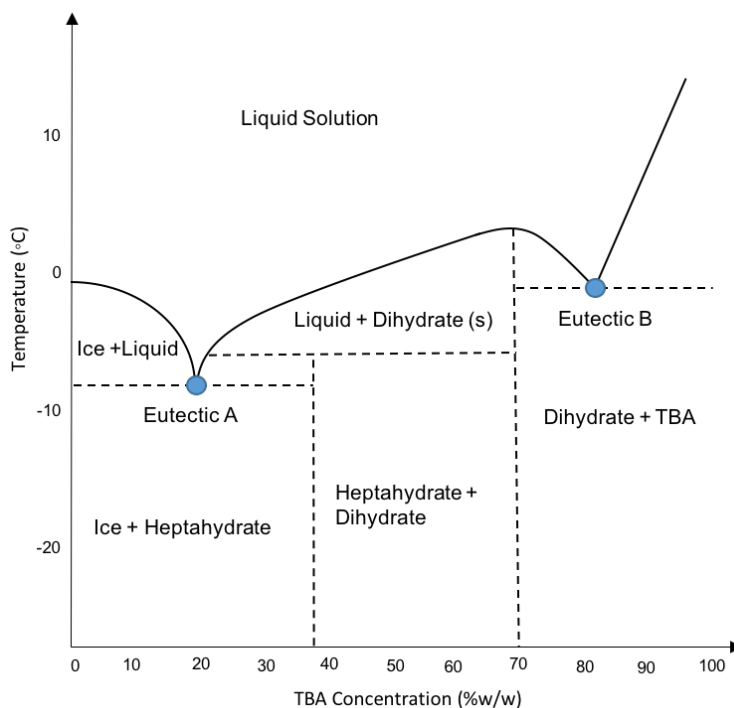


Figure 5.3 – Phase Diagram for Water and TBA

There are two eutectic points within the water-TBA phase diagram, one at roughly 25 wt% and one at 90 wt% TBA²³⁴ (labeled eutectic A and eutectic B in figure 5.3). As mentioned previously, when the solution at the eutectic point solidifies, a fine lamellar structure is formed.^{56,235} Away from the eutectic points the solidification of the solution is dictated by large crystals forming of the dominant component within the mixture. As these crystals form, the ratio of TBA and water alters until the eutectic point is reached, at which point the microstructured lamellar once again forms around the large crystals. As the water/TBA mixture is being used as a templating agent for porous materials the outcome of this is that away from the eutectic point the materials created are highly macroporous in nature, whereas the materials created within the eutectic points are more meso/microporous in nature.⁵⁶ The pore volume of the material also reaches a maximum around the eutectic points due to the high meso/microporosity created.^{56,233} This methodology allows for the production of mesoporous carbonaceous materials from a variety of polysaccharide feedstocks without the need for the solvent exchange and supercritical CO₂ drying steps.

As stated previously, a particular interest for utilisation of carbonaceous materials, in the setting of the current global situation – with climate change and environmental damage caused by humans now beyond question – is use of carbonaceous materials as gas adsorption agents. Especially relevant is CO₂ sequestration from mixed gas streams like those produced from fossil fuel based energy plants.

5.2 Specific Aims and Objectives

The aims within the chapter were to explore the utilisation of freeze dried derived carbonaceous materials produced from pectin extracted from the acid-free microwave biorefinery as CO₂ capture agents. With the following specific objectives:

- i. To fully characterise carbonaceous materials produced from extracted pectin at different carbonisation temperatures.
- ii. To explore the CO₂ adsorption capacity of these materials when compared to carbonaceous materials from other sources namely alginic acid and starch with comparison against commercially obtained activated carbon.
- iii. To explore the enthalpy of CO₂ adsorption onto the samples of mesoporous materials.
- iv. To draw conclusions based on the adsorption capacity for each material with reference to their physical material properties.

5.3 Results and Discussion

A range of Pecbon materials were created from Pecbon 300 (carbonised with a maximum of 300 °C) to Pecbon 800 (carbonised with a maximum of 800 °C). Carbonaceous materials produced from starch (Starbons) and alginic acid (Algibons) created within the group as well as commercial activated carbon were used for comparison purposes.

5.3.1 N₂ adsorption/desorption porosimetry

Porosimetry analysis using N₂ at 77 K was performed on the samples to determine the surface area, pore volume (both meso and micropore) and average pore radius. The results of which are shown in table 5.2. Full adsorption isotherms are given in the appendix (figure A.6).

Table 5.2 – Porosity Analysis of Pecbons

Sample	S _{BET} (m ² g ⁻¹)	V _{Total} (cm ³ g ⁻¹)	V _{Micropore} (cm ³ g ⁻¹)	% Micropores	Average Pore Radius (nm)
Pecbon 0	55	0.38	–	–	10.8
Pecbon 300	90	0.38	0	–	10.8
Pecbon 450	210	0.38	0.01	2.6	11.4
Pecbon 600	212	0.40	0.04	10.0	9.6
Pecbon 800	457	1.04	0.11	10.6	10.2
Starbon 800	546	0.45	0.17	37.8	8.9
Algibon 800	477	0.52	0.13	23.6	6.8
Activated Carbon	713	0.38	0.22	57.9	2.1

The porosity data in table 5.2 show that as carbonisation temperature is increased for the Pecbon samples, the surface area, total pore volume and micropore volume all increase. This is in good agreement with observations of other carbonaceous materials previously explored. When compared to activated carbon, all tested samples had a lower surface area and a markedly lower micropore volume but similar if not higher total pore volume. This indicates that activated carbon is mainly microporous in nature as indicated by its

high (57.9%) proportion of micropores and small average pore radius (2.1 nm). Other carbonaceous materials tested however, portray much more mesoporous character with the percentage of micropores being between 0 and 37.8% and the average pore radius being between 6.8 and 10.2 nm. The isotherms for the four best-performing materials with regards to CO₂ adsorption are given in figure 5.4 whilst isotherms for the other materials tested are given in figure A.6 in the appendix.

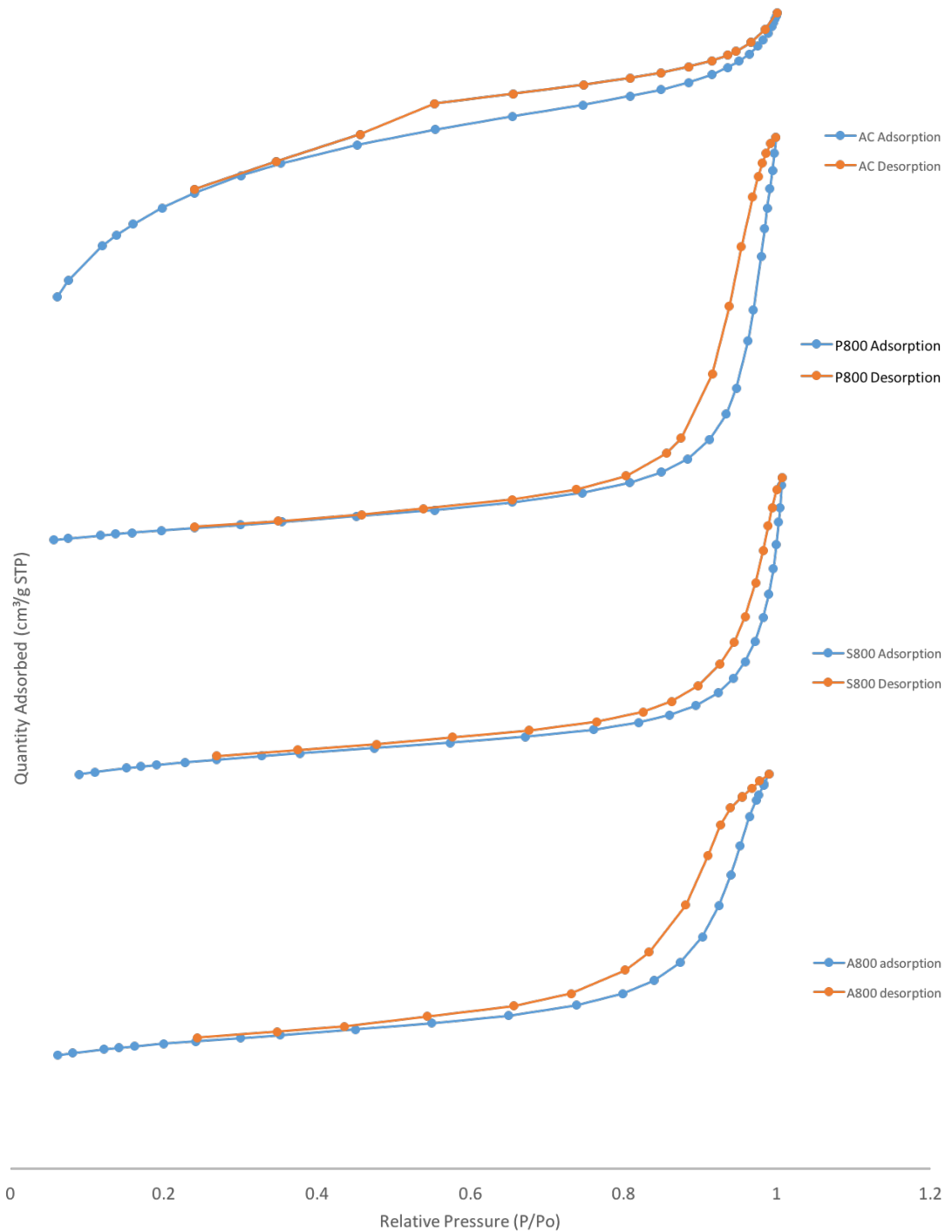


Figure 5.4 – Physisorption Isotherms for Different Materials. From Top to Bottom: Activated Carbon, P800, S800 and A800.

The isotherms shown in figure 5.4 allow more information regarding the pore character to be obtained. The isotherm for activated carbon shows a type I isotherm as defined by IUPAC.²³⁶ Type I isotherms are usually associated with very microporous materials, the isotherm also shows a H4-type hysteresis loop²³⁷ indicating narrow slit-pores.²³⁸ Both P800 and S800 show isotherms that portray mainly type III character with H3-type hysteresis²³⁷ which indicates materials that are mainly meso- or macroporous in nature with disordered, slit-shaped pores. The isotherm provided by A800 again shows mainly type III character, but the hysteresis loop shows similarities to H2 and H3 hystereses.²³⁷ This once again indicates a material that is highly meso- and macroporous in nature with potential interconnected ink-bottle shaped pores (H2-type hysteresis). The main differences between the materials tested and activated carbon is the degree of microporosity present. All experimentally derived carbonaceous materials showed more meso/macroporous character.

5.3.2 CO₂ Pressure Swing Adsorption studies

A pressure swing experiment was conducted to explore the CO₂ adsorption capabilities of the carbonaceous Pecbon materials compared to activated carbon, Starbon[®] and Algibon. Samples were first degassed on an Micromeritics ASAP 2020 porosimeter at 110 °C for 16h then cooled under vacuum, this sample was then subjected to five cycles of pressurised CO₂ at 10 bar for 30 minutes in a pressure reactor, followed by vacuum conditions at room temperature until the initial weight was once more achieved. The difference in mass between the post vacuum and post pressurised CO₂ conditions could then be used to calculate the amount of CO₂ adsorbed and hence the mmol of CO₂ the material was able to adsorb per gram. The averaged results across the five runs are given in figure 5.5 with the full pressure swing data being available in the appendix, tables A.34 – A.40

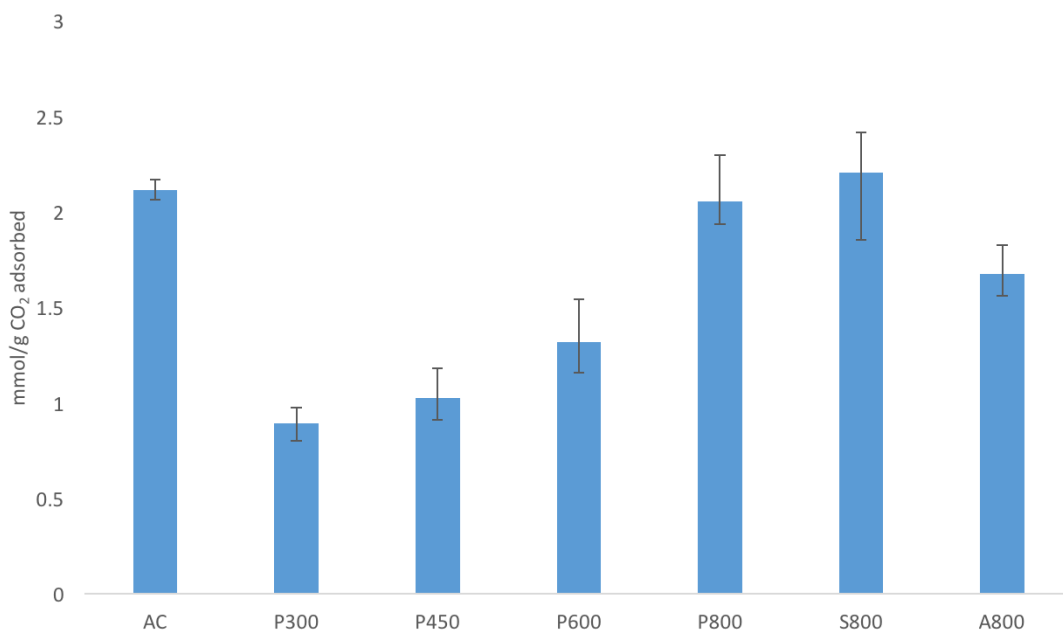


Figure 5.5 – mmol CO₂ Adsorbed per g Material

It can be seen from figure 5.5 that the higher the carbonisation temperature of the mesoporous material, the higher the amount of adsorbed CO₂. This is in good agreement with studies performed on carbonaceous materials produced from other biomass feedstocks.²³⁹ P800 is only slightly lower than the adsorption capacity of activated carbon and also slightly lower than S800, it is however a better CO₂ adsorber than A800.

5.3.3 Enthalpy of Adsorption

To help understand the nature of CO₂ adsorption onto the Pecbons, experiments were run on a simultaneous thermal analyzer (STA) to determine the enthalpy of adsorption at 308 K. The STA measures both the change in mass of the sample and the heat flow changes upon adsorption and desorption of CO₂. The enthalpy of adsorption and desorption of CO₂ can therefore be calculated.

5.3.3.1 CO₂/N₂ Swing

A CO₂/N₂ swing experiment was set up as outlined in the experimental section (2.3.1.5) to explore the enthalpy of adsorption and desorption of CO₂. Figure 5.6 shows the DSC

traces for P800, traces for the other materials can be found in figures A.7 and A.8 in the appendix.

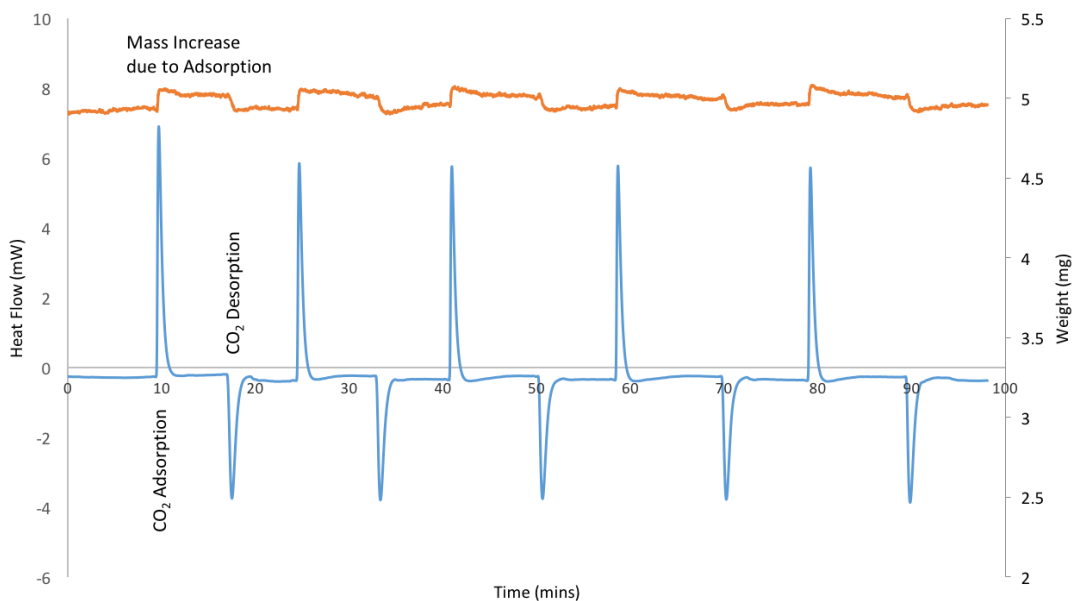


Figure 5.6 – Heat Flow and Weight Change During CO₂ Adsorption and Desorption using P800 at 308 K

From the DSC traces, the peak area associated with the adsorption/desorption of the CO₂ can be used in conjunction with the change in mass to calculate the enthalpy of adsorption associated with each material. Care has to be taken here, however, as these values do not take into account the buoyancy effect when changing gasses from N₂ to CO₂ in the STA. This may change the recorded mass of the sample slightly. If future tests were to be performed a calibration run swapping gasses under experimental conditions but with an empty sample cup should be performed to determine the magnitude of this effect. Figure 5.7 shows the calculated enthalpies of adsorption and desorption for the four best performing materials.

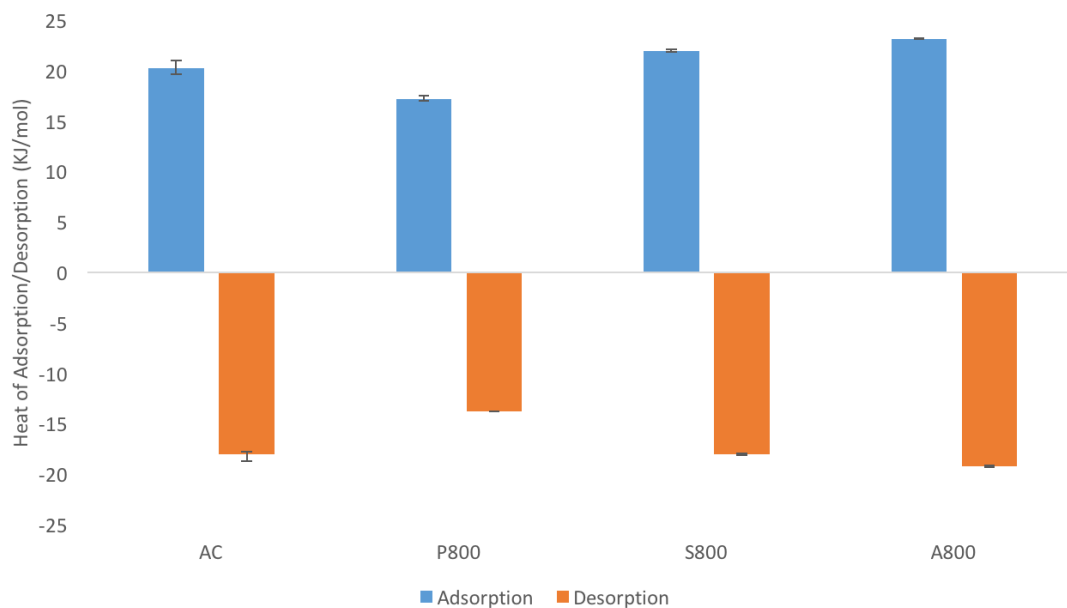


Figure 5.7 – Enthalpy of Adsorption/Desorption Determined via CO₂/N₂ Swing Experiments

Figure 5.7 shows that all the materials tested have similar enthalpies of adsorption ranging from 17.19 kJ/mol to 23.15 kJ/mol, These are in between values of heat of carbon dioxide vaporization (10.3 kJ/mol) and sublimation (26.1 kJ/mol)²⁴⁰ and so it can be concluded that physisorption is the primary mechanism for adsorption of CO₂ onto all four materials. This is to be expected due to the highly aromatic nature of materials carbonised at 800 °C.

5.3.3.2 Water Saturated CO₂/N₂ Swing

Real-world flue gas is heavily impregnated with moisture vapour. In an attempt to explore how this effects the adsorption of CO₂ onto the samples an experimental procedure was set up to allow the introduction of gaseous water vapour into the CO₂ gas stream for the STA analysis. The result for P800 of which are shown in figure 5.8, traces for the other materials can be found in figures A.9 and A.10 in the appendix.

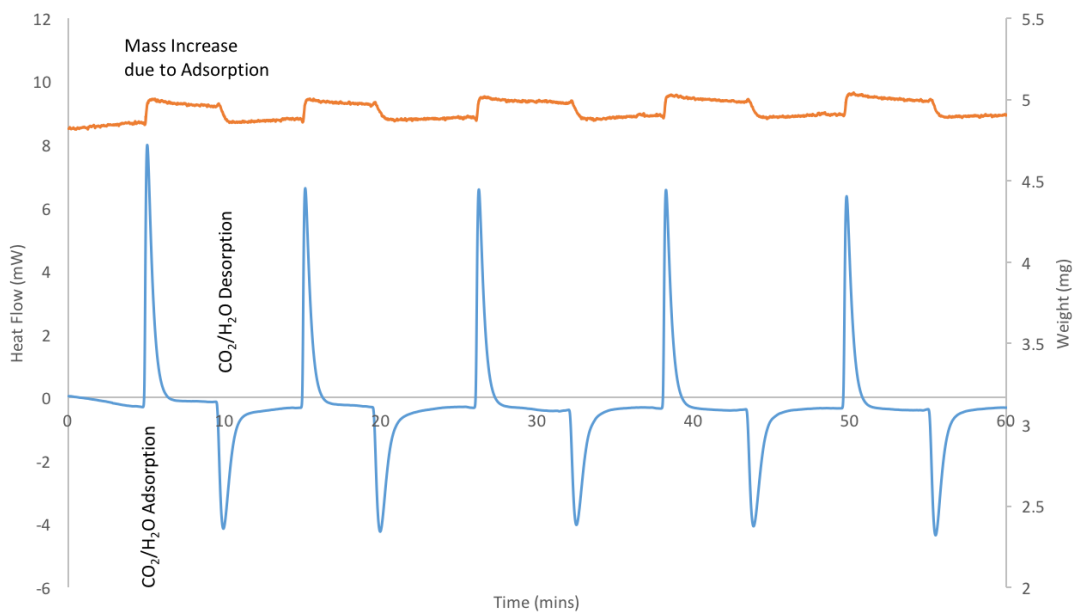


Figure 5.8 – Heat Flow and Weight Change During Water Saturated CO₂ Adsorption and Desorption using P800 at 308 K

Once again, the enthalpy of adsorption and desorption of CO₂ can be calculated from this data and compared to the results obtained from the ‘dry’ STA experiments. Figure 5.9 shows comparison of the ‘dry’ and moisture-loaded experiments for the four best-performing materials.

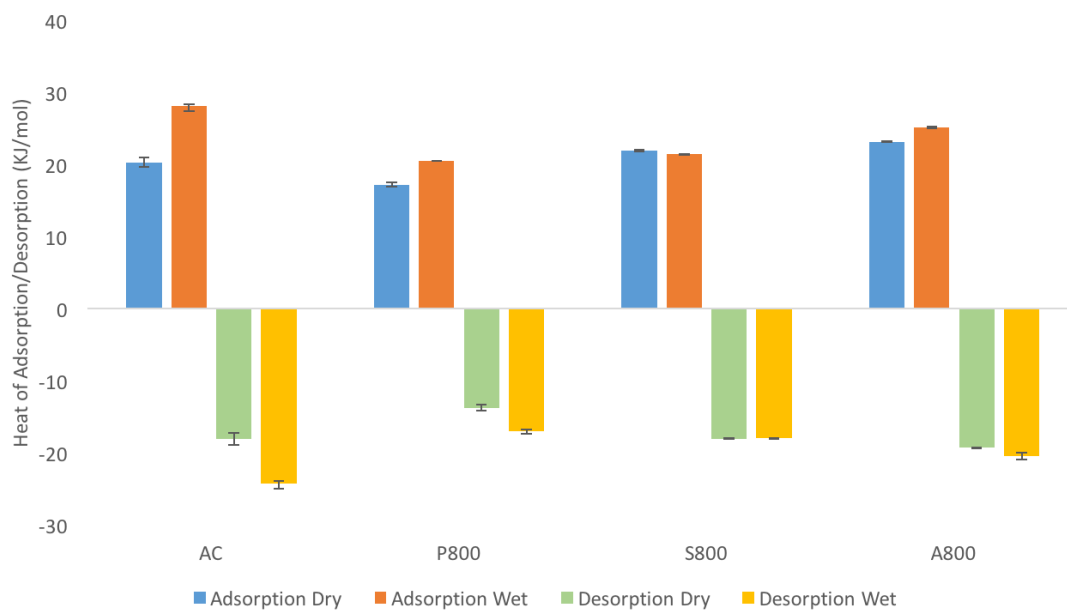


Figure 5.9 – Enthalpy of Adsorption and Desorption of CO₂ under Dry and Wet Conditions for Activated Carbon (AC), Pecbon 800 (P800), Starbon[®] 800 (S800) and Algibon 800 (A800)

The results obtained from the water-saturated thermal analysis of the adsorption and desorption of CO₂ onto the materials show a dramatic increase in enthalpy of adsorption for activated carbon and slight increases in P800 and A800, S800 showed no change. Because water is being introduced with the CO₂ the observed enthalpy of adsorption will be equal to the sum of the enthalpy of CO₂ adsorption and the enthalpy of H₂O adsorption. With this being the case, the dramatic increase in observed enthalpy for activated carbon indicates a large amount of water being adsorbed in combination with CO₂. Comparably the other materials tested do not show a large increase in observed enthalpy (with S800 showing none), this would indicate that very little water is being adsorbed onto these materials.

This preliminary exploration into water-saturated CO₂ adsorption indicates that all experimentally derived materials tested (P800, S800 and A800) are more resistant to water fouling than activated carbon. This is most likely due to the highly hydrophobic surface chemistry present in P800, S800 and A800, whereas activated carbon has undergone an activation procedure which will have altered the surface chemistry and potentially added hydrophilic functional groups.

Further experiments would have to be designed before this hypothesis can be confirmed, with calculation of the enthalpy of adsorption for water without CO₂ onto the materials and full adsorption isotherms for both water and water-saturated CO₂ being required. This is expanded upon in the future work section.

5.3.4 CO₂/N₂ Porosimetry

Chemisorption experiments were performed on the best-performing of each material: activated carbon, P800, S800 and A800, according to the methodology outlined in the experimental section (2.3.1.3). Experiments were run at 308 K to mimic conditions within a flue and isotherms for both N₂ and CO₂ were obtained. Unfortunately, due to sample size being small (<100 mg) the N₂ uptake onto the material was within the equipments error margin. Further experiments using a larger sample size would be required to explore if the N₂ uptake can be increased to recordable levels as covered in the future work section. For these experiments the uptake of N₂ onto the material is considered zero under the conditions tested. Full isotherms for the adsorption of CO₂ and N₂ at 308K and pressures ranging from 0-100 kPa for the four materials are shown in figure 5.10.

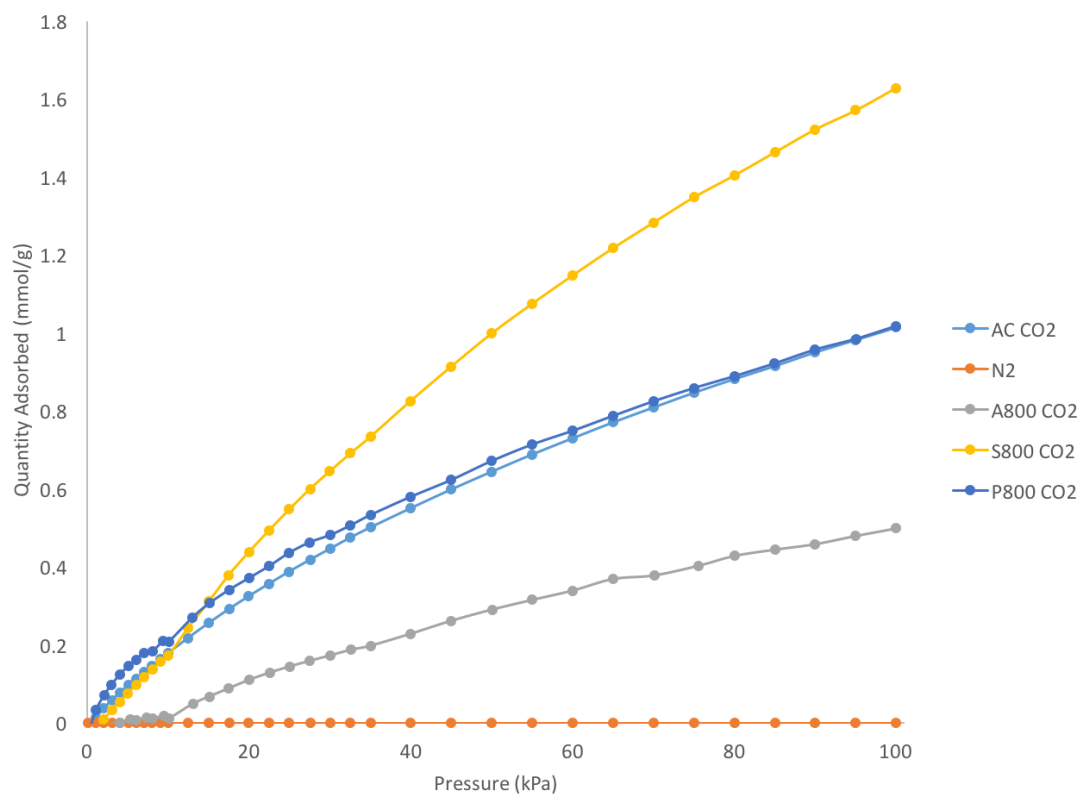


Figure 5.10 – Chemisorption Isotherms for Different Samples at 308K for both CO₂ and N₂

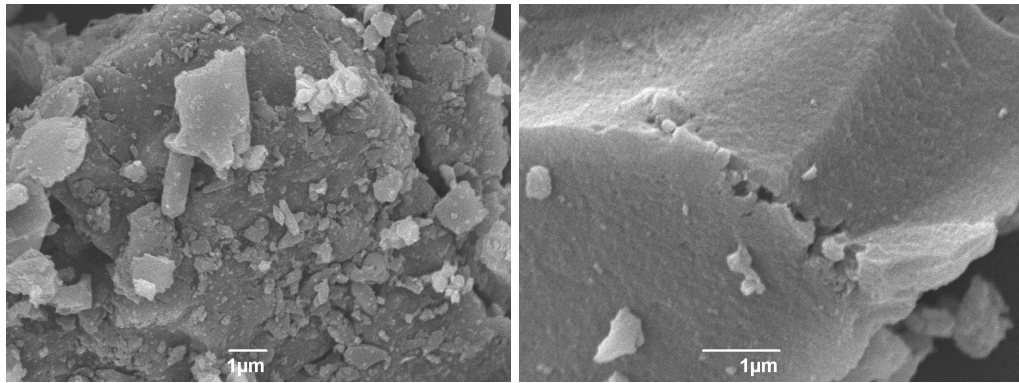
The isotherms shown in figure 5.10 indicate that all the materials tested had a higher affinity for adsorption of CO₂ than N₂ as shown by the much higher uptake. Looking at the maximum amount of CO₂ adsorbed onto each material, a similar trend to that observed in figure 5.5 is found. AC and P800 show similar CO₂ adsorption capacities with S800 being higher and A800 lower. Table 5.3 shows the maximum amount of gas adsorbed at 100 kPa for each of the materials (again, N₂ uptake was within the error of the instrument and is therefore reported as zero.)

Table 5.3 – Maximum Adsorption of CO₂ and N₂ onto Materials as Determined by Chemisorption Experiments

Sample	Maximum CO ₂ Adsorbed at 100 kPa (mmol/g)	Maximum N ₂ Adsorbed at 100 kPa (mmol/g)
AC	1.01	0
P800	1.02	0
S800	1.63	0
A800	0.50	0

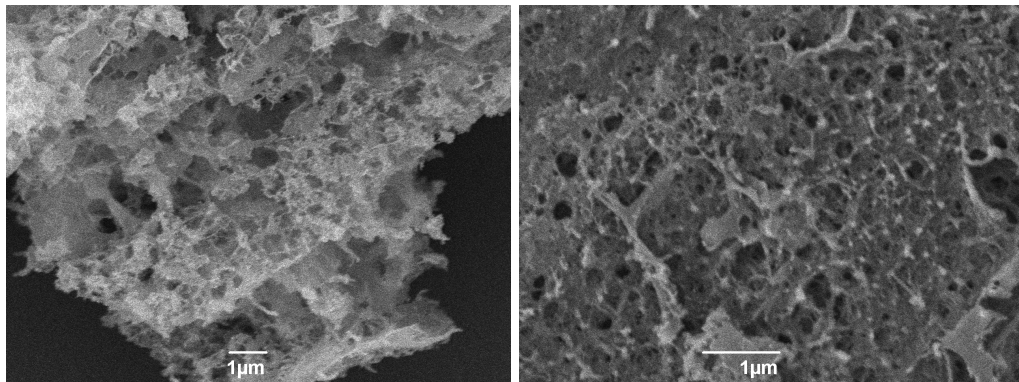
5.3.5 SEM Analysis

Scanning Electron Microscopy (SEM) was performed on the four best performing materials in an attempt to visualise the differences in surface structure. Figure 5.11 shows the images at 10,000x and 20,000x magnification. As expected, the activated carbon shows minimal macroporosity, showing a smooth surface (SEM is not sufficient to see micropores). The other materials tested, however, show extensive macroporosity, with very rough surfaces being observed. This reinforces the analysis performed via nitrogen porosimetry and indicate that the majority of the surface area for activated carbon is thanks to its extensive microposity, while with the other materials tested a large proportion of the surface area will be due to macro- and mesoporosity



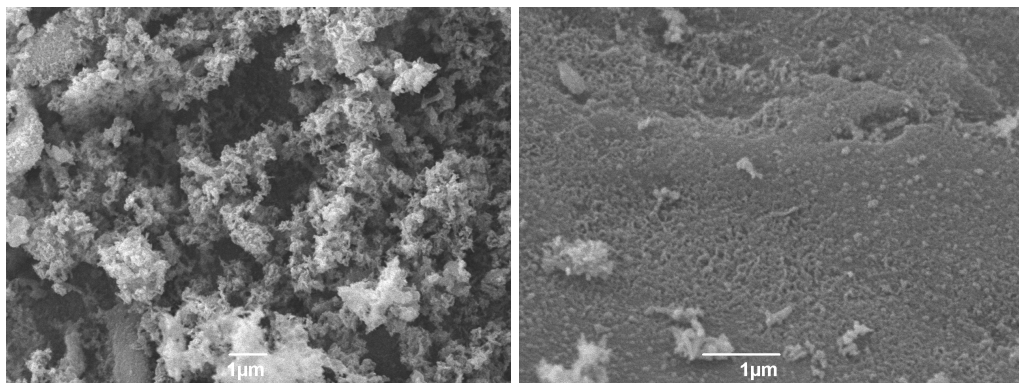
(a) SEM images of Activated Carbon 10,000x

(b) SEM images of Activated Carbon 20,000x



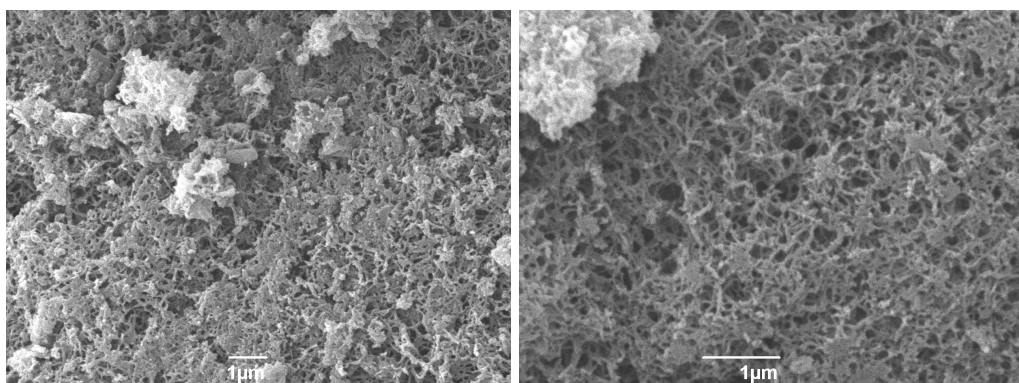
(c) SEM images of P800 10,000x

(d) SEM images of P800 20,000x



(e) SEM images of A800 10,000x

(f) SEM images of A800 20,000x



(g) SEM images of S800 10,000x

(h) SEM images of S800 20,000x

Figure 5.11 – SEM Images of different samples

5.3.6 Relationship Between Physical Properties and CO₂ Adsorption

Preliminary analysis comparing the physical properties of the materials tested and the adsorption capacity for CO₂ allows the properties that control CO₂ adsorption to be determined. Simply taking data from the physisorption table 5.2 and plotting it against CO₂ adsorption data from figure 5.5 shows little to no correlation between average pore diameter, percentage micropores and total pore volume. When total surface area and micropores are analysed however a correlation is found between both properties and the CO₂ adsorption capacity of the material, and while the R² values are not very high (8.54 and 8.53) a correlation is definitely present. Figures 5.12 and 5.13 show the correlation between BET surface area and micropore volume and CO₂ adsorption.

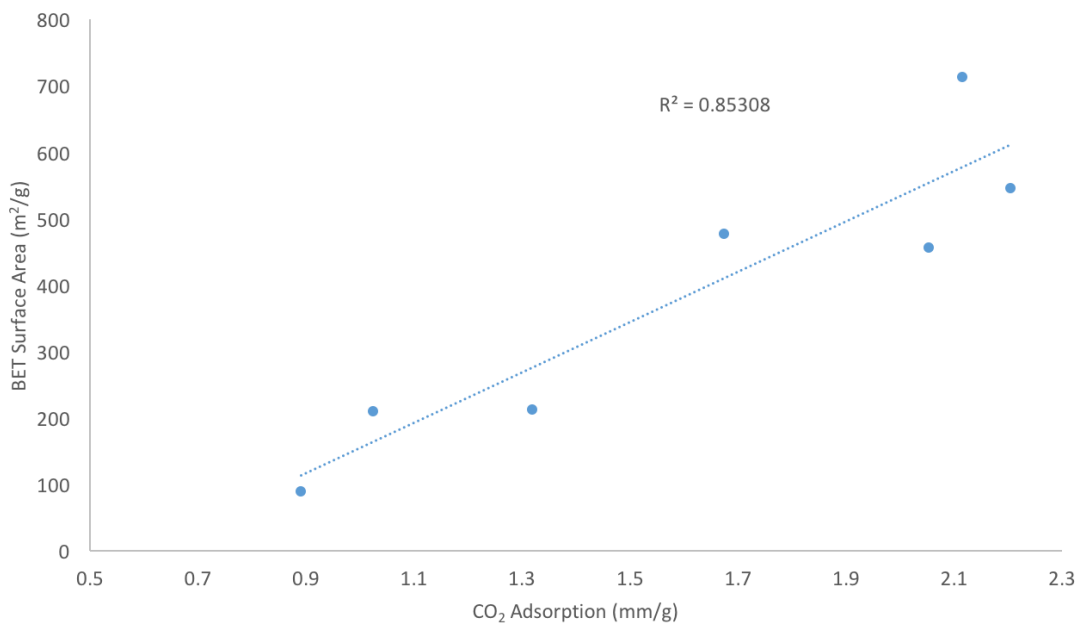


Figure 5.12 – Analysis of BET Surface Area against CO₂ Adsorption Capacity

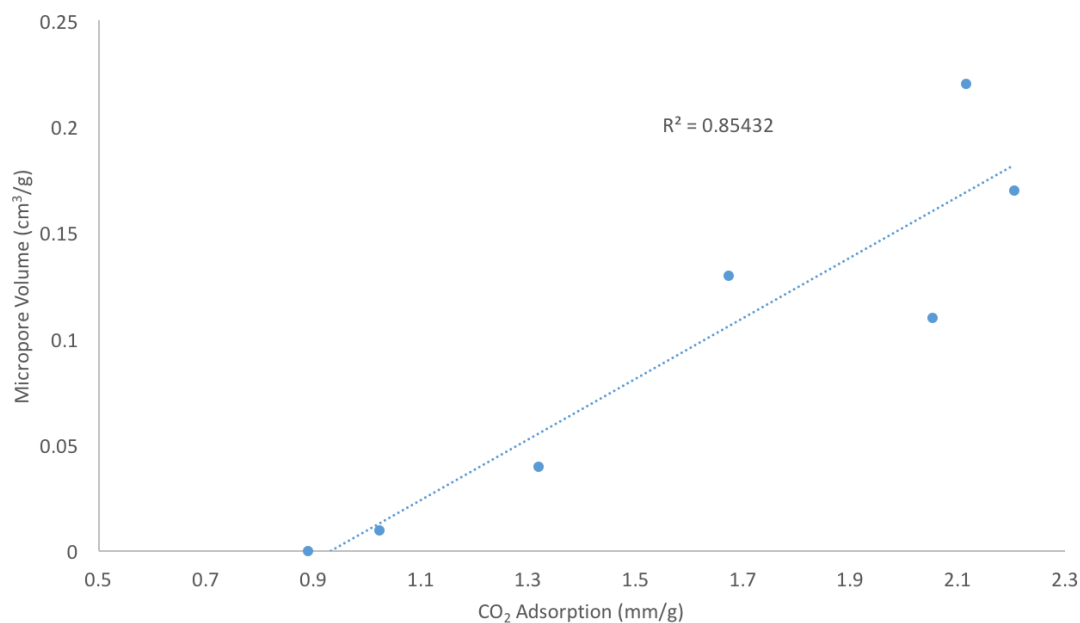


Figure 5.13 – Analysis of Micropore Volume against CO₂ Adsorption Capacity

Upon further analysis, a strong correlation between micropore volume and surface area was found (figure 5.14) with an R^2 value of 0.98. This could mean that the correlation between surface area and CO₂ capacity is down to the increase in micropore volume, more work would need to be performed to confirm this though, this is covered more in the future work section.

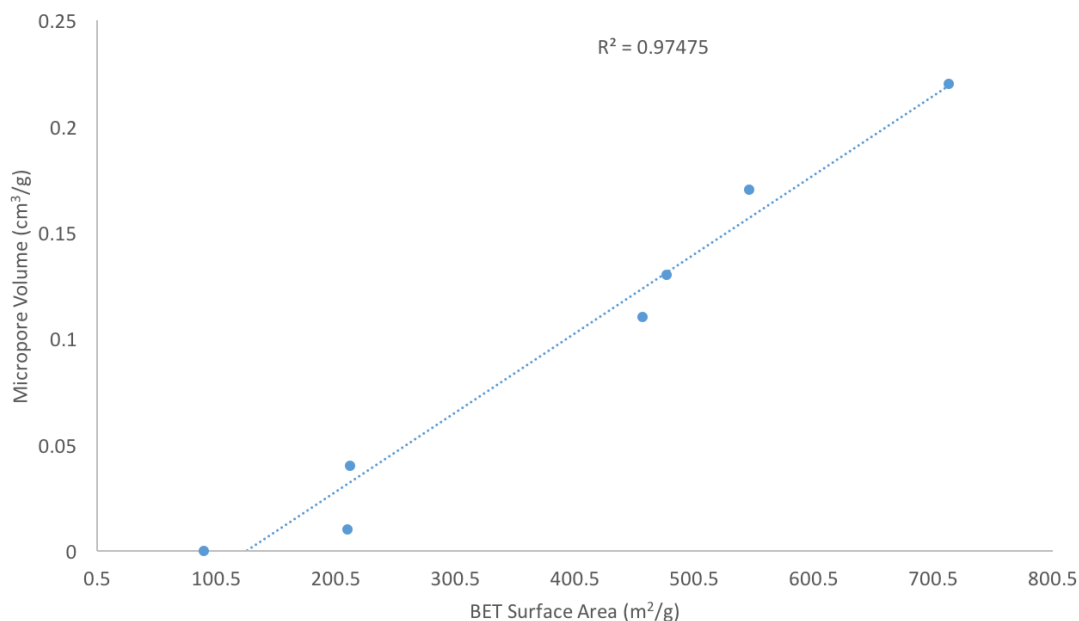


Figure 5.14 – Analysis of Micropore Volume against BET Surface Area

Ideally tests would be performed on samples with very high surface area and negligible microporosity to test whether the CO₂ adsorption is reliant on the micropore volume or surface area only, or whether it relies on a combination of both.

5.3.7 Effect of Material Preparation Methodology on CO₂ Adsorbance Capacities

The work presented in this chapter was a continuation of the work performed by Durá *et al.*²³⁹ who tested different Starbons and Algibons against activated carbon and concluded that S800 and A800 both performed markedly better than activated carbon at CO₂ adsorption. This is contrary to the results obtained in this chapter, upon exploration into why this could be the case it was discovered that Durá *et al.* created the carbonaceous materials via the original solvent exchange method as described in the introduction, whereas all materials produced for this work were obtained using the TBA:water templating followed by freeze drying as described in both the introduction and experimental sections.

Looking at the physical properties of the materials produced for this work and those used in the publication by Durá *et al.* it can be concluded that the freeze drying route creates

a more macroporous material than solvent exchange and supercritical CO₂ drying which creates more microporous materials in comparison. This result is interesting as it shows that although the freeze drying route has many advantages over the traditional solvent exchange route, if CO₂ adsorption is the aim for the materials produced, the lower degree of microporosity would appear to have a detrimental effect on the materials performance.

5.4 Conclusions

CO₂ capture is a topical area of research of great interest, and the development of new materials for this application is of paramount importance. Understanding how the properties of tested materials affect their CO₂ adsorption capacities allows for a more intelligent approach to designing them. This chapter outlines the initial work done into testing Pecbons as potential CO₂ capture agents and shows the promise of using porous, carbonaceous materials obtained from biomass for this application.

Pecbon carbonised up to 800 °C (P800) performed the best of those tested, with a maximum CO₂ adsorbance of 2.05 ± 0.24 mmol/g material. This is similar to the amount adsorbed by commercially available activated carbon (AC) (2.12 ± 0.05 mmol/g) as well as Starbon[®] 800 (S800) and Algibon 800 (A800) (2.21 ± 0.35 and 1.67 ± 0.15 mmol/g respectively).

Analysis of the physical properties of the materials showed that activated carbon had higher surface area than any of the other materials tested, with P800, S800 and A800 all having similar surface areas. Activated carbon once again had the highest micropore volume, followed by S800, A800, then P800, with lower carbonisation temperatures showing much smaller micropore volumes. This trend in micropore volume correlates to the quantity of CO₂ adsorbed with an R² value of 0.85.

The enthalpy and selectivity of CO₂ adsorbance were explored. All materials showed a much higher uptake of CO₂ than N₂ up to a pressure of 100 kPa; this shows initial evidence of a preferential adsorption of CO₂ from mixed gas streams, but more experiments would have to be performed utilising mixed gas streams to confirm this. The experimentally determined enthalpy of CO₂ adsorption onto the materials tested shows that the four best performing materials (AC, P800, S800 and A800) all have similar enthalpies of CO₂ adsorption that lie within the physisorption range. Upon addition of water saturated CO₂, however, elevated enthalpies are observed with AC giving the highest increase and the other materials tested much lower. This could indicate that more water is adsorbing in combination with CO₂ onto activated carbon suggesting the other tested materials are more resistant to water fouling.

Chapter 6

Future Work and Concluding Remarks

6.1 Future Work

6.1.1 Acid-Free Microwave Biorefinery Scheme for Citrus Waste

6.1.1.1 Full Analysis of Pectin Extraction from Agroterenas Case Study

While initial work has been performed on extraction of pectin from industrially sourced bagasse provided by Agroterenas, a full study with multiple repetitions to determine yield and full analysis as performed on other pectins needs to be performed to prove that the pectin obtained from this feedstock is of the same quality as that extracted from oranges juiced at lab scale. Full analysis of pectin obtained from healthy and HLB infected oranges would also be beneficial to further explore the effect of this disease on pectin quality. Pectin obtained from the yellow processing water would also need further analysis performed to determine whether or not it would be economically advantageous to pursue pectin as a product from the yellow water.

6.1.1.2 Scale-Up to Pilot-Scale

While work has been started scaling the acid-free microwave-assisted extraction of pectin from waste orange peel, there is still a lot of work to do on optimisation of methodologies both in terms of product yield and quality and energy and solvent minimisation. Initial results show that pectin extracted at large scale is of similar quality to lab scale experiments. Full life cycle assessment (LCA) would have to be carried out on the process as well during the optimisation phase to ensure that all parameters are considered, this would also allow the areas that could be most improved to be identified.

6.1.1.3 Mixed Feedstocks

One of the most desirable properties of a robust biorefinery system is its ability to cope with heterogeneous feedstocks. Biomass is typically non-uniform, so the biorefinery system would have to be able to cope with different loads depending on the harvest yield and different biomass quality. The variables that influence the biomass would

have to be fully explored and understood. Varietal differences between oranges and different citrus fruits as well as the effect of disease have been explored within this body of work. The effect of season, fruit ripeness, amount of time stored prior to extraction, inherent moisture content and many other variables, however, are still unexplored with relation to their effect on essential oil and pectin yield and quality.

To make the proposed system economically viable, a large amount of biomass would have to be processed daily. This would not be a problem for large citrus juicing companies such as those in Brazil, but it would be challenging for smaller companies to adopt this biorefinery system. It would be ideal, then, for the smaller companies to be able to sell their biomass to a centralised plant that could process the biomass from several different companies and therefore become economically viable. Even more attractive would be the ability to cope with mixed fruit feedstocks. If the plant could not only process citrus, but also other fruits such as apple, peach, pear etc. without affecting the pectin quality, a multitude of industries could valorise their waste through a centralised plant. Extensive research would have to be done into how mixed feedstocks would affect pectin yield and quality, however.

6.1.1.4 Combined Extraction Techniques

As alluded to in the introduction to Chapter 3, the combination of compatible extraction techniques could allow for a beneficial synergy of the advantages given by each separate technique. Exploration into the effect of ultrasound on microwave extraction, for example, would be an interesting avenue of research. The additional energy and equipment cost would have to be weighed against the potential improvement to yield and/or quality of the products to determine whether the addition of the second extraction technique was economically beneficial.

6.1.1.5 Other Valorisation Options – Proteins

Based on the work carried out in this project, it was decided that, as a potential addition to the acid-free microwave assisted biorefinery scheme outlined, initial research into the protein content and characteristics of orange peel waste should be pursued. While the protein content in oranges is known to be relatively low, it was hypothesised that if the

protein had not been extracted within the biorefinery process then a protein extraction step could easily be added onto the end. Herein preliminary results for this future area of work are briefly discussed.

i. Protein Content

Initial tests for protein were carried out on both wet and dry peel before and after extraction using the acid-free microwave assisted methodology. These tests were carried out using CHN analysis or the Kjeldahl method. For the wet orange peel, the nitrogen content was negligible in both samples, but for the dry peel, the removal of water allowed the nitrogen content of the biomass to be observed with greater accuracy. The results are shown in table 6.1

Table 6.1 – CHN Analysis of Dry Orange Peel Before and After Microwave Extraction

Sample	C(%)	H(%)	N(%)	Protein (%)
peel before extraction	42.458	6.592	0.596	2.77
peel after extraction	42.295	3.63	1.078	5.00
peel after conventional acid extraction	42.393	6.009	0.966	4.48

It can be seen that the acid-free microwave assisted extraction methodology does, in fact, increase the protein content within the peel residue from roughly 2.77% to roughly 5% on a dry weight basis. This has two-fold interest, as the residue from the biorefinery process could be used to extract a purified protein as described for potatoes or, if the residue was utilised as animal feed, the increased protein content as well as the removal of most of the bitter compounds during earlier microwave extractions would make higher quality feed.

Characterisation of the protein present was attempted by solubilising the protein in water, freeze drying and performing the analysis described below.

ii. SDS-PAGE

SDS-PAGE was performed on the protein-containing material in an effort to determine the molecular weight of the different proteins within oranges along with the diversity of proteins present. The SDS-PAGE is shown in figure 6.1

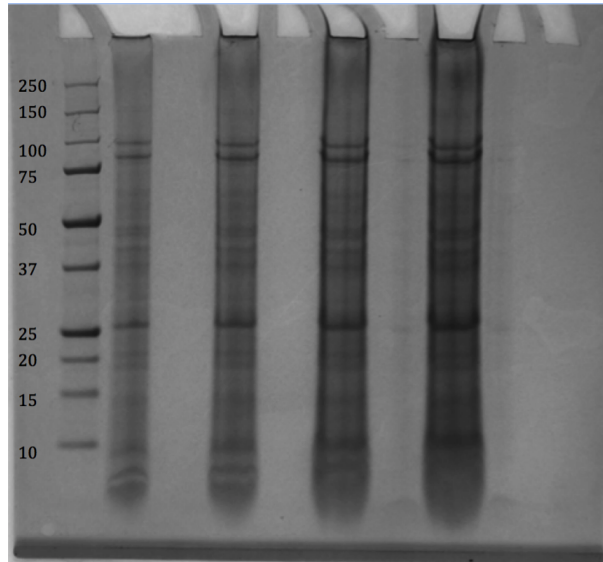


Figure 6.1 – SDS-PAGE gel for orange protein

As can be seen from figure 6.1, there are three main proteins present in the sample, one at roughly 25 kDa, and two between 75 and 100 kDa. Proteomic analysis was performed on these three bands to determine which proteins they represent.

iii. Identification of Proteins via Proteomics

Due to the fact there are only three major bands in the orange protein SDS-PAGE it was decided that proteomic analysis would be run on all three bands to determine the protein present. The 3 bands analysed were centred at roughly 100 kDa, 75 kDa and 25 kDa respectively. The results are shown in table 6.2

Table 6.2 – Proteomics Analysis of Orange Protein

Band	Position on Gel (kDa)	Protein Match	Molecular Weight of Protein (kDa)
1	25	germin-like protein subfamily 1 member 17	24.254
2	75	germin-like protein subfamily 1 member 17	24.254
2	75	elongation factor G-2, chloroplastic-like	86.083
3	100	germin-like protein subfamily 1 member 17	24.254

The results displayed in table 6.2 show clearly that the main protein present within the sample is the germin-like protein subfamily 1 member 17. Bands 2 and 3 also show peptide matches to this protein, and although the molecular mass does not match with these bands, this can be explained by the protein being a trimer or tetramer which would give matching molecular masses of 72.762 and 97.016 kDa respectively.

For full proteomic results see table 6.3. This preliminary work shows promise for development into another potential step to add into the described citrus waste biorefinery.

Table 6.3 – Proteomics Data For Orange Protien

Observed Mass	Mr (expt)	Mr (calc)	Expect Score	Peptide
Band 1				
Protein: Germin-like protein subfamily 1 member 17				
1917.0585	1916.0512	1915.9805	0.00026	R.IDYAPYGQRPPHIHPR.A
1927.9856	1926.9783	1926.9224	1.6e-06	R.AEDFFFSGLGKPGNTANR.L
2629.4089	2628.4017	2628.3395	4.6e-21	R.LGVDETDANVEQIPGLNTLGISAFR.I
Band 2				
Protein: elongation factor G-2, chloroplastic-like				
1597.8483	1596.8410	1596.8300	0.00013	K.IATDPFVGNLTFFR.V
Protein: Germin-like protein subfamily 1 member 17				
1916.9739	1915.9666	1915.9805	0.00022	R.IDYAPYGQRPPHIHPR.A
Band 3				
Protein: Germin-like protein subfamily 1 member 17				
1916.9825	1915.9753	1915.9805	5e-05	R.IDYAPYGQRPPHIHPR.A
1927.9288	1926.9216	1926.9224	5.9e-06	R.AEDFFFSGLGKPGNTANR.L
2629.3167	2628.3094	2628.3395	8.2e-15	R.LGVDETDANVEQIPGLNTLGISAFR.I

6.1.1.6 Full Life Cycle Assessment of Described Citrus Waste Biorefinery

The work described in this thesis has focused on the chemical and technological design of a citrus waste biorefinery, but if industrialisation of this process is to be performed, full Life Cycle Assessment (LCA) would need to be conducted. This would cover all aspects of the process including the areas explored within this thesis and would allow a map to be created with all outputs and inputs including electricity, heat, process water, waste etc. This map would highlight any inefficient processes within the biorefinery so they can be addressed. A full economic analysis of the potential profits against capital and operating costs would also have to be performed before an industry would consider implementation of this biorefinery.

6.1.2 Proteins from Potatoes

6.1.2.1 Testing in Food Applications

While potato protein is already currently used in many applications, there is potential for it to be used in many more in the future. As mentioned in the introduction to this body of work, the vegetable protein market is growing rapidly, so incorporation of vegetable – potato – protein into more products is likely. Thorough testing of the extracted protein in a host of different foodstuffs is therefore necessary to find which applications it is most suited to and what kind of effects it has on the textural, nutritional and sensory – taste and smell – properties of the food.

i. Testing of Extracted Protease Inhibitors as Appetite Suppressants

While studies have already been conducted into protease inhibitors extracted from potatoes in a conventional way, testing of the protease inhibitors extracted and purified as described here would be beneficial for commercialisation of these proteins.

6.1.2.2 Full Protease Inhibition Analysis

Continued work into developing easy colometric or fluorometric assays for testing inhibition of both trypsin and chymotrypsin by the target protease inhibitor would be beneficial in testing the inhibitor's activity and proving it is still in its active form after extraction and purification.

6.1.2.3 Crystallisation of Protease Inhibitor-Enzyme Complex

While complexation of PI2 with its target enzymes trypsin and chymotrypsin has been successfully performed, and crystallisation studies of the extracted PI2 protein are being performed, an interesting extension would be to crystallise the complex of PI2, trypsin and chymotrypsin. This would potentially allow a x-ray crystal structure of the complex to be obtained, giving valuable insight into the binding sites and protein conformation changes upon complexation. Computational predictions of the complex structure have been performed, but to date, no experimental crystal structure of PI2 complexed to trypsin and chymotrypsin has been obtained.

6.1.2.4 Full Life Cycle Assessment of Protein Extraction from Potatoes

As for the citrus waste biorefinery, if industrialisation of the described potato protein extraction is desired, a full LCA would need to be performed, for the same reasons.

6.1.3 Pecbons – a Carbonaceous Material for CO₂ Capture

6.1.3.1 Different Material Production Methodologies

As mentioned in the conclusions to Chapter 5, the method used for synthesis of the porous materials seems to heavily affect their ability to adsorb CO₂. To further explore this, direct comparisons would have to be made comparing different carbonaceous materials produced using either the solvent exchange method of drying, or the freeze-drying method. The same starting material, templating and carbonisation method should be used in both cases to reduce the number of variables.

6.1.3.2 Full Characterisation

Further characterisation of the materials produced needs to be performed to gain a thorough understanding of the effect of material properties on CO₂ adsorption. Testing in a real flue would also be beneficial because, while efforts were made to replicate the conditions in the lab, equipment limitations prohibited an exact replica of flue gas from being analysed.

i. Surface Chemistry Analysis

Although being carbonised to 800 °C should remove any functional groups present in the starting material and convert the material into graphitic carbon, experiments exploring whether any surface chemistry differences remain should be conducted. Algibons and Pecbons have a much higher carboxyl group concentration than activated carbon or Starbons, which could affect the CO₂ adsorption. Analysis of the activated carbon surface chemistry would also be beneficial in attempting to explain the increase in observed enthalpy of adsorption using water-saturated CO₂.

ii. Isotherms with Water and Mixed Gas Analysis

Full exploration into water adsorption onto the materials would be useful in drawing conclusions about the resistance to water fouling. Experimentals were performed using water-saturated CO₂ but using water-saturated N₂ followed by desorption using dry N₂ would allow for the enthalpy of adsorption of H₂O to be determined which would aid in analysis of the mixed enthalpies of adsorption.

Mixed gas analysis would also be needed to fully explore the complex interactions that would happen in a real-world flue. Porosimetry analysis using a mixed gas stream where the concentrations of each gas could be controlled would be an ideal solution, as this would allow isotherms at different partial pressures to be obtained and analysed. Reactions of different gases on the surface of the material could also occur in mixed gas streams, and extensive research would be needed to determine if this was the case and if so, what effect it would have on the adsorption capacity and regeneration of the material.

iii. Further Analysis into Physical Properties and CO₂ Adsorption Capacity

As alluded to in the results and discussion section of Chapter 5, it has not been determined if the micropore volume or the surface area has the greatest effect on CO₂ adsorption, as in the samples tested, these two properties correlated well. It would therefore be advantageous to test a high surface area material with negligible micro porosity to prove which of these two physical properties is the most important when it comes to designing future materials for use in CO₂ capture.

6.2 Concluding Remarks

Food waste is a serious concern in modern society. As the global population increases food production will have to increase in parallel. Food waste will grow at the same rate, unless practices are put in place to reduce food waste or to treat it as a feedstock for the production of energy, chemicals or edible products. The United Nations has highlighted waste prevention and development of sustainable consumption and production patterns in its Sustainable Development Goals, incentivising research into these areas. It is likely that research into sustainable industrial practices will continue in the future. The work contained in this thesis adds to the research into sustainable biorefinery routes for food waste, working towards the United Nation's Sustainable Development Goals and providing solutions to problems arising from our growing population.

Valorisation of both citrus juicing waste and potato production waste has been proven promising for the production of value-added products including: citrus oil, pectin, cellulosic fibres for water binding, protein, and appetite-suppressing dietary aids. Exploratory work has also been performed into the utilisation of pectin as a precursor for carbon capture agents and into scaling up the novel biorefinery processes for both citrus juicing waste and potato waste.

Appendix

A.1 Chapter 2

A.1.1 List of Equipment

Gas Chromatography-Flame Ionisation Detection (GC-FID)

GC-FID was carried out using an Agilent technologies 6890N Network GC System using a Phenomenex Zebron 5HT column equipped with a flame-ionisation detector.

Attenuated Total Reflection Infrared Spectroscopy (ATR-IR)

ATR-IR was carried out using a Bruker Vertex 70 spectrometer equipped with a Specac Golden gate. Spectra was taken from 4000 cm^{-1} to 600 cm^{-1} at 64 scans, with a spectral resolution of 2 cm^{-1} with a blank window for background.

Nuclear Magnetic Resonance (NMR)

Both ^1H (400 MHz) and ^{13}C NMR (100 MHz) along with ^{13}C DEPT 135 (Distortionless Enhancement by Polarisation Transfer) were performed on a JEOL 3cs400 spectrometer. Samples were dissolved in either deuterated chloroform (CDCl_3), deuterated methanol (CD_3OD) or DMSO.

Gas Chromatography Mass-Spectrometry (GC-MS)

GC-TOF was carried out using an Agilent 6890 GC coupled with a Pegasus IV TOF mass spectrometer (Leco) with the specs outlined below:

Table A.1 – GC-TOF Specification

Column	30 m x 0.25 mm Rxi-5Sil MS column (Thames Restek)
Film Thickness	0.25 μm
Carrier Gas	Helium
Flow Rate	Constant flow at 1 mL/min

Electro-Spray Ionisation Mass Spectrometry (ESI-MS)

ESI was performed using a Bruker MicroTOF instrument.

Thermo-Gravimetric Analysis (TGA)

TGA was carried out under a flow of nitrogen or carbon dioxide (50 mL min^{-1}) using a

NETZSCH Themische Analyse STA 409 cell.

STA analysis was carried out using a Stanton Redcroft STA 780 thermal analyser, using alumina crucibles.

Centrifuge

- Lab scale: A Thermo Scientific Heraeus Magafuge 40R centrifuge was used at a speed of 3000 rpm with an acceleration of 9 and deceleration of 3 RCF (Relative Centrifuge Force) was used for all experiments.
Brazil: Centrífuga eppendorf 5810 R at 7000 rpm with an acceleration of 9 and deceleration of 1 RCF.
- Scale up: Lemitec MD 60 decanter centrifuge with a throughput of 1-30 L/h.

Freeze Drier

- A VirTis SP Scientific sentry 2.0 freeze drier was used to dry both protein and pectin samples. The condenser was held below 100 °C and the pressure kept at below 100 mTorr and the samples were dried in appropriately sized round-bottomed flasks for at least 48 h to ensure complete removal of water. Samples were frozen prior to drying in liquid nitrogen.
- Brazil: Liofilizador E-C Modulyo freeze drier.
- Scale up: A VirTis Genesis 35 EL equipped with 5 Shelves (each 273 x 521 mm) with a shelf temperature range of <-67 °C to +65 °C and a condenser capacity of 35 L.

Microwaves

- CEM Discovery microwave.
- Milestone RotoSYNTH open vessel microwave equipped with a 4 L reactor.
- SEM MARS 6 with One Touch™ Technology, equipped with EasyPrep™ Plus Teflon 100 mL closed vessels. Microwave was fitted with a dual IR probe and a fiber optic probe to ensure accurate temperature readings. Pressure was also recorded for safety purposes.

- Brazil: Anton Paar Monowave 300 Microwave Synthesis Reactor.

Porosimetry

- Micromeritics ASAP 2020C Surface Area and Porosity Analyzer.
- Micromeritics TriStar.

High Performance Liquid Chromatography (HPLC)

Brazil: Agilent Technologies 1200 Series

High Performance Liquid Chromatography-Solid Phase Extraction-Nuclear Magnetic Resonance (HPLC-SPE-NMR)

Brazil: Agilent 1200 Bruker 600 Ultrashield Plus AVANCE III.

Ultra-filtration System

KrosFlo Research Ili Tangential Flow Filtration System fitted with a mPES MidiKros Filter Module with the properties listed below:

Table A.2 – Ultra-Filtration cartridge properties

Pore Rating (kD)	Fibre ID (mm)	Fibre Type	Surface Area (cm ²)	Packing
10	0.5	mPES	235	Dry

SDS-PAGE

XCell SureLoc Mini-Cell Electrophoresis System using NuPAGE Bis-Tris Mini Gels.

MALDI-TOF TOF

Bruker ultraflex III in reflectron mode.

Protein Purification Chromatography

GE Healthcare Life Sciences ÄKTA Pure M25

Equipped with multiple wavelength UV detector, conductivity monitoring and pH monitoring.

Protein fractions were collected in 96 well plates.

Columns used were:

- GE Healthcare Life Sciences HiTrap Q HPsepharose FastFlow

- GE Healthcare Life Sciences Sephadex S-75
- GE Healthcare Life Sciences Mono-Q

Protein Crystallisation

TTP Labtech Mosquito Crystal liquid handling robot for nano-drop sitting drop crystallisation screening integrated with a Hydra II 96-well dispensing robot to fill up reservoirs.

All crystal screen conditions were obtained from Hampton Research or Molecular Dimensions.

Plate Reader

An Biotek EpochTM Microplate Spectrophotometer was used to determine protein concentration in solution at a wavelength of 280nm.

Balances

- Kern ACJ/ACS ACJ 220-4M balance accurate to 0.1 mg
- Mettler AE163 balance accurate to 0.1 mg

A.2 Chapter 3

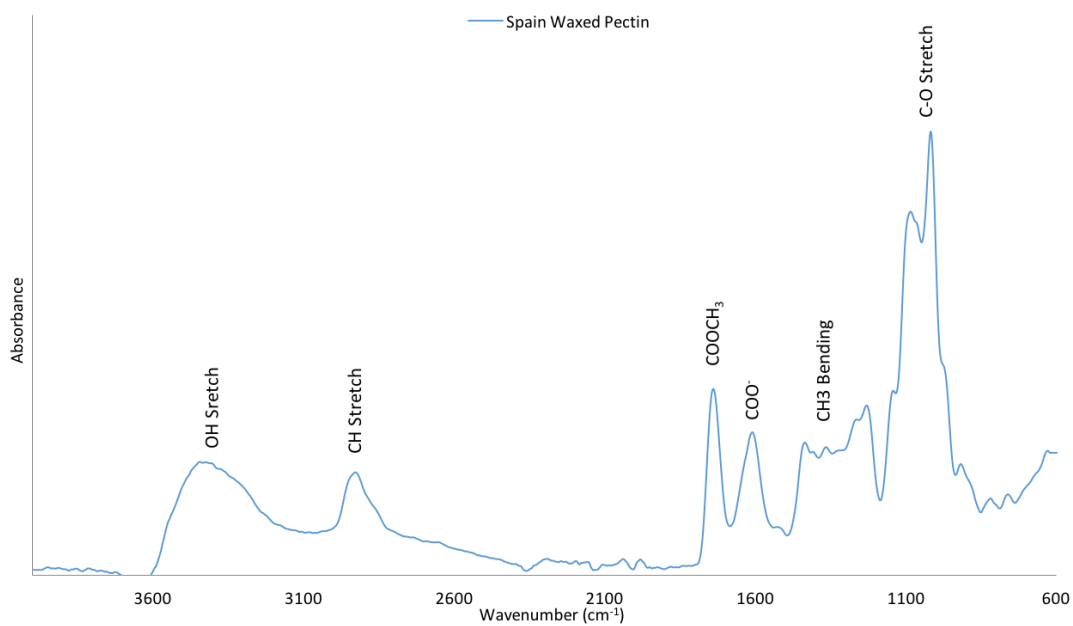


Figure A.1 – ATR-IR of Pectin Extracted from Oranges (Spain – Waxed)

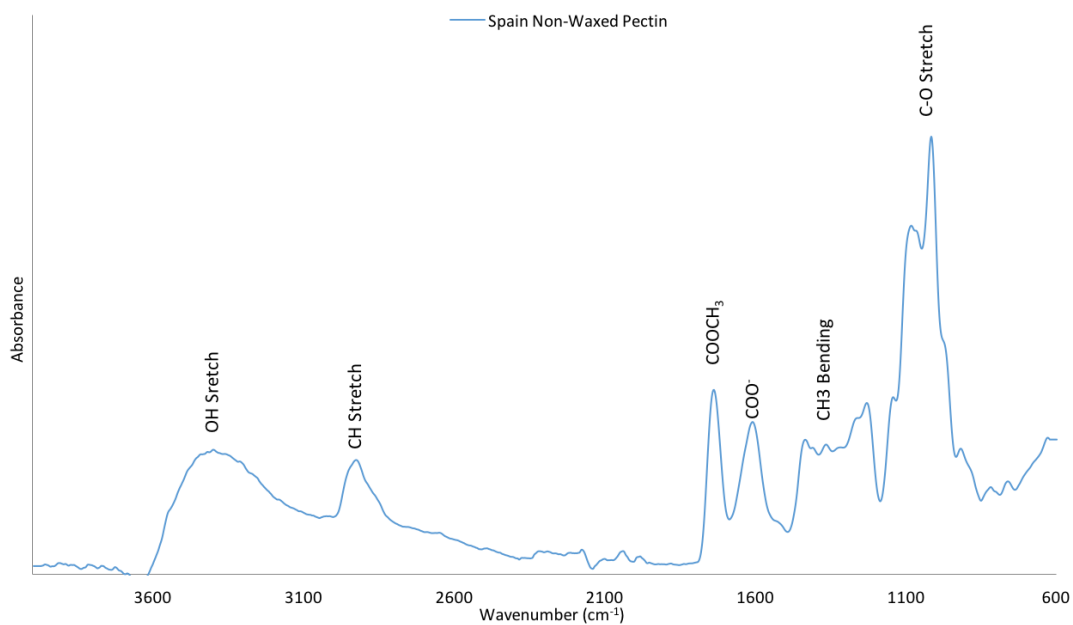


Figure A.2 – ATR-IR of Pectin Extracted from Oranges (Spain – Non-Waxed)

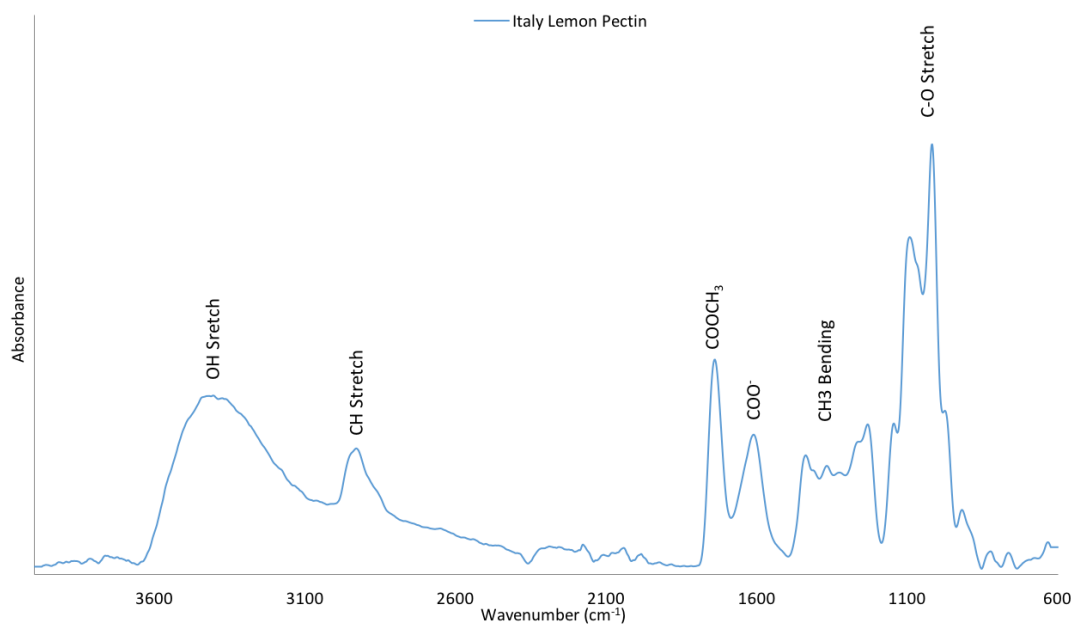


Figure A.3 – ATR-IR of Pectin Extracted from Lemons (Italy)

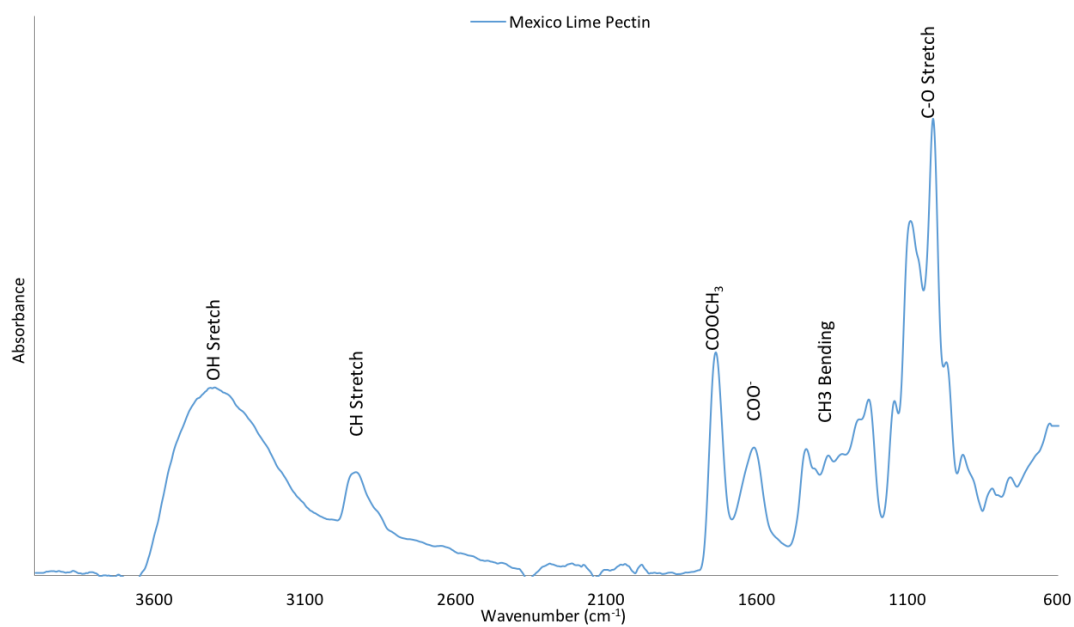


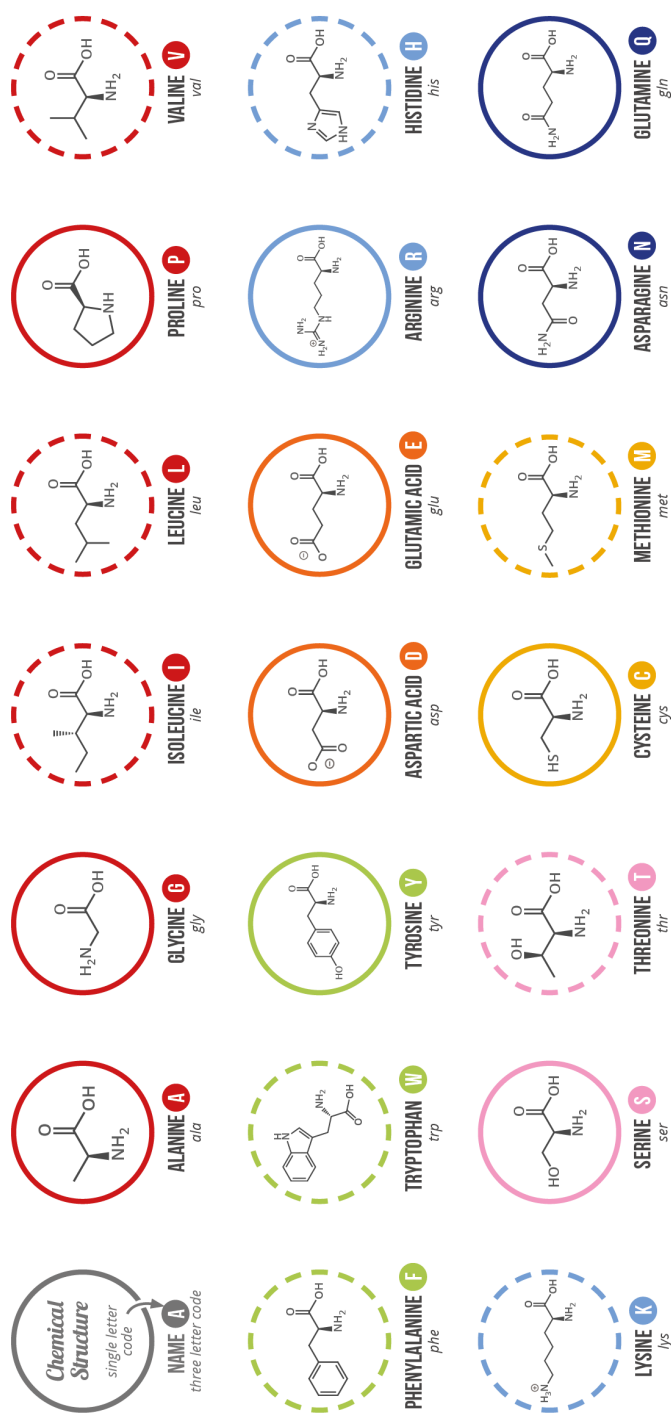
Figure A.4 – ATR-IR of Pectin Extracted from Limes (Mexico)

A.3 Chapter 4

A GUIDE TO THE TWENTY COMMON AMINO ACIDS

AMINO ACIDS ARE THE BUILDING BLOCKS OF PROTEINS IN LIVING ORGANISMS. THERE ARE OVER 500 AMINO ACIDS FOUND IN NATURE - HOWEVER, THE HUMAN GENETIC CODE ONLY DIRECTLY ENCODES 20. 'ESSENTIAL' AMINO ACIDS MUST BE OBTAINED FROM THE DIET, WHILST NON-ESSENTIAL AMINO ACIDS CAN BE SYNTHESISED IN THE BODY.

Chart Key: ● ALIPHATIC ● AROMATIC ● ACIDIC ● BASIC ● HYDROXYLIC ● SULFUR-CONTAINING ● AMIDIC ● NON-ESSENTIAL ○ ESSENTIAL



Note: This chart only shows those amino acids for which the human genetic code directly codes for. Selenocysteine is often referred to as the 21st amino acid, but is encoded in a special manner. In some cases, distinguishing between asparagine/aspartic acid and glutamine/glutamic acid is difficult. In these cases, the codes *asx* (B) and *glx* (Z) are respectively used.

© COMPOUND INTEREST 2014 - WWW.COMPOUNDCHEM.COM | Twitter: @compoundchem | Facebook: www.facebook.com/compoundchem

Shared under a Creative Commons Attribution-NonCommercial-NoDerivatives licence.



Table A.3 – Proteomics Data For Potato Band 1

Observed Mass	Mr (expt)	Mr (calc)	Expect Score	Peptide
Protein	PCPI 8.3=cysteine proteinase inhibitor [potatoes, tubers, Peptide, 180 aa]			
1727.9172	1726.9100	1726.8890	3.00E-09	-.LVLPEVYDQDGNPLR.I
2011.0759	2010.0687	2010.0714	3.20E-07	R.LVTVDDDKDFIPVFIK.A
Protein	Cysteine protease inhibitor 9 [Solanum tuberosum]			
1392.6968	1391.6895	1391.6802	0.02	K.LLHCPSHLQCK.N
2011.0759	2010.0687	2010.0714	3.20E-97	R.LVTVDDDKDFLFPVFIK.A

Table A.4 – Proteomics Data For Potato Band 2

Observed Mass	Mr (expt)	Mr (calc)	Expect Score	Peptide
Protein	PCPI 8.3=cysteine proteinase inhibitor [potatoes, tubers, Peptide, 180 aa]			
1254.5618	1253.5545	1253.5888	0.0024	R.KSES DYGDVVR.V
1727.8501	1726.8428	1726.8890	0.00022	-.LVLPEVYDQDGNPLR.I
2010.9911	2009.9838	2010.0714	0.00000033	R.LVTVDDDKDFIPVFIK.A
Protein	Cysteine protease inhibitor 9 [Solanum tuberosum]			
1254.5618	1253.5545	1253.5888	0.0024	R.KSES DYGDVVR.V
1392.6511	1391.6438	1391.6802	0.0062	K.LLHCPSHLQCK.N
2010.9911	2009.9838	2010.0714	3.30E-07	R.LVTVDDDKDFLFPVFIK.A

Table A.5 – Proteomics Data For Potato Band 3

Observed Mass	Mr (expt)	Mr (calc)	Expect Score	Peptide
Protein Aspartic protease inhibitor 8 [Solanum tuberosum]				
1348.6619	1347.6546	1347.6419	0.0000018	R.YNSDVGPSGTPVR.F
1518.6837	1517.6764	1517.6569	0.000046	K.SPNSDAPCPDGVFR.Y
1969.0818	1968.0745	1968.0680	0.0000005	R.RLALVNENPLDVLQEV.-
Protein PCPI 8.3=cysteine proteinase inhibitor				
1727.8956	1726.8884	1726.8890	0.012	-.LVLPEVYDQDGNPLR.I

Table A.6 – Proteomics Data For Potato Band 4

Observed Mass	Mr (expt)	Mr (calc)	Expect Score	Peptide
Protein cysteine protease inhibitor 8-like [Solanum tuberosum]				
1496.7928	1495.7856	1495.8147	0.000051	K.VAYSIVGPTHSPLR.F
Protein cysteine protease inhibitor 9-like [Solanum tuberosum]				
1595.8105	1594.8033	1594.8507	0.00065	R.LALNNKPYPFGFSK.V
Protein Aspartic protease inhibitor 8 [Solanum tuberosum]				
1518.6410	1517.6337	1517.6569	0.0058	K.SPNSDAPCPDGVFR.Y

Table A.7 – Proteomics Data For Potato Band 1 at 90 kDa

Observed Mass	Mr (expt)	Mr (calc)	Expect Score	Peptide
Protein	=Linoleate 9S-lipoxygenase 1			
1332.6792	1331.6719	1331.6470	7.7e-05	R.HTTDEIYLGQR.E
1411.7172	1410.7099	1410.6779	0.00038	R.TTLGGSAEYPYPR.R
1511.9263	1510.9190	1510.9123	4.3e-07	R.IPLILSLDIYVPR.D
1863.0437	1862.0364	1862.0567	0.0054	K.LFILNHHDVIIPYLR.R
2135.0779	2134.0706	2134.1099	2.2e-06	R.IFFANQPYP LPSETPELLR.K

Table A.8 – Proteomics Data For Potato Band 2 at 90 kDa

Observed Mass	Mr (expt)	Mr (calc)	Expect Score	Peptide
1332.6792	1331.6719	1331.6470	7.7e-05	R.HTTDEIYLGQR.E
1411.7172	1410.7099	1410.6779	0.00038	R.TTLGGSAEYPYPR.R
1511.9263	1510.9190	1510.9123	4.3e-07	R.IPLILSLDIYVPR.D
1863.0437	1862.0364	1862.0567	0.0054	K.LFILNHHDVIIPYLR.R
2135.0779	2134.0706	2134.1099	2.2e-06	R.IFFANQPYP LPSETPELLR.K

Table A.9 – Proteomics Data For Orange Band 1

Observed Mass	Mr (expt)	Mr (calc)	Expect Score	Peptide
Protein	Germin-like protein subfamily 1 member 17			
1917.0585	1916.0512	1915.9805	0.00026	R.IDYAPYGQRPPHIHPR.A
1927.9856	1926.9783	1926.9224	1.6e-06	R.AEDFFSGLGKPGNTANR.L
2629.4089	2628.4017	2628.3395	4.6e-21	R.LGVDETDANVEQIPGLNTLGISAFR.I

Table A.10 – Proteomics Data For Orange Band 2

Observed Mass	Mr (expt)	Mr (calc)	Expect Score	Peptide
Protein	elongation factor G-2, chloroplastic-like			
1597.8483	1596.8410	1596.8300	0.00013	K.IATDPFVGNLTFFR.V
Protein	Germin-like protein subfamily 1 member 17			
1916.9739	1915.9666	1915.9805	0.00022	R.IDYAPYGQRPPHIHPR.A

Table A.11 – Proteomics Data For Orange Band 3

Observed Mass	Mr (expt)	Mr (calc)	Expect Score	Peptide
Protein	Germin-like protein subfamily 1 member 17			
1916.9825	1915.9753	1915.9805	5e-05	R.IDYAPYGQRPPHIHPR.A
1927.9288	1926.9216	1926.9224	5.9e-06	R.AEDFFSGLGKPGNTANR.L
2629.3167	2628.3094	2628.3395	8.2e-15	R.LGVDETDANVEQIPGLNTLGISAFR.I

Table A.12 – Index Formulation Hampton Research - Copyright 2016 Part 1

Reagent No	[Salt]	Salt	[Buffer]	Buffer	pH	[Ppt 1]	Precipitant 1	[Ppt 2]	Precipitant 2	Average PH	Average Ref. Index	Average Conductivity
1			0.1 M	Citric acid	3.5	2 M	Ammonium sulfate			3.7	1.37249	187.2 mS/cm
2			0.1 M	Sodium acetate trihydrate	4.5	2 M	Ammonium sulfate			4.5	1.37084	162.3 mS/cm
3			0.1 M	BIS-TRIS	5.5	2 M	Ammonium sulfate			6.1	1.37345	197.2 mS/cm
4			0.1 M	BIS-TRIS	6.5	2 M	Ammonium sulfate			7.1	1.37348	196.8 mS/cm
5			0.1 M	HEPES	7.5	2 M	Ammonium sulfate			7.6	1.37364	196.1 mS/cm
6			0.1 M	Tris	8.5	2 M	Ammonium sulfate			8.2	1.37201	130.9 mS/cm
7			0.1 M	Citric acid	3.5	3 M	Sodium chloride			3.1	1.36382	174.4 mS/cm
8			0.1 M	Sodium acetate trihydrate	4.5	3 M	Sodium chloride			4.2	1.36211	180.9 mS/cm
9			0.1 M	BIS-TRIS	5.5	3 M	Sodium chloride			5.7	1.36433	176.4 mS/cm
10			0.1 M	BIS-TRIS	6.5	3 M	Sodium chloride			7.2	1.36449	176.1 mS/cm
11			0.1 M	HEPES	7.5	3 M	Sodium chloride			7.3	1.36478	174.4 mS/cm
12			0.1 M	Tris	8.5	3 M	Sodium chloride			8.6	1.36297	179.7 mS/cm
13			0.1 M	BIS-TRIS	5.5	0.3 M	Magnesium formate dihydrate			5.7	1.34272	31.5 mS/cm
14			0.1 M	BIS-TRIS	6.5	0.5 M	Magnesium formate dihydrate			6.5	1.34484	38.1 mS/cm
15			0.1 M	HEPES	7.5	0.5 M	Magnesium formate dihydrate			7.4	1.34695	36.5 mS/cm
16			0.1 M	Tris	8.5	0.3 M	Magnesium formate dihydrate			8.6	1.34117	28.6 mS/cm
17			1.4 M		5.6	1.26 M	Sodium phosphate monobasic monohydrate	0.14 M	Potassium phosphate dibasic	5.1	1.35423	55.6 mS/cm
18			1.4 M		6.9	0.49 M	Sodium phosphate monobasic monohydrate	0.91 M	Potassium phosphate dibasic	7	1.36075	101.9 mS/cm
19			1.4 M		8.2	0.056 M	Sodium phosphate monobasic monohydrate	1.344 M	Potassium phosphate dibasic	8.4	1.36167	127.1 mS/cm
20			0.1 M	HEPES	7.5	1.4 M	Sodium citrate tribasic dihydrate			8	1.39143	57 mS/cm
21						1.8 M	Ammonium citrate tribasic pH 7.0			7	1.40723	122.4 mS/cm
22						0.8 M	Succinic acid pH 7.0			7	1.35448	66.3 mS/cm
23						2.1 M	DL-Malic acid pH 7.0			7	1.38756	68.8 mS/cm
24						2.8 M	Sodium acetate trihydrate pH 7.0			7	1.36292	77.7 mS/cm
25						3.5 M	Sodium formate pH 7.0			7	1.35974	122.9 mS/cm
26						1.1 M	Ammonium tartrate dibasic pH 7.0			7	1.38364	106.8 mS/cm

Table A.13 – Index Formulation Hampton Research - Copyright 2016 Part 2

Reagent No	[Salt]	Salt	[Buffer]	Buffer	pH	[Ppt 1]	Precipitant 1	[Ppt 2]	Precipitant 2	Average PH	Average Ref. Index	Average Conductivity
27						2.4 M	Sodium malonate pH 7.0			7	1.38429	90.9 mS/cm
28						35 % v/v	Tacsimate pH 7.0			7	1.36096	80.3 mS/cm
29						60 % v/v	Tacsimate pH 7.0			7	1.37796	95.5 mS/cm
30	0.1 M	Sodium chloride	0.1 M	BIS-TRIS	6.5	1.5 M	Ammonium sulfate			6.9	1.36584	172.2 mS/cm
31	0.8 M	Potassium sodium tartrate tetrahydrate	0.1 M	Tris	8.5	0.5 % w/v	Polyethylene glycol monomethyl ether 5,000			8.9	1.35973	71.9 mS/cm
32	1 M	Ammonium sulfate	0.1 M	BIS-TRIS	5.5	1 % w/v	Polyethylene glycol 3,350			5.8	1.35756	125.4 mS/cm
33	1.1 M	Sodium malonate pH 7.0	0.1 M	HEPES	7	0.5 % v/v	Jeffamine ED-2001 pH 7.0			7.2	1.36332	76.9 mS/cm
34	1 M	Succinic acid pH 7.0	0.1 M	HEPES	7	1 % w/v	Polyethylene glycol monomethyl ether 2,000			7.1	1.3643	67.2 mS/cm
35	1 M	Ammonium sulfate	0.1 M	HEPES	7	0.5 % w/v	Polyethylene glycol 8,000			7.1	1.35725	123.5 mS/cm
36	15 % v/v	Tacsimate pH 7.0	0.1 M	HEPES	7	2 % w/v	Polyethylene glycol 3,350			7	1.35202	43.4 mS/cm
37						25 % w/v	Polyethylene glycol 1,500			6.3	1.36705	60.7 S/cm
38			0.1 M	HEPES	7	30 % v/v	Jeffamine M-600 pH 7.0			6.7	1.38366	11.6 mS/cm
39			0.1 M	HEPES	7	30 % v/v	Jeffamine ED-2001 pH 7.0			6.8	1.38249	6.7 mS/cm
40			0.1 M	Citric acid	3.5	25 % w/v	Polyethylene glycol 3,350			4.3	1.37035	2.9 mS/cm
41			0.1 M	Sodium acetate trihydrate	4.5	25 % w/v	Polyethylene glycol 3,350			5.1	1.36858	4.3 mS/cm
42			0.1 M	BIS-TRIS	5.5	25 % w/v	Polyethylene glycol 3,350			5.5	1.37088	3.4 mS/cm
43			0.1 M	BIS-TRIS	6.5	25 % w/v	Polyethylene glycol 3,350			6.5	1.37099	2.2 mS/cm
44			0.1 M	HEPES	7.5	25 % w/v	Polyethylene glycol 3,350			7.5	1.37144	1152 μ S/cm
45			0.1 M	Tris	8.5	25 % w/v	Polyethylene glycol 3,350			8.5	1.36942	1466.5 μ S/cm
46			0.1 M	BIS-TRIS	6.5	20 % w/v	Polyethylene glycol monomethyl ether 5,000			6.5	1.36412	2.7 mS/cm
47			0.1 M	BIS-TRIS	6.5	28 % w/v	Polyethylene glycol monomethyl ether 2,000			6.5	1.37502	1982 μ S/cm
48	0.2 M	Calcium chloride dihydrate	0.1 M	BIS-TRIS	5.5	45 % v/v	(+/-)-2-Methyl-2,4-pentanediol			3.4	1.39443	7.8 mS/cm
49	0.2 M	Calcium chloride dihydrate	0.1 M	BIS-TRIS	6.5	45 % v/v	(+/-)-2-Methyl-2,4-pentanediol			4.4	1.39392	7.1 mS/cm
50	0.2 M	Ammonium acetate	0.1 M	BIS-TRIS	5.5	45 % v/v	(+/-)-2-Methyl-2,4-pentanediol			6.3	1.39115	4.7 mS/cm

Table A.14 – Index Formulation Hampton Research - Copyright 2016 Part 3

Reagent No	[Salt]	Salt	[Buffer]	Buffer	pH	[Ppt 1]	Precipitant 1	[Ppt 2]	Precipitant 2	Average PH	Average Ref. Index	Average Conductivity
51	0.2 M	Ammonium acetate	0.1 M	BIS-TRIS	6.5	45 % v/v	(+/-)-2-Methyl-2,4-pentanediol			6.7	1.39107	4.3 mS/cm
52	0.2 M	Ammonium acetate	0.1 M	HEPES	7.5	45 % v/v	(+/-)-2-Methyl-2,4-pentanediol			7.4	1.39274	4 mS/cm
53	0.2 M	Ammonium acetate	0.1 M	Tris	8.5	45 % v/v	(+/-)-2-Methyl-2,4-pentanediol			8.3	1.38977	4 mS/cm
54	0.05 M	Calcium chloride dihydrate	0.1 M	BIS-TRIS	6.5	30 % v/v	Polyethylene glycol monomethyl ether 550			5.7	1.38511	4.4 mS/cm
55	0.05 M	Magnesium chloride hexahydrate	0.1 M	HEPES	7.5	30 % v/v	Polyethylene glycol monomethyl ether 550			7.3	1.38135	3.8 mS/cm
56	0.2 M	Potassium chloride	0.05 M	HEPES	7.5	35 % v/v	Pentaerythritol propoxylate (5/4 PO/OH)			7.4	1.38751	7.6 mS/cm
57	0.05 M	Ammonium sulfate	0.05 M	BIS-TRIS	6.5	30 % v/v	Pentaerythritol ethoxylate (15/4 EO/OH)			6.5	1.38511	3.7 mS/cm
58			0.1 M	BIS-TRIS	6.5	45 % v/v	Polypropylene glycol P 400			6.4	1.39821	872.5 μ S/cm
59	0.02 M	Magnesium chloride hexahydrate	0.1 M	HEPES	7.5	22 % w/v	Polyacrylic acid sodium salt 5,100			7.2	1.37252	39.7 mS/cm
60	0.01 M	Cobalt(II) chloride hexahydrate	0.1 M	Tris	8.5	20 % w/v	Polyvinylpyrrolidone K 15			7.7	1.37049	3.8 mS/cm
61	0.2 M	L-Proline	0.1 M	HEPES	7.5	10 % w/v	Polyethylene glycol 3,350			7.4	1.35407	1808.5 μ S/cm
62	0.2 M	Trimethylamine N-oxide dihydrate	0.1 M	Tris	8.5	20 % w/v	Polyethylene glycol monomethyl ether 2,000			8.6	1.36456	1583.5 μ S/cm
63	5 % v/v	Tacsimate pH 7.0	0.1 M	HEPES	7	10 % w/v	Polyethylene glycol monomethyl ether 5,000			6.9	1.3551	14.1 mS/cm
64	0.005 M	Cobalt(II) chloride hexahydrate	0.1 M	HEPES	7.5	12 % w/v	Polyethylene glycol 3,350			7.2	1.35388	4 mS/cm
	0.005 M	Nickel(II) chloride hexahydrate										
	0.005 M	Cadmium chloride hydrate										
	0.005 M	Magnesium chloride hexahydrate										
65	0.1 M	Ammonium acetate	0.1 M	BIS-TRIS	5.5	17 % w/v	Polyethylene glycol 10,000			5.9	1.36514	8.9 mS/cm
66	0.2 M	Ammonium sulfate	0.1 M	BIS-TRIS	5.5	25 % w/v	Polyethylene glycol 3,350			5.6	1.37512	16.2 mS/cm
67	0.2 M	Ammonium sulfate	0.1 M	BIS-TRIS	6.5	25 % w/v	Polyethylene glycol 3,350			6.5	1.37506	15.1 mS/cm
68	0.2 M	Ammonium sulfate	0.1 M	HEPES	7.5	25 % w/v	Polyethylene glycol 3,350			7.3	1.37542	14 mS/cm
69	0.2 M	Ammonium sulfate	0.1 M	Tris	8.5	25 % w/v	Polyethylene glycol 3,350			8.3	1.37355	14.5 mS/cm
70	0.2 M	Sodium chloride	0.1 M	BIS-TRIS	5.5	25 % w/v	Polyethylene glycol 3,350			5.4	1.37323	11.9 mS/cm
71	0.2 M	Sodium chloride	0.1 M	BIS-TRIS	6.5	25 % w/v	Polyethylene glycol 3,350			6.6	1.3731	10.8 mS/cm

Table A.15 – Index Formulation Hampton Research - Copyright 2016 Part 4

Reagent No	[Salt]	Salt	[Buffer]	Buffer	pH	[Ppt 1]	Precipitant 1	[Ppt 2]	Precipitant 2	Average PH	Average Ref. Index	Average Conductivity
72	0.2 M	Sodium chloride	0.1 M	HEPES	7.5	25 % w/v	Polyethylene glycol 3,350			7.4	1.37339	9.8 mS/cm
73	0.2 M	Sodium chloride	0.1 M	Tris	8.5	25 % w/v	Polyethylene glycol 3,350			8.5	1.37151	10.4 mS/cm
74	0.2 M	Lithium sulfate monohydrate	0.1 M	BIS-TRIS	5.5	25 % w/v	Polyethylene glycol 3,350			5.5	1.3747	11.5 mS/cm
75	0.2 M	Lithium sulfate monohydrate	0.1 M	BIS-TRIS	6.5	25 % w/v	Polyethylene glycol 3,350			6.5	1.37475	10.6 mS/cm
76	0.2 M	Lithium sulfate monohydrate	0.1 M	HEPES	7.5	25 % w/v	Polyethylene glycol 3,350			7.3	1.37561	9.5 mS/cm
77	0.2 M	Lithium sulfate monohydrate	0.1 M	Tris	8.5	25 % w/v	Polyethylene glycol 3,350			8.6	1.37334	10.2 mS/cm
78	0.2 M	Ammonium acetate	0.1 M	BIS-TRIS	5.5	25 % w/v	Polyethylene glycol 3,350			6.1	1.37313	9.8 mS/cm
79	0.2 M	Ammonium acetate	0.1 M	BIS-TRIS	6.5	25 % w/v	Polyethylene glycol 3,350			6.7	1.37346	8.9 mS/cm
80	0.2 M	Ammonium acetate	0.1 M	HEPES	7.5	25 % w/v	Polyethylene glycol 3,350			7.4	1.3737	8.1 mS/cm
81	0.2 M	Ammonium acetate	0.1 M	Tris	8.5	25 % w/v	Polyethylene glycol 3,350			8.4	1.37171	8.3 mS/cm
82	0.2 M	Magnesium chloride hexahydrate	0.1 M	BIS-TRIS	5.5	25 % w/v	Polyethylene glycol 3,350			5.5	1.37571	16.2 mS/cm
83	0.2 M	Magnesium chloride hexahydrate	0.1 M	BIS-TRIS	6.5	25 % w/v	Polyethylene glycol 3,350			6.5	1.37585	15.2 mS/cm
84	0.2 M	Magnesium chloride hexahydrate	0.1 M	HEPES	7.5	25 % w/v	Polyethylene glycol 3,350			7.3	1.37602	14.3 mS/cm
85	0.2 M	Magnesium chloride hexahydrate	0.1 M	Tris	8.5	25 % w/v	Polyethylene glycol 3,350			8.4	1.37409	17.4 mS/cm
86	0.2 M	Potassium sodium tartrate tetrahydrate				20 % w/v	Polyethylene glycol 3,350			7.4	1.36977	13.4 mS/cm
87	0.2 M	Sodium malonate pH 7.0				20 % w/v	Polyethylene glycol 3,350			7.4	1.36538	13.1 mS/cm
88	0.2 M	Ammonium citrate tribasic pH 7.0				20 % w/v	Polyethylene glycol 3,350			7	1.369	19.6 mS/cm
89	0.1 M	Succinic acid pH 7.0				15 % w/v	Polyethylene glycol 3,350			7.3	1.35632	8.8 mS/cm
90	0.2 M	Sodium formate				20 % w/v	Polyethylene glycol 3,350			7.3	1.35877	9.1 mS/cm
91	0.15 M	DL-Malic acid pH 7.0				20 % w/v	Polyethylene glycol 3,350			7.2	1.36488	9.8 mS/cm
92	0.1 M	Magnesium formate dihydrate				15 % w/v	Polyethylene glycol 3,350			6.9	1.35566	7.6 mS/cm
93	0.05 M	Zinc acetate dihydrate				20 % w/v	Polyethylene glycol 3,350			6.6	1.36193	2.2 mS/cm
94	0.2 M	Sodium citrate tribasic dihydrate				20 % w/v	Polyethylene glycol 3,350			8.3	1.36918	12.9 mS/cm
95	0.1 M	Potassium thiocyanate				30 % w/v	Polyethylene glycol monomethyl ether 2,000			6.8	1.3759	3.7 mS/cm
96	0.15 M	Potassium bromide				30 % w/v	Polyethylene glycol monomethyl ether 2,000			6.8	1.37615	6.6 mS/cm

Table A.16 – PEG ION Formulation Hampton Research - Copyright 2016 Part 1

Reagent No	[Salt]	Salt	pH	[Buffer]	Buffer	pH	[Ppt 1]	Precipitant 1	Average PH	Average Ref. Index	Average Conductivity
1	0.2 M	Sodium fluoride					20 % w/v	Polyethylene glycol 3,350	7.3	1.36145	8.8 mS/cm
2	0.2 M	Potassium fluoride					20 % w/v	Polyethylene glycol 3,350	7.2	1.36154	10.8 mS/cm
3	0.2 M	Ammonium fluoride					20 % w/v	Polyethylene glycol 3,350	6.2	1.36162	10.5 mS/cm
4	0.2 M	Lithium chloride					20 % w/v	Polyethylene glycol 3,350	6.8	1.36228	10 mS/cm
5	0.2 M	Magnesium chloride hexahydrate					20 % w/v	Polyethylene glycol 3,350	5.9	1.36516	17.3 mS/cm
6	0.2 M	Sodium chloride					20 % w/v	Polyethylene glycol 3,350	6.9	1.36241	13.1 mS/cm
7	0.2 M	Calcium chloride dihydrate					20 % w/v	Polyethylene glycol 3,350	5.1	1.36597	18.8 mS/cm
8	0.2 M	Potassium chloride					20 % w/v	Polyethylene glycol 3,350	6.9	1.36242	13.2 mS/cm
9	0.2 M	Ammonium chloride					20 % w/v	Polyethylene glycol 3,350	6.2	1.36253	13.6 mS/cm
10	0.2 M	Sodium iodide					20 % w/v	Polyethylene glycol 3,350	6.9	1.3647	11 mS/cm
11	0.2 M	Potassium iodide					20 % w/v	Polyethylene glycol 3,350	7	1.36548	12.6 mS/cm
12	0.2 M	Ammonium iodide					20 % w/v	Polyethylene glycol 3,350	5.9	1.36482	13.3 mS/cm
13	0.2 M	Sodium thiocyanate					20 % w/v	Polyethylene glycol 3,350	6.8	1.36376	9.9 mS/cm
14	0.2 M	Potassium thiocyanate					20 % w/v	Polyethylene glycol 3,350	6.9	1.36373	11.5 mS/cm
15	0.2 M	Lithium nitrate					20 % w/v	Polyethylene glycol 3,350	7	1.36198	9.7 mS/cm
16	0.2 M	Magnesium nitrate hexahydrate					20 % w/v	Polyethylene glycol 3,350	5.8	1.36473	16.9 mS/cm
17	0.2 M	Sodium nitrate					20 % w/v	Polyethylene glycol 3,350	6.8	1.36216	10.8 mS/cm
18	0.2 M	Potassium nitrate					20 % w/v	Polyethylene glycol 3,350	6.7	1.36207	12.1 mS/cm
19	0.2 M	Ammonium nitrate					20 % w/v	Polyethylene glycol 3,350	6.3	1.36275	13.1 mS/cm
20	0.2 M	Magnesium formate dihydrate					20 % w/v	Polyethylene glycol 3,350	7	1.36443	10.7 mS/cm
21	0.2 M	Sodium formate					20 % w/v	Polyethylene glycol 3,350	7.2	1.36208	9.1 mS/cm
22	0.2 M	Potassium formate					20 % w/v	Polyethylene glycol 3,350	7.2	1.36214	11 mS/cm
23	0.2 M	Ammonium formate					20 % w/v	Polyethylene glycol 3,350	6.6	1.36201	11.3 mS/cm
24	0.2 M	Lithium acetate dihydrate					20 % w/v	Polyethylene glycol 3,350	7.9	1.36264	6 mS/cm
25	0.2 M	Magnesium acetate tetrahydrate					20 % w/v	Polyethylene glycol 3,350	7.5	1.36564	7.9 mS/cm
26	0.2 M	Zinc acetate dihydrate					20 % w/v	Polyethylene glycol 3,350	6.3	1.36592	6.3 mS/cm

Table A.17 – PEG ION Formulation Hampton Research - Copyright 2016 Part 2

Reagent No	[Salt]	Salt	pH	[Buffer]	Buffer	pH	[Ppt 1]	Precipitant 1	Average PH	Average Ref. Index	Average Conductivity
27	0.2 M	Sodium acetate trihydrate					20 % w/v	Polyethylene glycol 3,350	8	1.3629	8 mS/cm
28	0.2 M	Calcium acetate hydrate					20 % w/v	Polyethylene glycol 3,350	7.5	1.36564	7.5 mS/cm
29	0.2 M	Potassium acetate					20 % w/v	Polyethylene glycol 3,350	7.8	1.36252	8 mS/cm
30	0.2 M	Ammonium acetate					20 % w/v	Polyethylene glycol 3,350	7.1	1.36277	7.1 mS/cm
31	0.2 M	Lithium sulfate monohydrate					20 % w/v	Polyethylene glycol 3,350	5.7	1.36449	5.9 mS/cm
32	0.2 M	Magnesium sulfate heptahydrate					20 % w/v	Polyethylene glycol 3,350	5.9	1.36506	5.9 mS/cm
33	0.2 M	Sodium sulfate decahydrate					20 % w/v	Polyethylene glycol 3,350	6.7	1.36435	6.6 mS/cm
34	0.2 M	Potassium sulfate					20 % w/v	Polyethylene glycol 3,350	6.7	1.36427	6.8 mS/cm
35	0.2 M	Ammonium sulfate					20 % w/v	Polyethylene glycol 3,350	6.1	1.36446	6 mS/cm
36	0.2 M	Sodium tartrate dibasic dihydrate					20 % w/v	Polyethylene glycol 3,350	7.2	1.36651	7.2 mS/cm
37	0.2 M	Potassium sodium tartrate tetrahydrate					20 % w/v	Polyethylene glycol 3,350	7.4	1.36664	7.3 mS/cm
38	0.2 M	Ammonium tartrate dibasic					20 % w/v	Polyethylene glycol 3,350	6.5	1.36688	6.6 mS/cm
39	0.2 M	Sodium phosphate monobasic monohydrate					20 % w/v	Polyethylene glycol 3,350	4.7	1.36351	4.7 mS/cm
40	0.2 M	Sodium phosphate dibasic dihydrate					20 % w/v	Polyethylene glycol 3,350	9.2	1.36537	9.1 mS/cm
41	0.2 M	Potassium phosphate monobasic					20 % w/v	Polyethylene glycol 3,350	4.9	1.36414	4.8 mS/cm
42	0.2 M	Potassium phosphate dibasic					20 % w/v	Polyethylene glycol 3,350	9.2	1.36535	9.2 mS/cm
43	0.2 M	Ammonium phosphate monobasic					20 % w/v	Polyethylene glycol 3,350	4.7	1.36344	4.6 mS/cm
44	0.2 M	Ammonium phosphate dibasic					20 % w/v	Polyethylene glycol 3,350	8	1.36529	8 mS/cm
45	0.2 M	Lithium citrate tribasic tetrahydrate					20 % w/v	Polyethylene glycol 3,350	8.3	1.36866	8.4 mS/cm
46	0.2 M	Sodium citrate tribasic dihydrate					20 % w/v	Polyethylene glycol 3,350	8.2	1.36943	8.3 mS/cm
47	0.2 M	Potassium citrate tribasic monohydrate					20 % w/v	Polyethylene glycol 3,350	8.2	1.36908	8.6 mS/cm
48	0.2 M	Ammonium citrate dibasic					20 % w/v	Polyethylene glycol 3,350	5.1	1.36792	5.1 mS/cm
49	0.1 M	Sodium malonate	4.0				12 % w/v	Polyethylene glycol 3,350	4.6	1.35106	5.7 mS/cm
50	0.2 M	Sodium malonate	4.0				20 % w/v	Polyethylene glycol 3,350	4.6	1.36269	8 mS/cm
51	0.1 M	Sodium malonate	5.0				12 % w/v	Polyethylene glycol 3,350	5.6	1.35178	8 mS/cm
52	0.2 M	Sodium malonate	5.0				20 % w/v	Polyethylene glycol 3,350	5.6	1.36473	10.7 mS/cm

Table A.18 – PEG ION Formulation Hampton Research - Copyright 2016 Part 3

Reagent No	[Salt]	Salt	pH	[Buffer]	Buffer	pH	[Ppt 1]	Precipitant 1	Average PH	Average Ref. Index	Average Conductivity
53	0.1 M	Sodium malonate	6.0				12 % w/v	Polyethylene glycol 3,350	6.4	1.35212	9.8 mS/cm
54	0.2 M	Sodium malonate	6.0				20 % w/v	Polyethylene glycol 3,350	6.5	1.36526	13 mS/cm
55	0.1 M	Sodium malonate	7.0				12 % w/v	Polyethylene glycol 3,350	7.4	1.35208	9.1 mS/cm
56	0.2 M	Sodium malonate	7.0				20 % w/v	Polyethylene glycol 3,350	7.4	1.36549	13.4 mS/cm
57	4 % v/v	Tacsimate	4.0				12 % w/v	Polyethylene glycol 3,350	4.4	1.35185	7.6 mS/cm
58	8 % v/v	Tacsimate	4.0				20 % w/v	Polyethylene glycol 3,350	4.5	1.36504	10.4 mS/cm
59	4 % v/v	Tacsimate	5.0				12 % w/v	Polyethylene glycol 3,350	5.4	1.35234	10.5 mS/cm
60	8 % v/v	Tacsimate	5.0				20 % w/v	Polyethylene glycol 3,350	5.4	1.36607	14 mS/cm
61	4 % v/v	Tacsimate	6.0				12 % w/v	Polyethylene glycol 3,350	6.3	1.35282	12.5 mS/cm
62	8 % v/v	Tacsimate	6.0				20 % w/v	Polyethylene glycol 3,350	6.3	1.3669	16.3 mS/cm
63	4 % v/v	Tacsimate	7.0				12 % w/v	Polyethylene glycol 3,350	7.2	1.35289	12.6 mS/cm
64	8 % v/v	Tacsimate	7.0				20 % w/v	Polyethylene glycol 3,350	7.2	1.367	16.5 mS/cm
65	4 % v/v	Tacsimate	8.0				12 % w/v	Polyethylene glycol 3,350	7.7	1.35287	13 mS/cm
66	8 % v/v	Tacsimate	8.0				20 % w/v	Polyethylene glycol 3,350	7.8	1.36713	16.9 mS/cm
67	0.1 M	Succinic acid	7.0				12 % w/v	Polyethylene glycol 3,350	7.2	1.35224	9.9 mS/cm
68	0.2 M	Succinic acid	7.0				20 % w/v	Polyethylene glycol 3,350	7.3	1.36594	13.2 mS/cm
69	0.1 M	Ammonium citrate tribasic	7.0				12 % w/v	Polyethylene glycol 3,350	7.1	1.3541	15.1 mS/cm
70	0.2 M	Ammonium citrate tribasic	7.0				20 % w/v	Polyethylene glycol 3,350	7.1	1.36964	19.6 mS/cm
71	0.1 M	DL-Malic acid	7.0				12 % w/v	Polyethylene glycol 3,350	7.1	1.35236	9.6 mS/cm
72	0.2 M	DL-Malic acid	7.0				20 % w/v	Polyethylene glycol 3,350	7.1	1.36642	12.5 mS/cm
73	0.1 M	Sodium acetate trihydrate	7.0				12 % w/v	Polyethylene glycol 3,350	6.8	1.35055	5.4 mS/cm
74	0.2 M	Sodium acetate trihydrate	7.0				20 % w/v	Polyethylene glycol 3,350	6.9	1.36272	7.6 mS/cm
75	0.1 M	Sodium formate	7.0				12 % w/v	Polyethylene glycol 3,350	6.8	1.35022	6.4 mS/cm
76	0.2 M	Sodium formate	7.0				20 % w/v	Polyethylene glycol 3,350	6.9	1.36211	9.3 mS/cm
77	0.1 M	Ammonium tartrate dibasic	7.0				12 % w/v	Polyethylene glycol 3,350	6.8	1.35264	12.2 mS/cm
78	0.2 M	Ammonium tartrate dibasic	7.0				20 % w/v	Polyethylene glycol 3,350	6.8	1.36674	16.2 mS/cm

Table A.19 – PEG ION Formulation Hampton Research - Copyright 2016 Part 4

Reagent No	[Salt]	Salt	pH	[Buffer]	Buffer	pH	[Ppt 1]	Precipitant 1	Average PH	Average Ref. Index	Average Conductivity
79	2 % v/v	Tacsimate	4.0	0.1 M	Sodium acetate trihydrate	4.6	16 % w/v	Polyethylene glycol 3,350	4.8	1.35729	8.6 mS/cm
80	2 % v/v	Tacsimate	5.0	0.1 M	Sodium citrate tribasic dihydrate	5.6	16 % w/v	Polyethylene glycol 3,350	5.9	1.36083	13.7 mS/cm
81	2 % v/v	Tacsimate	6.0	0.1 M	BIS-TRIS	6.5	20 % w/v	Polyethylene glycol 3,350	6.6	1.36575	7.1 mS/cm
82	2 % v/v	Tacsimate	7.0	0.1 M	HEPES	7.5	20 % w/v	Polyethylene glycol 3,350	7.4	1.36611	6 mS/cm
83	2 % v/v	Tacsimate	8.0	0.1 M	Tris	8.5	16 % w/v	Polyethylene glycol 3,350	8.6	1.35872	7.7 mS/cm
84			0.07 M		Citric acid,	3.4	16 % w/v	Polyethylene glycol 3,350	3.8	1.35817	1447.3 S/cm
			0.03 M		BIS-TRIS propane						
85			0.06 M		Citric acid,	4.1	16 % w/v	Polyethylene glycol 3,350	4.4	1.3585	1718.3 S/cm
			0.04 M		BIS-TRIS propane						
86			0.05 M		Citric acid,	5.0	16 % w/v	Polyethylene glycol 3,350	5.2	1.35892	1.9 mS/cm
			0.05 M		BIS-TRIS propane						
87			0.04 M		Citric acid,	6.4	20 % w/v	Polyethylene glycol 3,350	6.5	1.3647	1273 S/cm
			0.06 M		BIS-TRIS propane						
88			0.03 M		Citric acid,	7.6	20 % w/v	Polyethylene glycol 3,350	7.8	1.36484	1349.3 S/cm
			0.07 M		BIS-TRIS propane						
89			0.02 M		Citric acid,	8.8	16 % w/v	Polyethylene glycol 3,350	8.9	1.35939	1542 S/cm
			0.08 M		BIS-TRIS propane						
90	0.02 M	Calcium chloride dihydrate					20 % w/v	Polyethylene glycol 3,350	5.4	1.36202	5.2 mS/cm
	0.02 M	Cadmium chloride hydrate									
	0.02 M	Cobalt(II) chloride hexahydrate									
91	0.01 M	Magnesium chloride hexahydrate		0.1 M	HEPES sodium	7.0	15 % w/v	Polyethylene glycol 3,350	6.8	1.3586	8.2 mS/cm
	0.005 M	Nickel(II) chloride hexahydrate									
92	0.02 M	Zinc chloride					20 % w/v	Polyethylene glycol 3,350	4.4	1.36094	2.3 mS/cm
93	0.15 M	Cesium chloride					15 % w/v	Polyethylene glycol 3,350	6.9	1.35552	12.3 mS/cm
94	0.2 M	Sodium bromide					20 % w/v	Polyethylene glycol 3,350	6.8	1.36318	11.5 mS/cm
95	1 % w/v	Tryptone		0.05 M	HEPES sodium	7.0	12 % w/v	Polyethylene glycol 3,350	6.9	1.3537	4.3 mS/cm
	0.001 M	Sodium azide									
96	1 % w/v	Tryptone		0.05 M	HEPES sodium	7.0	20 % w/v	Polyethylene glycol 3,350	7	1.36455	3.3 mS/cm
	0.001 M	Sodium azide									

Table A.20 – Molecular Interactions PACT *premier*TM Crystallisation Screen

Part 1

Reagent No	[Salt]	Salt	[Buffer]	Buffer	pH	[Ppt 1]	Precipitant 1
1			0.1 M	SPG	4	25 % w/v	PEG 1500
2			0.1 M	SPG	5	25 % w/v	PEG 1500
3			0.1 M	SPG	6	25 % w/v	PEG 1500
4			0.1 M	SPG	7	25 % w/v	PEG 1500
5			0.1 M	SPG	8	25 % w/v	PEG 1500
6			0.1 M	SPG	9	25 % w/v	PEG 1500
7	0.2 M	Sodium chloride	0.1 M	Sodium acetate	5	20 % w/v	PEG 6000
8	0.2 M	Ammonium chloride	0.1 M	Sodium acetate	5	20 % w/v	PEG 6000
9	0.2 M	Lithium chloride	0.1 M	Sodium acetate	5	20 % w/v	PEG 6000
10	0.2 M	Magnesium chloride hexahydrate	0.1 M	Sodium acetate	5	20 % w/v	PEG 6000
11	0.2 M	Calcium chloride dihydrate	0.1 M	Sodium acetate	5	20 % w/v	PEG 6000
12	0.01 M	Zinc chloride	0.1 M	Sodium acetate	5	20 % w/v	PEG 6000
13			0.1 M	MIB	4	25 % w/v	PEG 1500
14			0.1 M	MIB	5	25 % w/v	PEG 1500
15			0.1 M	MIB	6	25 % w/v	PEG 1500
16			0.1 M	MIB	7	25 % w/v	PEG 1500
17			0.1 M	MIB	8	25 % w/v	PEG 1500
18			0.1 M	MIB	9	25 % w/v	PEG 1500
19	0.2 M	Sodium chloride	0.1 M	MES	6	20 % w/v	PEG 6000
20	0.2 M	Ammonium chloride	0.1 M	MES	6	20 % w/v	PEG 6000
21	0.2 M	Lithium chloride	0.1 M	MES	6	20 % w/v	PEG 6000
22	0.2 M	Magnesium chloride hexahydrate	0.1 M	MES	6	20 % w/v	PEG 6000
23	0.2 M	Calcium chloride dihydrate	0.1 M	MES	6	20 % w/v	PEG 6000
24	0.01 M	Zinc chloride	0.1 M	MES	6	20 % w/v	PEG 6000
25			0.1 M	PCTP	4	25 % w/v	PEG 1500
26			0.1 M	PCTP	5	25 % w/v	PEG 1500
27			0.1 M	PCTP	6	25 % w/v	PEG 1500
28			0.1 M	PCTP	7	25 % w/v	PEG 1500
29			0.1 M	PCTP	8	25 % w/v	PEG 1500
30			0.1 M	PCTP	9	25 % w/v	PEG 1500
31	0.2 M	Sodium chloride	0.1 M	HEPES	7	20 % w/v	PEG 6000
32	0.2 M	Ammonium chloride	0.1 M	HEPES	7	20 % w/v	PEG 6000
33	0.2 M	Lithium chloride	0.1 M	HEPES	7	20 % w/v	PEG 6000
34	0.2 M	Magnesium chloride hexahydrate	0.1 M	HEPES	7	20 % w/v	PEG 6000
35	0.2 M	Calcium chloride hexahydrate	0.1 M	HEPES	7	20 % w/v	PEG 6000

Table A.21 – Molecular Interactions PACT *premier*TM Crystallisation Screen

Part 2

Reagent No	[Salt]	Salt	[Buffer]	Buffer	pH	[Ppt 1]	Precipitant 1
36	0.01 M	Zinc chloride	0.1 M	HEPES	7	20 % w/v	PEG 6000
37			0.1 M	MMT	4	25 % w/v	PEG 1500
38			0.1 M	MMT	5	25 % w/v	PEG 1500
39			0.1 M	MMT	6	25 % w/v	PEG 1500
40			0.1 M	MMT	7	25 % w/v	PEG 1500
41			0.1 M	MMT	8	25 % w/v	PEG 1500
42			0.1 M	MMT	9	25 % w/v	PEG 1500
43	0.2 M	Sodium chloride	0.1 M	Tris	8	20 % w/v	PEG 6000
44	0.2 M	Ammonium chloride	0.1 M	Tris	8	20 % w/v	PEG 6000
45	0.2 M	Lithium chloride	0.1 M	Tris	8	20 % w/v	PEG 6000
46	0.2 M	Magnesium chloride hexahydrate	0.1 M	Tris	8	20 % w/v	PEG 6000
47	0.2 M	Calcium chloride dihydrate	0.1 M	Tris	8	20 % w/v	PEG 6000
48	0.002 M	Zinc chloride	0.1 M	Tris	8	20 % w/v	PEG 6000
49	0.2 M	Sodium fluoride			0	20 % w/v	PEG 3350
50	0.2 M	Sodium bromide			0	20 % w/v	PEG 3350
51	0.2 M	Sodium iodide			0	20 % w/v	PEG 3350
52	0.2 M	Potassium thiocyanate			0	20 % w/v	PEG 3350
53	0.2 M	Sodium nitrate			0	20 % w/v	PEG 3350
54	0.2 M	Sodium formate			0	20 % w/v	PEG 3350
55	0.2 M	Sodium acetate trihydrate			0	20 % w/v	PEG 3350
56	0.2 M	Sodium sulfate			0	20 % w/v	PEG 3350
57	0.2 M	Potassium sodium tartrate tetrahydrate			0	20 % w/v	PEG 3350
58	0.02 M	Sodium/potassium phosphate			0	20 % w/v	PEG 3350
59	0.2 M	Sodium citrate tribasic dihydrate			0	20 % w/v	PEG 3350
60	0.2 M	Sodium malonate dibasic monohydrate			0	20 % w/v	PEG 3350
61	0.2 M	Sodium fluoride	0.1 M	Bis-Tris propane	6.5	20 % w/v	PEG 3350
62	0.2 M	Sodium bromide	0.1 M	Bis-Tris propane	6.5	20 % w/v	PEG 3350
63	0.2 M	Sodium iodide	0.1 M	Bis-Tris propane	6.5	20 % w/v	PEG 3350
64	0.2 M	Potassium thiocyanate	0.1 M	Bis-Tris propane	6.5	20 % w/v	PEG 3350
65	0.2 M	Sodium nitrate	0.1 M	Bis-Tris propane	6.5	20 % w/v	PEG 3350
66	0.2 M	Sodium formate	0.1 M	Bis-Tris propane	6.5	20 % w/v	PEG 3350
67	0.2 M	Sodium acetate trihydrate	0.1 M	Bis-Tris propane	6.5	20 % w/v	PEG 3350
68	0.2 M	Sodium sulfate	0.1 M	Bis-Tris propane	6.5	20 % w/v	PEG 3350
69	0.2 M	Potassium sodium tartrate tetrahydrate	0.1 M	Bis-Tris propane	6.5	20 % w/v	PEG 3350
70	0.02 M	Sodium/potassium phosphate	0.1 M	Bis-Tris propane	6.5	20 % w/v	PEG 3350

Table A.22 – Molecular Interactions PACT *premier*TM Crystallisation Screen

Part 3

Reagent No	[Salt]	Salt	[Buffer]	Buffer	pH	[Ppt 1]	Precipitant 1
71	0.2 M	Sodium citrate tribasic dihydrate	0.1 M	Bis-Tris propane	6.5	20 % w/v	PEG 3350
72	0.2 M	Sodium malonate dibasic monohydrate	0.1 M	Bis-Tris propane	6.5	20 % w/v	PEG 3350
73	0.2 M	Sodium fluoride	0.1 M	Bis-Tris propane	7.5	20 % w/v	PEG 3350
74	0.2 M	Sodium bromide	0.1 M	Bis-Tris propane	7.5	20 % w/v	PEG 3350
75	0.2 M	Sodium iodide	0.1 M	Bis-Tris propane	7.5	20 % w/v	PEG 3350
76	0.2 M	Potassium thiocyanate	0.1 M	Bis-Tris propane	7.5	20 % w/v	PEG 3350
77	0.2 M	Sodium nitrate	0.1 M	Bis-Tris propane	7.5	20 % w/v	PEG 3350
78	0.2 M	Sodium formate	0.1 M	Bis-Tris propane	7.5	20 % w/v	PEG 3350
79	0.2 M	Sodium acetate trihydrate	0.1 M	Bis-Tris propane	7.5	20 % w/v	PEG 3350
80	0.2 M	Sodium sulfate	0.1 M	Bis-Tris propane	7.5	20 % w/v	PEG 3350
81	0.2 M	Potassium sodium tartrate tetrahydrate	0.1 M	Bis-Tris propane	7.5	20 % w/v	PEG 3350
82	0.02 M	Sodium/potassium phosphate	0.1 M	Bis-Tris propane	7.5	20 % w/v	PEG 3350
83	0.2 M	Sodium citrate tribasic dihydrate	0.1 M	Bis-Tris propane	7.5	20 % w/v	PEG 3350
84	0.2 M	Sodium malonate dibasic monohydrate	0.1 M	Bis-Tris propane	7.5	20 % w/v	PEG 3350
85	0.2 M	Sodium fluoride	0.1 M	Bis-Tris propane	8.5	20 % w/v	PEG 3350
86	0.2 M	Sodium bromide	0.1 M	Bis-Tris propane	8.5	20 % w/v	PEG 3350
87	0.2 M	Sodium iodide	0.1 M	Bis-Tris propane	8.5	20 % w/v	PEG 3350
88	0.2 M	Potassium thiocyanate	0.1 M	Bis-Tris propane	8.5	20 % w/v	PEG 3350
89	0.2 M	Sodium nitrate	0.1 M	Bis-Tris propane	8.5	20 % w/v	PEG 3350
90	0.2 M	Sodium formate	0.1 M	Bis-Tris propane	8.5	20 % w/v	PEG 3350
91	0.2 M	Sodium acetate trihydrate	0.1 M	Bis-Tris propane	8.5	20 % w/v	PEG 3350
92	0.2 M	Sodium sulfate	0.1 M	Bis-Tris propane	8.5	20 % w/v	PEG 3350
93	0.2 M	Potassium sodium tartrate tetrahydrate	0.1 M	Bis-Tris propane	8.5	20 % w/v	PEG 3350
94	0.02 M	Sodium/potassium phosphate	0.1 M	Bis-Tris propane	8.5	20 % w/v	PEG 3350
95	0.2 M	Sodium citrate tribasic dihydrate	0.1 M	Bis-Tris propane	8.5	20 % w/v	PEG 3350
96	0.2 M	Sodium malonate dibasic monohydrate	0.1 M	Bis-Tris propane	8.5	20 % w/v	PEG 3350

Table A.23 – PDB Minimal Crystallisation Screen Part 1

tube	Conc1	Reagent1	Conc2	Reagent2	Buffer Conc	Buffer	pH	Conc4	Reagent4
1	0.2 M	MAGNESIUM CHLORIDE	30% W/V	POLYETHYLENE GLYCOL 4000	0.1 M	TRIS	8.5		
2	0.2 M	SODIUM ACETATE	30% W/V	POLYETHYLENE GLYCOL 4000	0.1 M	TRIS	8.5		
3	20% W/V	POLYETHYLENE GLYCOL 4000	10% V/V	2-PROPANOL	0.1 M	HEPES	7.5		
4	25% W/V	POLYETHYLENE GLYCOL 3350			0.1 M	BIS-TRIS	5.5		
5	0.2 M	MAGNESIUM CHLORIDE	25% W/V	POLYETHYLENE GLYCOL 3350	0.1 M	BIS-TRIS	5.5		
6	2 M	AMMONIUM SULFATE			0.1 M	TRIS	8.5		
7	0.2 M	MAGNESIUM ACETATE	20% W/V	POLYETHYLENE GLYCOL 8000	0.1 M	SODIUM CACODYLATE	6.5		
8	0.2 M	AMMONIUM ACETATE	30% W/V	POLYETHYLENE GLYCOL 4000	0.1 M	SODIUM ACETATE	4.6		
9	1.6 M	AMMONIUM SULFATE	10% V/V	DIOXANE	0.1 M	MES	6.5		
10	0.2 M	AMMONIUM ACETATE	25% W/V	POLYETHYLENE GLYCOL 3350	0.1 M	BIS-TRIS	5.5		
11	0.2 M	SODIUM CHLORIDE	25% W/V	POLYETHYLENE GLYCOL 3350	0.1 M	BIS-TRIS	5.5		
12	2 M	AMMONIUM SULFATE			0.1 M	SODIUM ACETATE	4.6		
13	0.2 M	LITHIUM SULFATE	25% W/V	POLYETHYLENE GLYCOL 3350	0.1 M	BIS-TRIS	5.5		
14	12% W/V	POLYETHYLENE GLYCOL 20000			0.1 M	MES	6.5		
15	0.2 M	MAGNESIUM CHLORIDE	25% W/V	POLYETHYLENE GLYCOL 3350	0.1 M	BIS-TRIS	6.5		
16	2 M	AMMONIUM SULFATE	2% V/V	POLYETHYLENE GLYCOL 400	0.1 M	HEPES	7.5		
17	2 M	AMMONIUM SULFATE							
18	20% W/V	POLYETHYLENE GLYCOL 4000	20% V/V	2-PROPANOL	0.1 M	SODIUM CITRATE	5.6		
19	0.2 M	AMMONIUM SULFATE	25% W/V	POLYETHYLENE GLYCOL 4000	0.1 M	SODIUM ACETATE	4.6		
20	0.2 M	AMMONIUM SULFATE	30% W/V	POLYETHYLENE GLYCOL 8000	0.1 M	SODIUM CACODYLATE	6.5		
21	0.2 M	AMMONIUM SULFATE	25% W/V	POLYETHYLENE GLYCOL 3350	0.1 M	BIS-TRIS	5.5		
22	0.2 M	AMMONIUM SULFATE	25% W/V	POLYETHYLENE GLYCOL 3350	0.1 M	BIS-TRIS	6.5		
23	1.6 M	AMMONIUM SULFATE	0.1 M	SODIUM CHLORIDE	0.1 M	HEPES	7.5		
24	0.2 M	AMMONIUM ACETATE	30% W/V	POLYETHYLENE GLYCOL 4000	0.1 M	SODIUM CITRATE	5.6		
25	0.2 M	MAGNESIUM CHLORIDE	25% W/V	POLYETHYLENE GLYCOL 3350	0.1 M	HEPES	7.5		
26	0.2 M	AMMONIUM SULFATE	30% W/V	POLYETHYLENE GLYCOL MONOMETHYL ETHER 5000	0.1 M	MES	6.5		

Table A.24 – PDB Minimal Crystallisation Screen Part 2

tube	Conc1	Reagent1	Conc2	Reagent2	Buffer Conc	Buffer	pH	Conc4	Reagent4
27	2 M	SODIUM FORMATE			0.1 M	SODIUM ACETATE	4.6		
28	8% V/V	ETHYLENE GLYCOL	10% W/V	POLYETHYLENE GLYCOL 8000	0.1 M	HEPES	7.5		
29	20% W/V	POLYETHYLENE GLYCOL 10000			0.1 M	HEPES	7.5		
30	20% W/V	POLYETHYLENE GLYCOL MONOMETHYL ETHER 5000			0.1 M	BIS-TRIS	6.5		
31	0.2 M	CALCIUM ACETATE	20%	W/V POLYETHYLENE GLYCOL 8000			0.1 M	MES	6
32	0.02 M	CALCIUM CHLORIDE	30% V/V	2-METHYL-2,4-PENTANEDIOL	0.1 M	SODIUM ACETATE	4.6		
33	0.2 M	MAGNESIUM CHLORIDE	25% W/V	POLYETHYLENE GLYCOL 3350	0.1 M	TRIS	8.5		
34	1 M	TRISODIUM CITRATE	5% w/v	POLYETHYLENE GLYCOL 3350	0.1 M	HEPES	7.5		
35	0.2 M	AMMONIUM SULFATE	30% W/V	POLYETHYLENE GLYCOL MONOMETHYL ETHER 2000	0.1 M	SODIUM ACETATE	4.6		
36	0.2 M	LITHIUM SULFATE	30% W/V	POLYETHYLENE GLYCOL 4000	0.1 M	TRIS	8.5		
37	25% W/V	POLYETHYLENE GLYCOL 3350			0.1 M	HEPES	7.5		
38	0.2 M	CALCIUM CHLORIDE	28% V/V	POLYETHYLENE GLYCOL 400	0.1 M	HEPES	7.5		
39	2.4 M	SODIUM MALONATE pH7					7		
40	1.4 M	TRISODIUM CITRATE			0.1 M	HEPES	7.5		
41	0.2 M	POTASSIUM SODIUM TARTRATE	2 M	AMMONIUM SULFATE	0.1 M	SODIUM CITRATE	5.6		
42	0.2 M	AMMONIUM SULFATE	25% W/V	POLYETHYLENE GLYCOL 3350	0.1 M	HEPES	7.5		
43	1 M	SODIUM CITRATE			0.1 M	SODIUM CACODYLATE	6.5		
44	1 M	SODIUM CHLORIDE	10% w/v	POLYETHYLENE GLYCOL 3350	0.1 M	TRIS	7.5		
45	0.2 M	MAGNESIUM CHLORIDE	20% W/V	POLYETHYLENE GLYCOL 8000	0.1 M	TRIS	8.5		
46	20% W/V	POLYETHYLENE GLYCOL 3000			0.1 M	SODIUM CITRATE	5.5		
47	8% W/V	POLYETHYLENE GLYCOL 4000			0.1 M	SODIUM ACETATE	4.6		
48	10% W/V	POLYETHYLENE GLYCOL 6000	5% V/V	2-METHYL-2,4-PENTANEDIOL	0.1 M	HEPES	7.5		
49	2 M	AMMONIUM SULFATE			0.1 M	BIS-TRIS	5.5		
50	1 M	AMMONIUM SULFATE	1% W/V	POLYETHYLENE GLYCOL 3350	0.1 M	BIS-TRIS	5.5		
51	1.5 M	LITHIUM SULFATE			0.1 M	HEPES	7.5		
52	0.2 M	AMMONIUM ACETATE	25% W/V	POLYETHYLENE GLYCOL 3350	0.1 M	HEPES	7.5		

Table A.25 – PDB Minimal Crystallisation Screen Part 3

tube	Conc1	Reagent1	Conc2	Reagent2	Buffer Conc	Buffer	pH	Conc4	Reagent4
53	20% W/V	POLYETHYLENE GLYCOL 8000			0.1 M	HEPES	7.5		
54	0.2 M	LITHIUM SULFATE	25% W/V	POLYETHYLENE GLYCOL 3350	0.1 M	BIS-TRIS	6.5		
55	0.2 M	LITHIUM SULFATE	25% W/V	POLYETHYLENE GLYCOL 3350	0.1 M	HEPES	7.5		
56	2.4 M	AMMONIUM SULFATE			0.1 M	BICINE	9		
57	0.05 M	CALCIUM CHLORIDE	30% V/V	POLYETHYLENE GLYCOL MONOMETHYL ETHER 550	0.1 M	BIS-TRIS	6.5		
58	0.2 M	MAGNESIUM CHLORIDE	30% V/V	POLYETHYLENE GLYCOL 400	0.1 M	HEPES	7.5		
59	20% W/V	POLYETHYLENE GLYCOL 3350	0.2 M	MAGNESIUM ACETATE			7.7		
60	1.6 M	MAGNESIUM SULFATE			0.1 M	MES	6.5		
61	0.2 M	CALCIUM ACETATE	18% W/V	POLYETHYLENE GLYCOL 8000	0.1 M	SODIUM CACODYLATE	6.5		
62	2 M	AMMONIUM SULFATE			0.1 M	BIS-TRIS	6.5		
63	0.2 M	SODIUM ACETATE	30% W/V	POLYETHYLENE GLYCOL 8000	0.1 M	SODIUM CACODYLATE	6.5		
64	28% W/V	POLYETHYLENE GLYCOL MONOMETHYL ETHER 2000			0.1 M	BIS-TRIS	6.5		
65	0.2 M	CALCIUM ACETATE	10% W/V	POLYETHYLENE GLYCOL 8000	0.1 M	IMIDAZOLE	8.0		
66	60% V/V	TACSIMATE pH7.0					7		
67	2.1 M	DL-MALIC ACID 7.0					7		
68	0.15 M	DL-MALIC ACID 7.0	20 W/V	POLYETHYLENE GLYCOL 3350			7		
69	0.2 M	SODIUM CHLORIDE	2 M	AMMONIUM SULFATE					
70	4 M	SODIUM FORMATE							
71	1.4 M	SODIUM ACETATE			0.1 M	SODIUM CACODYLATE	6.5		
72	0.2 M	SODIUM CHLORIDE	25% W/V	POLYETHYLENE GLYCOL 3350	0.1 M	HEPES	7.5		
73	4.3 M	SODIUM CHLORIDE			0.1 M	HEPES	7.5		
74	0.2 M	AMMONIUM CHLORIDE	20% W/V	POLYETHYLENE GLYCOL 3350					
75	0.2 M	SODIUM FORMATE	20% W/V	POLYETHYLENE GLYCOL 3350					
76	0.2 M	AMMONIUM FORMATE	20% W/V	POLYETHYLENE GLYCOL 3350					
77	0.2 M	CALCIUM ACETATE	20% W/V	POLYETHYLENE GLYCOL 3350					
78	0.2 M	POTASSIUM SODIUM TARTRATE	2 M	AMMONIUM SULFATE	0.1 M	TRISODIUM CITRATE	5.6		

Table A.26 – PDB Minimal Crystallisation Screen Part 4

tube	Conc1	Reagent1	Conc2	Reagent2	Buffer Conc	Buffer	pH	Conc4	Reagent4
79	0.01 M	COBALT CHLORIDE	1.8 M	AMMONIUM SULFATE	0.1 M	MES	6.5		
80	1.2 M	SODIUM DIHYDROGEN PHOSPHATE	0.8 M	DIPOTASSIUM HYDROGEN PHOSPHATE	0.1 M	CAPS	10.5	0.2 M	LITHIUM SULFATE
81	0.2 M	CALCIUM ACETATE	40% V/V	POLYETHYLENE GLYCOL 300	0.1 M	SODIUM CACODYLATE	6.5		
82	2 M	AMMONIUM SULFATE			0.1 M	SODIUM ACETATE	4.5		
83	70% V/V	2-METHYL-2,4-PENTANEDIOL			0.1 M	HEPES	7.5		
84	20% W/V	POLYETHYLENE GLYCOL 4000	10% V/V	2-PROPANOL	0.1 M	SODIUM HEPES	7.5		
85	30% V/V	POLYETHYLENE GLYCOL MONOMETHYL ETHER 550	0.05 M	MAGNESIUM CHLORIDE	0.1 M	HEPES	7.5		
86	2 M	AMMONIUM SULFATE	2% V/V	POLYETHYLENE GLYCOL 400	0.1 M	SODIUM HEPES	7.5		
87	0.2 M	SODIUM CHLORIDE	25% W/V	POLYETHYLENE GLYCOL 3350	0.1 M	BIS-TRIS	6.5		
88	25% W/V	POLYETHYLENE GLYCOL 3350			0.1 M	TRIS	8.5		
89	0.2 M	LITHIUM SULFATE	30% W/V	POLYETHYLENE GLYCOL 8000	0.1 M	SODIUM ACETATE	4.5		
90	20% W/V	POLYETHYLENE GLYCOL 6000	1 M	LITHIUM CHLORIDE	0.1 M	MES	6		
91	3.5 M	SODIUM FORMATE	0.1 M			SODIUM ACETATE	4.6		
92	20% W/V	POLYETHYLENE GLYCOL 8000			0.1 M	CHES	9.5		
93	1 M	SODIUM CITRATE			0.1 M	CHES	9.5		
94	0.2 M	LITHIUM SULFATE	20% W/V	POLYETHYLENE GLYCOL 1000	0.1 M	PHOSPHATE-CITRATE	4.2		
95	2.8 M	SODIUM ACETATE					7.0		
96	1.6 M	SODIUM CITRATE					6.5		

Table A.27 – Qiagen[®] MPD Screen Conditions Part 1

Number	[Salt]	Salt	[Buffer]	Buffer	[Prec1]	Prec1
1	0.2 M	Cadmium chloride			40% (v/v)	MPD
2	0.2 M	Potassium fluoride			40% (v/v)	MPD
3	0.2 M	Ammonium fluoride			40% (v/v)	MPD
4	0.2 M	Lithium chloride			40% (v/v)	MPD
5	0.2 M	Magnesium chloride			40% (v/v)	MPD
6	0.2 M	Sodium chloride			40% (v/v)	MPD
7	0.2 M	Calcium chloride			40% (v/v)	MPD
8	0.2 M	Potassium chloride			40% (v/v)	MPD
9	0.2 M	Ammonium chloride			40% (v/v)	MPD
10	0.2 M	Sodium iodide			40% (v/v)	MPD
11	0.2 M	Potassium iodide			40% (v/v)	MPD
12	0.2 M	Ammonium iodide			40% (v/v)	MPD
13	0.2 M	Sodium thiocyanate			40% (v/v)	MPD
14	0.2 M	Potassium thiocyanate			40% (v/v)	MPD
15	0.2 M	Lithium nitrate			40% (v/v)	MPD
16	0.2 M	Magnesium nitrate			40% (v/v)	MPD
17	0.2 M	Sodium nitrate			40% (v/v)	MPD
18	0.2 M	Potassium nitrate			40% (v/v)	MPD
19	0.2 M	Ammonium nitrate			40% (v/v)	MPD
20	0.2 M	Zinc sulfate			40% (v/v)	MPD
21	0.2 M	Sodium formate			40% (v/v)	MPD
22	0.2 M	Potassium formate			40% (v/v)	MPD
23	0.2 M	Ammonium formate			40% (v/v)	MPD
24	0.2 M	Lithium acetate			40% (v/v)	MPD
25	0.2 M	Magnesium acetate			40% (v/v)	MPD
26	0.2 M	Sodium malonate			40% (v/v)	MPD
27	0.2 M	Sodium acetate			40% (v/v)	MPD
28	0.2 M	Calcium acetate			40% (v/v)	MPD
29	0.2 M	Potassium acetate			40% (v/v)	MPD
30	0.2 M	Ammonium acetate			40% (v/v)	MPD
31	0.2 M	Lithium sulfate			40% (v/v)	MPD
32	0.2 M	Magnesium sulfate			40% (v/v)	MPD
33	0.2 M	Cesium chloride			40% (v/v)	MPD
34	0.2 M	Nickel chloride			40% (v/v)	MPD
35	0.2 M	Ammonium sulfate			40% (v/v)	MPD

Table A.28 – Qiagen[®] MPD Screen Conditions Part 2

Number	[Salt]	Salt	[Buffer]	Buffer	[Prec1]	Prec1
36	0.2 M	di-Sodium tartrate			40% (v/v)	MPD
37	0.2 M	K/Na tartrate			40% (v/v)	MPD
38	0.2 M	di-Ammonium tartrate			40% (v/v)	MPD
39	0.2 M	Sodium phosphate			40% (v/v)	MPD
40	0.2 M	Potassium bromide			40% (v/v)	MPD
41	0.2 M	Sodium bromide			40% (v/v)	MPD
42	0.2 M	di-Potassium phosphate			40% (v/v)	MPD
43	0.2 M	Ammonium phosphate			40% (v/v)	MPD
44	0.2 M	di-Ammonium phosphate			40% (v/v)	MPD
45	0.2 M	tri-Lithium citrate			40% (v/v)	MPD
46	0.2 M	tri-Sodium citrate			40% (v/v)	MPD
47	0.2 M	tri-Potassium citrate			40% (v/v)	MPD
48	0.18 M	tri-Ammonium citrate			40% (v/v)	MPD
49			0.1 M	Citric acid pH 4.0	10% (v/v)	MPD
50			0.1 M	Sodium acetate pH 5.0	10% (v/v)	MPD
51			0.1 M	MES pH 6.0	10% (v/v)	MPD
52			0.1 M	HEPES pH 7.0	10% (v/v)	MPD
53			0.1 M	Tris pH 8.0	10% (v/v)	MPD
54			0.1 M	Bicine pH 9.0	10% (v/v)	MPD
55			0.1 M	Citric acid pH 4.0	20% (v/v)	MPD
56			0.1 M	Sodium acetate pH 5.0	20% (v/v)	MPD
57			0.1 M	MES pH 6.0	20% (v/v)	MPD
58			0.1 M	HEPES pH 7.0	20% (v/v)	MPD
59			0.1 M	Tris pH 8.0	20% (v/v)	MPD
60			0.1 M	Bicine pH 9.0	20% (v/v)	MPD
61			0.1 M	Citric acid pH 4.0	40% (v/v)	MPD
62			0.1 M	Sodium acetate pH 5.0	40% (v/v)	MPD
63			0.1 M	MES pH 6.0	40% (v/v)	MPD
64			0.1 M	HEPES pH 7.0	40% (v/v)	MPD
65			0.1 M	Tris pH 8.0	40% (v/v)	MPD
66			0.1 M	Bicine pH 9.0	40% (v/v)	MPD
67			0.1 M	Sodium acetate pH 4.0	65% (v/v)	MPD
68			0.1 M	Sodium acetate pH 5.0	65% (v/v)	MPD
69			0.1 M	MES pH 6.0	65% (v/v)	MPD
70			0.1 M	HEPES pH 7.0	65% (v/v)	MPD

Table A.29 – Qiagen[®] MPD Screen Conditions Part 3

Number	[Salt]	Salt	[Buffer]	Buffer	[Prec1]	Prec1
71			0.1 M	Tris pH 8.0	65% (v/v)	MPD
72			0.1 M	Bicine pH 9.0	65% (v/v)	MPD
73	0.1 M	tri-Sodium citrate	0.1 M	HEPES sodium salt pH 7.5	10% (w/v)	MPD
74	0.05 M	Magnesium chloride	0.1 M	TrisHCl pH 8.5	12% (w/v)	MPD
75	0.02 M	Calcium chloride	0.1 M	Sodium acetate pH 4.6	15% (w/v)	MPD
76			0.1 M	ImidazoleHCl pH 8.0	15% (w/v); 5% (w/v)	MPD; PEG 4000
77	0.2 M	Ammonium acetate	0.1 M	tri-Sodium citrate pH 5.6	15% (w/v)	MPD
78	0.2 M	Magnesium acetate	0.1 M	MES sodium salt pH 6.5	15% (w/v)	MPD
79	0.2 M	tri-Sodium citrate	0.1 M	HEPES sodium salt pH 7.5	15% (w/v)	MPD
80	0.1 M	tri-Sodium citrate	0.1 M	HEPES sodium salt pH 7.5	20% (w/v)	MPD
81			0.1 M	ImidazoleHCl pH 8.0	20% (w/v)	MPD
82	0.2 M	Sodium chloride			20% (w/v); 4% (w/v)	MPD; Glycerol
83	0.02 M	Calcium chloride	0.1 M	Sodium acetate pH 4.6	30% (w/v)	MPD
84	0.2 M	Ammonium acetate	0.1 M	tri-Sodium citrate pH 5.6	30% (w/v)	MPD
85	0.2 M	Magnesium acetate	0.1 M	MES sodium salt pH 6.5	30% (w/v)	MPD
86	0.5 M	Ammonium sulfate	0.1 M	HEPES sodium salt pH 7.5	30% (w/v)	MPD
87	0.2 M	tri-Sodium citrate	0.1 M	HEPES sodium salt pH 7.5	30% (w/v)	MPD
88			0.1 M	HEPES sodium salt pH 7.5	30% (w/v); 5% (w/v)	MPD; PEG 4000
89			0.1 M	ImidazoleHCl pH 8.0	30% (w/v); 10% (w/v)	MPD; PEG 4000
90					30% (w/v); 20% (w/v)	MPD; Ethanol
91					35% (w/v)	MPD
92			0.1 M	ImidazoleHCl pH 8.0	35% (w/v)	MPD
93			0.1 M	TrisHCl pH 8.5	40% (w/v)	MPD
94			0.1 M	HEPES sodium salt pH 7.5	47% (w/v)	MPD
95					47% (w/v); 2% (w/v)	MPD; tert-Butanol
96					50% (w/v)	MPD

Table A.30 – HT Formulation Hampton Research - Copyright 2016 Part 1

Reagent Number	[Salt 1]	Salt 1	[Salt 2]	Salt 2	[Buffer]	Buffer	[Prec 1]	Prec 1	[Prec 2]	Prec 2	Average pH
1	0.02 M				0.1 M	Sodium acetate trihydrate pH 4.6	30 % v/v	(+/-)-2-Methyl-2,4-pentanediol			5.1
2						pH	0.4 M	Potassium sodium tartrate tetrahydrate			8.4
3						pH	0.4 M	Ammonium phosphate monobasic			4.2
4					0.1 M	TRIS hydrochloride pH 8.5	2 M	Ammonium sulfate			8.2
5	0.2 M				0.1 M	HEPES sodium pH 7.5	30 % v/v	(+/-)-2-Methyl-2,4-pentanediol			7.4
6	0.2 M				0.1 M	TRIS hydrochloride pH 8.5	30 % w/v	Polyethylene glycol 4,000			8.5
7					0.1 M	Sodium cacodylate trihydrate pH 6.5	1.4 M	Sodium acetate trihydrate			6.8
8	0.2 M				0.1 M	Sodium cacodylate trihydrate pH 6.5	30 % v/v	2-Propanol			7
9	0.2 M				0.1 M	Sodium citrate tribasic dihydrate pH 5.6	30 % w/v	Polyethylene glycol 4,000			6.5
10	0.2 M				0.1 M	Sodium acetate trihydrate pH 4.6	30 % w/v	Polyethylene glycol 4,000			5.8
11					0.1 M	Sodium citrate tribasic dihydrate pH 5.6	1 M	Ammonium phosphate monobasic			4.7
12	0.2 M				0.1 M	HEPES sodium pH 7.5	30 % v/v	2-Propanol			6.9
13	0.2 M				0.1 M	TRIS hydrochloride pH 8.5	30 % v/v	Polyethylene glycol 400			8.8
14	0.2 M				0.1 M	HEPES sodium pH 7.5	28 % v/v	Polyethylene glycol 400			7.3
15	0.2 M				0.1 M	Sodium cacodylate trihydrate pH 6.5	30 % w/v	Polyethylene glycol 8,000			6.6
16					0.1 M	HEPES sodium pH 7.5	1.5 M	Lithium sulfate monohydrate			7.7
17	0.2 M				0.1 M	TRIS hydrochloride pH 8.5	30 % w/v	Polyethylene glycol 4,000			8.6
18	0.2 M				0.1 M	Sodium cacodylate trihydrate pH 6.5	20 % w/v	Polyethylene glycol 8,000			6.6
19	0.2 M				0.1 M	TRIS hydrochloride pH 8.5	30 % v/v	2-Propanol			8.3
20	0.2 M				0.1 M	Sodium acetate trihydrate pH 4.6	25 % w/v	Polyethylene glycol 4,000			4.9
21	0.2 M				0.1 M	Sodium cacodylate trihydrate pH 6.5	30 % v/v	(+/-)-2-Methyl-2,4-pentanediol			6.7
22	0.2 M				0.1 M	TRIS hydrochloride pH 8.5	30 % w/v	Polyethylene glycol 4,000			8.6
23	0.2 M				0.1 M	HEPES sodium pH 7.5	30 % v/v	Polyethylene glycol 400			7.3
24	0.2 M				0.1 M	Sodium acetate trihydrate pH 4.6	20 % v/v	2-Propanol			4.6
25					0.1 M	Imidazole pH 6.5	1 M	Sodium acetate trihydrate			6.9

Table A.31 – HT Formulation Hampton Research - Copyright 2016 Part 2

Reagent Number	[Salt 1]	Salt 1	[Salt 2]	Salt 2	[Buffer]	Buffer	[Prec 1]	Prec 1	[Prec 2]	Prec 2	Average pH
26	0.2 M				0.1 M	Sodium citrate tribasic dihydrate pH 5.6	30 % v/v	(+/-)-2-Methyl-2,4-pentanediol			6.5
27	0.2 M				0.1 M	HEPES sodium pH 7.5	20 % v/v	2-Propanol			7.4
28	0.2 M				0.1 M	Sodium cacodylate trihydrate pH 6.5	30 % w/v	Polyethylene glycol 8,000			6.9
29					0.1 M	HEPES sodium pH 7.5	0.8 M	Potassium sodium tartrate tetrahydrate			7.6
30	0.2 M					pH	30 % w/v	Polyethylene glycol 8,000			5.5
31	0.2 M					pH	30 % w/v	Polyethylene glycol 4,000			5.6
32						pH	2 M	Ammonium sulfate			5
33						pH	4 M	Sodium formate			8.5
34					0.1 M	Sodium acetate trihydrate pH 4.6	2 M	Sodium formate			5.5
35					0.1 M	HEPES sodium pH 7.5	0.8 M	Sodium phosphate monobasic monohydrate	0.8 M	Potassium phosphate monobasic	4.5
36					0.1 M	TRIS hydrochloride pH 8.5	8 % w/v	Polyethylene glycol 8,000			8.5
37					0.1 M	Sodium acetate trihydrate pH 4.6	8 % w/v	Polyethylene glycol 4,000			4.8
38					0.1 M	HEPES sodium pH 7.5	1.4 M	Sodium citrate tribasic dihydrate			7.9
39					0.1 M	HEPES sodium pH 7.5	2 % v/v	Polyethylene glycol 400	2 M	Ammonium sulfate	8
40					0.1 M	Sodium citrate tribasic dihydrate pH 5.6	20 % v/v	2-Propanol	20 % w/v	Polyethylene glycol 4,000	6.5
41					0.1 M	HEPES sodium pH 7.5	10 % v/v	2-Propanol	20 % w/v	Polyethylene glycol 4,000	7.3
42	0.05 M					pH	20 % w/v	Polyethylene glycol 8,000			5
43						pH	30 % w/v	polyethylene glycol 1,500			6.5
44						pH	0.2 M	Magnesium formate dihydrate			7.8
45	0.2 M				0.1 M	Sodium cacodylate trihydrate pH 6.5	18 % w/v	Polyethylene glycol 8,000			5.8
46	0.2 M				0.1 M	Sodium cacodylate trihydrate pH 6.5	18 % w/v	Polyethylene glycol 8,000			6.6
47					0.1 M	Sodium acetate trihydrate pH 4.6	2 M	Ammonium sulfate			4.6
48					0.1 M	TRIS hydrochloride pH 8.5	2 M	Ammonium phosphate monobasic			4.6
49	2 M					pH	10 % w/v	Polyethylene glycol 6,000			6.3
50	0.5 M	0.01 M	0.01 M	Magnesium chloride hexahydrate		pH	0.01 M	Hexadecyltrimethylammonium bromide			6
51						pH	25 % v/v	Ethylene glycol			5.7
52						pH	35 % v/v	1,4-Dioxane			5.1

Table A.32 – HT Formulation Hampton Research - Copyright 2016 Part 3

Reagent Number	[Salt 1]	Salt 1	[Salt 2]	Salt 2	[Buffer]	Buffer	[Prec 1]	Prec 1	[Prec 2]	Prec 2	Average pH
53	2 M					pH	5 % v/v	2-Propanol			5.3
54						pH	1 M	Imidazole pH 7.0			7
55						pH	10 % w/v	Polyethylene glycol 1,000	10 % w/v	Polyethylene glycol 8,000	5.8
56	1.5 M					pH	10 % v/v	Ethanol			6.1
57					0.1 M	Sodium acetate trihydrate pH 4.6	2 M	Sodium chloride			4.4
58	0.2 M				0.1 M	Sodium acetate trihydrate pH 4.6	30 % v/v	(+/-)-2-Methyl-2,4-pentanediol			5
59	0.01 M				0.1 M	Sodium acetate trihydrate pH 4.6	1 M	1,6-Hexanediol			4.8
60	0.1 M				0.1 M	Sodium acetate trihydrate pH 4.6	30 % v/v	Polyethylene glycol 400			4.8
61	0.2 M				0.1 M	Sodium acetate trihydrate pH 4.6	30 % w/v	Polyethylene glycol monomethyl ether 2,000			5
62	0.2 M				0.1 M	Sodium citrate tribasic dihydrate pH 5.6	2 M	Ammonium sulfate			5.7
63	0.5 M				0.1 M	Sodium citrate tribasic dihydrate pH 5.6	1 M	Lithium sulfate monohydrate			5.3
64	0.5 M				0.1 M	Sodium citrate tribasic dihydrate pH 5.6	2 % v/v	Ethylene imine polymer			5.6
65					0.1 M	Sodium citrate tribasic dihydrate pH 5.6	35 % v/v	tert-Butanol			6.3
66	0.01 M				0.1 M	Sodium citrate tribasic dihydrate pH 5.6	10 % v/v	Jeffamine M-600			5.6
67					0.1 M	Sodium citrate tribasic dihydrate pH 5.6	2.5 M	1,6-Hexanediol			6.3
68					0.1 M	MES monohydrate pH 6.5	1.6 M	Magnesium sulfate heptahydrate			6.6
69	0.1 M	0.1 M	0.1 M	Potassium phosphate monobasic	0.1 M	MES monohydrate pH 6.5	2 M	Sodium chloride			5.4
70					0.1 M	MES monohydrate pH 6.5	12 % w/v	Polyethylene glycol 20,000			6.5
71	1.6 M				0.1 M	MES monohydrate pH 6.5	10 % v/v	1,4-Dioxane			6.7
72	0.05 M				0.1 M	MES monohydrate pH 6.5	30 % v/v	Jeffamine M-600			6.5
73	0.01 M				0.1 M	MES monohydrate pH 6.5	1.8 M	Ammonium sulfate			6.8
74	0.2 M				0.1 M	MES monohydrate pH 6.5	30 % w/v	Polyethylene glycol monomethyl ether 5,000			6.3

Table A.33 – HT Formulation Hampton Research - Copyright 2016 Part 4

Reagent Number	[Salt 1]	Salt 1	[Salt 2]	Salt 2	[Buffer]	Buffer	[Prec 1]	Prec 1	[Prec 2]	Prec 2	Average pH
75	0.01 M				0.1 M	MES monohydrate pH 6.5	25 % v/v	Polyethylene glycol monomethyl ether 550			6.4
76						pH	1.6 M	Sodium citrate tribasic dihydrate pH 6.5			6.5
77	0.5 M				0.1 M	HEPES pH 7.5	30 % v/v	(+/-)-2-Methyl-2,4-pentanediol			7.3
78					0.1 M	HEPES pH 7.5	10 % w/v	Polyethylene glycol 6,000	5 % v/v	(+/-)-2-Methyl-2,4-pentanediol	7.4
79					0.1 M	HEPES pH 7.5	20 % v/v	Jeffamine M-600			7.5
80	0.1 M				0.1 M	HEPES pH 7.5	1.6 M	Ammonium sulfate			7.6
81					0.1 M	HEPES pH 7.5	2 M	Ammonium formate			7.4
82	0.05 M				0.1 M	HEPES pH 7.5	1 M	Sodium acetate trihydrate			7.4
83					0.1 M	HEPES pH 7.5	70 % v/v	(+/-)-2-Methyl-2,4-pentanediol			7.4
84					0.1 M	HEPES pH 7.5	4.3 M	Sodium chloride			7.8
85					0.1 M	HEPES pH 7.5	10 % w/v	Polyethylene glycol 8,000	8 % v/v	Ethylene glycol	7.4
86					0.1 M	HEPES pH 7.5	20 % w/v	Polyethylene glycol 10,000			7.4
87	0.2 M				0.1 M	Tris pH 8.5	3.4 M	1,6-Hexanediol			8.4
88					0.1 M	Tris pH 8.5	25 % v/v	tert-Butanol			8.3
89	0.01 M				0.1 M	Tris pH 8.5	1 M	Lithium sulfate monohydrate			8.5
90	1.5 M				0.1 M	Tris pH 8.5	12 % v/v	Glycerol			8.1
91	0.2 M				0.1 M	Tris pH 8.5	50 % v/v	(+/-)-2-Methyl-2,4-pentanediol			6.3
92					0.1 M	Tris pH 8.5	20 % v/v	Ethanol			8.4
93	0.01 M				0.1 M	Tris pH 8.5	20 % w/v	Polyethylene glycol monomethyl ether 2,000			8.3
94	0.1 M				0.1 M	BICINE pH 9	20 % v/v	Polyethylene glycol monomethyl ether 550			9.1
95					0.1 M	BICINE pH 9	2 M	Magnesium chloride hexahydrate			7.5
96					0.1 M	BICINE pH 9	2 % v/v	1,4-Dioxane	10 % w/v	Polyethylene glycol 20,000	9.5

A.4 Chapter 5

Table A.34 – Activated Carbon CO₂ Pressure Swing 10 bar pressure for 30mins

Run Number	Initial Weight	Final Weight	Difference	Normalised Difference	mmol CO2 Adsorbed	per g sample
1	17.7527	17.7812	0.0285	0.0094	0.2127	2.1057
2	17.7522	17.7809	0.0287	0.0096	0.2172	2.1507
3	17.7517	17.7800	0.0283	0.0092	0.2081	2.0607
4	17.7496	17.7784	0.0288	0.0097	0.2195	2.1732
5	17.7499	17.7783	0.0284	0.0093	0.2104	2.0832

Table A.35 – Pecbon 300 CO₂ Pressure Swing 10 bar pressure for 30mins

Run Number	Initial Weight	Final Weight	Difference	Normalised Difference	mmol CO2 Adsorbed	per g sample
1	17.7649	17.7886	0.0237	0.0043	0.0986	0.9519
2	17.7679	17.7917	0.0238	0.0044	0.1009	0.9738
3	17.7683	17.7914	0.0231	0.0037	0.0850	0.8203
4	17.7697	17.7932	0.0235	0.0041	0.0941	0.9080
5	17.7689	17.7919	0.0230	0.0036	0.0827	0.7983

Table A.36 – Pecbon 450 CO₂ Pressure Swing 10 bar pressure for 30mins

Run Number	Initial Weight	Final Weight	Difference	Normalised Difference	mmol CO2 Adsorbed	per g sample
1	17.9800	18.0048	0.0248	0.0053	0.1195	1.1798
2	17.9819	18.0066	0.0247	0.0052	0.1172	1.1574
3	17.9849	18.0084	0.0235	0.0040	0.0900	0.8882
4	17.9855	18.0094	0.0239	0.0044	0.0991	0.9780
5	17.9856	18.0092	0.0236	0.0041	0.0923	0.9107

Table A.37 – Pecbon 600 CO₂ Pressure Swing 10 bar pressure for 30mins

Run Number	Initial Weight	Final Weight	Difference	Normalised Difference	mmol CO ₂ Adsorbed	per g sample
1	17.9597	17.9861	0.0264	0.0068	0.1550	1.5404
2	17.9598	17.9857	0.0259	0.0063	0.1436	1.4275
3	17.9602	17.9854	0.0252	0.0056	0.1277	1.2694
4	17.9602	17.9851	0.0249	0.0053	0.1209	1.2016
5	17.9596	17.9843	0.0247	0.0051	0.1163	1.1564

Table A.38 – Pecbon 800 CO₂ Pressure Swing 10 bar pressure for 30mins

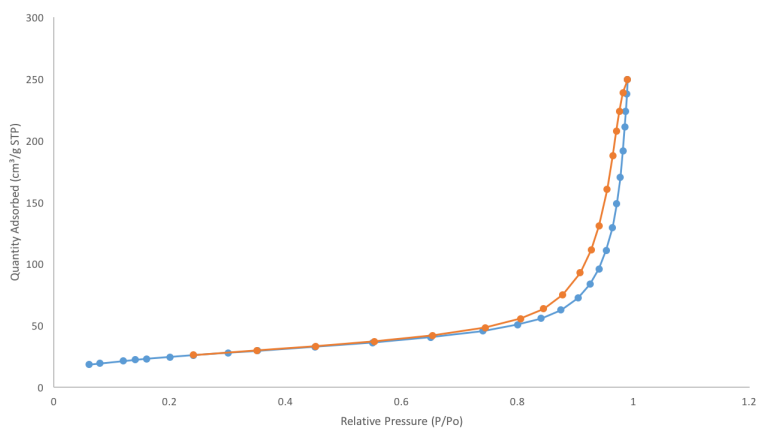
Run Number	Initial Weight	Final Weight	Difference	Normalised Difference	mmol CO ₂ Adsorbed	per g sample
1	17.7992	17.8281	0.0289	0.0101	0.2304	2.2971
2	17.7999	17.8279	0.0280	0.0092	0.2100	2.0932
3	17.8015	17.8289	0.0274	0.0086	0.1963	1.9573
4	17.8015	17.8288	0.0273	0.0085	0.1940	1.9347
5	17.8023	17.8298	0.0275	0.0087	0.1986	1.9800

Table A.39 – Starbon 800 CO₂ Pressure Swing 10 bar pressure for 30mins

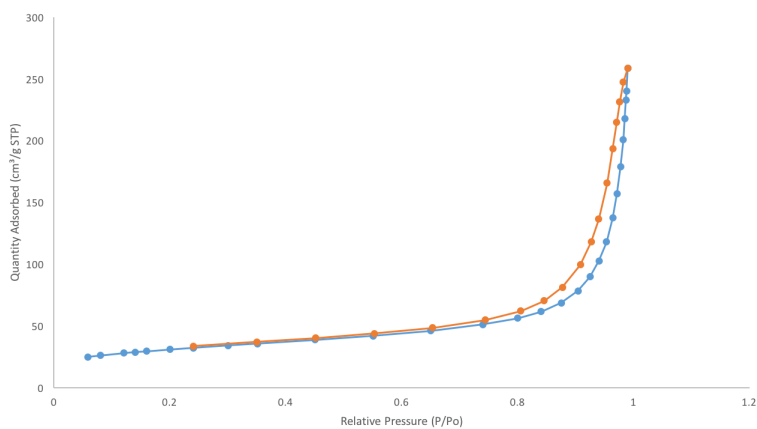
Run Number	Initial Weight	Final Weight	Difference	Normalised Difference	mmol CO ₂ Adsorbed	per g sample
1	17.9641	17.9944	0.0303	0.0105	0.2386	2.3716
2	17.9615	17.9920	0.0305	0.0107	0.2431	2.4168
3	17.9622	17.9914	0.0292	0.0094	0.2136	2.1231
4	17.9625	17.9923	0.0298	0.0100	0.2272	2.2587
5	17.9631	17.9911	0.0280	0.0082	0.1863	1.8521

Table A.40 – Algibon 800 CO₂ Pressure Swing 10 bar pressure for 30mins

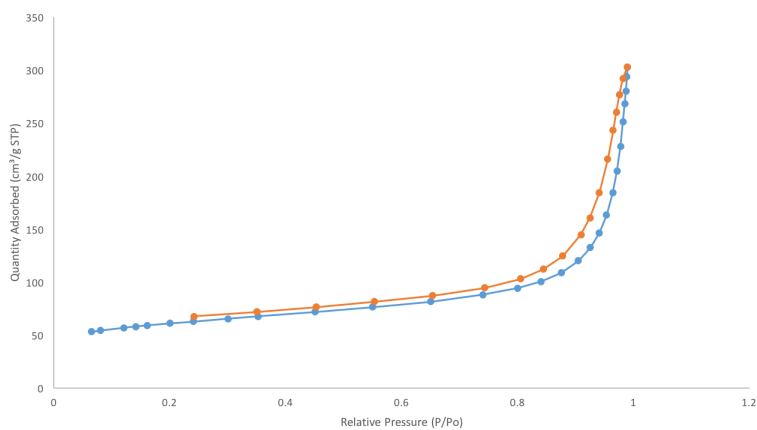
Run Number	Initial Weight	Final Weight	Difference	Normalised Difference	mmol CO ₂ Adsorbed	per g sample
1	17.9816	18.0087	0.0271	0.0073	0.1663	1.6243
2	17.9804	18.0084	0.0280	0.0082	0.1868	1.8240
3	17.9803	18.0082	0.0279	0.0081	0.1845	1.8018
4	17.9801	18.0069	0.0268	0.0070	0.1595	1.5577
5	17.9808	18.0076	0.0268	0.0070	0.1595	1.5577



(a) Isotherm for P300

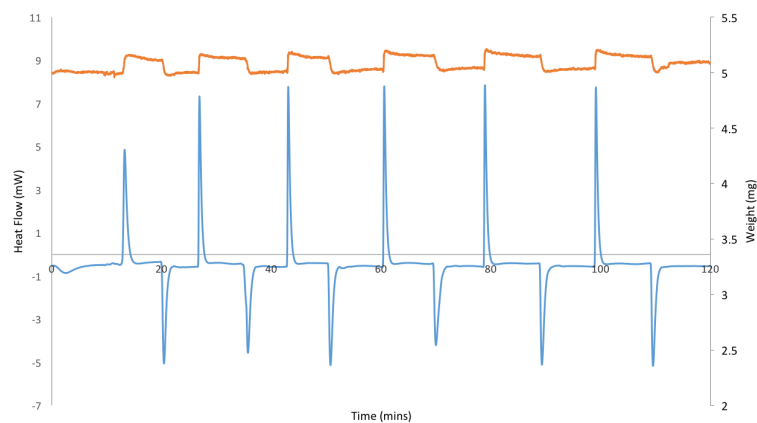


(b) Isotherm for P450

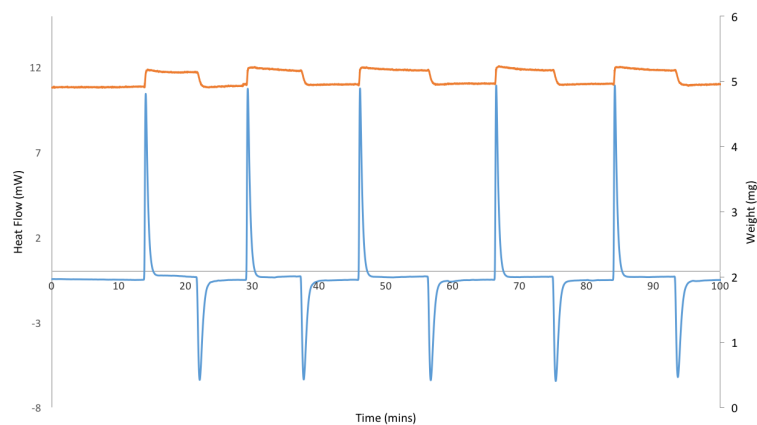


(c) Isotherm for P600

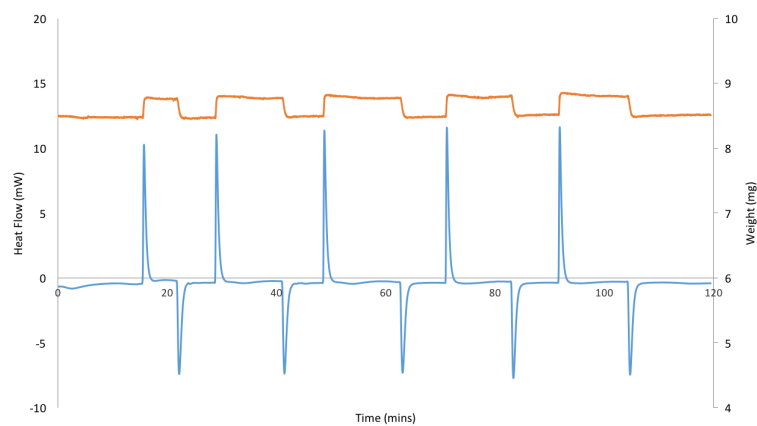
Figure A.6 – Isotherms for Different Samples



(a) Heat Flow and Weight Change on Addition of CO₂ and N₂ to A800

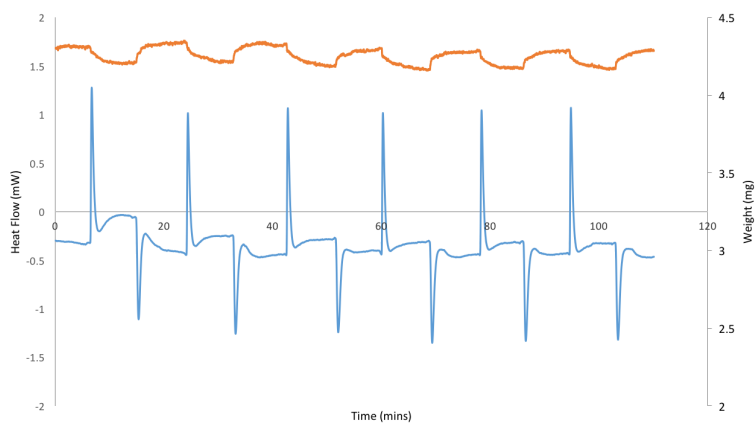


(b) Heat Flow and Weight Change on Addition of CO₂ and N₂ to P450

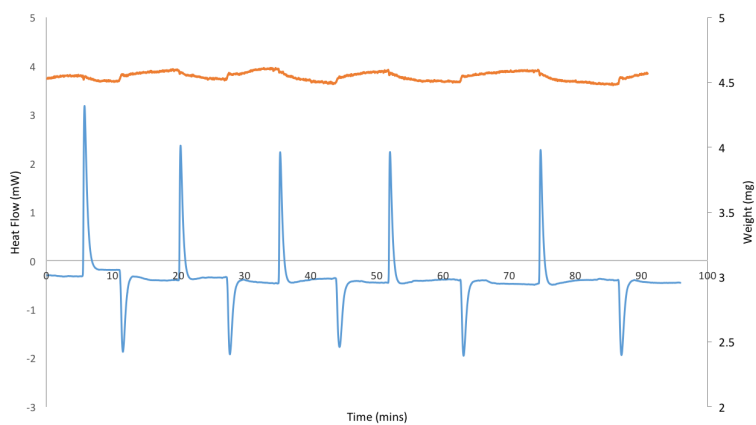


(c) Heat Flow and Weight Change on Addition of CO₂ and N₂ to P600

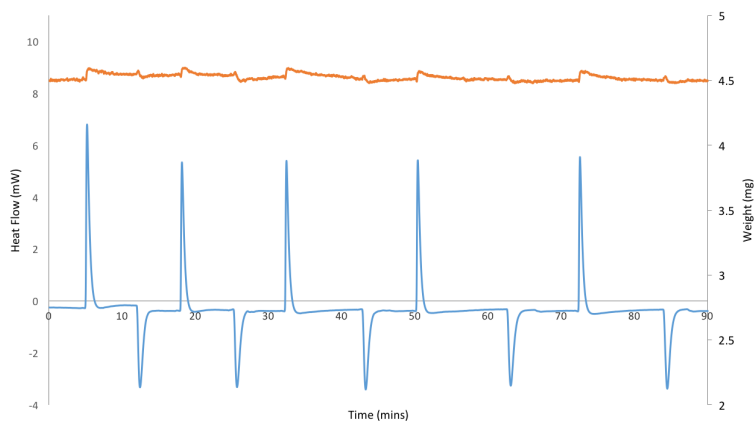
Figure A.7 – DSC Traces for A800, S800 and AC on Addition of CO₂ and N₂



(a) Heat Flow and Weight Change on Addition of CO₂ and N₂ to P300

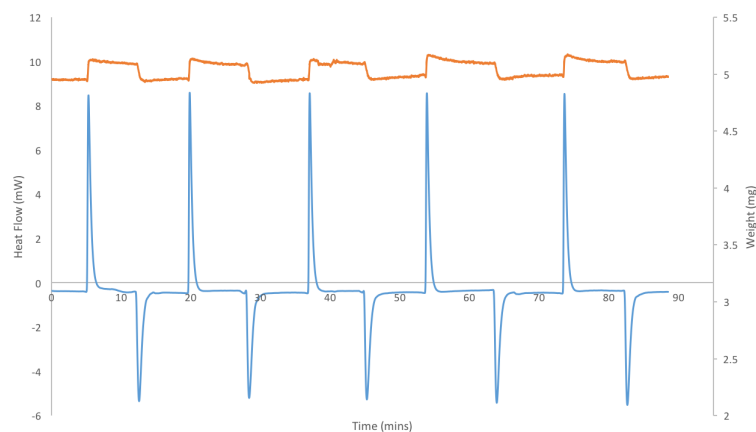


(b) Heat Flow and Weight Change on Addition of CO₂ and N₂ to P450

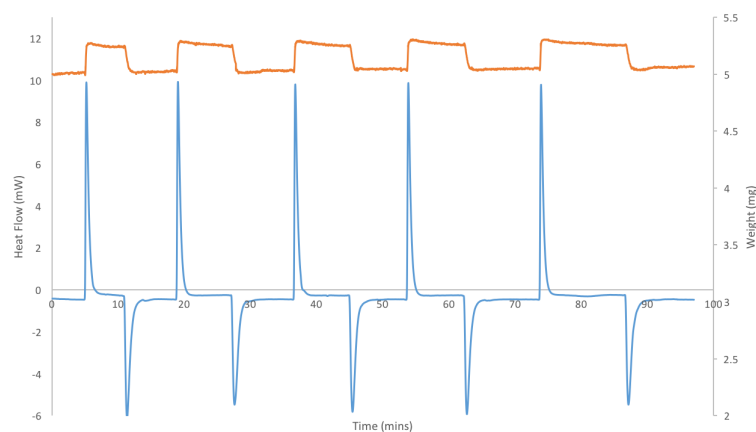


(c) Heat Flow and Weight Change on Addition of CO₂ and N₂ to P600

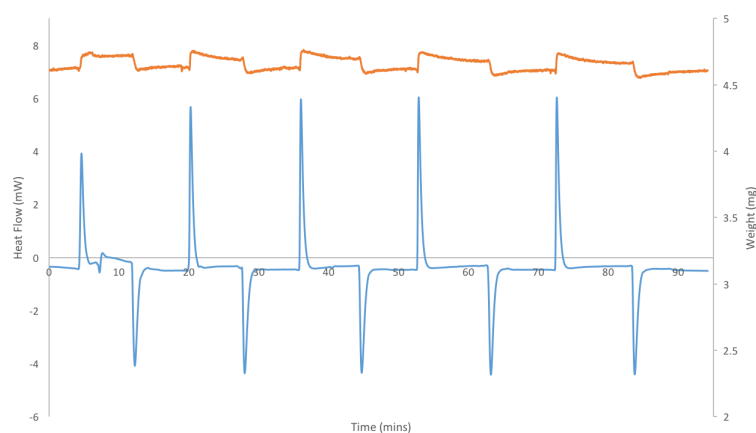
Figure A.8 – DSC Traces for P300, P450 and P600 on Addition of CO₂ and N₂



(a) Heat Flow and Weight Change on Addition of Moisture Loaded CO_2 and N_2 to P300

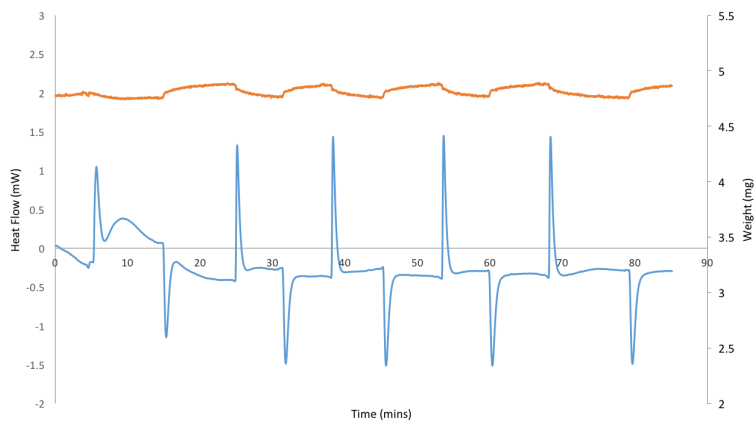


(b) Heat Flow and Weight Change on Addition of Moisture Loaded CO_2 and N_2 to P450

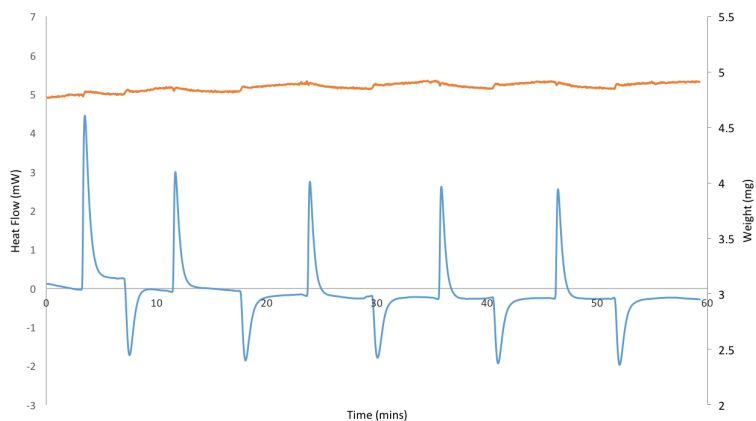


(c) Heat Flow and Weight Change on Addition of Moisture Loaded CO_2 and N_2 to P600

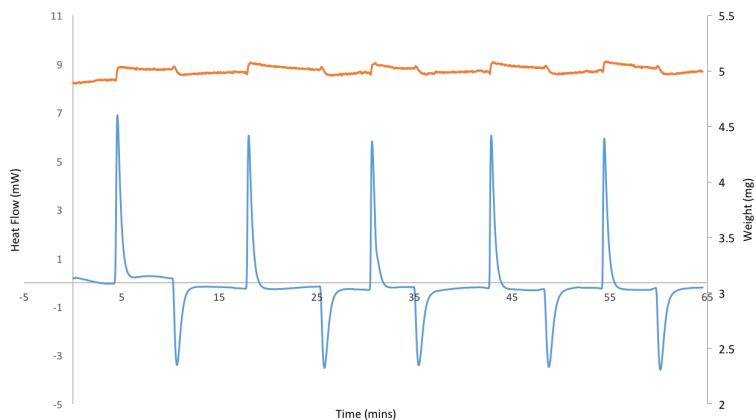
Figure A.9 – DSC Traces for A800, S800 and AC on Addition of Moisture Loaded CO_2 and N_2



(a) Heat Flow and Weight Change on Addition of Moisture Loaded CO₂ and N₂ to P300



(b) Heat Flow and Weight Change on Addition of Moisture Loaded CO₂ and N₂ to P450



(c) Heat Flow and Weight Change on Addition of Moisture Loaded CO₂ and N₂ to P600

Figure A.10 – DSC Traces for P300, P450 and P600 on Addition of Moisture Loaded CO₂ and N₂

Abbreviations

AC	Activated Carbon
ACC	Activated Carbon Cloths
ACF	Activated Carbon Fibers
AD	Anaerobic Digestion
ATR-IR	Attenuated Total Reflection - Infra Red
BJH	Barret-Joyner-Halenda
BMI	Body Mass Index
BV	Biological Value
CAGR	Compound Annual Growth Rate
CE	Circular Economy
CHN	Carbon Hydrogen Nitrogen
CCK	Cholecystokinin
CCS	Carbon Capture and Storage
CPMAS	Cross-Polarisation Magic Angle Spinning
CS	Chemical Score
DE	Degree of Esterification
DTE	Dithioerythritol
EAAI	Essential Amino Acid Index
EOL	End Of Life

ESI-MS	Electron Spray Ionisation - Mass Spectrometry
EI-MS	Electron-Ionisation - Mass Spectrometry
EU	European Union
FD	Freeze Dried
FDA	Food and Drugs Administration
FSC	Food Supply Chain
FW	Food Waste
GAC	Granular Activated Carbon
GC	Gas Chromatography
GHG	Green House Gas
GHI	Global Hunger Index
HLB	Huanglongbing
HPLC	High Performance Liquid Chromatography
HM	High Methoxyl
HMW	High Molecular Weight
ICP-AES	Inductively Coupled Plasma Atomic Emission Spectroscopy
IFPRI	International Food Policy Research Institute
IR	Infra Red
IUPAC	International Union of Pure and Applied Chemistry
LCA	Life Cycle Assessment
LM	Low Methoxyl
LMA	Low Methoxyl Amidated

LMW	Low Molecular Weight
MALDI	Matrix Assisted Laser Desorption/Ionisation
MAS	Magic Angle Spinning
MEA	MonoEthanolAmine
MOFs	Metal-Organic Frameworks
MDG	Millennium Development Goal
MS	Mass Spectrometry
MW	Microwave
NCBI	National Center for Biotechnology Information non-redundant protein
NMR	Nuclear Magnetic Resonance
NPU	Net Protein Utilisation
OPEC	Orange Peel Exploitation Company
PAC	Powdered Activated Carbon
PER	Protein Efficiency Ratio
PFJ	Potato Fruit Juice
PI2	Protease Inhibitor II
PI1	Protease Inhibitor I
REACH	Regulation, Evaluation and Authorisation of Chemicals
RCF	Relative Centrifugal Force
RPM	Revolutions Per Minute
SPE	Solid Phase Extraction
SDG	Sustainable Development Goal

SDS-PAGE Sodium Dodecyl Sulphate Polyacrylamide Gel Electrophoresis

STA Simultaneous Thermal Analysis

SVHC Substance of Very High Concern

TBA Tertiary Butyl Alcohol

TGA ThermoGravimetric Analysis

TOF Time Of Flight

UK United Kingdom

UN United Nations

USA United States of America

WOP Waste Orange Peel

Bibliography

1. Attard, T. M.; Hunt, A. J.; Matharu, A. S.; Houghton, J. A.; Polikarpov, I. In *Introduction to Chemicals from Biomass*; John Wiley & Sons, Ltd: 2015, pp 31–52.
2. Dugmore, T. I.; Clark, J. H.; Bustamante, J.; Houghton, J. A.; Matharu, A. S. *Top. Curr. Chem.* **2017**, *375*, 46.
3. Gonzalo, J. A.; Alfonseca, M. *World Population: Past, Present, & Future* **2016**, 29.
4. Gandini, A.; Lacerda, T. M. *Prog. Polym. Sci.* **2015**, *48*, 1–39.
5. Johansson, T. B.; Patwardhan, A. P.; Nakićenović, N.; Gomez-Echeverri, L., *Global energy assessment: toward a sustainable future*; Cambridge University Press: 2012.
6. Ding, X.; Zhong, W.; Shearmur, R. G.; Zhang, X.; Huisingh, D. *J. Clean. Prod.* **2015**, *109*, 62–75.
7. Millner, A.; Dietz, S. *Environ. Dev. Econ.* **2015**, *20*, 380–406.
8. Vos, R. O. *J. Chem. Technol. Boit.* **2007**, *82*, 334–339.
9. Toman, M. A. *The RFF reader in environmental and resource policy* **2006**, *2*.
10. Lee, B. X.; Kjaerulf, F.; Turner, S.; Cohen, L.; Donnelly, P. D.; Muggah, R.; Davis, R.; Realini, A.; Kieselbach, B.; MacGregor; Snyder, L.; Waller, I.; Gordon, R.; Moloney-Kitts, M.; Lee, G.; Gilligan, J. *J. Public Health Pol.* **2016**, *37*, 13–31.
11. Lin, C. S. K.; Pfaltzgraff, L. A.; Herrero-Davila, L.; Mubofu, E. B.; Abderrahim, S.; Clark, J. H.; Koutinas, A. A.; Kopsahelis, N.; Stamatelatou, K.; Dickson, F.; Thankappan, S.; Mohamed, Z.; Brocklesby, R.; Luque, R. *Energ. Environ. Sci.* **2013**, *6*, 426–464.
12. Parfitt, J.; Barthel, M.; Macnaughton, S. *Philos. Trans. R. Soc. London B Biol. Sci.* **2010**, *365*, 3065–3081.

BIBLIOGRAPHY

13. Dahiya, S.; Kumar, A. N.; Chatterjee, J. S. S. S.; Sarkar, O.; Mohan, S. V. *Bioresource Technol.* **2017**.
14. Gustavsson, J.; Cederberg, C.; Sonesson, U.; Otterdijk, R. V.; Meybeck, A. *Global food losses and food waste*; tech. rep.; Food and Agriculture Organization of the United Nations Rome, Italy, 2011.
15. WRAP *WRAP Gate Fees Report 2013*; tech. rep.; WRAP, 2013.
16. WRAP *WRAP Gate Fees Report 2009*; tech. rep.; WRAP, 2009.
17. Giroto, F.; Alibardi, L.; Cossu, R. *Waste manage.* **2015**, *45*, 32–41.
18. WRAP *Estimates of food and packaging waste in the UK grocery retail and hospitality chain*; tech. rep.; WRAP, 2013.
19. Monier, V. *Preparatory study on food waste across EU 27*; tech. rep.; European Commission, 2011.
20. FAO, I. *Food and Agriculture Organization Publications, Rome* **2016**.
21. Von Grebmer, K.; Bernstein, J.; Nabarro, D.; Prasai, N.; Amin, S.; Yohannes, Y.; Sonntag, A.; Patterson, F.; Towey, O.; Thompson, J., *2016 Global hunger index: Getting to zero hunger*; Intl Food Policy Res Inst: 2016.
22. Ray, D. K.; Mueller, N. D.; West, P. C.; Foley, J. A. *PloS one* **2013**, *8*, e66428.
23. Tai, A. P.; Martin, M. V.; Heald, C. L. *Nat. Clim. Change* **2014**, *4*, 817.
24. Aiking, H. *Am. J. Clin. Nutr.* **2014**, *100*, 483S–489S.
25. Sutton, C.; Dibb, S. *World Wildlife Fund, Food Ethics Council: Godalming, UK* **2013**.
26. Scarborough, P.; Appleby, P. N.; Mizdrak, A.; Briggs, A. D.; Travis, R. C.; Bradbury, K. E.; Key, T. J. *Climatic change* **2014**, *125*, 179–192.
27. Porter, S. D.; Reay, D. S.; Higgins, P.; Bomberg, E. *Sci. Total Environ.* **2016**, *571*, 721–729.
28. Schott, A. B. S.; Wenzel, H.; la Cour Jansen, J. *J. Clean. Prod.* **2016**, *119*, 13–24.
29. *Food wastage footprint & Climate Change*; tech. rep.; Food and Agriculture Organization of the United Nations, 2015.
30. Tilman, D.; Clark, M. *Nature* **2014**, *515*, 518–522.
31. Collins, T. J., *Letters to a young chemist*; Ghosh, A., Ed., 2011, p77–85.

32. S. L. Tang, R. L. Smith, M. P. Green. *Chem. 2005*, *7*, 761–762.
33. Anastas, P. T.; Kirchhoff, M. M. *Accounts. Chem. Res.* **2002**, *35*, 686–694.
34. Lenardão, E. J.; Freitag, R. A.; Dabdoub, M. J.; Batista, A. C. F.; Silveira, C. d. C. *Quim. Nova* **2003**, *26*, 123–129.
35. Poliakoff, M.; Fitzpatrick, J. M.; Farren, T. R.; Anastas, P. T. *Sci.* **2002**, *297*, 807–810.
36. Eghbali, P. A.; N. *Chem. Soc. Rev.* **2011**, *39*, 301–312.
37. . T. Anastas, L. B. Bartlett, M. M. Kirchhoff, T. C. W. *Catal. Today* **2000**, *55*, 11–22.
38. Baumeister, C.; Kilian, L. *The J. Econ. Perspect.* **2016**, *30*, 139–160.
39. Energy & Financial Markets - Crudeoil - U.S. Energy Information Administration (EIA)., https://www.eia.gov/finance/markets/crudeoil/spot{_}prices.php (accessed 08/14/2017).
40. R. Dobbs, J. Oppenheim, J. Manyika, S. S. Nyquist, C. R. *Resource revolution: meeting the world's energy, materials, food and water needs*; tech. rep.; McKinsey Global Institute, 2011.
41. Mohan, S. V.; Nikhil, G.; Chiranjeevi, P; Reddy, C. N.; Rohit, M.; Kumar, A. N.; Sarkar, O. *Bioresource Technol.* **2016**, *215*, 2–12.
42. Mohan, S. V.; Modestra, J. A.; Amulya, K; Butti, S. K.; Velvizhi, G *Trends Biotechnol.* **2016**, *34*, 506–519.
43. Ghisellini, P.; Cialani, C.; Ulgiati, S. *J. Clean. Prod.* **2016**, *114*, 11–32.
44. Lieder, M.; Rashid, A. *J. Clean. Prod.* **2016**, *115*, 36–51.
45. Cherubini, F. *Energ. Convers. Manage.* **2010**, *51*, 1412–1421.
46. Morais, A. R.; da Costa Lopes, A. M.; Bogel-Lukasik, R. *Chem. Rev.* **2014**, *115*, 3–27.
47. Bauer, F.; Coenen, L.; Hansen, T.; McCormick, K.; Palgan, Y. V. *Biofuel. Bioprod. Bior.* **2017**.
48. Elliott, K. *Biofuel Policies: Fuel versus Food, Forests, and Climate*; tech. rep.; Center for Global Development, 2015.
49. Maity, S. K. *Renew. Sust. Energ. Rev.* **2015**, *43*, 1427–1445.

BIBLIOGRAPHY

50. Nakajima, S.; Hira, T.; Tsubata, M.; Takagaki, K.; Hara, H. *J. Agric. Food Chem.* **2011**, *59*, 9491–9496.
51. Bustamante, J.; van Stempvoort, S.; García-Gallarreta, M.; Houghton, J. A.; Briers, H. K.; Budarin, V. L.; Matharu, A. S.; Clark, J. H. *J. Clean. Prod.* **2016**, *137*, 598–605.
52. Kratchanova, M; Panchev, I; Pavlova, E; Shtereva, L *Carbohydr. polym.* **1994**, *25*, 141–144.
53. Synytsya, A.; Copikova, J.; Brus, J. *Czech J. Food Sci.* **2003**, *21*, 1–12.
54. National Research Council (US) & the Committee on Specifications of the Food Chemicals Codex, ., *Food chemicals codex*; National Academies: 1972; Vol. 2.
55. Kawabata, S.-I.; Miura, T.; Morita, T.; Kato, H.; Fujikawa, K.; Iwanaga, S.; Takada, K.; Kimura, T.; Sakakibara, S. *The FEBS J.* **1988**, *172*, 17–25.
56. Borisova, A.; De Bruyn, M.; Budarin, V. L.; Shuttleworth, P. S.; Dodson, J. R.; Segatto, M. L.; Clark, J. H. *Macromol. Rapid Commun.* **2015**, *36*, 774–779.
57. Mikhail, R. S.; Brunauer, S.; Bodor, E. *J. Colloid Interf. Sci.* **1968**, *26*, 45–53.
58. Barrett, E. P.; Joyner, L. G.; Halenda, P. P. *J. Am. Chem. Soc.* **1951**, *73*, 373–380.
59. Reucroft, P.; Simpson, W.; Jonas, L. *J. Phys. Chem.* **1971**, *75*, 3526–3531.
60. Xu, Q.; Chen, L.-L.; Ruan, X.; Chen, D.; Zhu, A.; Chen, C.; Bertrand, D.; Jiao, W.-B.; Hao, B.-H.; Lyon, M. P.; Chen, J.; Gao, S.; Xing, F.; Lan, H.; Chang, J.-W.; Ge, X.; Lei, Y.; Hu, Q.; Miao, Y.; Wang, L.; Xiao, S.; Biswas, M. K.; Zeng, W.; Guo, F.; Cao, H.; Yang, X.; Xu, X.-W.; Cheng, Y.-J.; Xu, J.; Liu, J.-H.; Luo, O. J.; Tang, Z.; Guo, W.-W.; Kuang, H.; Zhang, H.-Y.; Roose, M. L.; Nagarajan, N.; Deng, X.-X.; Ruan, Y. *Nat. Genet.* **2013**, *45*, 59–66.
61. Mamma, D.; Christakopoulos, P. *Waste Biomass Valori.* **2014**, *5*, 529–549.
62. Escobedo-Avellaneda, Z.; Gutiérrez-Urbe, J.; Valdez-Fragoso, A.; Torres, J. A.; Welti-Chanes, J. *J. Funct. Foods* **2014**, *6*, 470–481.
63. FAO STAT., <http://faostat3.fao.org/> (accessed 04/15/2017).
64. United States Department of Agriculture *Citrus: World Markets and Trade*; tech. rep.; World Agricultural Outlook Board USDA, 2016.

65. Wikandari, R.; Nguyen, H.; Millati, R.; Niklasson, C.; Taherzadeh, M. J.; Wikandari, R.; Nguyen, H.; Millati, R.; Niklasson, C.; Taherzadeh, M. J. *Biomed Res. Int.* **2015**, *2015*, 1–6.
66. Negro, V.; Mancini, G.; Ruggeri, B.; Fino, D. *Bioresource Technol.* **2016**, *214*, 806–815.
67. Ferreira-Leitao, V.; Gottschalk, L. M. F.; Ferrara, M. A.; Nepomuceno, A. L.; Molinari, H. B. C.; Bon, E. P. *Waste Biomass Valori.* **2010**, *1*, 65–76.
68. Negro, V.; Mancini, G.; Ruggeri, B.; Fino, D. *Bioresource Technol.* **2016**, *214*, 806–815.
69. Aboagye, D; Banadda, N; Kiggundu, N; Kabenge, I *Renew. Sustainable Energy Rev.* **2017**, *70*, 814–821.
70. Ruiz, B.; Flotats, X. *Biochem. Eng. J.* **2016**, *109*, 9–18.
71. Su, H.; Tan, F.; Xu, Y. *Fuel* **2016**, *181*, 843–851.
72. Anjum, M.; Khalid, A.; Qadeer, S.; Miandad, R. *Waste Manage. Res.* **2017**, 0734242X17715904.
73. Negro, V.; Ruggeri, B.; Mancini, G.; Fino, D. *J. Chem. Technol. Boit.* **2017**, *92*, 1186–1191.
74. Boluda-Aguilar, M.; López-Gómez, A. *Ind. Crops Prod.* **2013**, *41*, 188–197.
75. Viuda-Martos, M.; Ruiz-Navajas, Y.; Fernández-López, J.; Pérez-Álvarez, J. *Food Control* **2008**, *19*, 1130–1138.
76. Paggiola, G.; Stempvoort, S. V.; Bustamante, J.; Barbero, J. M. V.; Hunt, A. J.; Clark, J. H. *Biofuels, Bioprod. and Bior.* **2016**, *10*, 686–698.
77. Lohrasbi, M.; Pourbafrani, M.; Niklasson, C.; Taherzadeh, M. J. *Bioresource Technol.* **2010**, *101*, 7382–7388.
78. Reddy, S. G. E.; Kirti Dolma, S.; Koundal, R.; Singh, B. *Nat. Prod. Res.* **2016**, *30*, 1834–1838.
79. ChemSec, SIN list 2.1., <http://www.chemsec.org> (accessed 03/21/2017).
80. *Proposal for a Directive of the European Parliament and of the Council amending Council Directive 67/548/EEC adapting it to the" REACH Regulation*; tech. rep.; European Commission, 2003.

BIBLIOGRAPHY

81. Abdollahnejad, F.; Kobarfard, F.; Kamalinejad, M.; Mehrgan, H.; Babaeian, M. *J. Essent. Oil Bear. Plants* **2016**, *19*, 574–581.
82. McHugh, M.; Krukonis, V., *Supercritical fluid extraction: principles and practice*; Elsevier: 2013.
83. Sicari, V.; Poiana, M. *J. Food Process Eng.* **2016**, n/a–n/a.
84. Xhaxhiu, K.; Wenclawiak, B. *J. Essent. Oil Bear. Plants* **2015**, *18*, 289–299.
85. Mouahid, A.; Crampon, C.; Toudji, S.-A. A.; Badens, E. *J. Supercrit. Fluids* **2016**, *116*, 271–280.
86. Sahraoui, N.; Boutekedjiret, C. In *Prog. Clean Energy, Vol. 1*; Springer International Publishing: Cham, 2015, pp 831–841.
87. Franco-Vega, A.; Ramírez-Corona, N.; Palou, E.; López-Malo, A. *J. Food Eng.* **2016**, *170*, 136–143.
88. Golmakani, M.-T.; Moayyedi, M. *Food Sci. Nutr.* **2015**, *3*, 506–518.
89. Cheok, C. Y.; Mohd Adzahan, N.; Abdul Rahman, R.; Zainal Abedin, N. H.; Hussain, N.; Sulaiman, R.; Chong, G. H. *Crit. Rev Food Sci.* **2017**, 1–27.
90. Mirabella, N.; Castellani, V.; Sala, S. *J. Clean. Prod.* **2014**, *65*, 28–41.
91. Matharu, A. S.; Houghton, J. A.; Lucas-Torres, C.; Moreno, A. *Green Chem.* **2016**, *18*, 5280–5287.
92. Thakur, B. R.; Singh, R. K.; Handa, A. K.; Rao, M. A. *Crit. Rev. Food Sci. Nutr.* **1997**, *37*, 47–73.
93. Voragen, A. G. J. In *5th Eur. Train. Course Carbohydrates*, 1998, p 47.
94. Harholt, J.; Suttangkakul, A.; Scheller, H. V. *Plant Physiol.* **2010**, *153*, 384–395.
95. *Global Pectin Market by Manufacturers, Regions, Type and Application, Forecast to 2021*; tech. rep.; GlobalInfoResearch, 2017.
96. May, C. D. *Carbohydr. polym.* **1990**, *12*, 79–99.
97. Koubala, B. B.; Kansci, G.; Garnier, C.; Mbome, I. L.; Durand, S.; Thibault, J.-F.; Ralet, M.-C. *Int. J. Food Sci. Technol.* **2009**, *44*, 1809–1817.
98. Bagherian, H.; Zokaee Ashtiani, F.; Fouladitajar, A.; Mohtashamy, M. *Chem. Eng. Process. Process Intensif.* **2011**, *50*, 1237–1243.
99. Yeoh, S.; Shi, J.; Langrish, T. *Desalination* **2008**, *218*, 229–237.

100. Guo, X.; Han, D.; Xi, H.; Rao, L.; Liao, X.; Hu, X.; Wu, J. *Carbohydr. Polym.* **2012**, *88*, 441–448.
101. Koubala, B.; Kansci, G.; Mbome, L.; Crépeau, M.-J.; Thibault, J.-F.; Ralet, M.-C. *Food Hydrocoll.* **2008**, *22*, 1345–1351.
102. Kliemann, E.; Simas, D.; Nunes, K.; Amante, E. R.; Prudêncio, E. S.; Teófilo, R. F.; Ferreira, M.; Amboni, R. D. M. C. *Int. J. food Sci. Technol.* **2009**, *44*, 476–483.
103. Merrill, R. C.; Weeks, M. *J. Am. Chem. Soc.* **1945**, *67*, 2244–2247.
104. Fraeye, I.; De Roeck, A.; Duvetter, T.; Verlent, I.; Hendrickx, M.; Van Loey, A. *Food Chem.* **2007**, *105*, 555–563.
105. Tapre, A.; Jain, R. *Int. Food Res. J.* **2014**, *21*.
106. Wikiera, A.; Mika, M.; Grabacka, M. *Food Hydrocoll.* **2015**, *44*, 156–161.
107. Jeong, H.-S.; Kim, H.-Y.; Ahn, S. H.; Oh, S. C.; Yang, I.; Choi, I.-G. *Food Chem.* **2014**, *157*, 332–338.
108. Puri, M.; Sharma, D.; Barrow, C. J. *Trends Biotechnol.* **2012**, *30*, 37–44.
109. Vasco-Correa, J.; Zapata, A. D. Z. *Food Sci. Tech-LWT* **2017**, *80*, 280–285.
110. Adetunji, L. R.; Adekunle, A.; Orsat, V.; Raghavan, V. *Food Hydrocoll.* **2017**, *62*, 239–250.
111. Azmir, J.; Zaidul, I.; Rahman, M.; Sharif, K.; Mohamed, A.; Sahena, F.; Jahurul, M.; Ghafoor, K.; Norulaini, N.; Omar, A. *J. Food Eng.* **2013**, *117*, 426–436.
112. Chemat, F.; Rombaut, N.; Sicaire, A.-G.; Meullemiestre, A.; Fabiano-Tixier, A.-S.; Abert-Vian, M. *Ultrason. Sonochem.* **2017**, *34*, 540–560.
113. Luque-Garca, J.; Luque de Castro, M. *Trends Anal. Chem.* **2003**, *22*, 41–47.
114. Ozel, M.; Gogus, F.; Lewis, A. C. *Food Chem.* **2003**, *82*, 381–386.
115. Xia, H.; Houghton, J. A.; Clark, J. H.; Matharu, A. S. *ACS Sus. Chem. Eng.* **2016**, *4*, 6002–6009.
116. Asl, A. H.; Khajenoori, M, DOI: 10.5772/54993.
117. Özel, M. Z.; Göü, F.; Hamilton, J. F.; Lewis, A. C. *Anal. Bioanal. Chem.* **2005**, *382*, 115–119.
118. Smith, R. M. *Anal. Bioanal. Chem.* **2006**, *385*, 419–421.

BIBLIOGRAPHY

119. Zakaria, S. M.; Kamal, S. M. M. *Food Eng. Rev.* **2016**, *8*, 23–34.
120. Maran, J. P.; Sivakumar, V; Thirugnanasambandham, K; Sridhar, R *Carbohydr. Polym.* **2013**, *97*, 703–709.
121. Venkatesh, M.; Raghavan, G. *Biosyst. Eng.* **2004**, *88*, 1–18.
122. Kratchanova, M; Pavlova, E; Panchev, I *Carbohydr. Polym.* **2004**, *56*, 181–185.
123. Fishman, M. L.; Chau, H. K.; Hoagland, P. D.; Hotchkiss, A. T. *Food Hydrocoll.* **2006**, *20*, 1170–1177.
124. Maran, J. P.; Swathi, K.; Jeevitha, P.; Jayalakshmi, J.; Ashvini, G. *Carbohydr. Polym.* **2015**, *123*, 67–71.
125. Wang, S.; Chen, F.; Wu, J.; Wang, Z.; Liao, X.; Hu, X. *J. Food Eng.* **2007**, *78*, 693–700.
126. Clark, J. H.; Pfaltzgraff, L. A.; Budarin, V. L.; De Bruyn, M. Microwave assisted citrus waste biorefinery., US Patent 9,382,339, 2016.
127. Cravotto, G.; Cintas, P. *Chem. Eur. J.* **2007**, *13*, 1902–1909.
128. Martina, K.; Tagliapietra, S.; Barge, A.; Cravotto, G. *Top. Curr. Chem.* **2016**, *374*, 79.
129. Liew, S. Q.; Ngoh, G. C.; Yusoff, R.; Teoh, W. H. *Int. J. Biol. Macromol.* **2016**, *93*, 426–435.
130. Citrus Diseases - Huanglongbing (HLB)., [http://idtools.org/id/citrus/diseases/factsheet.php?name=Huanglongbing+\(HLB\)](http://idtools.org/id/citrus/diseases/factsheet.php?name=Huanglongbing+(HLB)) (accessed 01/11/2017).
131. De Miranda, S. H. G.; de Oliveira Adami, A. C.; Bassanezi, R. B. In *Poster presented at the International Association of Agricultural Economists (IAAE) Triennial Conference*, 2012.
132. Gottwald, T. R.; Graham, J. H. *CAB Reviews* **2014**, *9*, 1–11.
133. Burlingame, B.; Mouillé, B.; Charrondière, R. *J. Food Compos. Anal.* **2009**, *22*, 494–502.
134. Litaladio, N.; Castaldi, L. *J. Food Compos. Anal.* **2009**, *22*, 491–493.
135. FAO STAT., <http://faostat3.fao.org/> (accessed 07/04/2017).
136. *Waste, Reducing Supply Chain and Consumer Potato*; tech. rep.; WRAP, 2012.

137. Matharu, A. S.; de Melo, E. M.; Houghton, J. A. *Bioresource Technol.* **2016**, *215*, 123–130.
138. Fritsch, C.; Staebler, A.; Happel, A.; Cubero Márquez, M. A.; Aguiló-Aguayo, I.; Abadias, M.; Gallur, M.; Cigognini, I. M.; Montanari, A.; López, M. J.; Suárez-Estrella, F.; Brunton, N.; Luengo, E.; Sisti, L.; Ferri, M.; Belotti, G. *Sustainability* **2017**, *9*, 1492.
139. Lutosa dehydrated potato flakes., <http://www.lutosa.com/uk/products/food-service/flakes/>. (accessed 05/07/2017).
140. Products, Dehydrated Potato., <http://www.potatopro.com/product-types/dehydrated-potato-products>. (accessed 05/06/2017).
141. Keijbets, M. *Potato Research* **2008**, *51*, 271–281.
142. *McCance and Widdowson's The Composition of Foods*; Royal Society of Chemistry: 2014.
143. Waglay, A.; Karboune, S.; Alli, I. *Food Chem.* **2014**, *142*, 373–382.
144. Narasimhamoorthy, B; hao, L. Q.; Liu, X; Essah, S. Y. C.; Holm, D. G.; Greaves, J. A. *Am. J. potato Res.* **2013**, *90*, 561–569.
145. Visvanathan, R.; Jayathilake, C.; Chaminda Jayawardana, B.; Liyanage, R. *J. Sci. Food Agr.* **2016**, *96*, 4850–4860.
146. Ng, M.; Fleming, T.; Robinson, M.; Thomson, B.; Graetz, N.; Margono, C.; Mullany, E. C.; Biryukov, S.; Abbafati, C.; Abera, S. F. *Lancet* **2014**, *384*, 766–781.
147. Ku, S. K.; Sung, S. H.; Choung, J. J.; Choi, J.-S.; Shin, Y. K.; Kim, J. W. *Exp. Ther. Med.* **2016**, *12*, 354–364.
148. World Health Organisation Obesity and Overweight Risk Factor Database., http://www.who.int/gho/ncd/risk_factors/overweight/en/ (accessed 07/21/2017).
149. Klijs, B.; Mackenbach, J. P.; Kunst, A. E. *BMC Public Health* **2011**, *11*, 378.
150. Komarnytsky, S.; Cook, A.; Raskin, I. *Int. J. Obes.* **2011**, *35*, 236–243.
151. Kim, D. D.; Basu, A. *Value Heal.* **2016**, *19*, 602–613.
152. Muennig, P.; Lubetkin, E.; Jia, H.; Franks, P. *Am. J. Public Health* **2006**, *96*, 1662–8.

BIBLIOGRAPHY

153. Bergthaller, W.; Witt, W.; Goldau, H. *Starch–Stärke* **1999**, *51*, 235–242.
154. Wu, D. *Procedia Environ. Sci.* **2016**, *31*, 108–112.
155. Eliasson, A.-C., *Starch in food: Structure, function and applications*; CRC Press: 2004.
156. L. Thomsen *International Starch*; tech. rep.; Danish Starch Industry.
157. The uses of Starch., <http://www.starch.eu/the-uses-of-starch> (accessed 04/04/2017).
158. Kraak, A *Ind. Crop. Prod.* **1992**, *1*, 107–112.
159. Dabestani, S.; Arcot, J.; Chen, V. *J. Food Eng.* **2017**, *195*, 85–96.
160. Zwijnenberg, H. J.; Kemperman, A. J.; Boerrigter, M. E.; Lotz, M.; Dijksterhuis, J. F.; Poulsen, P. E.; Koops, G.-H. *Desalination* **2002**, *144*, 331–334.
161. *2017 Market Research Report on Global Potato Protein*; tech. rep.; QYR Food and Beverages Research Center, 2017.
162. Albanese, A., *Protein and amino acid nutrition*; Elsevier: 2012.
163. Bártová, V.; Bárta, J.; Brabcová, A.; Zdráhal, Z.; Horáčková, V. *J. Food Compos. Anal.* **2015**, *40*, 78–85.
164. Bártová, V. Q.; Bárta, J.; Brabcová, A.; Zdráhal, Z.; Horáčková, V. *J. Food Compos. Anal.* **2014**, DOI: 10.1016/j.jfca.2014.12.006.
165. Friedman, M.; McDonald, G. M.; Filadelfi-Keszi, M. *CRC. Crit. Rev. Plant Sci.* **1997**, *16*, 55–132.
166. Potato, tuber, raw — Feedipedia - Animal Feed Resources Information System., <http://www.feedipedia.org/node/12472> (accessed 04/08/2017).
167. Claussen, I.; Ustad, T.; Strømmen, I.; Walde, P. *Dry. Technol.* **2007**, *25*, 947–957.
168. Liapis, A. I.; Bruttini, R. *Handbook of industrial drying* **2014**, 259.
169. Noble, R. D.; Stern, S. A., *Membrane separations technology: principles and applications*; Elsevier: 1995; Vol. 2.
170. Elford, W. J. *Proceedings of the Royal Society of London. Series B, Containing Papers of a Biological Character* **1933**, *112*, 384–406.
171. Scopes, R. K., *Protein purification: principles and practice*; Springer Science & Business Media: 2013.

172. Ghosh, R. *J. Chromatogr. A* **2002**, *952*, 13–27.
173. Janson, J.-C., *Protein purification: principles, high resolution methods, and applications*; John Wiley & Sons: 2012; Vol. 151.
174. Yamamoto, S.; Nakanishi, K.; Matsuno, R., *Ion-exchange chromatography of proteins*; CRC Press: 1988.
175. Zhu, Y.; Lasrado, J. A.; Hu, J. *Food Funct.* **2017**.
176. Zhu-Salzman, K.; Zeng, R. *Annu. Rev. Entomol.* **2015**, *60*, 233–252.
177. Jamal, F.; Pandey, P. K.; Singh, D.; Khan, M. *Phytochem. Reviews* **2013**, *12*, 1–34.
178. Ryan, C. A. *Annu. Rev. Phytopathol.* **1990**, *28*, 425–449.
179. Koiwa, H.; Bressan, R. A.; Hasegawa, P. M. *Trends Plant Sci.* **1997**, *2*, 379–384.
180. Sharma, K. *Int J Curr Res Aca Rev* **2015**, *3*, 55–70.
181. Bludell, J.; Lawton, C.; Cotton, J.; Macdiarmid, J. I. *Annu. Rev. Nutr.* **1996**, *16*, 285–319.
182. Peikin, S.; Springer, C.; Dockray, G.; Calam, J In *Gastroenterology*, 1987; Vol. 92, pp 1570–1570.
183. Schwartz, J. G.; Guan, D.; Green, G. M.; Phillips, W. T. *Diabetes Care* **1994**, *17*, 255–262.
184. Peters, H.; Foltz, M; Kovacs, E.; Mela, D.; Schuring, E.; Wiseman, S. *Int. J. Obesity* **2011**, *35*, 244.
185. DelMar, E.; Largman, C; Brodrick, J.; Geokas, M. *Anal. Biochem.* **1979**, *99*, 316–320.
186. D’Alessandro, D.; Smit, B.; Long, J. *Angew. Chemie Int. Ed.* **2010**, *49*, 6058–6082.
187. Raupach, M. R.; Marland, G.; Ciais, P.; Le Quéré, C.; Canadell, J. G.; Klepper, G.; Field, C. B. *Proceedings of the National Academy of Sciences* **2007**, *104*, 10288–10293.
188. Boot-Handford, M. E.; Abanades, J. C.; Anthony, E. J.; Blunt, M. J.; Brandani, S.; Mac Dowell, N.; Fernández, J. R.; Ferrari, M.-C.; Gross, R.; Hallett, J. P.; Haszeldine, R. S.; Heptonstall, P.; Lyngfelt, A.; Makuch, Z.; Mangano, E.; Porter, R. T. J.; Pourkashanian, M.; Rochelle, G. T.; Shah, N.; Yao, J. G.; Fennell, P. S. *Energ. Environ. Sci.* **2014**, *7*, 130–189.

BIBLIOGRAPHY

189. Sumida, K.; Rogow, D. L.; Mason, J. A.; McDonald, T. M.; Bloch, E. D.; Herm, Z. R.; Bae, T.-H.; Long, J. R. *Chem. Rev* **2012**, *112*, 724–781.
190. Field, C. B.; Raupach, M. R., *The global carbon cycle: integrating humans, climate, and the natural world*; Island Press: 2004; Vol. 62.
191. Rochelle, G. T. *Science (80-.)*. **2009**, *325*.
192. Figueroa, J. D.; Fout, T.; Plasynski, S.; McIlvried, H.; Srivastava, R. D. *Int. J. Greenh. Gas Control* **2008**, *2*, 9–20.
193. Yong, Z.; Mata, V.; Rodrigues, A. E. *Sep. Purif. Technol.* **2002**, *26*, 195–205.
194. Li, K.; Leigh, W.; Feron, P.; Yu, H.; Tade, M. *Appl. Energ.* **2016**, *165*, 648–659.
195. Luis, P. *Desalination* **2016**, *380*, 93–99.
196. Abu-Zahra, M. R.; Niederer, J. P.; Feron, P. H.; Versteeg, G. F. *Int. J. Greenh. Gas Con.* **2007**, *1*, 135–142.
197. Soltani, S. M.; Fennell, P. S.; Mac Dowell, N. *Int. J. Greenh. Gas Con.* **2017**, *63*, 321–328.
198. Yu, C.-H.; Huang, C.-H.; Tan, C.-S. *Aerosol Air Qual. Res* **2012**, *12*, 745–769.
199. Yang, S.; Qian, Y.; Yang, S. *Ind. Eng. Chem. Res.* **2016**, *55*, 6186–6193.
200. Aaron, D.; Tsouris, C. *Sep. Sci. Technol.* **2005**, *40*, 321–348.
201. Ben-Mansour, R; Habib, M.; Bamidele, O.; Basha, M; Qasem, N.; Peedikakkal, A; Laoui, T; Ali, M. *Appl. Energ.* **2016**, *161*, 225–255.
202. Zhou, H.-C.; Long, J. R.; Yaghi, O. M., *Introduction to metal–organic frameworks*; ACS Publications: 2012.
203. Xiang, S.; He, Y.; Zhang, Z.; Wu, H.; Zhou, W.; Krishna, R.; Chen, B. *Nat. Commun.* **2012**, *3*, 954.
204. Li, J.-R.; Ma, Y.; McCarthy, M. C.; Sculley, J.; Yu, J.; Jeong, H.-K.; Balbuena, P. B.; Zhou, H.-C. *Coordin. Chem. Rev.* **2011**, *255*, 1791–1823.
205. Yaumi, A.; Bakar, M. A.; Hameed, B. *Energy* **2017**, *124*, 461–480.
206. Sanders, D. F.; Smith, Z. P.; Guo, R.; Robeson, L. M.; McGrath, J. E.; Paul, D. R.; Freeman, B. D. *Polymer* **2013**, *54*, 4729–4761.
207. Kenarsari, S. D.; Yang, D.; Jiang, G.; Zhang, S.; Wang, J.; Russell, A. G.; Wei, Q.; Fan, M. *RSC Adv.* **2013**, *3*, 22739–22773.

208. Bernardo, P; Drioli, E; Golemme, G *Ind. Eng. Chem. Res.* **2009**, *48*, 4638–4663.
209. Lopes, F. V.; Grande, C. A.; Ribeiro, A. M.; Loureiro, J. M.; Evaggelos, O.; Nikolakis, V.; Rodrigues, A. E. *Sep. Sci. and Technol.* **2009**, *44*, 1045–1073.
210. Hu, B.; Wang, K.; Wu, L.; Yu, S.-H.; Antonietti, M.; Titirici, M.-M. *Adv. Mater.* **2010**, *22*, 813–828.
211. Sun, M.-H.; Huang, S.-Z.; Chen, L.-H.; Li, Y.; Yang, X.-Y.; Yuan, Z.-Y.; Su, B.-L. *Chem. Soc. Rev.* **2016**, *45*, 3479–3563.
212. Berberoglu, S.; Gupta, V.; Carrott, P.; Singh, R.; Chaudhary, M.; Kushwaha, S. *Bioresource Technol.* **2016**, *216*, 1066–1076.
213. Hu, Z.; Srinivasan, M. P.; Ni, Y. *Adv. Mater.* **2000**, *12*, 62–65.
214. Ma, Q.; Yu, Y.; Sindoro, M.; Fane, A. G.; Wang, R.; Zhang, H. *Adv. Mater.* **2017**.
215. Maleki, H. *Chem. Eng. J.* **2016**, *300*, 98–118.
216. Ioannidou, O; Zabaniotou, A *Renew. Sust. Energ. Rev.* **2007**, *11*, 1966–2005.
217. Abioye, A. M.; Ani, F. N. *Renew. Sust. Energ. Rev.* **2015**, *52*, 1282–1293.
218. White, R. J.; Budarin, V.; Luque, R.; Clark, J. H.; Macquarrie, D. J. *Chem. Soc. Rev.* **2009**, *38*, 3401–3418.
219. You, P.; Kamarudin, S *Chem. Eng. J.* **2017**, *309*, 489–502.
220. Köseoğlu, E.; Akmil-Başar, C. *Adv. Powder Technol.* **2015**, *26*, 811–818.
221. Van Hilst, F.; Hoefnagels, R.; Junginger, M.; Shen, L.; Wicke, B. *Sustainable biomass for energy and materials: A greenhouse gas emission perspective*; tech. rep.; Working paper: Copernicus Institute of Sustainable Development, Utrecht University, Heidelberglaan 2, 3584 CS Utrecht, the Netherlands. Available at: https://uu.nl/sites/default/files/sustainable_biomass_for_energy_and_materials.pdf (Last accessed February 2017), 2017.
222. Dias, J. M.; Alvim-Ferraz, M. C.; Almeida, M. F.; Rivera-Utrilla, J.; Sánchez-Polo, M. *J. Environ. Manage.* **2007**, *85*, 833–846.
223. Jain, A.; Balasubramanian, R.; Srinivasan, M. *Chem. Eng. J.* **2016**, *283*, 789–805.
224. Marsh, H.; Reinoso, F. R., *Activated carbon*; Elsevier: 2006.

BIBLIOGRAPHY

225. Aygün, A.; Yenisoy-Karakaş, S.; Duman, I. *Micropor. Mesopor Mat.* **2003**, *66*, 189–195.
226. Bansal, R. C.; Goyal, M., *Activated carbon adsorption*; CRC press: 2005.
227. Yahya, M. A.; Al-Qodah, Z; Ngah, C. Z. *Renew. Sust. Energ. Rev.* **2015**, *46*, 218–235.
228. Inagaki, M.; Toyoda, M.; Soneda, Y.; Tsujimura, S.; Morishita, T. *Carbon* **2016**, *107*, 448–473.
229. Budarin, V.; Clark, J. H.; Hardy, J. J. E.; Luque, R.; Milkowski, K.; Tavener, S. J.; Wilson, A. J. *Angew. Chemie Int. Ed.* **2006**, *118*, 3866–3870.
230. Titirici, M.-M.; White, R. J.; Brun, N.; Budarin, V. L.; Su, D. S.; del Monte, F.; Clark, J. H.; MacLachlan, M. J. *Chem. Soc. Rev.* **2015**, *44*, 250–290.
231. White, R.; Budarin, V.; Clark, J. *Chem. Eur. J.* **2010**, *16*, 1326–1335.
232. Nireesha, G.; Divya, L; Sowmya, C; Venkateshan, N; Babu, M. N.; Lavakumar, V. *International journal of novel trends in pharmaceutical sciences* **2013**, *3*, 87–98.
233. Guizard, C.; Leloup, J.; Deville, S. *J. Am. Ceram. Soc.* **2014**, *97*, ed. by White, M. A., 2020–2023.
234. Kasraian, K.; DeLuca, P. P. *Pharm. Res.* **1995**, *12*, 484–490.
235. Tang, Y.; Qiu, S.; Wu, C.; Miao, Q.; Zhao, K. *J. Eur. Ceram. Soc.* **2016**, *36*, 1513–1518.
236. Donohue, M.; Aranovich, G. *Adv. Colloid Interfac.* **1998**, *76*, 137–152.
237. Thommes, M.; Kaneko, K.; Neimark, A. V.; Olivier, J. P.; Rodriguez-Reinoso, F.; Rouquerol, J.; Sing, K. S. *Pure Appl. Chem.* **2015**, *87*, 1051–1069.
238. AlOthman, Z. A. *Materials* **2012**, *5*, 2874–2902.
239. Durá, G.; Budarin, V. L.; Castro-Osma, J. A.; Shuttleworth, P. S.; Quek, S. C.; Clark, J. H.; North, M. *Angew. Chemie Int. Ed.* **2016**, *128*, 9319–9323.
240. Harris, J. G.; Yung, K. H. *J. Phys. Chem.* **1995**, *99*, 12021–12024.